Universidade do Minho
Escola de Engenharia

Patrícia Brandão de Athayde Malafaya Baptista

OSTEOCHONDRAL TISSUE ENGINEERING CONSTRUCTS COMBINING PARTICLE AGGREGATED SCAFFOLDING AND BIOACTIVE DELIVERY STRATEGIES

Março de 2008

OSTEOCHONDRAL TISSUE ENGINEERING CONSTRUCTS COMBINING PARTICLE AGGREGATED SCAFFOLDING AND BIOACTIVE DELIVERY STRATEGIES
Patrícia Brandão de Athayde Malafaya Baptista
UMinho|2008

Universidade do Minho
Escola de Engenharia

Patrícia Brandão de Athayde Malafaya Baptista

OSTEOCHONDRAL TISSUE ENGINEERING CONSTRUCTS COMBINING PARTICLE AGGREGATED SCAFFOLDING AND BIOACTIVE DELIVERY STRATEGIES

Tese de Doutoramento em Engenharia Biomédica

Trabalho efectuado sob a orientação do
Professor Rui Luís Gonçalves dos Reis

Março de 2008

TO ALL THAT SOMEHOW

CONTRIBUTED TO THIS THESIS

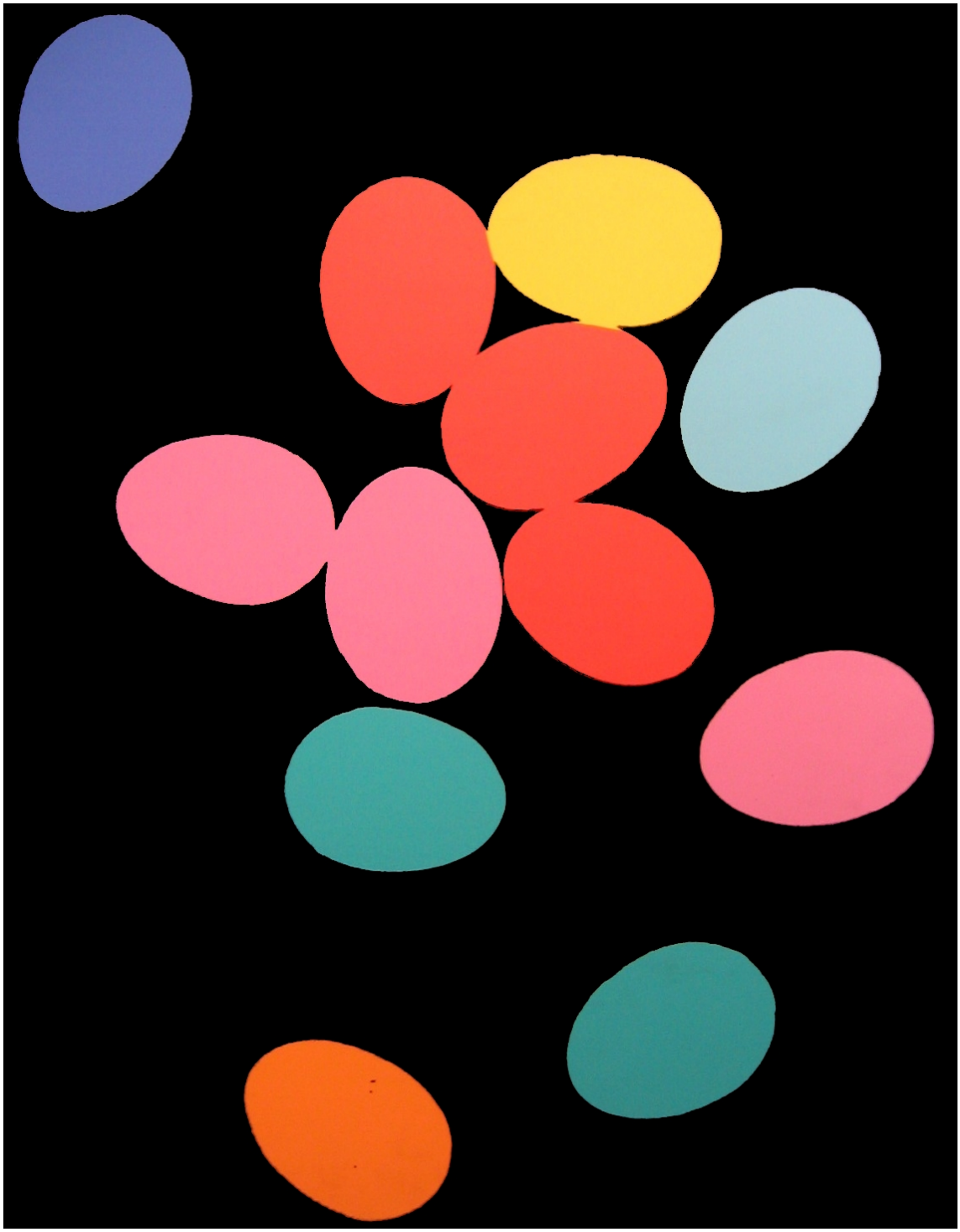

EGGS
Andy Warhol, 1982
Acrylic and silkscreen ink on canvas
Founding Collection, Contribution The Andy Warhol Foundation for the Visual Arts, Inc.
1998.1.259

ACKNOWLEDGEMENTS

The preparation of this thesis would not be possible without the support of several persons and institutions. To express my gratitude, I dedicate this thesis to them. Nevertheless, I feel the need to acknowledge some in particular.

For the obvious reasons, I have to start thanking my supervisor, Prof. Rui Reis, without whom this thesis, and what I have accomplished, would not be possible. He has always supported my ideas and decisions, giving me the right motivation 'cues' needed to reach this moment, namely when this writing stage turned out to be more challenging due to the *in silico* obstacle. He also gave me the opportunity to be involved in other processes beyond this thesis, which were so important to me and from which I have learned so much. I will always admire the way he continuously faces and overcomes his challenges. I sincerely hope you feel proud of this, as you said once, last (but not least) thesis of the genesis of your research group.

To Prof. Mauli Agrawal from the University of Texas, Health Science Center at San Antonio that, even without practical translation to this thesis, formally accepted to be my PhD co-supervisor.

To LBI and RCROSS in Austria, namely to Prof. Heinz Redl, Dr. Martijn van Griensven and Dr. Anja Peterbauer that, in the scope of the FP6 European project HIPPOCRATES, have sustained this interesting and fruitful collaboration, which has resulted in several joint publications.

To the Portuguese Foundation for Science and Technology for the financial support through a PhD grant (SFRH/BD/11155/2002). This work was also partially supported by FCT through POCTI and/or FEDER programmes, by the INTERREG IIIA project PROTEUS, by EU project HIPPOCRATES (NMP3-CT-2003-505758) and carried out in the scope of European NoE EXPERTISSUES (NMP3-CT-2004-500283). I would like also to acknowledge the Calouste Gulbenkian Foundation for the several travel awards to attend international scientific meetings.

During this PhD period in my research group, which is always under a very dynamic metamorphosis, I have made friends, met some really special people and received truthful support from many colleagues. I have to thank you all for your attention, support and sincere enthusiasm throughout the very good and less good moments. Namely to Adriano Pedro and Miguel Oliveira for their 'extra work' when I had to be more dedicated on writing this thesis, as well as to our 'MT' people for their logistical and friendly support. A special thanks to my dear friends Catarina

Alves, Vitor Correlo, Ana Martins and Ariana Santos for sharing so many good moments and for their endless positive energy during this period.

I want also to acknowledge the technical support of Elsa Ribeiro during the SEM analysis. To Life and Health Sciences Research Institute (ICVS) at the University of Minho, for the use their facilities, namely to Luís Martins for his perseverance with the histological chitosan sections slicing. I would also like to acknowledge the technical staff of the Central Laboratory of Analysis from the University of Aveiro, namely to Dr. Lina Carvalho and Dr. Eugénio Soares for their promptness with ICP analysis.

I need to thank to all my very best friends, Ana, Dorita, Cristina, Pituca, Belinha and João Menina (and *sus muchachos*..) for their priceless support, enthusiasm, motivation and... tireless hears! I am a lucky person to have you around. My very special words to Ana that, by our endless friendship and deeper understanding on this long journey, was always there with the right word at the right moment, even when more important issues were nearby. Thank you for being you!

I would like also to express my sincere gratitude to João's parents, Manuel e Emília, for their almost daily warm support and availability, namely for their assistance after the *in silico* problem.

My special thankfulness to my family, namely my sister and Roberto and our youngest member, my lovely Inês. I'm sure that she will forgive me for my absence in this writing stage, especially because at this period of life mobiles are just to have fun! To my mother and my father for their unconditional love, endless support and enthusiasm on my accomplishments.

Finally, the hardest emotional task at this point. As it is easy to understand, the right words to express my gratitude to someone so unique and so special to me were not invented yet. João, your unconditional support was essential to get to the end of this journey, mainly when my motivation and strength were somehow down. You and your love were always there and I deeply thank you for that. Thank you for stand by me with your strength as a source of motivation that kept me ongoing in an 'easier way'. Like someone said one day: '*Aos meus olhos agradeço o facto de terem encontrado os teus*'…

ABSTRACT

Osteochondral defects are lesions of the articular cartilage where the underlying bone tissue is also damaged. Although some studies have achieved success in repairing small cartilage defects, there is no widely accepted method for complete repair of large osteochondral defects. This is due to different factors, for instances, the ones associated with mechanical instability, among others. The requirements for a successful regeneration of an osteochondral defect could potentially be met by using a tissue-engineered osteochondral hybrid construct. Therefore, the need for a simultaneous regeneration of both cartilage and subchondral bone should be considered, making osteochondral tissue engineering an interesting challenge to the present research since it requires the combination of both bone and cartilage tissue engineering principles. Some researchers suggest that osteochondral defects could be regenerated from single-layer scaffolds, engineering complex tissue grafts with gradients of molecular, structural, and functional properties. Nevertheless, it has been better accepted that a bilayered structure would be more adequate to regenerate an osteochondral defect. This structure should be able to support the growth and development of different types of cells while providing a mechanical and biochemical environment able to promote the formations of the two distinct tissues.

The main goal of this thesis was to develop and assess the potential of several possible strategies for osteochondral tissue engineering. This includes: (1) the development of the cell culturing to be performed independently in the two components that are integrated before implantation; (2) the biphasic scaffold with adequate properties for both cartilage and bone parts to be used in a special bioreactor with two separate chambers where two different cell types can be seeded, and (3) the biphasic scaffold loaded with distinct differentiation agents able to provide the adequate biochemical cues to common progenitor cells. Furthermore, and as a key requisite for biomedical applications including tissue engineering, the presented work also tried to keep present the needs for (4) the *in vivo* biofunctionality of the new materials. These were the main challenges addressed in this thesis. The work described intends mainly to be yet another positive contribute for the design of a successful approach for osteochondral tissue engineering, having always in mind that, to date, there is no accepted method for complete repair of large osteochondral defects.

In this PhD research, an innovative methodology for scaffolds production is proposed, based on the aggregation of pre-fabricated degradable particles. This methodology allowed to produce scaffolds with high interconnectivity and mechanical stability. The processing route was also used efficiently for the production of bilayered scaffolds by assembling both polymeric and composite particles. The obtained bilayered scaffolds present a very good integration between both components which is critical, since any discontinuity is likely to cause long-term device failure.

By using the particles aggregation methodology, and as described in this work, it was possible to successfully produce polymeric, composite and bilayered scaffolds. Chitosan was selected as polymeric matrix due to its structural similarity to

glycosaminoglycans (GAGs) found in extracellular matrices including native articular cartilage. On the other hand, hydroxylapatite was used as bioactive ceramic filler, since this it is the main mineral present in bone composition, approaching in this way the developed composite scaffolds to the bone composite structure. An extensive materials characterization was carried out, with a particular emphasis on the morphometric analysis and mechanical performance of the developed materials that have demonstrated to be adequate, corroborating the claimed advantages of the proposed methodology.

Preliminary studies with human adipose stem cells were also carried out, clearly indicating the presence of cells with osteogenic and chondrogenic morphology in the 3D particle agglomerated scaffolds. The influence of the 3D support on the cells differentiation ability is further suggested, since no events of osteogenic or chondrogenic differentiation in the control cells without the scaffolds were detected.

A specific double-chamber bioreactor was designed in order to allow, as an ultimate goal, for the simultaneous culturing of chondrocytes and osteoblasts or the same source of progenitor cells with distinct differentiation mediums. As proof of concept, dynamic bioactivity tests are described using bilayered chitosan scaffolds.

Insulin-loaded chitosan particle aggregated scaffolds are proposed as a potential model system to induce chondrogenic differentiation. The *in vitro* release profiles and the effect of these systems on a pre-chondrogenic cell line were investigated. The most promising results were obtained for cells seeded in the higher insulin-loaded scaffolds that showed a typical chondrocytic round morphology, were positively stained for toluidine blue, presented a high GAGs production, and expressed genes encoding cartilaginous markers. This approach opens the possibility to assemble the developed systems in bilayered constructs, in order to provide the adequate biochemical cues to promote selective differentiation of cartilage and bone in osteochondral applications.

The final study described in this work is focused on the assessment of the *in vivo* biofunctionality of polymeric chitosan scaffolds. The scaffolds *in vivo* performance is one obvious key requirement for tissue engineering applications. The scaffolds properties shown to be favourable to the connective tissues ingrowth into the scaffolds, demonstrating a good integration with the host tissue. Furthermore, the scaffolds were able to promote an organization of the extracellular matrix and an increasing neo-vascularization with the time of implantation, which is rather promising and not typical at all for porous biodegradable systems.

As a general remark, and in the context of possible strategies for osteochondral tissue engineering, the chitosan-based scaffolds produced by particle aggregation are morphologically and mechanically competent. In addition, the developed scaffolds are able to incorporate adequate biochemical cues, and present an *in vivo* biocompatible behaviour, and may thereby be potential candidates for large osteochondral tissue engineering applications. Each of the individual performed work opens the possibility to better accomplish an osteochondral hybrid strategy following the different discussed options. This is the main innovation coming from this thesis.

Engenharia de Tecidos de Defeitos Osteocondrais Combinando Estratégias de Design de Suportes Processados por Agregação de Partículas e de Libertação Controlada de Agentes Bioactivos

RESUMO

Os defeitos osteocondrais são lesões na cartilagem articular onde o tecido ósseo adjacente está também danificado. Apesar do sucesso alcançado em alguns estudos na regeneração de pequenos defeitos da cartilagem, não existe actualmente um método consensual para a reabilitação completa de grandes defeitos osteocondrais. Isto é devido a diferentes factos, entre os associados com instabilidade mecânica. Os requisitos para uma regeneração bem sucedida de um defeito osteocondral podem ser potencialmente preenchidos utilizando um suporte híbrido desenvolvido através de engenharia de tecidos. Por isso, a necessidade da regeneração simultânea da cartilagem e do osso subcondral deve ser considerada, tornando a engenharia de tecidos osteocondral num desafio interessante para a investigação actual, uma vez que requer a combinação dos princípios de engenharia de tecidos do osso e da cartilagem. Alguns investigadores sugerem que os defeitos osteocondrais podem ser regenerados a partir de suportes monofásicos, desenvolvendo implantes tecidulares complexos com gradientes de propriedades moleculares, estruturais e funcionais. No entanto, tem sido melhor aceite que uma estrutura bifásica pode ser mais adequada para regenerar um defeito osteocondral. Esta estrutura deve ser capaz de sustentar o crescimento e desenvolvimento de diferentes tipos de células, providenciando um ambiente bioquímico e mecânico capaz de promover a formação dos dois tecidos distintos.

O principal objectivo desta tese foi desenvolver e avaliar o potencial de várias estratégias possíveis para engenharia de tecidos osteocondrais. Estas incluem: (i) o desenvolvimento de cultura de células para ser efectuado nos dois componentes independentemente que são integrados antes da implantação; (ii) o suporte bifásico com propriedades adequadas para a regeneração de osso e cartilagem é utilizado num bioreactor específico com duas câmaras separadas, onde os dois tipos de células diferentes podem ser cultivados; e (iii) os agentes de diferenciação são incorporados no suporte bifásico, de modo a proporcionar estímulos bioquímicos adequados às células progenitoras comuns. Para além disso, e como um pré-condição essencial para aplicações biomédicas incluindo engenharia de tecidos, este trabalho tentou ter sempre presente os requisitos de biofuncionalidade *in vivo* de novos materiais. Estes são os principais desafios propostos nesta tese. O trabalho descrito pretende principalmente ser mais um contributo positivo para o design de uma estratégia de sucesso na engenharia de tecidos osteocondrais, não esquecendo que até à data não existe um método consensual para a reabilitação completa de grandes defeitos osteocondrais.

Nesta investigação de doutoramento, é proposta uma metodologia inovadora para a produção de suportes para engenharia de tecidos com base na agregação de partículas biodegradáveis pré-processadas. Esta metodologia permitiu a produção de suportes para engenharia de tecidos com elevada interconectividade e estabilidade mecânica. Mais ainda, foi aplicada eficazmente na produção de suportes bifásicos combinando partículas poliméricas e compósitas. Os suportes bifásicos obtidos apresentam uma boa integração entre os dois componentes. Este facto é crítico, dado que é provável que qualquer descontinuidade provoque a falha do dispositivo a longo prazo.

Utilizando a metodologia de agregação de partículas, e tal como é descrito neste trabalho, foi possível produzir com sucesso estruturas poliméricas, compósitas e bifásicas. O quitosano foi seleccionado como matriz polimérica devido à sua semelhança estrutural com os glicosaminoglicanos (GAGs) presentes nas matrizes extra-celulares, incluindo na cartilagem articular. Por outro lado, a hidroxiapatite foi utilizada como reforço cerâmico bioactivo, dado que é o principal mineral presente na composição do osso, aproximando deste modo os materiais compósitos desenvolvidos à estrutura compósita do osso. Uma extensa caracterização dos materiais foi realizada, com particular ênfase na análise morfométrica e desempenho mecânico dos materiais desenvolvidos que demonstraram ser adequados, comprovando assim as vantagens reivindicadas da metodologia proposta.

Estudos preliminares com células estaminais do tecido adiposo foram efectuados, indicando claramente a presença de células com morfologia osteogénica e condrogénica nos suportes desenvolvidos. A influência da estrutura tridimensional na capacidade de diferenciação das células é também sugerida, uma vez que não foram detectadas evidências de diferenciação osteogénica e condrogénica nas células sem os suportes utilizadas como controle. Um bioreactor específico de câmara dupla foi também desenhado de modo a permitir, como objectivo final, a cultura simultânea de condrócitos e osteoblastos ou o mesmo tipo de células progenitoras com diferentes meios de diferenciação. Como prova de conceito foram efectuados estudos dinâmicos de bioactividade utilizando suporte bifásicos de quitosano. Suportes produzidos por agregação de partículas carregados com insulina são propostos como um potencial modelo para induzir a diferenciação condrogénica. Os perfis de libertação *in vitro* e o efeito destes sistemas numa linha celular pré-condrogénica foram investigados. Os resultados mais promissores foram obtidos com células cultivadas nos suportes com maior concentração de insulina tendo as células demonstrado uma morfologia típica de condrócitos e marcado positivamente para o azul de toluidina. Verificou-se também um aumento na produção de glicosaminoglicanos e na expressão de genes associados a marcadores típicos de cartilagem. Esta aproximação abre a possibilidade de associar os sistemas desenvolvidos em suportes bifásicos, fornecendo sinais bioquímicos adequados à promoção selectiva da diferenciação em cartilagem e osso, tendo em vista aplicações osteocondrais.

O estudo final descrito neste trabalho foca-se na avaliação da biofuncionalidade *in vivo* dos suportes poliméricos de quitosano. O comportamento destes materiais *in vivo* é um pré-requisito óbvio para aplicações no campo de engenharia de tecidos. As propriedades dos suportes mostraram ser favoráveis ao crescimento dos tecidos conectivos para o interior dos mesmos, apresentando uma boa integração com o tecido hospedeiro. Os materiais foram ainda capazes de promover a organização da matriz extra-celular e um aumento da neo-vascularização durante a implantação, o que é bastante promissor e de todo invulgar para sistemas porosos biodegradáveis.

Como comentário final, e no contexto de possíveis estratégias para engenharia de tecidos osteocondrais, os suportes à base de quitosano processados por agregação de partículas são morfológica e mecanicamente competentes. Para além disso, os materiais desenvolvidos são capazes de incorporar sinais bioquímicos adequados apresentando um comportamento biocompatível *in vivo*, podendo deste modo ser considerados potenciais candidatos para aplicações de engenharia de tecidos de grandes defeitos osteocondrais. Cada um dos trabalhos realizados abre uma possibilidade de alcançar uma estratégia híbrida osteocondral tendo em conta as opções discutidas. Esta é a principal inovação resultante desta tese.

TABLE OF CONTENTS

LIST OF ABBREVIATIONS

#	
0.05	polymeric chitosan scaffolds loaded with 0.05% of insulin
0.5	polymeric chitosan scaffolds loaded with 0.5% of insulin
5	polymeric chitosan scaffolds loaded with 5% of insulin
2D	two dimensional
3D	three dimensional
A	
agg	aggrecan
ASC	adipose stem cells
ATDC5	pre-chondrogenic murine mesenchymal cell line
ATR	attenuated total reflectance
B	
BCA	bicinchoninic acid
BDNF	brain derived neutrophic factor
bFGF	basic fibroblast growth factor
BiCCHA	bilayered chitosan/chitosan-hydroxylapatite scaffolds
BMP	bone morphogenetic protein
BMP-2	bone morphogenetic protein-2
BS	bone surface
BS/BV	bone surface-to-volume ratio
BV	bone volume
β-NGF	beta-nerve growth factor
C	
C, Ch	polymeric chitosan scaffolds
CaP	calcium phosphate
CCD-18Co	normal colon fibroblast cells derived from human colon
CHA	composite chitosan-hydroxylapatite scaffolds
col I	collagen type I
col II	collagen type II
CT	computed tomography
D	
DA	structural degree of anisotropy
DMA	dynamic mechanical analysis
DMB	1,9-dimethylmethylene blue
DMEM	xvydroxyl's modified eagle's medium
E	
E*	complex modulus
E'	storage modulus
E''	loss modulus
ECACC	xvydroxyl collection of cell cultures
ECM	extracellular matrix
EDS	energy dispersive spectroscopy
EGF	epidermal growth factor
Ethisorb210	non-woven fleece composed of a polyglycolic-polylactic-copolymer punctually glued with polydioxanon
F	
F12	Ham's F-12 Nutrient Mixture with 15 mM HEPES
FGF	fibroblast growth factor
FGF-2	fibroblast growth factor-2
FTIR	fourier-transform infrared spectroscopy
G	
GAG	glycosaminoglycans
Gly-X-Y	glycine-X-Y
H	
HA	hydroxylapatite
HA sint	sintered hydroxylapatite
HA unsint	unsintered hydroxylapatite
HDMECA	adult human dermal microvascular endothelial cells
H&E	hematoxylin-eosin
HMDS	hexamethyldisilazane reagent
HUVEC	human umbilical vein endothelial cells
I	
ICP	inductively coupled plasma
IGF-I	insulin growth factor-1
INS	cell culture medium supplemented with 10 μg/ml of insulin

L

L929	rat lung fibroblasts cell line

M

M	molar
Micro-BCA™	Protein Assay Kit 23235, Pierce
MIMICS®	materialise Interactive Medical Image Control System
m_I	initially loaded weight of protein
mM	milimolar
m_p	weight of dry particles prior to *in vitro* release studies
Mpa	mega Pascal
m_r	weight of protein in precipitation solution
MRI	magnetic resonance imaging
MSC	mesenchymal stem cells
MTS	4,5-dimethylthiazol-2-yl)-5-(3-carboxylmethoxyphenyl) -2-(4-sulfophenyl)-2H tetrazolium
µ-CT micro-CT	micro-computed tomography
µg	micrograms
µl	microliters
µm	micrometers

N

NGF	nerve growth factor
nglBMP-2	non-glycosylated form of bone morphogenetic protein-2
NT-3	neurotrophin-3

P

PBS	phosphate buffer solution
PCL	polycaprolactone
PCR	polymerase chain reaction
PDGF	platelet-derived growth factor
PDGF-BB	platelet-derived growth factor-BB
PGA	polyglycolic acid
pH	potencial of hydrogen
PLA	polylactic acid
PLGA	poly(lactide-co-glycolide) copolymer
PP	polypropylene
PS	polysulfone
PVA	poly(vinyl alcohol)

R

RGD	Arg-Gly-Asp peptides
RH	relative humidity
rhBMP-2	recombinant bone morphogenetic protein-2
rhOP-1	recombinant human osteogenic protein-1
RT	room temperature

S

SBF	simulated body fluid
SEM	scanning electron microscopy
SMA	smooth muscle actin
SSF	simulated synovial fluid

T

T	temperature
Tb. Sp	trabecular separation
Tb.Th	trabecular thickness
TCP	tricalcium phosphate
TGF-β	transforming growth factor beta
TGF-β1	transforming growth factor-beta1

V

VECs	mitral valve endothelial cells
VEGF	vascular endothelial growth factor
VICs	mitral valve interstitial cells
vWF	von Willebrand factor

W

W_i	initial weight
W_w	wet weight

LIST OF FIGURES

SECTION 2

CHAPTER II

Materials and Methods

SECTION 3

CHAPTER III

Chitosan particle agglomerated scaffolds for cartilage and osteochondral tissue engineering approaches with adipose tissue derived stem cells

CHAPTER IV

Bilayered chitosan-based scaffolds for osteochondral tissue engineering: influence of hydroxylapatite on *in vitro* cytotoxicity and dynamic bioactivity studies in a specific double chamber bioreactor

CHAPTER V

The effect of insulin-loaded chitosan particle-aggregated scaffolds in chondrogenic differentiation

CHAPTER VI

Morphometric, mechanical characterization and in vivo neo-vascularization of novel chitosan particle aggregated tissue engineering scaffolding architectures

LIST OF TABLES

SECTION 1

CHAPTER I

Natural-origin polymers as carriers and scaffolds for biomolecules and cell delivery in tissue engineering applications

SECTION 2

CHAPTER II.

Materials and Methods

SECTION 3

CHAPTER IV.

Bilayered chitosan-based scaffolds for osteochondral tissue engineering: influence of hydroxylapatite on *in vitro* cytotoxicity and dynamic bioactivity studies in a specific double chamber bioreactor

CHAPTER V.

The effect of insulin-loaded chitosan particle-aggregated scaffolds in chondrogenic differentiation

CHAPTER VI.

Morphometric, mechanical characterization and *in vivo* neo-vascularization of novel chitosan particle aggregated tissue engineering scaffolding architectures

SHORT *CURRICULUM VITAE*

Patrícia B. Malafaya was born in 1974 in Porto, Portugal. She presently lives in Matosinhos and works, as a researcher, in the 3B's Research Group (Biomaterials, Biodegradables and Biomimetics), at the University of Minho, Braga, Portugal directed by Prof. Rui L. Reis. This research group is one of the Units of the Institute for Biotechnology and Bioengineering (PT Government Associated Laboratory).

Her background includes a five-year graduation in Metallurgical Engineering and Materials Science in the Faculty of Engineering of the University of Porto. During the final year of her graduation, she developed two important works of initiation to scientific research in the biomaterials field on the general topic of 'Processing and Characterization of Porous Polymeric and Ceramic Materials for Orthopaedic Application', both supervised by Prof. Rui L. Reis.

In 1998, she was formally invited to help starting a new biomaterials group at the University of Minho, known today as the 3B's Research Group. She has a Master Degree in Polymer Engineering by the University of Minho also with the supervision of Prof. Rui L. Reis in collaboration with Consejo Superior de Investigaciones Cientificas (CSIC) in Madrid with local supervision of Prof. Julio San Róman. In January 2003, she was awarded with a grant from the Portuguese Foundation for Science and Technology (FCT) for her PhD in the 3B's Research Group at the University of Minho under the supervision of Prof. Rui L. Reis, in collaboration with the University of Texas Health Science Center at San Antonio, under the local co-supervision of Prof. C. Mauli Agrawal.

As a researcher in the 3B's Research Group, she has been involved in the preparation of several grants proposal both at National and European levels, including the EXPERTISSUES – the only funded FP6 Network of Excellence in the tissue engineering field. She is also actively involved in HIPPOCRATES, a FP6 STREP entitled 'A Hybrid Approach for Bone and Cartilage Tissue Engineering using Natural Origin Scaffolds, Progenitor Cells and Growth Factors'. She was invited as an Expert Evaluator for FP7 proposals evaluation for the call FP7-NMP-SME-1 'Rapid manufacturing concepts for small series industrial production' both in stage 1 and 2. She is a referee in several international scientific journals, namely Journal of Controlled Release and Materials Science and Engineering C, among others. She was also involved in the development of the business plan of STEMMATERS which is the biotechnological spin-off of the 3B's Research Group. Moreover, she is actively involved in the new building project at Avepark, which includes the new home for the 3B´s, the headquarters for EXPERTISSUES NoE and the spin-off STEMMATERS. She was also part of the organization of several scientific meetings, namely two NATO-ASI (Advanced Study Institute) Courses and currently, the 2008 Annual Meeting of TERMIS-EU (Tissue Engineering and Regenerative Medicine International Society – EU chapter).

As results of her research work, she attended several of the most important international meetings in the present field of research. Presently, she is author of 20 papers in international peer reviewed journals (14 published and 6 submitted), 17 book chapters, 62 abstracts published in international proceedings.

LIST OF PUBLICATIONS

The work performed during this PhD resulted in the following publications:

INTERNATIONAL JOURNAL WITH REFEREES

PB Malafaya, GA Silva, RL Reis. Natural-origin polymers as carriers and scaffolds for biomolecules and cell delivery in tissue engineering applications. Advanced Drug Delivery Reviews (2007) 59(4-5):207-233

PB Malafaya, AJ Pedro, A. Peterbauer, C. Gabriel, H. Redl, RL Reis. Chitosan particles agglomerated scaffolds for cartilage and osteochondral tissue engineering approaches with adipose tissue derived stem cells. Journal of Materials Science: Materials in Medicine: (2005) 16:1077-1085

PB Malafaya, RL Reis. Bilayered chitosan-based scaffolds for osteochondral tissue engineering: influence of hydroxylapatite on *in vitro* cytotoxicity and dynamic bioactivity studies in a specific double chamber bioreactor. Acta Biomaterialia (2008) submitted

PB Malafaya, JT Oliveira, RL Reis. The effect of insulin-loaded chitosan particle aggregated scaffolds in chondrogenic differentiation. Biomaterials (2008) submitted

PB Malafaya, TC Santos, M van Griensven, RL Reis. Morphometric, mechanical characterization and *in vivo* neo-vascularization of novel chitosan particle aggregated tissue engineering scaffolding architectures. Tissue Engineering: Part A (2008) submitted

BOOK CHAPTERS

PB Malafaya, RL Reis. Production of particle-aggregated scaffolds to be used in cartilage, bone and osteochondral tissue engineering applications. In: A manual for biomaterials/scaffold fabrication technology, A (Manuals in Biomedical Research, vol. 4) ed: G Khang, MS Kim, HB Lee, World Scientific Publishers, Singapore, Singapore (2007) 77-90

PB Malafaya, GA Silva, RL Reis. Strategies for delivering bone and cartilage regeneration factors. In: Biodegradable Systems in Tissue Engineering and Regenerative Medicine, ed: RL Reis, J San Román. CRC Press, Boca Raton, USA (2004) 253-280

PB Malafaya, RL Reis. Porous bioactive composites from marine origin based in chitosan and hydroxylapatite particles. In: Bioceramics 15, Sidney (AUT), Key Engineering Materials, ed: B Ben-Nissan, D Sher, W Walsh. Trans Tech Pub, Zurich, Switzerland (2003) 240-2:39-42

PB Malafaya, ME Gomes, AJ Salgado, RL Reis. Polymer based scaffolds and carriers for bioactive agents from different natural origin materials. In: Tissue Engineering, Stem Cells, and Gene Therapies, ed: YM Elçin. Advances In Experimental Medicine and Biology Series, Kluwer Academic/Plenum Publishers, London, UK (2003) 534:201-233

INTERNATIONAL CONFERENCES

PB Malafaya, JT Oliveira, TC Santos, M van Griensven, RL Reis. Morphometric and mechanical characterization, insulin loading and in vivo biocompatibility of chitosan particles aggregated scaffolds for tissue engineering. TERMIS-EU 2008 Meeting, Porto, PT, Tissue Engineering (2008) accepted as oral presentation

PB Malafaya, JT Oliveira, RL Reis. Development and characterization of natural-origin bilayered scaffolds for osteochondral tissue engineering under the scope of HIPPOCRATES project. TERMIS-EU 2008 Meeting, Porto, PT, Tissue Engineering (2008) invited lecture

PB Malafaya, RL Reis. Optimization of chitosan-based composite and bilayered scaffolds produced by particles aggregation for osteochondral tissue engineering: influence of hydroxylapatite. TERMIS-EU 2008 Meeting, Tissue Engineering, Porto, PT (2008) accepted as poster presentation

PB Malafaya, RL Reis. Design of bone, cartilage and osteochondral tissue engineering chitosan-based scaffolds produced by a particle aggregation methodology. 31st Annual Meeting of the Society for Biomaterials – SFB'06, Pittsburgh, Pennsylvania, USA (2006) 244, poster

PB Malafaya, AJ Pedro, A Peterbauer, H Redl, C Gabriel, RL Reis. An osteochondral tissue engineering approach based in chitosan particle agglomerated scaffolds and adipose derived stem cells. 2006 Regenerate – World Congress on Tissue Engineering and Regenerative Medicine, Pittsburgh, Pennsylvania, USA (2006) 594, oral presentation

PB Malafaya, AJ Pedro, A Peterbauer, H Redl, C Gabriel, RL Reis. Preliminary assessment of osteogenic and chondrogenic differentiation of adipose tissue derived stem cells seeded in chitosan particle agglomerated scaffolds. 1st Annual International Meeting of the Portuguese Society for Stem Cells and Cellular Therapies (SPCE-TE), Funchal, Madeira, Portugal (2006) 17, poster

PB Malafaya, AJ Pedro, A Peterbauer, H Redl, C Gabriel, RL Reis. Chitosan particle agglomerated scaffolds and adipose tissue derived stem cells for osteochondral tissue engineering. 1st Marie Curie Cutting Edge InVENTS Conference on New

Developments on Polymers for Tissue Engineering, Replacement and Regeneration, Funchal, Madeira, Portugal (2006) oral presentation

PB Malafaya, AJ Pedro, JT Oliveira, A Peterbauer, C Gabriel, H Redl, RL Reis. Strategies for osteochondral tissue engineering applications tailoring chitosan-based bilayered scaffolds and surface interactions. 2nd Marie Curie Cutting Edge InVENTS Conference on Recent advances on polymeric based systems for controlled delivery of bioactive agents: Applications in Tissue Engineering, Alvor, Algarve, Portugal (2006) O12, oral presentation

PB Malafaya, RL Reis. Chitosan-based particle agglomerated scaffolds developed for bone, cartilage and osteochondral tissue engineering applications. 6th International Symposium on Frontiers in Biomedical Polymers – FBPS'05, Granada, Spain (2005) O19, oral presentation

PB Malafaya, AJ Pedro, A. Peterbauer, H. Redl, C. Gabriel, RL Reis. Bone and cartilage tissue engineering approaches using chitosan particle agglomerated scaffolds and adipo derived stem cells. 19th European Conference on Biomaterials – ESB2005, Sorrento, Italy (2005) T173, oral presentation

PB Malafaya, RL Reis. Development and characterization of pH responsive chitosan and chitosan/HA scaffolds processed by a microsphere-based aggregation route. 7th World Biomaterials Congress, Sydney, Australia (2004) 1285, poster

PB Malafaya, CM Alves, RL Reis. Polymeric and composite porous biomaterials entirely from marine origin: development and characterization. 29th Annual Meeting of the Society for Biomaterials, Reno, Nevada, USA (2003) 634, poster

PB Malafaya, ET Baran, K. Tuzlakoglu, RM Silva, RL Reis. Polymeric and composite constructs from marine origin for bone regeneration. NATO/ASI on Learning from Nature How to Design New Implantable Biomaterials: From Biomineralization Fundamentals to Biomimetic Materials and Processing Routes, Alvor, Portugal (2003) 61, poster

PB Malafaya, RL Reis. Porous bioactive composites from marine origin based in chitosan and hydroxylapatite particles. Bioceramics 15, Sidney, Australia (2002) 240-2:39-42, oral presentation

From the work developed in collaboration with colleagues in the 3B's Research Group, the following publications have resulted:

INTERNATIONAL JOURNAL WITH REFEREES

AM Martins, QP Pham, PB Malafaya, RL Reis, AG Mikos. Natural stimulus responsive scaffolds/cells for bone tissue engineering: influence of lysozyme upon scaffold degradation and osteogenic differentiation of cultured marrow stromal cells induced by CaP coatings. Tissue Engineering: Part A (2008) submitted

AM Martins, MI Santos, HS Azevedo, PB Malafaya, RL Reis. Natural origin "smart" scaffolds with in situ pore forming capability for bone tissue engineering applications. Acta Biomaterialia (2008) submitted

JM Oliveira, SA Costa, IB Leonor, PB Malafaya, JF Mano, RL Reis. Novel xxxydroxylapatite/ carboxymethylchitosan composite scaffolds prepared through an innovative "auto-catalytic" electroless co-precipitation route. Journal of Biomedical Materials Research: Part A (2008) in press

JT Oliveira, VM Correlo, PC Sol, AR Costa-Pinto, PB Malafaya, AJ Salgado, M Bhattacharya, P Charbord, NM Neves, RL Reis. Assessment of the Suitability of Chitosan/PolyButylene Succinate Scaffolds Seeded with Mouse Mesenchymal Progenitor Cells for a Cartilage Tissue Engineering Approach. Tissue Engineering: Part A (2008) in press

JM Oliveira, SS Silva, PB Malafaya, MT Rodrigues, N Kotobuki, M Hirose, ME Gomes, JF Mano, H Ohgushi, RL Reis. Macroporous xxxydroxylapatite scaffolds for bone tissue engineering applications: Physicochemical characterization and assessment of rat bone marrow stromal cells viability. Journal of Biomedical Materials Research: Part A (2008) in press

AL Oliveira, PB Malafaya, SA Costa, RA Sousa, RL Reis. Micro-Computed Tomography (μ-CT) as a potential tool to assess the effect of dynamic coating routes on the formation of biomimetic apatite layers on 3D-plotted biodegradable polymeric scaffolds. Journal of Materials Science: Materials in Medicine (2007) 18(2):211-223

JF Mano, GA Silva, HS Azevedo, PB Malafaya, RA Sousa, SS Silva, LF Boesel, JM Oliveira, TC Santos, AP Marques, NM Neves, RL Reis. Natural origin biodegradable systems in tissue engineering and regenerative medicine: present status and some moving trends. Journal of the Royal Society Interface (2007) 4(17): 999-1030

JM Oliveira, MT Rodrigues, SS Silva, PB Malafaya, ME Gomes, CA Viegas, IR Dias, JT Azevedo, JF Mano, RL Reis. Novel xxxydroxylapatite/chitosan bilayered scaffold for osteochondral tissue-engineering applications: Scaffold design and its performance when seeded with goat bone marrow stromal cells. Biomaterials (2006) 27:6123-6137

AL Oliveira, PB Malafaya, RL Reis. Sodium silicate gel as a precursor for the in vitro nucleation and grow of a bone-like apatite coating in compact and porous polymeric structures. Biomaterials (2003) 24:2575-2584

BOOK CHAPTERS

ME Gomes, HS Azevedo, PB Malafaya, SS Silva, JM Oliveira, GA Silva, RA Sousa, JF Mano, RL Reis. Natural polymers in tissue engineering applications. In: Textbook on Tissue Engineering, ed: C Van Blitterswijk, A Lindahl, P Thomsen, D Williams, J Hubbell, R Cancedda, Elsevier, Amsterdam, Netherlands, (2008) in press

VM Correlo, ME Gomes, K Tuzlakoglu, JM Oliveira, PB Malafaya, JF Mano, NM Neves, RL Reis. Tissue Engineering Using Natural Polymers. In: Biomedical Polymers. Ed: M. Jenkins. Woodhead Publishing Ltd, Cambridge, UK (2007) 197-217

HS Azevedo, ME Gomes, PB Malafaya, AP Marques, AJ Salgado, RL Reis. Natural origin degradable polymers in biomedical applications. In: Handbook of biodegradable polymeric materials and their applications. Ed: SK Mallapragada, B Narasimhan. American Scientific Publishers, California, USA (2006) 2:13-31

ME Gomes, PB Malafaya, RL Reis. Fiber bonding and particle aggregation as promising methodologies for the fabrication of biodegradable scaffolds for hard tissue engineering. In: Biodegradable Systems in Tissue Engineering and Regenerative Medicine, ed: RL Reis, J San Román. CRC Press, Boca Raton, USA (2004) 53-65

RM Silva, PB Malafaya, JF Mano, RL Reis. Bioactive composite chitosan membranes to be used in bone regeneration applications. In: Bioceramics 15, Sidney (AUT), Key Engineering Materials, ed: B Ben-Nissan, D Sher, W Walsh. Trans Tech Pub, Zurich, Switzerland (2003) 240-2:423-426

CM Alves, PB Malafaya, RL Reis. Biocompatibility study of biodegradable hydroxylapatite particulates for bone/dentistry fillers. In: Bioceramics 15, Sidney (AUT), Key Engineering Materials, ed: B Ben-Nissan, D Sher, W Walsh. Trans Tech Pub, Zurich, Switzerland (2003) 240-2:725-728

AL Oliveira, ME Gomes, PB Malafaya, RL Reis. Biomimetic coating of starch based polymeric foams produced by a calcium silicate based methodology. In: Bioceramics 15, Sidney (AUT), Key Engineering Materials, ed: B Ben-Nissan, D Sher, W Walsh. Trans Tech Pub, Zurich, Switzerland (2003) 240-2:101-104

AL Oliveira, IB Leonor, PB Malafaya, CM Alves, HS Azevedo, RL Reis. Tailoring the bioactivity of natural origin based polymers systems: from bone-analogue composites to an all range of biomimetic calcium-phosphate coating methodologies. In: Bioceramics 15 Sidney (AUT), Key Engineering Materials, ed: B Ben-Nissan, D Sher, W Walsh. Trans Tech Pub, Zurich, Switzerland (2003) 240-2:111-142, invited chapter

ME Gomes, PB Malafaya, RL Reis. Methodologies for processing biodegradable and natural origin hybrid scaffolds for bone and cartilage tissue engineering applications. In: Biopolymer Methods in Tissue Engineering, ed: AP Hollander, PV Hatton. Methods in Molecular Biology Series, The Humana Press Inc, Totowa, USA (2003) 65-76

INTERNATIONAL CONFERENCES

JF Mano, JT Oliveira, CM Alves, PB Malafaya, RL Reis. Bone, cartilage and osteochondral tissue engineering strategies using natural origin polymers and ceramics, growth factors and progenitor cells. TERMIS-EU 2008 Meeting, Porto, PT, Tissue Engineering (2008) accepted as oral presentation

JM Oliveira, RA Sousa, N Kotobuki, PB Malafaya, M Tadokoro, M Hirose, JF Mano, RL Reis, H Ohgushi. Dexamethasone-loaded carboxymethylchitosan/poly(amidoamine) dendrimer nanoparticles enhances bone formation in vivo. TERMIS-EU 2008 Meeting, Porto, PT, Tissue Engineering (2008) accepted as oral presentation

JT Oliveira, R Picciochi, TC Santos, L Martins, LG Pinto, PB Malafaya, R A Sousa, AP Marques, AG Castro, JF Mano, NM Neves, RL Reis. Injectable gellan gum hydrogels as supports for cartilage tissue engineering applications. TERMIS-EU 2008 Meeting, Porto, PT, Tissue Engineering (2008) accepted as oral presentation

AM Martins, QP Pham, PB Malafaya, RM Raphael, FK Kasper, RL Reis, AG Mikos. "Smart" and stimulus responsive chitosan-based scaffolds /cells for bone tissue engineering: influence of lysozyme upon scaffold degradation and osteogenic differentiation of cultured marrow stromal cells induced by CaP coatings. TERMIS-EU 2008 Meeting, Porto, PT, Tissue Engineering (2008) accepted as oral presentation

JT Oliveira, R Picciochi, TC Santos, PB Malafaya, RA Sousa, AP Marques, AG Castro, JF Mano, NM Neves, RL Reis. Injectable gellan gum hydrogels as supports for cartilage tissue engineering applications: in vitro characterization and initial in vivo studies. 8th World Biomaterials Congress – WBC'08, Amsterdam, Netherlands (2008) accepted as oral presentation

AM Martins, QP Pham, PB Malafaya, RA Sousa, ME Gomes, K Kasper, RL Reis, AG Mikos. The role of lipase and α-amylase in both the degradation of starch/polycaprolactone fiber meshes and the osteogenic differentiation of rat marrow stromal cells. 8th World Biomaterials Congress - WBC'08, Amsterdam, Netherlands (2008) accepted as poster presentation

A Martins, ED Pinho, PB Malafaya, AP Marques, RL Reis, NM Neves. Micro-nano composite mesh scaffold in mouse MPCs osteogenic differentiation. TERMIS-EU 2007 Meeting, London, UK, Tissue Engineering (2007) 13(7):1727, oral presentation

JT Oliveira, R Picciochi, PB Malafaya, RA Sousa, TC Santos, AP Marques, L Martins, L Goretti, R Fernandes, G Castro, JF Mano, NM Neves, RL Reis. Gellan gum hydrogels as supports for cartilage tissue engineering approaches: in vitro and in vivo evaluation. 4th Marie Curie Cutting Edge InVENTS Conference on Biocompatibility evaluation and biological behaviour of polymeric biomaterials, Alvor, Algarve, Portugal (2007) oral presentation

AL Oliveira, RA Sousa, PB Malafaya, SA Costa, RL Reis. Micro-CT a valuable tool to study the effect of dynamic coating routes on the formation of biomimetic apatite layers on 3D-plotted biodegradable polymeric scaffolds. 20th European Conference on Biomaterials – ESB2006, Nantes, France (2006) T170, oral presentation

AL Oliveira, PB Malafaya, RA Sousa, RL Reis. Development of bone tissue engineering scaffolds through integration of melt based rapid prototyping and dynamic biomimetic coating routes. 2nd Marie Curie Cutting Edge InVENTS Conference on Recent advances on polymeric based systems for controlled delivery of bioactive agents: Applications in Tissue Engineering, Alvor, Algarve, Portugal (2006) P11, poster

JT Oliveira, R Picciochi, AR Pinto, L Martins, PB Malafaya, RA Sousa, JF Mano, NM Neves, RL Reis. Gellan gum hydrogels as supports for human articular chondrocytes and human bone marrow cells for cartilage tissue engineering applications. ESF/EMBO Symposium on Stem Cells in Tissue Engineering: isolation, culture, characterisation and applications, Sant Feliu de Guixols, Spain (2006) oral presentation

G Zanoni, PB Malafaya, A MacIntosh, RL Reis, PV Hatton, H Redl. 3D visualization of non X-Ray absorbing tissue engineering scaffolds in micro-computer tomography (μ-CT). 4th Annual Meeting of the European Tissue Engineering Society – ETES'05, Munich, Germany (2005) 337, poster

AM Martins, PB Malafaya, HS Azevedo, MI Santos, OP Coutinho, RL Reis. Natural origin scaffolds with in situ gradual pore forming capability: development and characterization. 7th World Biomaterials Congress, Sydney, Australia (2004) 1525, poster

IB Leonor, PB Malafaya, ET Baran, M Kawashita, RL Reis, T Kokubo, T Nakamura. Growth of a bonelike apatite layer on chitosan microparticles after a calcium silicate treatment. 7th World Biomaterials Congress – WBC'04, Sydney, Australia (2004) 1792, poster

AM Martins, MI Santos, HS Azevedo, PB Malafaya, OP Coutinho, RL Reis. Chitosan/starch scaffolds with an in situ pore forming capability for tissue engineering applications, 7th International Meeting of the Tissue Engineering Society International (TESI), Lausagne, Switzerland (2004) 105, oral presentation

AM Martins, PB Malafaya, HS Azevedo, RL Reis. Chitosan/starch scaffolds with gradual in vivo pore forming ability. 18th European Conference on Biomaterials – ESB'03, Stuttgart, Germany (2003) P027, poster

AL Oliveira, PB Malafaya, ME Gomes, RL Reis. Pre-mineralization of starch based bone tissue engineering scaffolds by a calcium silicate based process. 18th European Conference on Biomaterials – ESB'03, Stuttgart, Germany (2003) T028, oral presentation

RM Silva, PB Malafaya, JF Mano, RL Reis. Bioactive membranes of marine origin for guided bone regeneration. NATO/ASI on Learning from Nature How to Design New Implantable Biomaterials: From Biomineralization Fundamentals to Biomimetic Materials and Processing Routes, Alvor, Portugal (2003) 99, poster

AL Oliveira, CM Alves, ME Gomes, PB Malafaya, RL Reis. Silicate gels as precursors of biomimetic mineralization on degradable scaffolds. NATO/ASI on Learning from Nature How to Design New Implantable Biomaterials: From Biomineralization Fundamentals to Biomimetic Materials and Processing Routes, Alvor, Portugal (2003) 31, oral presentation

OTHER PUBLICATIONS

Book front cover photograph: Biomedical Polymers. Ed: M. Jenkins. Woodhead Publishing Ltd, Cambridge which as resulted from the publication: VM Correlo, ME Gomes, K Tuzlakoglu, JM Oliveira, PB Malafaya, JF Mano, NM Neves, RL Reis. Tissue Engineering Using Natural Polymers. In: Biomedical Polymers. Ed: M. Jenkins. Woodhead Publishing Ltd Cambridge, UK (2007) 197-217

Book front cover figure (with help of João Pereira): Biodegradable Systems in Tissue Engineering and Regenerative Medicine, ed: RL Reis, J San Román. CRC Press, Boca Raton, USA which as resulted from the publication of: PB Malafaya, GA Silva, RL Reis. Strategies for delivering bone and cartilage regeneration factors. In: Biodegradable Systems in Tissue Engineering and Regenerative Medicine, ed: RL Reis, J San Román. CRC Press, Boca Raton, USA (2004) 253-280

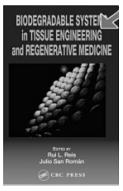

INTRODUCTION TO THE THESIS FORMAT

This present thesis is divided into four sections containing seven different chapters, with four of them being experimental research. According to the 3B's Research Group long-ago implemented philosophy, the thesis format is based on published or submitted papers, including the introduction section (a review paper). The contents of each chapter are summarized below.

SECTION I (Chapter I)

Chapter I is based on a review paper and presents a comprehensive overview on the natural-origin polymers that are being applied as carriers and scaffolds for biomolecules and cell delivery in tissue engineering applications. The described applications included mainly bone, cartilage and osteochondral defects, but other tissues/organs are also addressed. A review on the literature on the recently emerging strategies is discussed, revealing the importance of this key strategy as second generation scaffolds to achieve a successful tissue engineering approach. Furthermore, some examples of commercially available natural-origin polymers with applications in research or in clinical use in several applications are also presented.

SECTION 2 (Chapter II)

Chapter II presents in detail the materials and experimental procedures used to accomplish the proposed work plan. This chapter includes also some additional considerations in order to give a more clear vision to the reader of the selected options.

SECTION 3 (Chapter III to VI) consists in the different experimental studies.

Chapter III describes the development and characterization of chitosan-based scaffolds produced by particles aggregation which are the basis of this thesis. Preliminary work on one of the possible strategies to engineer an osteochondral defect is explored based in the separate cell seeding in separate scaffolds. For that, biphasic scaffolds and osteogenic and chondrogenic differentiation of human adipose stem cells are described.

Chapter IV is based on the optimization and extensive characterization of bilayered scaffolds produced by assembling polymeric and composite chitosan-based particles. A detailed morphometric characterization is presented using micro-computed tomography (μ-CT). This chapter describes also the approaches to overcome

an unexpected cytotoxic behaviour of composite scaffolds produced with unsintered hydroxylapatite. Furthermore, it presents a proof of concept of a double-chamber bioreactor specifically designed for osteochondral applications. This can be considered a second possible strategy for these applications.

Chapter V proposes the use of insulin-loaded scaffolds for chondrogenic differentiation, since insulin in considered to be a potential differentiation agent. The *in vitro* release studies of the developed systems and its effect on a pre-chondrogenic cell line are investigated. This strategy was followed as part of the ideal strategy for osteochondral applications, where the scaffold is able by itself to provide the adequate biochemical cues in order to promote the selective but simultaneous differentiation of both cartilage and bone tissues using the same cell source.

Chapter VI is focused in the assessment of the *in vivo* biofunctionality of polymeric chitosan scaffolds as one of the key requirements for biomaterials applications in tissue engineering. This chapter explores the effects of the scaffolds' properties on supporting the connective tissues ingrowth into the materials and on promoting the *in vivo* neo-vascularization. A morphometric and mechanical characterization of the scaffolds is also included.

SECTION 4 (Chapter VII)

Chapter VII contains the general conclusions regarding the overall work carried out under the scope of this thesis, as well as some final remarks and future directions.

As a final note to this introduction, the present thesis was also developed under the scope of the European Project HIPPOCRATES, on which the author is actively involved. HIPPOCRATES is a FP6 STREP (NMP3-CT-2003-505758) entitled 'A Hybrid Approach for Bone and Cartilage Tissue Engineering using Natural Origin Scaffolds, Progenitor Cells and Growth Factors'.

SECTION 1.

CHAPTER I.

Natural-origin polymers as carriers and scaffolds for biomolecules and cell delivery in tissue engineering applications

CHAPTER I.

Natural-origin polymers as carriers and scaffolds for biomolecules and cell delivery in tissue engineering applications *

ABSTRACT

The present paper intends to overview a wide range of natural-origin polymers with special focus on proteins and polysaccharides (the systems more inspired on the extracellular matrix) that are being used in research, or might be potentially useful as carriers systems for active biomolecules or as cell carriers with application in the tissue engineering field targeting several biological tissues. The combination of both applications into a single material has proven to be very challenging though. The paper presents also some examples of commercially available natural-origin polymers with applications in research or in clinical use in several applications. As it is recognized, this class of polymers is being widely used due to their similarities with the extracellular matrix, high chemical versatility, typically good biological performance and inherent cellular interaction and, also very significant, the cell or enzyme-controlled degradability. These biocharacteristics classify the natural–origin polymers as one of the most attractive options to be used in the tissue engineering field and drug delivery applications.

---

* This chapter is based in the following publication:

PB Malafaya[#], GA Silva[#], RL Reis. Natural-origin polymers as carriers and scaffolds for biomolecules and cell delivery in tissue engineering applications. Advanced Drug Delivery Reviews (2007) 59(4-5):207-233

[#] Equally contributing authors

---

1. GENERAL INTRODUCTION

Tissue engineering is the promising therapeutic approach that combines cells, biomaterials, and microenvironmental factors to induce differentiation signals into surgically transplantable formats and promote tissue repair and/or functional restoration. Despite many advances, tissue engineers still face significant challenges in repairing or replacing tissues that serve predominantly biomechanical functions such as articular cartilage. One obstacle can be identified as the scaffolds play an important role as the extracellular matrix but they are often unable to create the exact/correct microenvironment during the engineered tissue development to promote the accurate *in vitro* tissue development. The emerging and promising next generation of engineered tissues is relying on producing scaffolds with an informational function, e.g., material containing growth factors sequence which facilitates cell attachment, proliferation and differentiation that is far better than non-informational polymers. The use of growth factors has been considered as a way to manipulate not only the host healing response at the site of injury to facilitate the tissue repair, but also to manipulate and improve the *in vitro* tissue growth in order to produce more biofunctional engineered tissues. Hence, the strategy is to mimic matrix and provide the necessary information or signalling for cell attachment, proliferation and differentiation to meet the requirement of dynamic reciprocity for tissue engineering. This justifies the importance of drug delivery in tissue engineering applications.

Moreover, natural polymers perform a diverse set of functions in their native setting. For example, polysaccharides function in membranes and intracellular communication and also as storage, and proteins function as structural materials and catalysts [1]. The current trend is to mimic nature and what better way than materials from nature to do it? Natural biopolymers illustrate, as an impressive example, how all the properties displayed by biological materials and systems are exclusively determined by the physical-chemical properties of the monomers and their sequence. A well-defined molecular structure can lead to a rich complexity of structure and function on the mesoscale [2]. Here, competing interactions, structural flexibility and functional properties are tailored by the succession of monomeric units taken from a rather limited set. Because macromolecules bridge the span of nanometers up to micrometers by virtue of their length and flexibility, they enable a unique control of hierarchical organization and long-range interactions. Regardless of the tissue/organ involved, there are many concepts that can be extrapolated from nature and therefore applicable in the tissue engineering field to

repair/ regenerate the tissue/organ. In many cases, the matrices and scaffolds would ideally be made of biodegradable polymers whose properties closely resemble those of the extracellular matrix (ECM), a soft, tough, and elastomeric proteinaceous network that provides mechanical stability and structural integrity to tissues and organs [3].

If the constantly evolving knowledge on how our body works and the needs to achieve repair, there is the need to congregate into a sole construct both structural support and drug delivery properties. For the purpose of this review, cell encapsulation will be considered as a delivery system, as this is believed to be a promising therapeutic approach. Encapsulation physically isolates a cell mass from an outside environment and aims to maintain normal cellular physiology within a desired permeability barrier [4]. Encapsulation techniques are generally classified as microencapsulation (involving small spherical vehicles and conformal coated tissues) and macroencapsulation (involving larger flat-sheet and hollow-fiber membranes) [4]. The encapsulated cells can then be cultured *in vitro* or transplanted *in vivo*, either to repopulate a defect site or to produce growth factors or other molecules that will have an effect over the targeted cell population. Within the latter, cells have been transfected with genes of interest (including BMPs, among others) to make them true cellular factories to produce and deliver active growth factors.

2. PROTEIN-ORIGIN POLYMERS

2.1. INTRODUCTION

In this paper, the attention is focused in several protein-based polymers that found application in research works for drug or cell delivery within the tissue engineering field, namely collagen, gelatin, silk fibroin, fibrin (fibrinogen) and other proteins such elastin or soybean. These protein-based polymers and their applications in the field are described in more detail in the following sections.

Protein-based polymers have the advantage of mimicking many features of extracellular matrix and thus have the potential to direct the migration, growth and organization of cells during tissue regeneration and wound healing and for stabilization of encapsulated and transplanted cells. In a molecular perspective, proteins may be considered as polymer structures composed by 20 distinct amino acids

linked by amide (or peptide) bonds. Amino acids are therefore the building blocks of polypeptides and proteins, which consist of a central carbon linked to an amine group, a carboxyl group, a hydrogen atom, and a side chain (R groups). R groups can be classified as non-polar groups, uncharged polar groups or charged polar groups, and their distribution along the protein backbone renders proteins with distinct characteristics.

One of the drawbacks of the natural-origin polymers is their possible batch variation. One interesting strategy to overcome this issue is the recombinant protein technologies where the monodispersity and precisely defined properties of polymers as well as the predictable placement of crosslinking groups, binding moieties at specific sites along the polypeptide chain or their programmable degradation rates makes them very attractive and useful for drug delivery and tissue engineering [2]. One example is presented when describing the elastin like polypeptides. Our attempt to mimic nature to create materials is routinely accomplished with exceptional high yield and efficiency by the cellular systems of protein biosynthesis. Protein biosynthesis is implemented with an absolute control of the amino-acid sequence [2,5,6], from the first amino acid to the last, with complete absence of randomness. Additionally, the protein biosynthesis machinery is able to process and produce any amino-acid sequence stored in the elements of information called genes, so its flexibility is absolute. If one controls the information that genes deliver into the machinery, one completely controls the biosynthesis process itself. The key issue to retain is to use highly purified and defined polymers in order to have the perfect control over the developed final product.

2.2. COLLAGEN

Collagen is regarded by many as an ideal scaffold or matrix for tissue engineering as it is the major protein component of the extracellular matrix, providing support to connective tissues such as skin, tendons, bones, cartilage, blood vessels, and ligaments [7-11]. In its native environment, collagen interacts with cells in connective tissues and transduces essential signals for the regulation of cell anchorage, migration, proliferation, differentiation, and survival [12]. Twenty-seven types of collagens have been identified to date, but collagen type I is the most abundant and the most investigated for biomedical applications. The different collagens are first synthesized as large precursor molecules known as procollagens [13]. After secretion of procollagen into the extracellular matrix, both C-and N-

propeptides are cleaved and the molecules then self-assemble into fibrils (a detailed review can be found in [12]). Fibril-forming collagen molecules used in tissue engineering applications consist of three polypeptide chains of glycine-X-Y (Gly-X-Y) amino acid repeats twined around one another to form triple helices [14,15].

Collagen is defined by high mechanical strength, good biocompatibility, low antigenicity and ability of being crosslinked, and tailored for its mechanical, degradation and water-uptake properties. Collagen is mainly isolated from animal tissues, and an additional concern has been raised about the safety of the collagen derived from animal tissues, based on the potential for viral and prion contamination. However, purification techniques using enzymatic treatments may be employed to eliminate the immunogenic telopeptides, the major cause of foreign body response [16,17], as well as the development of recombinant and non-recombinant human collagens as a replacement for animal tissue-derived material. However, alternatives to animal origin collagens - those produced by recombinant technologies - still present a high cost. Additionally, collagen is hard to process and the extent and rate of degradability is hard to control. For the latter, several factors have an impact on degradability of collagen, for instance, the penetration of cells into the structure causes contraction, as well as the fact that, besides collagenase and gelatinase, several other non-specific proteinases are able to digest collagen [18]. Crosslinking is necessary in order to tailor the degradation of collagen and this has obviously to have into account the application, as fluid movement, pressure and nature of the tissue where the material is implanted contribute to a faster degradation rate. In addition to the difficulties in processability, the sterilization of collagen is also a problem, as nearly all sterilization methods incur some degree of alteration of collagen [18].

Collagen has been widely applied in tissue engineering applications and in some extent in delivery systems in this field. Table 1 intends to summarize some relevant applications reported as research works.

→

Table 1. Collagen-based matrices/scaffolds for drug, cell and gene delivery used in different tissue engineering applications.

POLYMER(S)/CARRIER/SCAFFOLD STRUCTURE	TE APPLICATION	ACTIVE BIOMOLECULE	ENCAPSULATED/SEEDED CELL TYPE (SOURCE)	ANIMAL MODEL	REFS
Collagen/hydroxylapatite	Bone	NGF	–	Calvaria defects	[19]
Collagen sponge	Cartilage	bFGF	Chondrocytes	Nude mice subcutaneous implantation	[20]
Collagen gel	Bone Cartilage	BMP-2	Bone marrow stromal cells	Mouse femoral muscle	[21]
Collagen gel	Skin	PDGF-A PDGF-B	–	Rabbit dermal ulcer Swine dermal wound	[22]
Collagen gel	Vascularization	VEGF	–	Chorioallantoic membrane	[23]
Collagen/heparin sulfate matrix	Vascularization	bFGF	–	Rat	[24]
Collagen gel with gelatin microspheres	Adipose	FGF-2	–	Mouse groin	[25]
Collagen-agarose beads	Not defined	–	Adults mesenchymal stem cells	–	[26]
Collagen sponge	Bone	–	Alveolar osteoblasts Gingival fibroblasts	Critical-size defect in mouse skull	[27]
Collagen electrospun nanofibers	Bone	–	Bone marrow-derived mesenchymal stem cells (adult)	–	[28]
Collagen sponge and hydrogel	Intervertebral disc	–	Human intervertebral disc cells	–	[29,30]
Collagen sponge	Tooth	–	Porcine third molar cells	Omentum of immunocompromised rats	[31]
Collagen sponge	Cartilage	–	Chondrocytes (autologous)	Sheep chondral defects	[32]
Collagen membrane	Cartilage	–	Chondrocytes	Medial femoral condyle of New Zealand rabbits	[33]
Collagen sponge	Adipose	–	Preadipocytes (human)	Nude mice subcutaneous implantation	[34]
Collagen-GAG scaffold	Cardiovascular	–	Bone marrow-derived mesenchymal stem cells	Rat myocardial infarction	[35]

Abbreviations: NGF: nerve growth factor; bFGF: basic fibroblast growth factor; BMP-2: bone morphogenetic protein-2; PDGF: platelet-derived growth factor; VEGF: vascular endothelial growth factor; FGF-2: fibroblast growth factor-2; GAG: glycosaminoglycans. Compiled from references [19-37].

Recently, a broad range of tissue engineering products based on animal-sourced collagen scaffolds have been developed and commercialized. For example, bilayered collagen gels seeded with human fibroblasts in the lower part and human keratinocytes in the upper layer have been used as the 'dermal' matrix of an artificial skin product are commercialized by Organogenesis in USA under the name of

Apligraf® and was the first bio-engineered skin to receive FDA approval in 1998. Organogenesis has other collagen-based products currently under development such as Revitix™ (topical cosmetic product), VCTO1™ (bilayered bio-engineered skin) or Forta-Derm™ Antimicrobial (anti-microbial wound dressing). inFUSE® Bone Graft are collagen sponges have been used as an osteoconductive carrier of bone morphogenetic protein (BMP-2) for spinal fusion marketed by Medtronic Sofamor Danek in USA. Collagen sponges have been use also for the treatment of long bone fractures [12]. Collagraft® commercialized by Angiotech Pharmaceuticals, Inc. in Canada is a mixture of porous hydroxylapatite and tricalcium phosphate and animal-derived collagen I, has been used clinically for the treatment of long bone fractures for more than a decade. Healos® Bone Graft Replacement marketed by DePuy Orthopaedics in USA is an osteoconductive matrix constructed of crosslinked collagen fibers that are fully coated with hydroxylapatite and has been approved recently for clinical use as a bone graft substitute in spinal fusions [12] and Biomend® is a collagen membrane conventionally used in the regeneration of periodontal tissue and is a registered trademark of Integra LifeSciences Corp. in USA [36].

2.3. GELATIN

Gelatin is a natural polymer that is derived from collagen, and is commonly used for pharmaceutical and medical applications because of its biodegradability and biocompatibility in physiological environments as reviewed by Tabata and Mikos [38,39]. These characteristics have contributed to gelatin's safety as a component in drug formulations or as a sealant for vascular prostheses [40]. Moreover, gelatin has relatively low antigenicity because of being denatured in contrast to collagen which is known to have antigenicity due to its animal origin. Gelatin contains a large number of glycine, proline and 4-hydroxyproline residues.

Gelatin is a denatured protein obtained by acid and alkaline processing of collagen. As a result, two different types of gelatin can be produced depending on the method in which collagen is pre-treated, prior to the extraction process [40]. This pre-treatment affects also the electrical nature of collagen, producing gelatin with different isoelectric points. The alkaline process targets the amide groups of asparagine and glutamine and hydrolyses them into carboxyl groups, thus converting many of these residues to aspartate and glutamate. In contrast, acidic pre-treatment does little to affect the amide

groups present. The result is that gelatin processed with an alkaline pre-treatment is electrically different from acidic-processed gelatin. This is due to hydrolysis of amide groups of collagen yields gelatin with a higher density of carboxyl groups present in the alkaline processed gelatin rendering it negatively charge and lowering its isoelectric point [38]. In contrast, the electrostatic nature of collagen is hardly modified through the acid process because of a less invasive reaction to amide groups of collagen. As a result, the isoelectric point of gelatin that is obtained with the acid process will remain similar to that of collagen [39]. By utilizing this technique, manufacturers now offer gelatin in a variety of isoelectric point values, being the most used the basic gelatin with an isoelectric point of 9.0 and the acidic gelatin with an isoelectric point of 5.0.

It is well accepted that a positively or negatively charged polyelectrolyte electrostatically interacts with an oppositely charged molecule to form a polyion complex [38]. The different processing conditions of gelatin allows for flexibility in terms of enabling polyion complexation of a gelatin carrier with either positively or negatively charged biomolecules. It is theoretically possible for gelatin to form polyion complexes with any type of charged biomolecules, although the strength of the interaction depends on the type of biomolecules used. If the biomolecule to be released is acidic, basic gelatin with an isoelectric point of 9.0 is preferable as a matrix, while acidic gelatin with an isoelectric point of 5.0 should be applicable to the control release of a basic protein. Both gelatins are insoluble in water to prepare a hydrogel through chemical crosslinking, for instance, with water-soluble carbodiimides and glutaraldehyde [39].

The gelatin hydrogels forming polyion complexes with proteins will facilitate the release of biologically active proteins. Generally, the release is controlled by matrix degradation [39] and therefore the time period for biomolecule release can be regulated by tailoring the hydrogel degradation. The biodegradable hydrogel matrices are prepared by chemical crosslinking of acidic or basic gelatin and are enzymatically degraded in the body with time. The degradation is controllable by changing the extent of crosslinking, which, in turn, produces hydrogels with different water contents [41]. In addition, as already referred, depending on the manufacturing method, variations in the electrical and physical properties of gelatin-based systems can be achieved. It is this flexibility in processing that has allowed gelatin-based systems to find several applications in fields ranging from tissue engineering to drug delivery and gene therapy.

The properties of gelatin as a typical rigid-chain high molecular weight compound are in many issues analogous to those of rigid-chain synthetic polymers [42]. Gelatin exhibits essentially the same common properties typical of polymeric substances, which is not the case with native collagen. Thus, in a similar way to linear-chain synthetic polymers, in aqueous solutions gelatin macromolecules assume, at elevated temperatures, the conformation of a statistical coil [42]. Under specific conditions, such as temperature, solvent or pH, gelatin macromolecules present sufficient flexibility to realize a variety of conformations. This makes it possible to vary also all the gelatin characteristics dependent on its molecular structure. Besides, gelatin, similar to synthetic high polymers, shows a rather wide molecular weight distribution [42]. Structural diversity of gelatin chain units determines the specific features of gelatin properties. Most synthetic polymers show no such features that are typical of most biopolymers, such as the presence of both acidic and basic functional groups in the gelatin macromolecules. Due to its promising properties, safety and mainly to the possibility of polyion complexation, gelatin is been used in drug delivery for tissue engineering applications targeting several tissues as we try to summarize in Table 2. Targeted tissues include bone, cartilage and skin, but others such as adipose tissue have applied gelatin as carrier to delivery an active biomolecule to improve the temporary cell functions. Due to its easy processability and gelation properties, gelatin as been manufactured in a range of shapes including sponges and injectable hydrogels, but definitively the most used carriers are gelatin microspheres which normally are incorporated in a second scaffold such as a hydrogel.

One of the most common strategies using gelatin microspheres is the encapsulation of biomolecules or cells in the microspheres with further incorporation of those in a second matrix. The group of Mikos [44-47,54,55] together with Tabata vast work with gelatin [49,50,53] has been commonly using this strategy to incorporate a single biomolecule such as TGF-β1 [44,45], or in combination with IGF-1 for dual release [46] as well as the encapsulation of marrow stromal osteoblasts in the surface of the gelatin microspheres [54,55]. The results from these studies show the efficacy and safety of using gelatin based microspheres as carriers for tissue engineering applications. Besides the incorporation of growth factors and cells, the incorporation of cell adhesion proteins and peptides is also a strategy to be implemented to achieve a successful tissue engineering approach. Ito *et al.* [51] present a biodegradable gelatin hydrogels prepared through crosslinking of gelatin with transglutaminase (TGase) with fibronectin, vitronectin and RGD peptides (RGDLLQ and RGDLLG) incorporated to be applied as artificial skin or for bone and cartilage tissue engineering. NIH/3T3 fibroblasts were then added into the aqueous solution of gelatin to be part of the construct. Vitronectin and fibronectin can bind with gelatin

by the action of TGase and as a cell adhesion factors it is expected to increase the cell growth. In fact, this study has shown that the gelatin matrices incorporating the cell adhesion factors such as vitronectin, fibronectin and RGD peptides by the action of TGase enhanced cell proliferation.

Using gelatin carriers for cell delivery as shown to be also a promising technology for tissue engineering applications. Several examples include bovine and human chondrocytes [47,56], mesenchymal stem cells [57,58] and human preadipocytes [53] as described in Table 2. The strategies range the co-implantation of loaded microspheres [53] to the incorporation of the cells into porous scaffolds [57] and, in general, the *in vivo* results shown the higher efficiency of using gelatin carriers-based technology.

There are several commercially available gelatin based carriers for drug delivery that are being applied in tissue engineering applications [48,56,57]. The most commonly used ones are Gelfoam® commercialized now by Pfizer in USA (former Pharmacia and Upjohn) which is an absorbable gelatin sponge being also available in the powder form by milling the gelatin sponges. Gelfoam® is a sterile and workable surgical sponge prepared from specially treated and purified gelatin solution and it is used as a hemostatic device. Pfizer has also a commercially available Gelfilm® that is an absorbable gelatin film designed for use as an absorbable gelatin implant in neurosurgery and thoracic and ocular surgery. Surgifoam® is another commercially available porous, absorbable gelatin disks. This product is distributed by Ethicon Inc. in USA. CultiSpher-G® is another gelatin based product marketed by Percell Biolytica AB in Sweden which is a macroporous gelatin microcarrier beads used as microcarrier cell culture. CultiSpher-S® is the same product with a different crosslinking procedure conferring a higher thermal and mechanical stability.

→

Table 2. Gelatin-based matrices/scaffolds for drug and cell delivery used in different tissue engineering applications.

POLYMER(S)/CARRIER/ SCAFFOLD STRUCTURE	TE APPLICATION	ACTIVE BIOMOLECULE	ENCAPSULATED/ SEEDED CELL TYPE (SOURCE)	ANIMAL MODEL	REFS
Gelatin (hydrogel)	Bone	bFGF	–	Nude mice subcutaneous implantation	[38]
Gelatin-siloxane (porous freeze-dried scaffolds)	Bone	Gentamicin sulfate	Osteoblast-like MC3T3-E1 cell line	–	[43]
Gelatin microspheres encapsulated in a hydrogel injectable matrix	Cartilage	TGF-β1	–	–	[44,45]
Gelatin microspheres encapsulated in a hydrogel injectable matrix	Cartilage	TGF-β1 IGF-I	–	–	[46]
Gelatin microspheres encapsulated in a hydrogel injectable matrix	Cartilage	TGF-β1	Bovine chondrocytes	–	[47]
Porous gelatin disks (Surgifoam®)	Cartilage	TGF-β1 (medium)	Human adipose-derived adult stem cells	–	[48]
Gelatin sponge	Bone Cartilage	BMP-2	–	Tracheal cartilage rings in canine cervix	[49,50]
Transglutaminase crosslinked gelatin (hydrogel)	Bone Cartilage Artificial skin	Vitronectin Fibronectin RGD peptides	Fibroblasts-like NIH/3T3 cell line	–	[51]
Gelatin microspheres incorporated in collagen gel	Adipose	FGF-2	–	Tissue engineering chambers in mouse groins	[25]
Photocured styrenated gelatin microspheres	Adipose	bFGF insulin IGF-I	–	Nude mice subcutaneous implantation	[52]
Gelatin microspheres incorporated in a collagen sponge	Adipose	bFGF	Human preadipocytes	Nude mice subcutaneous implantation	[53]
Gelatin microspheres encapsulated in an hydrogel matrix	Bone	–	Rat marrow stromal osteoblasts	–	[54,55]
Macroporous gelatin microcarriers beads (CultiSpher G®)	Cartilage	–	Human nasal chondrocytes	Nude mice subcutaneous implantation	[56]
Porous gelatin sponge (Gelfoam®)	Cartilage	–	Adult human mesenchymal stem cells	Osteochondral defect in the rabbit femoral condyle	[57]
Gelatin and chemically modified hyaluronic acid injectable hydrogel	Osteochondral	–	Rabbit bone marrow-derived mesenchymal stem cells	Rabbit osteochondral knee joint	[58]

Abbreviations: bFGF: basic fibroblast growth factor; TGF-β1: transforming growth factor-β1; BMP-2: bone morphogenetic protein-2; RGD: Arg-Gly-Asp peptides; FGF-2: fibroblast growth factor-2; IGF-I: insulin growth factor-1. Compiled from references [25,38,43-58].

2.4. SILK FIBROIN

Silk is generally defined as protein polymers that are spun into fibers by some *lepidoptera* larvae such as silkworms, spiders, scorpions, mites and flies [59]. Spider silk is an intriguing biomaterial that is lightweight, extremely strong and elastic, and exhibits mechanical properties comparable to the best synthetic fibers produced by modern technology [60]. Spider silk is spun near ambient temperatures and pressures using water as the solvent, which gives rise to an environmentally safe, biodegradable material [60]. However, it is not possible to maintain domesticated spiders to produce massive amounts of silk. Therefore, the attention was turned to silk fibroin, a mass-producible natural polymer produced by silk-worms, commonly used as a textile fiber. In the medical field, silk has long been used for surgical sutures [61].

The silkworm *Bombyx mori* produces silk to weave its cocoon, and its major components are fibroin and sericin. Fibroin is a fibrous protein constituting the core of silk, while sericin is a glue-like protein surrounding fibroin. Fibroin is composed of fibroin H-chain (FH), fibroin L-chain (FL), and fibrohexamerin at a molar rate of 6:6:1 [62]. Silks are attractive biomaterials for tissue engineering, because of their biocompatibility [59,63], slow degradability [64] and excellent mechanical properties. Some examples are shown in Table 3.

Table 3. Silk fibroin-based matrices/scaffolds for drug and cell delivery used in different tissue engineering applications.

POLYMER(S)/CARRIER/ SCAFFOLD STRUCTURE	TE APPLICATION	ACTIVE BIOMOLECULE	ENCAPSULATED/SEEDED CELL TYPE (SOURCE)	ANIMAL MODEL	REFS
Silk fibroin fibre scaffolds	Bone	BMP-2	Bone marrow-derived mesenchymal stem cells	–	[67]
Silk fibroin hydrogel	Bone	–	Osteoblasts	Rabbit distal femurs	[68]
Silk fibroin non-woven net	Angiogenesis	–	Endothelial cells	–	[69,70]
Silk fibroin porous scaffolds	Cartilage	–	Mesenchymal stem cells	–	[71]
Silk fibroin electrospun fiber scaffolds	Wound dressing	–	Keratinocytes and fibroblasts	–	[72]
Silk fibroin/collagen scaffolds	Liver	–	Hepatocytes	–	[73]
Silk fibroin multi-fiber matrix	Anterior crucial ligament	–	Bone marrow-derived mesenchymal	–	[74]

Abbreviations: BMP-2: bone morphogenetic protein-2. Compiled from references [67-74].

Degradable silk is a mechanically robust biomaterial that offers a wide range of mechanical and functional properties for biomedical applications including drug delivery [65,66]. Besides the applications that can be found in Table 3, a very interesting approach is the one described by Hino and co-workers [75] where the authors aimed to prepare a novel type of bFGF delivery system using fibroin as a scaffold. They generated transgenic silkworms that bore a gene encoding FL fused with bFGF (FL/bFGF). The transgenic silkworms spun cocoons whose fibroin layers were composed of both inherent gene-derived natural fibroin (nF) and the recombinant FL/bFGF, r(FL/bFGF). When human umbilical vein endothelial cells (HUVECs) were seeded in the scaffold, they were able to grow in the refolded r(FL/bFGF)nF-containing culture media, showing that bFGF in r(FL/bFGF) was biologically active [75]. r(FL/ bFGF)nF immobilized on a culture dish also supported the growth of HUVECs in bFGF-free media, suggesting the usefulness of r(FL/bFGF)nF as a new biomaterial for tissue engineering [75].

2.5. FIBRIN

Fibrin and fibrinogen have a well-established application in research in tissue engineering due to their innate ability to induce improved cellular interaction and subsequent scaffold remodelling compared to synthetic scaffolds. Furthermore, due to its biochemical characteristics, mainly in cellular interactions, fibrin-based materials also found applications in the field of drug delivery with special focus in cell delivery.

Fibrin is a protein matrix produced from fibrinogen, which can be autologously harvested from the patient [76], providing an immunocompatible carrier for delivery of active biomolecules, specially cells. Polymerized fibrin is a major component of blood clots and plays a vital role in the subsequent wound healing response [77]. *In vivo*, formation of fibrin clots is initiated by vascular injury, which causes the release of the enzyme thrombin, a serine protease that activates many constituents of the coagulation cascade [78]. Thrombin cleaves peptide fragments from the soluble plasma protein fibrinogen, yielding insoluble fibrin peptides that aggregate to form fibrils [79]. A fibrin meshwork is formed, which entraps platelets and other blood-borne components to create a clot that is stabilized through crosslinking by the transglutaminase Factor XIII [79,80]. In addition, fibrin naturally contains sites for cell binding, and

therefore has been investigated as a substrate for cell adhesion, spreading, migration and proliferation [81].

Fibrin glue is a biological adhesives also used in surgery (abdominal, thoracic, vascular, oral, endoscopic) due to its haemostatic, chemotactic and mitogenic properties [82]. Fibrin glue mimics the last step of the *in vivo* coagulation cascade through activation of fibrinogen by thrombin, resulting in a clot of fibrin with adhesive properties [83]. Fibrinogen is converted into a monomeric form of fibrin by thrombin which forms the fibrin clot. Mechanisms of fibrin production and clot assembly have been elucidated primarily from studies in which a specific amount of thrombin is added to purified fibrinogen as clearly described in [79]. The concentration of fibrinogen is 20–40 times higher in fibrin sealant products than in body fluid. The formation of the fibrin clot and the physiological properties are then enhanced. This concentration also determines the properties of the fibrin clot (adhesive strength, rate of formation, network conformation, permeability and fiber diameter) and modifications to concentrations can be made to allow the fibrin glue to fit the application [82].

A number of variables other than the concentration of thrombin and fibrinogen can also influence the structure of a fibrin gel, including the local pH, ionic strength, and concentrations of calcium [79]. The relative influence of fibrinogen and thrombin concentration in the final gel structure and properties when comparing with each other is still not clear. There are works showing that fibrinogen concentration is more critical to the final properties [84,85] as well as works showing that thrombin concentrations lead to more modifications in the structure of the clot than modifications to fibrinogen concentrations [78,83]. Extremely low concentrations of thrombin (<1 nM, <0.1 U/mL) are sufficient to cleave fibrino-peptides and catalyze fibrin polymerization [79]. These low thrombin concentrations produce fibrin clots that are turbid and composed of thick, loosely-woven fibrin strands. Higher concentrations of thrombin produce fibrin clots that are composed of relatively thinner, more tightly-packed fibrin strands.

There are a several works trying to stabilizing and modulate the properties of the fibrin gels with thrombin in order to get more stable gels [78,79]. However, this important fibrin characteristic of increasing instability and solubility over time *in vitro* and *in vivo* is due to fibrinolysis which could be an advantage for in wound sealing or other surgical applications as well as for cell and growth factor delivery. Fibrin provides a material that can be rapidly invaded, remodelled and replaced by cell-associated proteolytic activity [80]. Moreover, due to its biomimetic and physical properties it is also

widely used as a cell carrier to many cell types, such as keratinocytes [86], urothelium cells [86], tracheal epithelial cells [86], murine embryonic stem cells [87] mesenchymal progenitor cells [88] and also very used to encapsulate chondrocytes for cartilage tissue engineering [89-91]. But rapid degradation can represent a problem for use as a shape-specific scaffold in tissue engineering, therefore optimizing fibrin composition is a fundamental approach to obtain a scaffold system providing optimal shape stability and integrity for specific applications in tissue engineering. In spite of this factor, fibrin as a carrier of active biomolecules and particularly as support for cell delivery as been applied to the tissue engineering field as presented in Table 4. The table summarizes the polymer and carriers shape used in the system, the aimed tissue engineering application, the biologically active biomolecule to be delivered, the source of the cells used to test the developed systems *in vitro* or the cell type incorporated in the system in the last part of the table. When applicable the used animal model is also referred. One interesting work is presented by Aper *et al.* [76] where autologous blood vessels are engineered from peripheral blood sample. The objective is the development of a bioartificial vascular graft by means of an autologous scaffold material seeded with endothelial progenitor cells separated from the peripheral blood of a single donor. With regard to a later clinical application, the scaffold material should be generated easily without the need for surgical procedure to harvest it from the body of the later recipient [76].

Fibrinogen and thrombin from different sources including human are commercially available in the usual chemical sup-pliers and normally are used to produce the fibrin gel in research works. Nevertheless, there is an already available industrially produced homologous fibrin sealant. The most used one is Tisseel VH® commercialized by Baxter, USA and consists of a two-component fibrin biomatrix with highly concentrated human fibrinogen. Moreover, it is possible also to produce fibrin gel from a blood sample [76]. There are several commercially available devices that allow for this. An example is the CryoSeal® Fibrin Sealant System manufactured by Thermogenesis in USA which enables the production of autologous fibrin sealant components from a single unit of a patient's blood plasma in about 60 min. Another example is Vivostat® System commercialized by Vivolution, Denmark which is an automated system for the on-site preparation and application of patient-derived fibrin sealant or platelet-rich fibrin. There is a published study [106] which compares the properties in different aspects concluding that there are clear differences between the commercially available ways to obtain fibrin gel.

Table 4. Fibrin-based matrices/scaffolds for drug and cell delivery described for different tissue engineering applications.

POLYMER(S)/CARRIER/ SCAFFOLD STRUCTURE	TE APPLICATION	ACTIVE BIOMOLECULE	ENCAPSULATED/ SEEDED CELL TYPE (SOURCE)	ANIMAL MODEL	REFS
Fibrin films	Not defined	FGF-2 (patterning)	MG63 cell line	–	[92]
Fibrin gel (Tisseel®)-plotted PCL/TCP	Bone	rhBMP-2	Human osteoblasts	–	[93]
Fibrin gel	Bone	ngl BMP-2	–	Rat calvarium and dog inter-carpal fusion	[80]
Fibrin gel containing heparin-nanospheres	Vascularization	bFGF	Human umbilical vein endothelial cells	Mouse limb ischemia	[94,95]
Fibrin gel	Vascularization	VEGF variants	Human umbilical vein endothelial cells	–	[81]
Fibrin gel	Skin Cardiovascular	TGF-β1, insulin and plasmin (medium)	Human foreskin fibroblasts cell line	–	[77]
Fibrin gel and beads	Spinal cord injury	NT-3	Chick dorsal root ganglia cell culture	Rat suction ablation spinal cord injury	[96,97]
Fibrin gel	Nerve regeneration	bFGF, VEGF, β-NGF, NT-3	Chick dorsal root ganglia cell culture	Rat sciatic nerve defect	[98-100]
Fibrin gel	Intervertebral disc	–	Human intervertebral disc cells	–	[30]
Fibrin-collagen gel	Cartilage	–	Embryonic chondrogenic cells	–	[91]
Fibrin gel	Cartilage	–	Bovine articular chondrocytes	–	[89,90,101]
Fibrin gel in a PGA non-woven mesh	Cartilage	–	Pig chondrocytes	–	[102]
Porous fibrin gel	Cartilage	–	Human articular chondrocytes	–	[103]
Fibrin glue (Tisseel®) - plotted PCL	Osteochondral	–	Rabbit bone marrow mesenchymal cells	Rabbit medial femoral condyle	[104]
Fibrin scaffold	Spinal cord injury	–	Murine embryonic stem cells	–	[87]
Fibrin tubes (autologous)	Vascularization	–	Outgrowth endothelial cells	–	[76]
Fibrin gel	Vascularization	–	Rat aortic smooth muscle cells	–	[78]
Fibrin gel in a fiber-based scaffold	Cardiovascular	–	Human venous myofibroblasts	–	[105]

Abbreviations: FGF-2: fibroblast growth factor-2; bFGF: basic fibroblast growth factor; NT-3: neurotrophin-3; NGF: nerve growth factor; β-NGF: beta-nerve growth factor; VEGF: vascular endothelial growth factor; PCL: polycaprolactone; TCP: tricalcium phosphate; rhBMP-2: recombinant bone morphogenetic protein-2; nglBMP-2: non-glycosylated form of bone morphogenetic protein-2; PGA: polyglycolic acid; TGF-β1: transforming growth factor-beta 1. Compiled from references [30,76-78,80,81,87,89-105].

2.6. OTHER PROTEIN-BASED POLYMERS

There are other very interesting and attractive protein-origin polymers namely elastin and soybean that have been applied in some extent in the tissue engineering applications. We have decided to include them just as a general overview due to the limited application as drug delivery carriers or cell carriers in the tissue engineering field but justifying their use in tissue engineering.

Elastin is the dominant extracellular matrix protein deposited in the arterial wall and can contribute up to 50% of its dry weight. The protein product of the elastin gene is synthesized by vascular smooth muscle cells and secreted as a tropoelastin monomer that is soluble, non-glycosylated and highly hydrophobic [107]. Elastin is the responsible component conferring elasticity, preventing dynamic tissue creep by stretching under load and recoiling to their original configurations after the load is released. In addition to the mechanical responsiveness, elastin is a potent autocrine regulator of vascular smooth muscle cells activity and this regulation is important for preventing fibrocellular pathology [6]. Given elastin importance in governing the mechanical properties of native vessels and their role in vascular smooth muscle cells activity, the development of processable elastin-based biomaterials could advance the design of biofunctional blood vessel replacements, in vascular tissue engineering (where the main application is found) or achieving vascularization in bone regeneration. Such elastin-based biomaterials may not need to initially resemble the precise structural organization of native elastin, but could serve as templates for cellular remodeling and reorganization, being a critical issue in the referred applications as reviewed by Patel *et al*. [6]. Nevertheless, the development of elastin-based biomaterials is still an exploitable area for other application rather than vascular tissue engineering.

Examples of applications in this field are proposed by Buttafoco *et al*. [108] where the addition of polyethylene oxide and sodium chloride was necessary to spin continuous and homogeneous elastin fibers by an electrospinning method. The formation of a confluent multi-layer of smooth muscle cells, growing on top of each nanofiber meshes was observed by means of histology [108]. Other application is proposed by Lu *et al*. [107] the attempt to create porous structures for cell repopulation removing selectively matrix components from decellularized porcine aorta to obtain two types of scaffolds, namely elastin and collagen scaffolds. Fibroblasts were used for cell culture and they infiltrated about 120 μm into elastin scaffolds and about 40 μm into collagen scaffolds after 4 weeks of rotary cell culture. These results indicated that the developed novel aortic elastin matrices have the potential to serve as scaffolds for cardiovascular tissue engineering. Moreover, Leach *et al*. [109] propose a simple synthesis technique for creating elastin-based biomaterials. They present a versatile system of two commercially

available and water-soluble components: α-elastin (a well-characterized elastin digest) and ethylene glycol diglycidylether (a diepoxy crosslinker) to develop a pH-dependent crosslinking scheme to yield insoluble α-elastin biomaterials. Studies of vascular smooth muscle cells attachment and proliferation were used to confirm the predicted cell response to α-elastin substrates [109]. The results suggest that crosslinked α-elastin could provide a platform for complex composite materials with both mechanical and bioactive properties that closely mimic native vascular tissue.

Recombinant protein technologies have allowed the synthesis of well-defined elastin-derived polypeptides (ELPs), which have driven insightful structure-function studies of tropoelastin (the soluble precursor of crosslinked elastin) and have gained more attention. ELPs are artificial biopolymers composed of the pentapeptide repeat Val-Pro-Gly-Xaa-Gly (VPGXG), which is derived from the hydrophobic domain of tropoelastin. At low temperatures, ELPs are soluble in aqueous solution, but as the solution temperature is raised, they become insoluble and aggregate at a critical temperature, termed the 'inverse transition temperature' (T_t), a phenomenon similar to the lower critical solution temperature transition [5]. This process is typically reversible so that subsequent cooling of the solution below the T_t results in the re-solubilization of the ELP. This transition has become the key issue in the development of new peptide-based polymers as molecular machines and materials. The basic structure of ELPs is a repeating sequence originating in the repeating sequences found in the mammalian elastic protein, elastin [2]. Some of their main characteristics of these ELPs are derived from the natural protein they are based on. For example, the crosslinked matrices of these polymers retain most of the striking mechanical properties of elastin, i.e. almost ideal elasticity with Young's modulus, elongation at break, etc. in the range of the natural elastin and outstanding resistance to fatigue [5]. ELPs have found application in the drug delivery field due to the ability to synthesize them with a precise molecular weight and low poly-dispersity, their potential biocompatibility and controlled degradation.

In the tissue engineering field, the biodegradation and bio-compatibility of ELPs are suitable for preparing bulk implants and/or injectables. These implants can hold cells, providing a substrate for tissue engineering. In one approach, Betre *et al.* [110] investigated the potential of a genetically engineered ELPs to promote the chondrocytic differentiation of human adipose derived adult stem cells without exogenous chondro-genic supplements. The results demonstrate that ELPs can provide the appropriate physical and biochemical environment to maintain chondrocyte differentiation and support cartilage matrix synthesis *in vitro* and suggest the potential utility of ELPs to serve as a scaffold for

cartilage repair. Moreover, the study suggests that ELPs can promote chondrogenesis for human adipose derived adult stem cells in the absence of exogenous TGF-β1 and dexamethasone, especially under low oxygen tension conditions [110]. Finally the potential of ELPs to self-assemble into nanostructures in response to environmental cues, a nascent area of research, will lead to a host of new applications of these recombinant polymers.

Soybean, from the most cultivated plant in the world, is rich in proteins (40–50%), lipids (20–30%) and carbohydrates (26–30%), and consequently the subject of extensive scientific research [111]. The soybean (USA and UK) or soya bean (UK) (from an annual plant, *Glycine Max L. Merrill* [112]) is a species of legume native that can be processed into three kinds of protein-rich products; soy flour, soy concentrate, and soy isolate which varies in protein content. Isolated soy protein (highly refined or purified form), the most concentrated source of soy protein by definition contains 90% protein on a dry weight basis, followed by soy concentrate (soybean without the water-soluble carbohydrates) at 70% protein and soy flour (made by grinding soybeans into a fine powder) at 50% protein on a dry weight basis. The major soy proteins (greater than 85%) are glycinin, or 11S, and β-conglycinin, or 7S, which represent 34% and 27%, respectively, of the proteins occurring in the isolate [111,113]. Soy protein is abundant, renewable, inexpensive and biodegradable, making it an attractive source of degradable materials for tissue engineering uses. Nevertheless, the application of soy-based polymers in this field is still very narrow, especially if one considers application for growth factor or cell delivery. The main field of soy application is by far the food industry and more recently as environment-friendly biodegradable 'green' alternatives for biolpolymers and composites for use in various applications including computer casings and electronic chip packaging [112]. However, soy is also expected to present a tailorable degradation profile [114] varying with the crosslinking degree which constitutes an advantage for drug delivery systems design. Furthermore to improve soy properties (namely mechanical, degradation, solubility and hydrophilicity) it is common to mix with other polymers such as dextran [115,116], chitosan [117], gelatin [118], carrageenan [119], and starch [116,120]. The use of soy-based polymers for drug delivery and tissue engineering applications is proposed by the group of Reis *et al.* [117,121-123] where soy-based thermoplastics and membranes are described and characterized as biomaterials and carriers for drug delivery applications.

3. POLYSACCHARIDIC POLYMERS

3.1. INTRODUCTION

Polysaccharides are a class of biopolymers constituted by simple sugar monomers [124]. The monomers (monosaccharides) are linked together by *O*-glycosidic bonds that can be made to any of the hydroxyl groups of a monosaccharide, conferring polysaccharides the ability to form both linear and branched polymers. Differences in the monosaccharide com-position, chain shapes and molecular weight dictate their physical properties including solubility, gelation and surface properties. These biological polymers can be obtained from different sources: microbial, animal and vegetal [125]. Several advantages can be derived from the use of these macromolecules. First of all, probably because of the chemical similarities with heparin, polysaccharides show good hemocompatibility properties. They are non-toxic, show interaction with living cells and, with few exceptions, have low costs in comparison with others biopolymers such as collagen [125,126]. These polysaccharidic polymers have been widely proposed as scaffold materials in tissue engineering applications as well as carriers for drug delivery systems as described in more detail in the following sections.

3.2. CHITOSAN

Chitosan is a cationic polymer obtained from chitin com-prising copolymers of β(1→4)-glucosamine and *N*-acetyl-D-glucosamine. Chitin is a natural polysaccharide found particularly in the shell of crustacean, cuticles of insects and cell walls of fungi and is the second most abundant polymerized carbon found in nature. Chitosan, the fully or partially deacetylated form of chitin, due to its properties as attracted much attention in the tissue engineering and drug delivery fields with a wide variety of applications ranging from skin, bone, cartilage and vascular grafts to substrates for mammalian cell culture. It has been proved to be biologically renewable, biodegradable, biocompatible, non-antigenic, non-toxic and biofunctional [127].

The term chitosan is used to describe a series of polymers of different degrees of deacetylation defined in terms of the percentage of primary amino groups in the polymer backbone and average molecular weights. The degree of deacetylation of typical commercial chitosan is usually between 70% and 95%,

and the molecular weight between 10 and 1000 kDa [128]. The properties, biodegradability and biological role of chitosan are dependent on the relative proportions of *N*-acetyl-D-glucosamine and D-glucosamine residues [129]. In preparing chitosan, ground shells are deproteinated and demineralized by sequential treatment with alkali and acid, after which the extracted chitin is deacetylated to chitosan by alkaline hydrolysis at high temperature. Production of chitosan from these sources is inexpensive, easy and can provide additional control over chitosan final properties. In addition, chitosan molecule has amino and hydroxyl groups which can be modified chemically providing a high chemical versatility and is metabolized by certain human enzymes, especially lysozyme being considered biodegradable.

Chitosan is also a bioadhesive material. The adhesive properties of chitosan in a swollen state have been shown to persist well during repeated contacts of chitosan and the substrate [128] which implies that, in addition to the adhesion by hydration, many other mechanisms, such as hydrogen bonding and ionic interactions might also have be involved. Moreover, chitosan exhibits a pH-sensitive behavior as a weak poly-base due to the large quantities of amino groups on its chain. Chitosan dissolves easily at low pH while it is insoluble at higher pH ranges. The mechanism of pH-sensitive swelling involves the protonation of amine groups of chitosan under low pH conditions. This property has held chitosan to be widely investigated as a delivery matrix. Crosslinking is often used to tailor chitosan-based materials properties. The most common crosslinkers used to crosslink chitosan are dialdehydes such as glyoxal [130] and glutaraldehyde [131]. The aldehyde groups form covalent imine bonds with the amino groups of chitosan due to the resonance established with adjacent double ethylinic bonds via a Schiff reaction [128]. Dialdehydes allow the crosslinking to happen by direct reaction in aqueous media and under mild conditions. Moreover, dihaldehydes such as glutaraldehyde stabilize the collagen structure, prevent tissue digestion by enzymes or bacteria and reduce the antigenicity of the material [132]. It also adds to retaining the biocompatibility of the polymer. Natural crosslinkers like genipin [133] are gaining wide acceptance for crosslinking chitosan.

Porous chitosan matrix may be suggested as a potential candidate as a bone regenerative material due to its proper biological and physical properties. Biological activity of chitosan on bone regeneration has been demonstrated in many reports [134,135]. However, chitosan has some limitations in inducing rapid bone regeneration at initial stages. Bone formation after implanting these matrices occurs over a long period (several months or years) [127]. Additional functions for chitosan materials are necessary to shorten bone forming period and improve their efficacy. Incorporation of active biomolecules such as

growth factors has been used as a strategy which is highly beneficial for obtaining improved bone regeneration.

Concerning cartilage engineering, chitosan is structurally similar to glycosaminoglycans (GAGs) found in extracellular matrices as in native articular cartilage and are very important in playing a key role in modulating chondrocytes morphology, differentiation and function. This characteristic together with the ones previously described makes chitosan also an attractive natural-origin polymer to engineered cartilage. In addition, chitosan was found to enhance blood coagulation [136] accelerating wound healing [137,138], thus it can act as an ideal wound dressing as it exhibits a positive charge, film-forming capacity, mild gelation characteristics and a strong tissue-adhesive property. Research work indicates that chitosan enhances the functions of inflammatory cells such as polymorphonuclear leukocytes, macrophages and fibroblasts promoting granulation and organization [136]. Therefore, chitosan can be used for large open wounds [139]. A study showed that chitosan-treated wounds were epithelized when compared with wounds of the control group after the treatment [137,139]. Table 5 intends to summarize some relevant application of chitosan-based materials in the tissue engineering field and drug delivery aiming several tissues. The incorporation of a wide range of bioactive molecule highlights the potential of this natural origin to these applications, including gene delivery.

Some commercially available formats of chitosan include the geniaBeads® CN commercialize by Genialab in Germany which are hydrogel beads made from chitosan. Due to chitosan properties in wound healing, a commercially available product is HemCon® bandage from HemCon Medical Technologies Inc. in USA which is a chitosan bandage. This bandage can be applied with pressure to a severe external wound and in several minutes attracts blood cells (negatively charged surface) that merge with chitosan forming a blood clot. The bleeding stops and the bandage adhere tightly to the wound, so the person can be moved without more bleeding. Chitosan has also been marketed throughout the world as a component in non-medical products, as a fat binder in cholesterol-lowering and slimming formulations. It has been claimed that chitosan entraps lipids in the intestine due to its cationic nature.

Table 5. Chitosan-based matrices/scaffolds for drug, cell and gene delivery described for different tissue engineering applications.

POLYMER(S)/CARRIER/ SCAFFOLD STRUCTURE	TE APPLICATION	ACTIVE BIOMOLECULE	ENCAPSULATED/SEEDED CELL TYPE (SOURCE)	ANIMAL MODEL	REFS
Chitosan-alginate fibers	Not defined	Dexamethasone, PDGF-BB	–	–	[140]
Galactosylated chitosan coating	Not defined	EGF	Mouse hepatocytes	–	[141]
Chitosan granules in a TCP/ chitosan hydrogel	Bone	PDGF	–	Rat femur defect	[142]
Chitosan freeze-dried scaffolds	Bone	PDGF-BB	Rat calvarial osteoblasts	–	[135]
Chitosan/collagen scaffolds	Periodontal bone	TGF-β1 plasmid	Human periodontal ligament cells	Nude mice subcutaneous implantation	[143]
Chitosan/coral scaffolds	Periodontal bone	PDGFB plasmid	Human periodontal ligament cells	Nude mice subcutaneous implantation	[144]
Chitosan freeze-dried sponge	Periodontal bone	PDGF-BB	Fetal rat calvarial osteoblastic cells	Rat calvarial defect	[145]
Chitosan/gelatin freeze-dried scaffolds	Cartilage	TGF-β1 plasmid	Rabbit articular chondrocytes	–	[146]
Chitosan microspheres in chitosan freeze-dried scaffolds	Cartilage	TGF-β1	Porcine articular chondrocytes	–	[147]
Chitosan microspheres in chondroitin sulphate-collagen-chitosan freeze-dried scaffolds	Cartilage	TGF-β1	Rabbit articular chondrocytes	–	[148]
Chitosan-glycerol phosphate hydrogel	Osteochondral	Autologous blood	–	Rabbit osteochondral defect	[149]
Chitosan/heparinoid injectable hydrogels	Vascularization	FGF-2	HUVEC	Mice back subcuits	[150]
Chitosan hydrogels	Vascularization	FGF-2	–	Rabbit myocardial infarction	[151]
Chitosan/chitin tubular device with PLGA microspheres	Peripheral nerve regeneration	EGF	Mice neural stem cells	–	[152]
Chitosan hydrogel	Skin	hEGF	–	Rat burn wounds	[139]
Photocrosslinkable chitosan hydrogel	Skin	FGF-2	–	Mice full-thickness skin incisions	[153]
Particle aggregated chitosan scaffolds	Bone Cartilage	–	Human adipose-derived adult stem cells	–	[131]

Abbreviations: TCP: tricalcium phosphate; PLGA: poly(lactide-co-glycolide); PDGF: platelet-derived growth factor; EGF: epidermal growth factor; TGF-β1: transforming growth factor-β1; FGF-2: fibroblast growth factor-2; HUVEC: Human umbilical vein endothelial cells. Compiled from references [131,135,139-153].

3.3. STARCH

Starch is one of the most promising natural polymers because of its inherent biodegradability, overwhelming abundance and renewability. It is composed of a mixture of glycans that plants synthesize and deposited in the chloroplasts as their principal food reserve. Starch is stored as insoluble granules composed of α-amylose (20–30%) and amylopectin (70–80%) [154]. α-Amylose is a linear polymer of several thousands of glucose residues linked by α(1→4) bonds. The α-glycosidic bonds of α-amylose cause it to adopt a helical conformation (left-handed helix) [154]. Amylopectin consists mainly of α(1→4)-linked glucose residues but it is a branched molecule with α(1→6) branch points every 24 to 30 glucose residues in average. Amylopectin molecules contain up to 106 glucose residues, making them some of the largest molecules in nature [154].

Starch by itself is extremely difficult to process and is brittle when used without the addition of a plasticizer. In most applications, the semi-crystalline native starch granule structure is either destroyed or reorganized, or both [155]. Water is the usual plasticizer in starch processing, and the physical properties of starch are greatly influenced by the amount of water present [155]. Therefore, the use of other plasticizers, such as low molecular weight alcohols, especially for the production of thermoplastic starches, renders starch more processable [155]. Additionally, blending two or more chemically and physically dissimilar natural polymers has shown potential to overcome these difficulties.

Over the years several materials have been blended with starch to improve its processability, including, but not restricted to, several synthetic polymers, such as polyethylene [156], polycaprolactone [157], polyethylene-co-vinyl alcohol [158], poly(hydroxybutyrate-co-valerate) [159], among others [160,161], or even other natural origin materials such as other polysaccharides [162] and proteins [163]. Starch has also been extensively modified by chemical methods such as oxidation [164] and grafting of acryl reactive groups [165]. Due to its degradation by amylases [166], this constitutes another strategy to tailor the degradation of starch-based materials [167,168]. A very important feature of most natural origin materials when considered for biomedical applications is the reaction of the host to degradation products (in the case of starch, degradation products are oligosaccharides that can be readily metabolized to produce energy).

Starch has been extensively used for drug delivery applications, including cancer therapy [169], nasal administration of insulin [170] among others [171,172]. Reis and co-workers [173,174] have proposed starch-based materials (blends of starch with different synthetic polymers, such as ethylene vinyl alcohol, polylactic acid, cellulose acetate and polycaprolactone) as materials with potential for biomedical applications. Since then, others have studied the ability of these materials for biomedical applications, namely as porous scaffolds [175,176]. The work of Reis and co-workers has been focused on a wide range of biomedical applications, such as scaffolds for bone tissue engineering applications [174,177], bone cements [178,179] and as drug delivery systems [174,180–182]. These materials have been shown to be biocompatible in vitro [183], and to possess a good in vivo performance [184]. More recently, these materials have been shown to permit the adhesion of endothelial cells [185], an indicator of the ability of starch-based fiber-based scaffolds to permit vascularization to occur. This finding builds on the already proven potential of these materials for tissue engineering applications.

Table 6 intends to summarize some relevant application of starch-based materials in the tissue engineering field and drug delivery.

Table 6. Starch-based matrices/scaffolds for drug and cell delivery described for different tissue engineering applications.

POLYMER(S)/CARRIER/ SCAFFOLD STRUCTURE	TE APPLICATION	ACTIVE BIOMOLECULE	ENCAPSULATED/SEEDED CELL TYPE (SOURCE)	ANIMAL MODEL	REFS
Starch-based porous scaffolds	Bone	Non-steroid anti-inflammatory agent	–	–	[174]
Starch-based microparticles	Bone	Non-steroid anti-inflammatory agent	–	–	[180]
Starch-based microparticles	Bone	Corticosteroids	–	–	[181]
Starch-based microparticles	Bone	PDGF	–	–	[182]
Starch-based microparticles	Bone	–	Osteoblasts	–	[186]
Starch-based fiber meshes scaffolds	Bone	–	Bone marrow stromal cells	–	[187]
Starch-based fiber meshes scaffolds	Vascularization	–	Micro (HPMEC-ST1.6R) and macrovascular (HUVEC) endothelial cells	–	[185]

Abbreviations: PDGF: platelet-derived growth factor. Compiled from references [174,180-182,185-187].

3.4. ALGINATE

Alginate is one of the most studied and applied polysaccharidic polymers in tissue engineering and drug delivery field. They are abundant in nature and are found as structural components of marine brown algae and as capsular polysaccharides in some soil bacteria. Commercial alginates are extracted from three species of brown algae. These include *Laminaria hyperborean*, *Ascophyllum nodosum*, and *Macrocystis pyrifera* in which alginate comprises up to 40% of the dry weight [128]. Bacterial alginates have also been isolated from *Azotobacter vinelandii* and several Pseudomonas species [128]. Alginates are naturally derived polysaccharide block copolymers composed of regions of sequential β-D-mannuronic acid monomers (M-blocks), regions of α-L-guluronic acid (G-blocks), and regions of interspersed M and G units [188]. The length of the M-and G-blocks and sequential distribution along the polymer chain varies depending on the source of the alginate. Alginates undergo reversible gelation in aqueous solution under mild conditions through interaction with divalent cations such as Ca^{2+} that can cooperatively bind between the G-blocks of adjacent alginate chains creating ionic inter-chain bridges. This gentle property has led to their wide use as cell transplantation vehicles to grow new tissues and as wound dressings. Moreover, alginate as an anionic polymer with carboxyl end groups is a good mucoadhesive agent [128]. However, alginate hydrogels used in these applications have uncontrollable degradation kinetics and gels dissolve in an uncontrollable manner following the loss of divalent cations releasing high and low molecular weight alginate units. Attempts have been made to covalently crosslink sodium alginate with gelatin and sodium tetraborate [189] or with albumin [190].

The hydrogel is formed because blocks of guluronic residues bind to cations resulting in a three dimensional network of alginate fibers held together with ionic interactions. The model that best describes this network is the “egg-box model” [191]. The resultant network is a function of the frequency and length of contiguous guluronic acid residues as well as the concentration and type of the cation [192]. The changes in frequency and length of adjacent guluronic acid units, as well as, changes in cation concentration can alter the number of alginate fibers held together changing the overall strength of the network. In a few words, alginates possessing a high guluronic acid content develop stiffer, more porous gels which maintain their integrity for longer periods of time. During cationic crosslinking, they do not undergo excessive swelling and subsequent shrinking, thus they better maintain their form [193]. On the other hand, alginates rich in mannuronic acid residues develop softer, less porous gels that tend to

disintegrate with time. Consequently, they are characterized by a high degree of swelling and shrinking during cationic crosslinking [193].

The effects of alginate composition on the growth characteristics and metabolic activity of encapsulated cells have yet to be fully assessed. Nevertheless, the referred parameters that defined the alginate network strength may be the majority responsible for the differences in the growth characteristics of cells encapsulated in different alginates as reported since by Simpson and co-workers [193], as the network strength is a conditional parameter to the nutrient diffusion and cell-to-cell contact. The work of Yoon et al. [194] also reports the influence of alginate concentration and cell concentration in the expression of insulin-like growth factor-1 (IGF-1) of encapsulated chondrocytes.

Alginate-based materials are pH-sensitive. Biomolecules release from alginate-based materials in low pH solutions is significantly reduced which could be advantageous in the development of a delivery system. Theoretically, alginate shrinks at low pH and the encapsulated drugs are not released. This pH-dependent behavior of alginate is exploited to tailor release profiles and in the development of 'smart' systems. However, at higher pH alginate undergoes a rapid dissolution which may result in burst release of protein drugs and subsequently their denaturation by proteolytic enzymes. Therefore, many modifications in the physicochemical properties are needed for the prolonged controlled release of protein drugs [195,196].

Due to its biocharacteristics and the mild gelation process conditions, alginate templates are by far one of the natural origin polymers applied in tissue engineering applications even considering growth factor delivery or cell encapsulation, as Table 7 demonstrates. If one analyses the vast examples in the table, cartilage tissue engineering arises as the major application mainly to the need of the 3D culture of chondrocytes. Alginate beads/hydrogels can be prepared by extruding/maintaining a solution of sodium alginate containing the desired protein or cells, as droplets/blocks, in to a divalent crosslinking solution such as Ca^{2+},Sr^{2+},or Ba^{2+}. Monovalent cations and Mg^{2+} ions do not induce gelation [128]. Although alginate beads/hydrogels can be prepared by simple and mild procedures, this method has a major limitation that is the drug loss during bead/hydrogel preparation, by leaching through the pores in the beads/hydrogels.

Table 7. Alginate-based matrices/scaffolds for drug and cell delivery described for different tissue engineering applications.

POLYMER(S)/CARRIER/ SCAFFOLD STRUCTURE	TE APPLICATION	ACTIVE BIOMOLECULE	ENCAPSULATED/SEEDED CELL TYPE (SOURCE)	ANIMAL MODEL	REFS
Alginate–chitosan fibers	Not defined	Dexamethasone, PDGF-BB	–	–	[140]
Alginate hydrogel	Bone/cartilage	BMP-2 gene	Bone marrow stromal cells	Mouse femoral muscle	[21]
Alginate beads	Cartilage	BMP-2	Human articular chondrocytes	–	[197]
Alginate beads	Cartilage	IGF-1, TGF-β2 and FGF-2	Bovine articular chondrocytes	–	[198]
Alginate beads	Cartilage	rhOP-1 (medium)	Bovine articular chondrocytes	–	[199]
Alginate hydrogel and film	Cartilage	FGF-2 and TGF-β (medium)	Rabbit periostal explants	–	[188,200]
Alginate beads	Cartilage	BMP-2,4,5,6,7	Chondrocytes (transfected)	Nude mice subcutaneous implantation	[201]
Alginate beads	Cartilage	TGF-β	–	Rabbit knee osteochondral defects	[202]
Alginate hydrogel	Cartilage	TGF-β1, TGF-β2, TGF-β3 or BMP-2	Bovine synovium-derived progenitor cells	–	[203]
Alginate beads	Cartilage	Human platelet supernatant	Human articular chondrocytes	–	[204]
Alginate beads	Cartilage	Porcine platelet-rich plasma	Porcine articular chondrocytes	–	[205]
Alginate beads	Vascularization	bFGF, VEGF, EGF	–	Rat myocardial infarction	[206]
Alginate hydrogel	Vascularization	VEGF and bFGF	–	Nude mice subcutaneous implantation	[207]
Alginate beads with bioactive glass	Vascularization	VEGF conditioned medium	Human CCD-18Co fibroblast cells and HDMECA	–	[208]
Alginate gels in PP and PS hollow-fibers	Vascularization	Endothelial cell growth supplement	–	Rat subcutaneous implantation	[209]
Alginate beads	Peripheral nerve regeneration	BDNF	–	Rat sciatic nerve	[210]
Alginate hydrogels with RGD-containing peptides	Bone	BMP-2 and TGF-β3	Rat bone marrow stromal cells	Nude mice subcutaneous implantation	[211]

(CONT.)

Table 7 (cont). Alginate-based matrices/scaffolds for drug and cell delivery described for different tissue engineering applications.

POLYMER(S)/CARRIER/ SCAFFOLD STRUCTURE	TE APPLICATION	ACTIVE BIOMOLECULE	ENCAPSULATED/SEEDED CELL TYPE (SOURCE)	ANIMAL MODEL	REFS
Alginate hydrogel	Intervertebral disc	TGF-β1	Human intervertebral disc cells	–	[29,30,212]
Alginate beads and disks	Cartilage	–	Human adipose-derived adult stem cells	Nude mice subcutaneous implantation	[48,213]
Alginate hydrogel	Cartilage	Glucose (medium)	Cattle articular chondrocytes	–	[214]
Alginate freeze-dried sponges and combined with hyaluronic acid	Cartilage	–	Rat chondrocytes	Rat full-thickness cartilage defect	[215]
Alginate hydrogel in Ethisorb210	Cartilage	–	Bovine articular chondrocytes	Nude mice subcutaneous implantation	[216]
Alginate hydrogel	Cartilage	–	Bovine articular chondrocytes	–	[101,194]
Alginate gel alone and in PGA-PLA pads	Cartilage	–	Rabbit rib chondro-progenitor cells	Rabbit knee osteochondral defects	[217]
Alginate–chitosan microcapsules	Bone/cartilage	–	Human bone marrow cells and human articular chondrocytes	Nude mice subcutaneous implantation	[218]
Oxidized alginate injectable hydrogel	Liver	–	Rat hepatocytes	–	[189]
Alginate beads	Pancreas	–	Murine insulinoma βTC3 cells	–	[193]

Abbreviations: PDGF-BB: recombinant human platelet-derived growth factor-BB; BMP: bone morphogenetic protein; IGF-1: insulin growth factor; TGF-β: transforming growth factor; FGF: fibroblast growth factor; rhOP-1: recombinant human osteogenic protein-1; EGF; epidermal growth factor; VEGF: vascular endothelial growth factor; BDNF: brain derived neutrophic factor; CCD-18Co: normal colon fibroblast cells derived from human colon; HDMECA: adult human dermal microvascular endothelial cells; PGA-PLA: co-polymer of polyglycolic acid-polylactic acid; Ethisorb210: non-woven fleece composed of a polyglycolic-polylactic-copolymer punctually glued with polydioxanon; PP: polypropylene, PS: polysulfone. Compiled from references [21,29,30,48,101,140,188,189,193,194,197-218].

One nature-inspired approach that has been attracting more attention is the use of biological multi-protein supplements as source of several growth factors to improve cell behavior. The biochemical stimulus provided in the initial critical stages of cell culture for engineered tissues may differ from that for single growth factor delivery. One example of this potential approach is given by Gaissmaier and co-workers [204] by using human platelet supernatant. As it is known, platelets are a rich source of many growth factors including transforming growth factor-β and platelet-derived growth factor. However, the authors report that in spite of the addition of human platelet supernatant accelerate chondrocytes expansion can lead to their dedifferentiation. Other reported approach is the use of platelet-rich plasma

isolated from autologous blood (porcine source) suggesting that the cells remain phenotypically stable in the presence of platelet-rich plasma [205]. Another strategy is proposed for angiogenic growth factors by using endothelial cell growth supplement [209] as source for vascular endothelial growth factor (VEGF), several endothelial cell growth factors (ECGFs) and basic fibroblast growth factor (bFGF). The study demonstrates that the controlled release of endothelial cell growth supplement leads to a two-fold increase in neovascularization at the material-tissue interface. However, the study does not include any comparison with the effect of any single growth factor.

For cartilage tissue engineering, periosteum can be use not only as source for chondrogenic growth factors but also as source for chondrogenic precursor cells as reported in the work of Stevens and colleagues [188]. Besides these, other advantage of periosteum over cell cultures for cartilage or osseous tissue engineering include the fact that it can serve as a template for directional evolution of tissue. The periosteum contains a source of chondrogenic growth factors that if supplemented in vitro by the morphogen TGF-β1 can drive the terminal differentiation of the precursor cells into a chondrocyte phenotype [188]. The *in vitro* culture of periosteal explants within the alginate hydrogel, showed that after 6 weeks more than 50% of the total area of the periosteal explants was composed of cartilage that was hyaline-like in appearance in contrast to the results obtained with encapsulated chondrocytes where constructs supported the in vitro culture for a period of several weeks but did not form a hyaline-like cartilaginous tissue [188].

Concerning the commercially available products, alginate has been widely marketed as wound dressings. Examples are Nu-Derm® commercialized by Johnson & Johnson in USA, Curasorb® by Kendall or AlgiSite® by Smith & Nephew in USA Genialab in Germany is marketing geniaBeads® CA which are hydrogel beads made from calcium alginate. The hydrogel beads' size can be chosen from a wide range of 0.2 to 3 mm to give them the desired properties regarding eye-appeal, release properties, or technical demands in general. A more tissue engineering driven product is commercialize by Articular Engineering LCC in USA for research purposes that has a variety of available products ranging engineered tissues, isolated cells, native tissues and cryopreserved cells from cartilage, synovium and intervertebral disc from both bovine or human origin using alginate beads with the alginate-recovered-chondrocyte or ARC™ method. A study was published on further development in this technology using osteogenic protein-1 [199].

3.5. HYALURONAN

Hyaluronic acid is most frequently referred to as hyaluronan due to the fact that it exists *in vivo* as a polyanion and not in the protonated acid form [219]. Hyaluronan is a naturally occurring non-sulfated glycosaminoglycan and a major macromolecular component of the intercellular matrix of most connective tissues such as cartilage, vitreous of the human eye, umbilical cord and synovial fluid [219]. Hyaluronic acid is a linear polysaccharide that consists of alternating disaccharide units of α-1,4-D-glucuronic acid and β-1,3-*N*-acetyl-D-glucosamine, linked by β(1→3) bonds [220]. Hyaluronan and its associated networks have many physiological roles that include tissue and matrix water regulation, structural and space-filling properties, lubrication, and a number of macromolecular functions [219].Especially for its enhanced viscoelastic properties, hyaluronan works as a lubricant and shock absorber in synovial fluid [124]. Hyaluronan has been widely studied for drug delivery, for dermal, nasal, pulmonary, parenteral, liposome-modified, implantable delivery devices and for gene delivery (reviewed in Liao *et al.* [219]). Hyaluronan for tissue engineering has been focused on cartilage, bone and osteochondral applications, most likely due to the fact that it is a major macromolecular component of the extracellular matrix. The most relevant applications are summarize in Table 8.

Commercially available hyaluronan is obtained from different sources, mainly by extraction from umbilical cord, rooster comb, synovial fluid, or vitreous humour. In addition, hyaluronic acid can be easily and controllably produced in large scales through microbial fermentation, from strains of bacteria such as *Streptococci* [219], enabling the scale-up of derived products and avoiding the risk of animal-derived pathogens. Hyaluronan is available for several applications, for lubrication and mechanical support for the joints in osteoarthritis (Hyalgan® and Hyalubrix® from Fidia in Italy; Artz® from Seikagaku Corporation in Japan) as a viscoelastic gel for surgery and wound healing (Bionect® from CSC Pharmaceutical in USA; Jossalind® from Hexal in Germany), for im-plantation of artificial intraocular lens (Healon® from OVD from Advanced Medical Optics in USA, Opegan R® from Seikagaku in Japan, Opelead® from Shiseido in Japan, Orthovisc® from Anika in USA) and as culture media for use in *in vitro* fertilization (EmbryoGlue® from Vitrolife, USA) [219]. Hyaff® commercialized by Fidia in Italy has been widely used as a biomaterial for biomedical applications as described in Table 8. From a chemical standpoint, Hyaff® is a benzyl ester of hyaluronic acid and its main characteristics are that HYAFF® maintains the biological characteristics of the natural molecule from which1 it derives, the natural degradation of Hyaff® releases hyaluronic acid, which is then degraded through well-known metabolic

pathways and that depending on the levels of esterification (e.g. the percentage of carboxylic groups interested by the esterification reaction), it is possible to obtain polymers with different levels of hydrophobicity.

Table 8. Hyaluronan-based matrices/scaffolds for drug and cell delivery described for different tissue engineering applications.

POLYMER(S)/CARRIER/ SCAFFOLD STRUCTURE	TE APPLICATION	ACTIVE BIOMOLECULE	ENCAPSULATED/SEEDED CELL TYPE (SOURCE)	ANIMAL MODEL	REFS
Hyaluronic acid hydrogel nanofiber scaffold	Not defined	Fibronectin	NIH 3T3 fibroblasts	–	[221]
Hyaluronan–alginate scaffold	Not defined	bFGF	–	–	[222]
Hyaluronate gel	Bone Cartilage	BMP-2 gene	Bone marrow stromal cells	Mouse femoral muscle	[21]
Hyaluronic acid gel	Vascularization	bFGF	–	Nude mice subcutaneous implantation	[223]
Hyaluronan–methylcellulose	Spinal cord	–	–	Spinal cord injury	[224]
Hyaluronic acid (Hyaff®11) fiber scaffold	Cartilage	–	Chondrocytes	Nude mice subcutaneous implantation	[225]
Hyaluronic acid hydrogel	Cartilage	–	Auricular chondrocytes	Nude mice subcutaneous implantation	[226]
Hyaluronic acid (Hyaff®11) non-woven mesh scaffold	Osteochondral	–	Bone marrow mesenchymal cells	Rabbit osteochondral knee lesion	[227]
Hyaluronic acid (native)	Vascularization	DNA	HUVECs	Rat hind limb	[228]
Hyaluronic acid (Hyaff®11) non-woven scaffold	Vascularization	–	Human saphenous vein endothelial cells	–	[229]
Hyaluronic acid membrane	Skin	–	Melanocytes Keratinocytes	–	[230]
Hyaluronic acid (Hyaff®11) sponge-hyaluronic acid coating	Adipose	–	Preadypocytes	Nude mice subcutaneous implantation	[34]

Abbreviations: BMP-2: bone morphogenetic protein-2; bFGF: basic fibroblast growth factor. Compiled from references [21,34,221-230].

3.6. CHONDROITIN SULPHATE

Extracellular matrix components are valuable building blocks for the preparation of biomaterials involved in tissue engineering, especially if their biological, chemical and physical characteristics can be controlled. An example is chondroitin sulfate, one of the most physiologically important

glycosaminoglycans. Glycosaminoglycans (GAGs) are found in the lubricating fluid of the joints and as components of cartilage, synovial fluid, bone, and heart valves. With the exception of hyaluronan, these polysaccharides are covalently linked to a protein core, thereby forming proteoglycans [231]. Biocharacteristics of GAGs include the binding and modulation of growth factors and cytokines, the inhibition of proteases, and the involvement in adhesion, migration, proliferation and differentiation of cells [232]. Furthermore, GAGs are practically non-immunogenic and degrade to non-toxic oligosaccharides. These characteristics together with their defined physical and chemical characteristics make them very interesting materials for tissue engineering. Due to its GAG nature, chondroitin sulfate is an attractive natural-origin polymer applied essentially in cartilage tissue engineering. Nevertheless, and due to its biological properties (mainly the ability to interact with various growth-active molecules), is often used in other tissue engineering applications to valorize other polymers in order to interact with cells and proteins improving cell behavior of the developed materials.

Chondroitin sulfate consists of repeating disaccharide units of D-glucuronic acid and *N*-acetyl galatosamine sulfated at either 4-or 6-positions [233]. Chondroitin sulfate can bind with core protein to produce highly absorbent aggregan, which is a major structure inside cartilage and acts as a shock absorber, or it can produce sydecan, which is a cell receptor which can interact with adhesion proteins, cells and the extracellular matrix (ECM) [233]. *In vitro* studies suggest that chondroitin sulfate is also able to increase matrix component production by human chondrocytes [234]. Furthermore, chondroitin sulfate proteoglycans have a critical role in regeneration and plasticity in the central nervous system as reviewed by Galtrey and Fawcett [235].

However, the readily water-soluble nature of chondroitin sulfate limits its application as a solid-state drug delivery vehicle. Therefore, it is usual to carry out a crosslinking treatment to tailor the properties of chondroitin sulfate as reported in several works [233,236,237] or to combine it with other polymers, such as chitosan [238], gelatin and hyaluronan [239,240], collagen [241,242], poly(vinyl alcohol) [233] or poly-(lactic-co-glycolic acid) [240] in order to produce more stable materials. Moreover, and since chondroitin sulfate in negatively charged, interaction with positively charged molecules such as polymers or growth factors is anticipated being a key issue to facilitate the design of delivery systems. For instances this characteristic is used to produce chondroitin sulphate-chitosan sponges as delivery systems for platelet-derived growth factor-BB (PDGF-BB) for bone regeneration as reported by Jeong Park *et al.* [238] where this interaction shown to induce more prolonged release of the growth factor. As previously

referred, due to its biocharacteristics, chondroitin sulfate has been used in some extent in the tissue engineering field, mainly in cartilage applications. The aim of the following in Table 9 is to show the diversified applications (besides cartilage) of this natural occurring polymer as carrier for growth factor or cell delivery in this field.

An interesting approach using chondroitin sulfate is proposed by Daamen *et al.* [245] by reporting the preparation of molecularly-defined collagen-elastin-glycosaminoglycan scaffolds. Given the large heterogeneity in the body's scaffolds, it is the purpose of this study to demonstrate that tailor-made, molecularly-defined scaffolds can be produced from the main components of the extracellular matrix using in this case highly purified collagen, elastin, and chondroitin sulfate in order to produce organ-specific scaffolds for tissue engineering. The developed scaffolds present the combination of adhesive properties and tensile strength of collagen with the elasticity of elastin (which is crucial for instances in blood vessels) and the bind capacity to growth-active molecules of chondroitin sulfate. This interesting approach is also one example of the effort that has to be done in trying to reduce the variability generally found of natural-origin polymers by using highly purified and characterized polymers producing molecularly-defined scaffolds.

In terms of commercially availability, chondroitin sulfate is widely marketed in USA and Europe as a nutritional supplement together with glucosamine used in the treatment of osteoarthritic patients. Chondroitin sulfate is also a component of the dermal layer of the FDA-approved skin substitute for treating burns [233]. An available commercial product is Integra® Dermal Regeneration Template marketed by Integra in USA which a bilayered membrane system for skin replacement that provides a scaffold for dermal regeneration. The dermal replacement layer is made of a porous matrix of fibers of crosslinked bovine tendon collagen and a glycosaminoglycan (chondroitin-6-sulfate) manufactured with a controlled porosity and defined degradation rate. According to the manufacturer, Integra® Dermal Regeneration Template is the first and only FDA-approved tissue engineered product for burn and reconstructive surgery. As hyaluronan, chondroitin sulfate is also used as a surgical aid in anterior segment procedures including cataract extraction and intraocular lens implantation. An example is Viscoat® from Alcon Laboratories in UK which is a solution of 4% chondroitin sulfate and 3% sodium hyaluronate.

Table 9. Chondroitin sulfate-based matrices/scaffolds for drug and cell delivery used in different tissue engineering applications.

POLYMER(S)/CARRIER/ SCAFFOLD STRUCTURE	TE APPLICATION	ACTIVE BIOMOLECULE	ENCAPSULATED/SEEDED CELL TYPE (SOURCE)	ANIMAL MODEL	REFS
Chondroitin 4-sulfate hydrogels	Not defined	Vasopressin, aprotinin, lysozyme, albumin	–	–	[243]
Chondroitin sulphate-collagen coated discs	Bone	rhBMP-2	–	Rat hind limbs	[242]
Chondroitin sulphate-chitosan sponges	Bone	PDGF-BB	Rat calvarial cells	–	[238]
Chondroitin sulphate-collagen-chitosan freeze-dried scaffolds with chitosan microspheres	Cartilage	TGF-β1	Rabbit articular chondrocytes	–	[148]
Chondroitin sulfate A	Vascularization	VEGF	Porcine vascular endothelial cells	–	[244]
Chondroitin sulfate injectable hydrogels	Vascularization	bFGF	NIH 3T3 fibroblasts	Nude mice subcutaneous implantation	[223]
Chondroitin sulphate-collagen-elastin freeze-dried scaffolds	Not defined	–	Human myoblasts and human HFL1 lung fibroblasts	–	[245]
Chondroitin/gelatin hyaluronate-PLGA porous scaffolds	Cartilage	–	Rabbit mesenchymal stem cells	Rabbit full-thickness cartilage defect	[240]
Chondroitin sulphate-gelatin-hyaluronan freeze-dried scaffolds	Cartilage	–	Porcine articular chondrocytes	Porcine articular and osteochondral defects	[239,246]
Chondroitin sulphate-collagen scaffolds	Cartilage	–	Bovine articular chondrocytes	–	[247]
Chondroitin sulphate-collagen hydrogels	Heart valve	–	Porcine VICs and VECs	–	[241]
Chondroitin sulphate-PVA hydrogels	Kidney	–	Baby-hamster kidney (BHK) cells	–	[233]

Abbreviations: bFGF: basic fibroblast growth factor; rhBMP-2: recombinant human bone morphogenetic protein-2; TGF-β1: transforming growth factor-β1; VEGF: vascular endothelial growth factor; PDGF-BB: Platelet-derived growth factor-BB; PVA: poly(vinyl alcohol); PLGA: poly-(lactic-co-glycolic acid); VICs and VECs: mitral valve interstitial cells (VICs) and endothelial cells (VECs); Compiled from references [148,223,233,238–247].

3.7. OTHER POLYSACCHARIDIC POLYMERS

Other polysaccharides have been studied for tissue engineering applications. Some of them, the so-called cold set gels which form a gel on cooling the solution [124] like agarose, carrageenans and gellan

gum have been studied in some extent the frame of drug delivery for tissue engineering and are described as follows. Due to their still narrow applications (but potential) as the drug delivery carriers in the tissue engineering field, the authors have chosen to overview them together in this section.

Dextran is a branched, high molecular weight polymer of D-glucose, produced by different bacterial strains from sucrose via the action of dextransucrase enzyme [248], consisting of α(1→6)-linked D-glucose residues with some degree of branching via α(1→3) linkages. Dextran is readily available in a wide range of molecular weights along with several derivatives and it is biodegradable and biocompatible. These properties make it suitable for a whole range of applications, such as plasma-expanders and blood substitutes, since it binds to erythrocytes, platelets and vascular endothelium by reducing their aggregation and adhesiveness, respectively. Additionally, it has also been shown to be a bone healing promoter and also for dermal and subcutaneous augmentation and for drug delivery [125].

Agar, the native polysaccharide of agarose, forms thermo-reversible gels when dissolved in water. It consists of two main components, agarose and agaropectin. Agarose is a linear polysaccharide consisting on (1→3)-β-D-galactopyranose-(1→4)3,6-anhydro-α-L-galactopyranose as the basic unit and contains a few ionized sulfate groups [249]. Agarose is normally insoluble in organic solvents and cannot form gels. Apparently the gelling possibility in aqueous solutions is a consequence of the structure of water. The arrangement of the agarose chains that join together and adopt a double helix so tight that any gaps are closed, trapping any water inside the helix [249]. These double stranded helices are the result of specific intermolecular hydrogen bonding that contributes to the rigidity of the polymer chains [249]. Adding hydrogen bond decomposing agents like urea can have a tremendously negative effect on the gelling properties. Gelation occurs at temperatures below 40°C, whereas the melting temperature appears to be 90°C [250]. The viscoelastic properties of aqueous agarose gels depend strongly on the degree of desulfation of its native polysaccharide agar: the propensity to form gels increases with increasing desulfation [250].

Carrageenans are a family of sulfated polysaccharides extracted from red marine algae and that are widely utilized in the industry because they can form reasonably stiff and thermoreversible gels in the presence of so-called gel-promoting salts at room temperature [251]. These polysaccharides are linear polymers consisting of chains of (1→3)-linked β-D-galactose and (1→4)-linked α-D-galactose units which are variously substituted and modified to the 3,6-anhydro derivative, depending on the source and

extraction conditions [113]. Three major types of carrageenan are recognized on the basis of their patterns of sulfate esterification: κ (kappa), ι (iota), and λ (lambda). All carrageenans are highly flexible molecules, which, at higher concentrations, wind around each other to form double-helical structures. A particular advantage is that they are thixotropic [252], i.e., they thin under shear stress and recover their viscosity once the stress is removed. Due to the strong ionic nature, these carrageenans exhibit a high degree of protein reactivity. These materials have been used in the field of drug delivery [253–255], which creates the potential for their use as drug delivery systems in tissue engineering. Carrageenans have been used mainly in the food industry, and several companies commercialize it - FMC BioPolymer or Carrageenan Company. Genialab in Germany is marketing genia-Beads® CG which are hydrogel beads made from carrageenan.

Gellan gum is a high molecular weight microbial exopolysaccharide produced by *Pseudomonas elodea*. It is a linear anionic heteropolysaccharide composed of the tetrasaccharide (1→4)-L-rhamnose-α(1→3)-D-glucose-β(1→4)-D-glucuronic acid-β(1→4)-D-glucose as repeating unit, with carboxylic side groups. Gellan gum is widely used in the food industry thanks to its ability to form transparent gels resistant to heat and acid in comparison to other polysaccharide gels. In its native or high acyl form, two acyl substituents D-acetate and D-glycerate are present. Both substituents are located in the same glucose residue. The high acyl form produces transparent, soft, elastic and flexible gels which are resistant to heat and acid, whereas the low acyl form produces firm, non-elastic brittle [125]. Gel formation is due to a conformational heat-reversible transition from a state of single random macromolecules to a more ordered state where macromolecules pair with each other to form double helixes [125]. A single macromolecule can be involved in the formation of more than one helix. In this way junctions among the helixes are formed and consequently a gel is obtained [125]. Gellan gum has been studied for drug delivery applications, both as adjuvants [256] and as vehicle for drug delivery [257]. Its use for tissue engineering applications is taking the first steps, documented in Suri and Banerjee [258], where the authors have used a gellan gum gel as a substitute for the vitreous of the eye, and its properties were comparable to the commonly used material (silicone). Commercially available gellan gum, Gelrite®, a novel ophthalmic vehicle, gels in the presence of mono- or divalent-cations present in the lacrimal fluid. It efficacy was comparable to marketed eye drops in efficacy of treatment of bacterial conjunctivitis that was induced artificially in rabbits [259]. Its properties, similar to other materials already studied in the tissue engineering field, make this material a suitable candidate for both cell encapsulation and drug delivery applications.

Cellulose is often referred as the most abundant organic polymer in the world [260] and therefore it is readily available and has a low cost. The ease in which it can be converted to derivatives makes it an attractive raw material [124]. In nature, it is the primary structural component of plant cell walls [261]. This is a linear polysaccharide of D-glucose units linked by β(1→4) glycosidic bonds [261,262] where every other glucose residue is rotated approximately 180° [262]. As a result, cellobiose is the structural repeating unit of the glucan chains in cellulose [262]. The glucan chains in cellulose are parallel to each other and are packed side by side to form microfibrils, which stabilizes the structure, minimizing its flexibility [263]. This highly cohesive, hydrogen-bonded structure, gives cellulose fibers exceptional strength and makes them water insoluble despite their hydrophilicity [263]. Cellulosic materials exhibit, however, poor degradation *in vivo* [264]. A cellulose sponge has been evaluated in rats' femurs for its permissibility for bone formation and it was found to need more time to regenerate than the control [265]. However, with growth factors' supplementation, this material can further display a desirable enhancement of bone formation.

Several works have investigated the use of cellulose for cartilage [266,267], bone [268,269] and cardiac [264] applications. Hydroxypropylcellulose is a non-ionic water-soluble cellulose ether with a remarkable combination of properties. It combines organic-solvent solubility, thermo-plasticity and surface activity. The molecular weight is varied by controlling the degree of polymerization of the cellulose backbone, which, in turn, controls the viscosity of hydroxypropylcellulose; as the degree of polymerization increases, the viscosity of the polymer increases. Hydroxypropylcellulose is used in pharmaceutical formulations for various purposes: low-viscosity grades are used as tablet binders in immediate-release dosage forms and medium-and high-viscosity grades are used in sustained-release matrix formulations. Hydroxyethylcellulose is a nonionic water-soluble polymer derived from cellulose.

There is a commercially available hydroxyethylcellulose named Natrosol® 250HX distributed by Hercules in USA and has a degree of substitution of 1.5 (three hydroxyls substituted/two units). Genialab in Germany is also marketing geniaBeads® MC which are hydrogel beads made from modified cellulose. The following in Table 10 present some relevant examples of the previously described polysaccharidic polymers as matrices or scaffolds in the tissue engineering field.

Table 10. Polysaccharides-based matrices/scaffolds for drug, cell and gene delivery used in different tissue engineering applications.

POLYMER(S)/CARRIER/ SCAFFOLD STRUCTURE	TE APPLICATION	ACTIVE BIOMOLECULE	ENCAPSULATED/ SEEDED CELL TYPE (SOURCE)	ANIMAL MODEL	REFS
Dextran beads (in Ca-P porous scaffolds)	Bone	rhBMP-2	–	Dog class III furcation defect	[270]
Dextran/gelatin hydrogel microspheres	Bone	IGF-I	–	Periodontal defect	[271]
Dextran hydrogel porous scaffolds	Guided cell and axonal regeneration	ECM-derived peptides (adhesion)	Primary embryonic chick dorsal root ganglia cells	–	[272]
Carboxymethyl-Dextran hydrogel membranes	Not defined	Lysozyme	–	–	[273]
Agarose film	Cartilage	FGF-2	Periostal explants	Rabbit knee	[200]
Agarose gel	Bone/cartilage	BMP-2 gene	Bone marrow stromal cells (transfected)	Mouse femoral muscle	[21]
Agarose sponge	Pancreas	Insulin	Pancreatic islets and insulinoma cells	–	[274]
Agarose gel	Intervertebral disc	TGF-β1	Human intervertebral disc cells	–	[29,30,212]
Agarose gel	Cartilage	–	Bovine articular chondrocytes	–	[101]
Agarose–fibrin gel	Cornea	–	Epithelial, stromal and endothelial cells	Rabbit cornea	[275]
Gellan gum (Gelrite®)	Ophthalmology	Antibiotic	–	Rabbit bacterial conjunctivitis	[259]
Gellan gum hydrogel	Eye (vitreous)	–	–	–	[258]
Cellulose hollow-fibers	Not defined	Fibronectin	Bovine coronary artery	–	[276]
Cellulose porous scaffold	Cartilage	–	Bovine and human chondrocytes	–	[277]

Abbreviations: rhBMP-2: recombinant human bone morphogenetic protein-2; IGF-1: insulin growth factor-I; ECM: extracellular matrix; FGF-2: fibroblast growth factor-2; BMP-2: bone morphogenetic protein-2; TGF-β1: transforming growth factor-β1. Compiled from references [21,29,30,101,200,212,258,259,270-277].

4. POLYHYDROXYALKANOATES

In nature, a special group of polyesters is produced by a wide variety of microorganisms as an internal carbon and energy storage, as part of their survival mechanism [278]. Poly(β-hydroxybutyrate) (PHB) was first mentioned in the scientific literature as early as 1901 [1]. Bacterially synthesized polyhydoxyalkanoates (PHAs) have attracted much attention because they can be produced from a

variety of renewable resources, and are truly biodegradable and highly biocompatible thermoplastic materials [1]. Although a great variety of materials of this family can be produced, the use of PHAs in tissue engineering has been mainly restricted to PHBs and poly(hydroxybutyrate-co-valerate) (PHBV) [279,280].

The brittleness of PHB was improved through copolymerization of β-hydroxybutyrate with β-hydroxyvalerate [281], which was first commercialized in 1990, but the high price of PHBV is still the major barrier to its wide spread usage [1]. The copolymerization produces less crystalline, more flexible and more readily processable materials than pure PHB. Depending on the requirements of different applications, PHA can be either blended, surface modified or combined with other polymers, enzymes or even inorganic materials, such as hydroxylapatite, to further adjust their mechanical properties or biocompatibility [279]. Interesting physical properties of polyhydroalkanoates include nonlinear optical activity and piezoelectricity [282], i.e. the capacity of a material to suffer electric polarization due to mechanical stress. Such properties can be very useful to tailor the material in question, increasing further promise applications of these polymers in areas such as tissue engineering and drug delivery.

Nevertheless, polyhydroxybutyrates have already been studied to some extent for tissue engineering applications [279], mainly for scaffold materials in combination with ceramic materials [283– 285], as a vehicle for drug delivery [286,287] and also as a material for cardiac tissue engineering [288]. Commercially available PHBs (poly-β-hydroxybutyrate homopolymer) BIOPOLGO4 is commercialized by IC1 Biological Products in the form of compression-molded sheets with 0.5mm thick. Similarly, ICI commercialized BIOPOLP05, the co-polymer poly(β-hydroxybutyrate-co-β-hydroxyvalerate) containing 24% hydroxyvalerate.

5. FINAL REMARKS AND FUTURE DIRECTIONS

Natural origin polymers have received considerable interest for drug delivery and tissue engineering applications. However, the combination of both applications into a single material has proven to be very challenging. This paper reviews the properties of natural-origin materials that render them attractive for applications where the combination of a scaffold material and a carrier for an active biomolecules is desirable. We also review research works were this combination of properties has been described, and

summarize them in comprehensive tables for each polymer. The described systems include mainly growth factors delivery or cell carriers with application in the tissue engineering field targeting, as described, a range of biological living tissues. The most relevant properties for the aimed applications of the natural-origin polymers were described with a special focus in the description of protein-based polymers and polysaccharides due to their similarity with the extracellular matrix. The use of porous scaffolds, microparticles, membranes, hydrogels and injectable systems from such kind of materials is also focused, especially on what concerns to the present status of the research in this field that should lead towards their final application.

Some examples of commercially available natural-origin polymers or systems that can find use in research or in the clinical were also identified and described. Moreover, the bio-logical performance of the described systems based on natural-based polymers is presented, based on several examples aiming at different clinical-relevant applications. Although natural origin materials present some drawbacks namely the difficulties in controlling the variability from batch to batch, mechanical properties or limited processability, their advantages clearly surplus the drawbacks. Their degradability, biocompatibility, low cost and availability, similarity with the extracellular matrix and intrinsic cellular interaction makes them attractive very candidates for biomedical applications, in particular as drug delivery systems for tissue engineering applications as described in this paper.

The aforementioned drawbacks are obviously limiting the widespread use of natural-origin polymers, mainly in clinical purposes. To try to overcome this disadvantage and for rational design of carriers/scaffolds for tissue engineering, it is essential to study the effect of individual components. To do so, templates have to be designed starting with highly purified molecules and the contribution of each component in the scaffold has to be controlled. Furthermore, when biomolecules such as growth factors are incorporated a further insightful study is needed in terms of interactions. Molecular design of these materials has clearly an important role in determining their suitability in such applications. Emerging technologies such as recombinant protein technologies and the development of molecularly-defined polymers can hinder this, by producing the polymer in a controlled, reliable and reproducible approach. A described example is the use of elastin-derived polypeptides or molecularly-defined polymers. Therefore, a better controlled development in methods for production, purification, or in material properties such as molecular weight, mechanical behavior or degradation rate is essential to widespread the use of these class of polymers.

In this paper, the authors have also presented some few examples of commercially available natural-origin products. However it is in some way limited because the availability of products with clinical relevance is still very narrowed especially if we limited the application to drug delivery field for tissue engineering applications. It is our conviction that a great deal of research work is still needed in order to obtain an increased number of commercially available and clinically successful natural-based systems and that emerging knowledge and technology is leading to a noteworthy exponential growth in this area. Undoubtedly, natural-origin polymers or nature-inspired materials appear as the natural and desired choice for the referred applications.

REFERENCES

1. L. Yu, K. Dean, L. Li, Polymer blends and composites from renewable resources, Prog. Polym. Sci. 31 (2006) 576–602.
2. J.C. Rodriguez-Cabello, J. Reguera, A. Girotti, M. Alonso, A.M. Testera, Developing functionality in elastin-like polymers by increasing their molecular complexity: the power of the genetic engineering approach, Prog. Polym. Sci. 30 (2005) 1119–1145.
3. X.D. Guo, Q.X. Zheng, J.Y. Du, S.H. Yang, H. Wang, Z.W. Shao, E.J. Sun, Molecular tissue engineering: concepts, status and challenge, J. Wuhan Univ. Technol. 17 (2002) 30–34.
4. H. Uludag, P. De Vos, P.A. Tresco, Technology of mammalian cell encapsulation, Adv. Drug Deliv. Rev. 42 (2000) 29–64.
5. A. Chilkoti, T. Christensen, J.A. MacKay, Stimulus responsive elastin biopolymers: applications in medicine and biotechnology, Curr. Opin. Chem. Biol. 10 (2006) 652–657.
6. A. Patel, B. Fine, M. Sandig, K. Mequanint, Elastin biosynthesis: the missing link in tissue-engineered blood vessels, Cardiovasc. Res. 71 (2006) 40–49.
7. B. Chevallay, D. Herbage, Collagen-based biomaterials as 3D scaffolds for cell cultures: application for tissue engineering and gene therapy, Med. Biol. Eng. Comput. 38 (2000) 211–218.
8. D.R. Eyre, Collagen: molecular diversity in the body's protein scaffold, Science 207 (1980) 1315–1322.
9. P.D. Kemp, Tissue engineering and cell-populated collagen matrices, Methods Mol. Biol. 139 (2000) 287–293.
10. C.H. Lee, A. Singla, Y. Lee, Biomedical applications of collagen, Int. J. Pharmacogn. 221 (2001) 1–22.
11. C. Wong Po Foo, D.L. Kaplan, Genetic engineering of fibrous proteins: spider dragline silk and collagen, Adv. Drug Deliv. Rev. 54 (2002) 1131–1143.
12. Y. Chunlin, P.J. Hillas, J.A. Buez, M. Nokelainen, J. Balan, J. Tang, R. Spiro, J.W. Polarek, The application of recombinant human collagen in tissue engineering, BioDrugs 18 (2004) 103–119.
13. K.I. Kivirikko, Collagen biosynthesis: a mini-review cluster, Matrix Biol. 16 (1998) 355–356.

14. R. Berisio, L. Vitagliano, L. Mazzarella, A. Zagari, Recent progress on collagen triple helix structure, stability and assembly, Prot. Pept. Lett. 9 (2002) 107–116.

15. B. Brodsky, J.A. Ramshaw, The collagen triple-helix structure, Matrix Biol. 15 (1997) 545–554.

16. P.F. Davidson, L. Levine, M.P. Drake, A. Rubin, S. Bump, The serologic specificity of tropocollagen telopeptides, J. Exp. Med. 126 (1967) 331–346.

17. A.K. Lynn, I.V. Yannas, W. Bonfield, Antigenicity and immunogenicity of collagen, J. Biomed. Mater. Res., B. Appl. Biomater. 71B (2004) 343–354.

18. W. Friess, Collagen: biomaterial for drug delivery, Eur. J. Pharm. Biopharm. 45 (1998) 113–136.

19. A. Letic-Gavrilovic, A. Piattelli, K. Abe, Nerve growth factor beta delivery via a collagen/hydroxyapatite composite and its effects on new bone growth, J. Mater. Sci., Mater. Med. 14 (2003) 95–102.

20. T. Fujisato, T. Sajiki, Q. Liu, Y. Ikada, Effect of basic fibroblast growth factor on cartilage regeneration in chondrocyte-seeded collagen sponge scaffold, Biomaterials 17 (1996) 155–162.

21. X.L. Xu, J. Lou, T.T. Tang, K.W. Ng, J.H. Zhang, C.F. Yu, K.R. Dai, Evaluation of different scaffolds for BMP-2 genetic orthopedic tissue engineering, J. Biomed. Mater. Res., B Appl. Biomater. 75B (2005) 289–303.

22. L.A. Chandler, D.L. Gu, C.L. Ma, A.M. Gonzalez, J. Doukas, T. Nguyen, G.F. Pierce, M.L. Phillips, Matrix-enabled gene transfer for cutaneous wound repair, Wound Repair Regen. 8 (2000) 473–479.

23. S. Koch, C. Yao, G. Grieb, P. Prevel, E.M. Noah, G.C.M. Steffens, Enhancing angiogenesis in collagen matrices by covalent incorporation of VEGF, J. Mater. Sci., Mater. Med. 17 (2006) 735–741.

24. J. Pieper, T. Hafmans, P. Van Wachem, M. Van Luyn, L. Brouwer, J. Veerkamp, T. Kuppevelt, Loading of collagen-heparan sulfate matrices with bFGF promotes angiogenesis and tissue regeneration in rats, J. Biomed. Mater. Res. 62 (2002) 185–194.

25. A.V. Vashi, K.M. Abberton, G.P. Thomas, W.A. Morrison, A.J. O'Connor, J.J. Cooper-White, E.W. Thompson, Adipose tissue engineering based on the controlled release of fibroblast growth factor-2 in a collagen matrix, Tissue Eng. 12 (2006) 3035–3043.

26. A. Batorsky, J.H. Liao, A.W. Lund, G.E. Plopper, J.P. Stegemann, Encapsulation of adult human mesenchymal stem cells within collagen-agarose microenvironments, Biotechnol. Bioeng. 92 (2005) 492–500.

27. Y. Xiao, H. Qian, W.G. Young, P.M. Bartold, Tissue engineering for bone regeneration using differentiated alveolar bone cells in collagen scaffolds, Tissue Eng. 9 (2003) 1167–1177.

28. Y.R.V. Shih, C.N. Chen, S.W. Tsai, Y.J. Wang, O.K. Lee, Growth of mesenchymal stem cells on electrospun type I collagen nanofibers, Stem Cells 24 (2006) 2391–2397.

29. H.E. Gruber, G.L. Hoelscher, K. Leslie, J.A. Ingram, E.N. Hanley, Three-dimensional culture of human disc cells within agarose or a collagen sponge: assessment of proteoglycan production, Biomaterials 27 (2006) 371–376.

30. H.E. Gruber, K. Leslie, J. Ingram, H.J. Norton, E.N. Hanley, Cell-based tissue engineering for the intervertebral disc: *in vitro* studies of human disc cell gene expression and matrix production within selected cell carriers, Spine J. 4 (2004) 44–55.

31. Y. Sumita, M.J. Honda, T. Ohara, S. Tsuchiya, H. Sagara, H. Kagami, M. Ueda, Performance of collagen sponge as a 3-D scaffold for tooth-tissue engineering, Biomaterials 27 (2006) 3238–3248.

32. R. Dorotka, U. Bindreiter, K. Macfelda, U. Windberger, Marrow stimulation and chondrocyte transplantation using a collagen matrix for cartilage repair, Osteoarthr. Cartil. 13 (2005) 655–664.

33. L.D. Franceschi, B. Grigolo, L. Roseti, A. Facchini, M. Fini, G. Giavaresi, M. Tschon, R. Giardino, Transplantation of chondrocytes seeded on collagen-based scaffold in cartilage defects in rabbits, J. Biomed. Mater. Res., A 75A (2005) 612–622.

34. K. Hemmrich, D.V. Heimburg, R. Rendchen, C.D. Bartolo, E. Milella, N. Pallua, Implantation of preadipocyte-loaded hyaluronic acid-based scaffolds into nude mice to evaluate potential for soft tissue engineering, Biomaterials 26 (2005) 7025–7037.

35. Z. Xiang, R. Liao, M.S. Kelly, M. Spector, Collagen–GAG scaffolds grafted onto myocardial infarcts in a rat model: a delivery vehicle for mesenchymal stem cells, Tissue Eng. 12 (2006) 2467–2478.

36. C. Danielsson, S. Ruault, A. Basset-Dardare, P. Frey, Modified collagen fleece, a scaffold for transplantation of human bladder smooth muscle cells, Biomaterials 27 (2006) 1054–1060.

37. P.C. Wang, T. Takezawa, Reconstruction of renal glomerular tissue using collagen vitrigel scaffold, J. Biosci. Bioeng. 99 (2005) 529–540.

38. Y. Tabata, Y. Ikada, Protein release from gelatin matrices, Adv. Drug Deliv. Rev. 31 (1998) 287–301.

39. S. Young, M. Wong, Y. Tabata, A.G. Mikos, Gelatin as a delivery vehicle for the controlled release of bioactive molecules, J. Control. Release 109 (2005) 256–274.

40. K.B. Djagny, Z. Wang, S. Xu, Gelatin: a valuable protein for food and pharmaceutical industries: review, Crit. Rev. Food Sci. Nutr. 41 (2001) 481–492.

41. D. Olsen, C. Yang, M. Bodo, R. Chang, S. Leigh, J. Baez, D. Carmichael, M. Perala, E.-R. Hamalainen, M. Jarvinen, J. Polarek, Recombinant collagen and gelatin for drug delivery, Adv. Drug Deliv. Rev. 55 (2003) 1547–1567.

42. S.B. Ross-Murphy, Structure and rheology of gelatin gels: recent progress, Polymer 33 (1992) 2622–2627.

43. L. Ren, A. Osaka, B. Yu, W. Shi, D.T. Ge, S. Chen, Q.Q. Zhang, Bioactive Gelatin–Siloxane Hybrids as Tissue Engineering Scaffolds, in: C.J. Sun, J. Ding, M. Gupta, G.M. Chow, L. Kurihara, L. Kabacoff (Eds.), Solid State Phenomena: Science and Technology Hybrid Materials, vol. 111, Trans Tech Publications, Switzerland, 2006, pp. 13–18.

44. T.A. Holland, Y. Tabata, A.G. Mikos, *In vitro* release of transforming growth factor-beta1 from gelatin microparticles encapsulated in biodegradable, injectable oligo(poly(ethylene glycol) fumarate) hydrogels, J. Control. Release 91 (2003) 299–313.

45. T.A. Holland, J.K.V. Tessmar, Y. Tabata, A.G. Mikos, Transforming growth factor-beta1 release from oligo(poly(ethylene glycol) fumarate) hydrogels in conditions that model the cartilage wound healing environment, J. Control. Release 94 (2004) 101–114.

46. T.A. Holland, Y. Tabata, A.G. Mikos, Dual growth factor delivery from degradable oligo(poly(ethylene glycol) fumarate) hydrogel scaffolds for cartilage tissue engineering, J. Control. Release 101 (2005) 111–125.

47. H. Park, J.S. Temenoff, T.A. Holland, Y. Tabata, A.G. Mikos, Delivery of TGF-beta1 and chondrocytes via injectable, biodegradable hydrogels for cartilage tissue engineering applications, Biomaterials 26 (2005) 7095–7103.

48. H.A. Awad, M. Quinn Wickham, H.A. Leddy, J.M. Gimble, F. Guilak, Chondrogenic differentiation of adipose-derived adult stem cells in agarose, alginate, and gelatin scaffolds, Biomaterials 25 (2004) 3211–3222.

49. T. Okamoto, Y. Yamamoto, M. Gotoh, C.-L. Huang, T. Nakamura, Y. Shimizu, Y. Tabata, H. Yokomise, Slow release of bone morphogenetic protein 2 from a gelatin sponge to promote regeneration of tracheal cartilage in a canine model, J. Thorac. Cardiovasc. Surg. 127 (2004) 329–334.

50. T. Okamoto, Y. Yamamoto, M. Gotoh, D. Liu, M. Kihara, K. Kameyama, E. Hayashi, K. Nakamura, A. Yamauchi, C.L. Huang, H. Yokomise, M. Yamamoto, T. Nakamura, Y. Shimizu, Y. Tabata, Cartilage regeneration using slow release of bone morphogenetic protein-2 from a gelatin sponge to treat experimental canine tracheomalacia: a preliminary report, Asaio J. 49 (2003) 63–69.

51. A. Ito, A. Mase, Y. Takizawa, M. Shinkai, H. Honda, K.-I. Hata, M. Ueda,T. Kobayashi, Transglutaminase-mediated gelatin matrices incorporating cell adhesion factors as a biomaterial for tissue engineering, J. Biosci. Bioeng. 95 (2003) 196–199.

52. T. Masuda, M. Furue, T. Matsuda, Photocured, styrenated gelatin-based microspheres for *de novo* adipogenesis through co-release of basic fibroblast growth factor, insulin, and insulin-like growth factor I, Tissue Eng. 10 (2004) 523–535.

53. Y. Kimura, M. Ozeki, T. Inamoto, Y. Tabata, Adipose tissue engineering based on human preadipocytes combined with gelatin microspheres containing basic fibroblast growth factor, Biomaterials 24 (2003) 2513–2521.

54. R.G. Payne, J.S. McGonigle, M.J. Yaszemski, A.W. Yasko, A.G. Mikos, Development of an injectable, *in situ* crosslinkable, degradable polymeric carrier for osteogenic cell populations. Part 2. Viability of encapsulated marrow stromal osteoblasts cultured on crosslinking poly(propylene fumarate), Biomaterials 23 (2002) 4373–4380.

55. R.G. Payne, M.J. Yaszemski, A.W. Yasko, A.G. Mikos, Development of an injectable, *in situ* crosslinkable, degradable polymeric carrier for osteogenic cell populations. Part 1. Encapsulation of marrow stromal osteoblasts in surface crosslinked gelatin microparticles, Biomaterials 23 (2002) 4359–4371.

56. J. Malda, E. Kreijveld, J.S. Temenoff, C.A.V. Blitterswijk, J. Riesle, Expansion of human nasal chondrocytes on macroporous microcarriers enhances redifferentiation, Biomaterials 24 (2003) 5153–5161.

57. M.S. Ponticiello, R.M. Schinagl, S. Kadiyala, F.P. Barry, Gelatin-based resorbable sponge as a carrier matrix for human mesenchymal stem cells in cartilage regeneration therapy, J. Biomed. Mater. Res. 52 (2000) 246–255.

58. Y. Liu, X.Z. Shu, G.D. Prestwich, Osteochondral defect repair with autologous bone marrow derived mesenchymal stem cells in an injectable, in situ, cross-linked synthetic extracellular matrix, Tissue Eng. 12 (2006) 3405–3416.

59. G.H. Altman, F. Diaz, C. Jakuba, T. Calabro, R.L. Horan, J. Chen, H. Lu, J. Richmond, D.L. Kaplan, Silk-based biomaterials, Biomaterials 24 (2003) 401–416.

60. M.B. Hinman, J.A. Jones, R.V. Lewis, Synthetic spider silk: a modular fiber, Trends Biotech. 18 (2000) 374–379.

61. Y. Tamada, New process to form a silk fibroin porous 3-D structure, Biomacromolecules 6 (2005) 3100–3106.

62. S. Inoue, K. Tanaka, F. Arisaka, S. Kimura, K. Ohtomo, S. Mizuno, Silk fibroin of Bombyx mori is secreted, assembling a high molecular mass elementary unit consisting of H-chain, L-chain and P25, with a 6:6:1 molar ratio, J. Biol. Chem. 275 (2000) 40517–40528.

63. I. Dal Pra, G. Freddi, J. Minic, U. Armato, *De novo* engineering of reticular connective tissue in vivo by silk fibroin nonwoven materials, Biomaterials 26 (2005) 1987–1999.

64. R.L. Horan, K. Antle, A.L. Collette, Y. Wang, J. Huang, J.E. Moreau, In vitro degradation of silk fibroin, Biomaterials 26 (2005) 3385–3393.

65. S. Hofmann, C. Foo, F. Rossetti, M. Textor, G. Vunjak-Novakovic, D.L. Kaplan, H.P. Merkle, L. Meinel, Silk fibroin as an organic polymer for controlled drug delivery, J. Control. Release 111 (2006) 219–227.

66. S. Sofia, M.B. MacCarthy, G. Gronowiz, D.L. Kaplan, Functionalized silk based biomaterials, J. Biomed. Mater. Res. 54 (2001) 139–148.

67. C. Li, C. Vepari, H.-J. Jin, H.J. Kim, D.L. Kaplan, Electrospun silk-BMP¬2 scaffolds for bone tissue engineering, Biomaterials 27 (2006) 3115–3124.

68. M. Fini, A. Motta, P. Torricelli, G. Glavaresi, N.N. Aldini, M. Tschon, R. Giardino, C. Migliaresi, The healing of confined critical size cancellous defects in the presence of silk fibroin hydrogel, Biomaterials 26 (2005) 3527–3536.

69. S. Fuchs, A. Motta, C. Migliaresi, C.J. Kirkpatrick, Outgrowth endothelial cells isolated and expanded from human peripheral blood progenitor cells for endothelialization as a potential source of autologous of silk fibroin biomaterials, Biomaterials 27 (2006) 5399–5408.

70. R.E. Unger, K. Peters, M. Wolf, A. Motta, C. Migliaresi, C.J. Kirkpatrick, Endothelialization of a non-woven silk fibroin net for use in tissue engineering: growth and gene regulation of human endothelial cells, Biomaterials 25 (2004) 5137–5146.

71. Y. Wang, U.-J. Kim, D.J. Blasioli, H.-J. Kim, D.L. Kaplan, In vitro cartilage tissue engineering with 3D porous aqueous-derived silk scaffolds and mesenchymal stem cells, Biomaterials 26 (2005) 7082–7094.

72. B.M. Min, G. Lee, S.H. Kim, Y.S. Nam, T.S. Lee, Electrospinning of silk fibroin nanofibers and its effect on the adhesion and spreading of normal human keratinocytes and fibroblasts in vitro, Biomaterials 25 (2004) 1289–1297.

73. Q. Lv, Q. Feng, K. Hu, F. Cui, Three-dimensional fibroin/collagen scaffolds derived from aqueous solution and the use for HepG2 culture, Polymer 46 (2005) 12662–12669.

74. G.H. Altman, R.L. Horan, H.H. Lu, J.E. Moreau, I. Martin, J.C. Richmond, D.L. Kaplan, Silk matrix for tissue engineered anterior cruciate ligaments, Biomaterials 23 (2002) 4131–4141.

75. R. Hino, M. Tomito, K. Yoshizato, The generation of germline transgenic silkworms for the production of biologically active recombinant fusion proteins of fibroin and human basic fibroblast growth factor, Biomaterials 27 (2006) 5715–5724.

76. T. Aper, A. Schmidt, M. Duchrow, H.-P. Bruch, Autologous blood vessels engineered from peripheral blood sample, Eur. J. Vasc. Endovasc. Surg. 33 (2007) 33–39.

77. M.R. Neidert, E.S. Lee, T.R. Oegema, R.T. Tranquillo, Enhanced fibrin remodeling in vitro with TGF-beta1, insulin and plasmin for improved tissue-equivalents, Biomaterials 23 (2002) 3717–3731.

78. S.L. Rowe, S. Lee, J.P. Stegemann, Influence of thrombin concentration on the mechanical and morphological properties of cell-seeded fibrin hydrogels, Acta Biomaterialia 3 (2007) 59–67.

79. A.S. Wolberg, Thrombin generation and fibrin clot structure, Blood Rev. 21 (2007) 131–142.

80. H. Schmoekel, J.C. Schense, F.E. Weber, K.W. Gratz, D. Gnagi, R. Muller, J.A. Hubbell, Bone healing in the rat and dog with nonglycosylated BMP-2 demonstrating low solubility in fibrin matrices, J. Orthop. Res. 22 (2004) 376–381.

81. M. Ehrbar, A. Metters, P. Zammaretti, J.A. Hubbell, A.H. Zisch, Endothelial cell proliferation and progenitor maturation by fibrin-bound VEGF variants with differential susceptibilities to local cellular activity, J. Control. Release 101 (2005) 93–109.

82. D. Le Nihouannen, L.L. Guehennec, T. Rouillon, P. Pilet, M. Bilban, P. Layrolle, G. Daculsi, Micro-architecture of calcium phosphate granules and fibrin glue composites for bone tissue engineering, Biomaterials 27 (2006) 2716–2722.

83. J. Oju, R. Soo Hyun, C. Ji Hyung, B.-S. Kim, Control of basic fibroblast growth factor release from fibrin gel with heparin and concentrations of fibrinogen and thrombin, J. Control. Release 105 (2005) 249–259.

84. S. Cox, M. Cole, B. Tawil, Behavior of human dermal fibroblasts in three-dimensional fibrin clots: dependence on fibrinogen and thrombin concentration, Tissue Eng. 10 (2004) 942–954.

85. W. Ho, B. Tawil, J.C.Y. Dunn, B.M. Wu, The behavior of human mesenchymal stem cells in 3D fibrin clots: dependence on fibrinogen concentration and clot structure, Tissue Eng. 12 (2006) 1587–1595.

86. G. Wechselberger, R. Russell, M. Neumeister, T. Schoeller, H. Piza-Katzer, C. Rainer, Successful transplantation of three tissue-engineered cell types using capsule induction technique and fibrin glue as a delivery vehicle, Plastic Reconst. Surg. 110 (2002) 123–129.

87. S.M. Willerth, K.J. Arendas, D.I. Gottlieb, S.E. Sakiyama-Elbert, Optimization of fibrin scaffolds for differentiation of murine embryonic stem cells into neural lineage cells, Biomaterials 27 (2006) 5990–6003.

88. J.T. Schantz, A. Brandwood, D. Hutmacher, H. Khor, K. Bittner, Osteogenic differentiation of mesenchymal progenitor cells in computer designed fibrin–polymer–ceramic scaffolds manufactured by fused deposition modeling, J. Mater. Sci., Mater. Med. 16 (2005) 807–819.

89. D. Eyrich, F. Brandl, B. Appel, H. Wiese, G. Maier, M. Wenzel, R. Staudenmaier, A. Goepferich, T. Blunk, Long-term stable fibrin gels for cartilage engineering, Biomaterials 28 (2007) 55–65.

90. C.J. Hunter, J.K. Mouw, M.E. Levenston, Dynamic compression of chondrocyte-seeded fibrin gels: effects on matrix accumulation and mechanical stiffness, Osteoarthr. Cartil. 12 (2004) 117–130.

91. C. Perka, O. Schultz, K. Lindenhayn, R.S. Spitzer, M. Muschik, M. Sittinger, G.R. Burmester, Joint cartilage repair with transplantation of embryonic chondrocytes embedded in collagen–fibrin matrices, Clin. Exper. Rheumatol. 18 (2000) 13–22.

92. E.D. Miller, G.W. Fisher, L.E. Weiss, L.M. Walker, P.G. Campbell, Dose-dependent cell growth in response to concentration modulated patterns of FGF-2 printed on fibrin, Biomaterials 27 (2006) 2213–2221.

93. B. Rai, S.H. Teoh, D.W. Hutmacher, T. Cao, K.H. Ho, Novel PCL-based honeycomb scaffolds as drug delivery systems for rhBMP-2, Biomaterials 26 (2005) 3739–3748.

94. O. Jeon, S.-W. Kang, H.-W. Lim, J. Chung, B.-S. Kim, Long-term and zero-order release of basic fibroblast growth factor from heparin-conjugated poly(l-lactide-co-glycolide) nanospheres and fibrin gel, Biomaterials 27 (2006) 1598–1607.

95. O. Jeon, S.H. Ryu, J. Chung, B.-S. Kim, Control of basic fibroblast growth factor release from fibrin gel with heparin and concentrations of fibrinogen and thrombin, J. Control. Release (2005) 249–259.

96. S.J. Taylor, J.W. McDonald, S.E. Sakiyama-Elbert, Controlled release of neurotrophin-3 from fibrin gels for spinal cord injury, J. Control. Release 98 (2004) 281–294.

97. S.J. Taylor, E.S. Rosenzweig, J.W. McDonald III, S.E. Sakiyama-Elbert, Delivery of neurotrophin-3 from fibrin enhances neuronal fiber sprouting after spinal cord injury, J. Control. Release 113 (2006) 226–235.

98. A.C. Lee, V.M. Yu, J.B. Lowe, M.J. Brenner, D.A. Hunter, S.E. Mackinnon, S.E. Sakiyama-Elbert, Controlled release of nerve growth factor enhances sciatic nerve regeneration, Exp. Neurol. 184 (2003) 295–303.

99. S.E. Sakiyama-Elbert, J.A. Hubbell, Controlled release of nerve growth factor from a heparin-containing fibrin-based cell in growth matrix, J. Control. Release 69 (2000) 149–158.

100. S.E. Sakiyama-Elbert, J.A. Hubbell, Development of fibrin derivatives for controlled release of heparin-binding growth factors, J. Control. Release 65 (2000) 389–402.

101. J.K. Mouw, N.D. Case, R.E. Guldberg, A.H.K. Plaas, M.E. Levenston, Variations in matrix composition and GAG fine structure among scaffolds for cartilage tissue engineering, Osteoarthr. Cartil. 13 (2005) 828–836.

102. G.A. Ameer, T.A. Mahmood, R. Langer, A biodegradable composite scaffold for cell transplantation, J. Orthop. Res. 20 (2002) 16–19.

103. C. Perka, R.S. Spitzer, K. Lindenhayn, M. Sittinger, O. Schultz, Matrix-mixed culture: new methodology for chondrocyte culture and preparation of cartilage transplants, J. Biomed. Mater. Res. 49 (2000) 305–311.

104. X.X. Shao, D.W. Hutmacher, S.T. Ho, J.C.H. Goh, E.H. Lee, Evaluation of a hybrid scaffold/cell construct in repair of high-load-bearing osteochondral defects in rabbits, Biomaterials 27 (2006) 1071–1080.

105. A. Mol, M.I. van Lieshout, C.G. Dam-de Veen, S. Neuenschwander, S.P. Hoerstrup, F.P.T. Baaijens, C.V.C. Bouten, Fibrin as a cell carrier in cardiovascular tissue engineering applications, Biomaterials 26 (2005) 3113–3121.

106. C. Buchta, H.C. Hedrich, M. Macher, P. Hocker, H. Redl, Biochemical characterization of autologous fibrin sealants produced by CryoSeal and Vivostat in comparison to the homologous fibrin sealant product Tissucol/Tisseel, Biomaterials 26 (2005) 6233–6241.

107. Q. Lu, K. Ganesan, D.T. Simionescu, N.R. Vyavahare, Novel porous aortic elastin and collagen scaffolds for tissue engineering, Biomaterials 25 (2004) 5227–5237.

108. L. Buttafoco, N.G. Kolkman, P. Engbers-Buijtenhuijs, A.A. Poot, P.J. Dijkstra, I. Vermes, J. Feijen, Electrospinning of collagen and elastin for tissue engineering applications, Biomaterials 27 (2006) 724–734.

109. J.B. Leach, J.B. Wolinsky, P.J. Stone, J.Y. Wong, Crosslinked alpha-elastin biomaterials: towards a processable elastin mimetic scaffold, Acta Biomaterialia 1 (2005) 155–164.

110. H. Betre, S.R. Ong, F. Guilak, A. Chilkoti, B. Fermor, L.A. Setton, Chondrocytic differentiation of human adipose-derived adult stem cells in elastin-like polypeptide, Biomaterials 27 (2006) 91–99.

111. B.F. Gibbs, A. Zougman, R. Masse, C. Mulligan, Production and characterization of bioactive peptides from soy hydrolysate and soy-fermented food, Food Res. Int. 37 (2004) 123–131.

112. P. Lodha, A.N. Netravali, Characterization of stearic acid modified soy protein isolate resin and ramie fiber reinforced 'green' composites, Compos. Sci. Tech. 65 (2005) 1211–1225.

113. C.H. Tang, H. Wu, Z. Chen, X.Q. Yang, Formation and properties of glycinin-rich and beta-conglycinin-rich soy protein isolate gels induced by microbial transglutaminase, Food Res. Int. 39 (2006) 87–97.

114. C.M. Vaz, L.A. de Graaf, R.L. Reis, A.M. Cunha, *In vitro* degradation behaviour of biodegradable soy plastics: effects of crosslinking with glyoxal and thermal treatment, Polym. Degrad. Stability 81 (2003) 65–74.

115. N. Diftis, V. Kiosseoglou, Physicochemical properties of dry-heated soy protein isolate–dextran mixtures, Food Chem. 96 (2006) 228–233.

116. J.J. Guan, A.Y. Qiu, X.Y. Liu, Y.F. Hua, Y.H. Ma, Microwave improvement of soy protein isolate–saccharide graft reactions, Food Chem. 97 (2006) 577–585.

117. S.S. Silva, J.M. Oliveira, J.A. Mano, R.L. Reis, Physicochemical characterization of novel chitosan–soy protein/TEOS porous hybrids for tissue engineering applications, Mater. Sci. Forum (2006) 1000–1004.

118. N. Cao, Y. Fu, J. He, Mechanical properties of gelatin films cross-linked, respectively, by ferulic acid and tannin acid, Food Hydrocoll. 21 (2007) 575–584.

119. S.E. Molina Ortiz, M.C. Puppo, J.R. Wagner, Relationship between structural changes and functional properties of soy protein isolates-carrageenan systems, Food Hydrocolloids 18 (2004) 1045–1053.

120. K.J. Ryan, M.S. Brewer, Purification and identification of interacting components in a wheat starch–soy protein system, Food Chem. 89 (2005) 109–124.

121. C.M. Vaz, M. Fossen, R.F. van Tuil, L.A. de Graaf, R.L. Reis, A.M. Cunha, Casein and soybean protein-based thermoplastics and composites as alternative biodegradable polymers for biomedical applications, J. Biomed. Mater. Res. 65A (2003) 60–70.

122. C.M. Vaz, P.F. Van Doeveren, R.L. Reis, A.M. Cunha, Soy matrix drug delivery systems obtained by melt-processing techniques, Biomacromolecules 4 (2003) 1520–1529.

123. C.M. Vaz, P.F.N.M. van Doeveren, R.L. Reis, A.M. Cunha, Development and design of double-layer co-injection moulded soy protein based drug delivery devices, Polymer 44 (2003) 5983–5992.

124. K. Nishinari, R. Takahashi, Interaction in polysaccharide solutions and gels, Curr. Opin. Colloid Interface Sci. 8 (2003) 396–400.

125. M.G. Cascone, N. Barbani, C. Cristallini, P. Giusti, G. Ciardelli, L. Lazzeri, Bioartificial polymeric materials based on polysaccharides,J. Biomater. Sci., Polym. Ed. 12 (2001) 267–281.

126. J. Venugopal, S. Ramakrishna, Applications of polymer nanofibers in biomedicine and biotechnology, Appl. Biochem. Biotechnol. 125 (2005) 147–157.

127. E. Khor, L.Y. Lim, Implantable applications of chitin and chitosan, Biomaterials 24 (2003) 2339–2349.

128. M. George, T.E. Abraham, Polyionic hydrocolloids for the intestinal delivery of protein drugs: alginate and chitosan - a review, J. Control. Release 114 (2006) 1–14.

129. Y. Huang, S. Onyeri, M. Siewe, A. Moshfeghian, S.V. Madihally, In vitro characterization of chitosan–gelatin scaffolds for tissue engineering, Biomaterials 26 (2005) 7616.

130. V.R. Patel, M.M. Amiji, Preparation and characterization of freezedried chitosan-poly(ethylene oxide) hydrogels for site-specific antibiotic delivery in the stomach, Pharmac. Res. 13 (1996) 588–593.

131. P.B. Malafaya, A. Pedro, A. Peterbauer, C. Gabriel, H. Redl, R. Reis, Chitosan particles agglomerated scaffolds for cartilage and osteochondral tissue engineering approaches with adipose tissue derived stem cells, J. Mater. Sci., Mater. Med. 16 (2005) 1077–1085.

132. M. Julien, D.R. Letouneau, Y. Marois, A. Cardou, M.W. King, R. Guidoin, D. Chachra, J.M. Lee, Shelf-life of bioprosthetic heart valves: a structural and mechanical study, Biomaterials 18 (1997) 605–612.

133. S.C. Chen, Y.C. Wu, F.L. Mi, Y.H. Lin, L.C. Yu, H.W. Sung, A novel pH-sensitive hydrogel composed of N,O-carboxymethyl chitosan and alginate cross-linked by genipin for protein drug delivery, J. Control. Release 96 (2004) 285–300.

134. A. Di Martino, M. Sittinger, M.V. Risbud, Chitosan: a versatile biopolymer for orthopaedic tissue-engineering, Biomaterials 26 (2005) 5983–5990.

135. J.Y. Lee, S.H. Nam, S.Y. Im, Y.J. Park, Y.M. Lee, Y.J. Seol, C.P. Chung, S.J. Lee, Enhanced bone formation by controlled growth factor delivery from chitosan-based biomaterials, J. Control. Release 78 (2002) 187–197.

136. Y. Okamoto, R. Yano, K. Miyatake, I. Tomohiro, Y. Shigemasa, S. Minami, Effects of chitin and chitosan on blood coagulation, Carbohyd. Polym. 53 (2003) 337–342.

137. D.K. Kweon, S.B. Song, Y.Y. Park, Preparation of water-soluble chitosan/heparin complex and its application as wound healing accelerator, Biomaterials 24 (2003) 1595–1601.

138. H. Ueno, T. Mori, T. Fujinaga, Topical formulations and wound healing applications of chitosan, Adv. Drug Deliv. Rev. 52 (2001) 105–115.

139. C. Alemdaroglu, Z. Degim, N. Celebi, F. Zor, S. Ozturk, D. Erdogan, An investigation on burn wound healing in rats with chitosan gel formulation containing epidermal growth factor, Burns 32 (2006) 319–327.

140. I.C. Liao, A.C.A. Wan, E.K.F. Yim, K.W. Leong, Controlled release from fibers of polyelectrolyte complexes, J. Control. Release 104 (2005) 347–358.

141. I.K. Park, J. Yang, H.J. Jeong, H.S. Bom, I. Harada, T. Akaike, S.I. Kim, C.S. Cho, Galactosylated chitosan as a synthetic extracellular matrix for hepatocytes attachment, Biomaterials 24 (2003) 2331–2337.

142. J.J. Delgado, C. Evora, E. Sanchez, M. Baro, A. Delgado, Validation of a method for non-invasive in vivo measurement of growth factor release from a local delivery system in bone, J. Control. Release 114 (2006) 223–229.

143. Y. Zhang, X. Cheng, J. Wang, Y. Wang, B. Shi, C. Huang, X. Yang, T. Liu, Novel chitosan/collagen scaffold containing transforming growthfactor-beta1 DNA for periodontal tissue engineering, Biochem. Biophys. Res. Commun. 344 (2006) 362–369.

144. Y. Zhang, Y. Wang, B. Shi, X. Cheng, A platelet-derived growth factor releasing chitosan/coral composite scaffold for periodontal tissue engineering, Biomaterials 28 (2007) 1515–1522.

145. Y. Jeong Park, Y. Moo Lee, S. Nae Park, S. Yoon Sheen, C. Pyoung Chung, S.J. Lee, Platelet derived growth factor releasing chitosan sponge for periodontal bone regeneration, Biomaterials 21 (2000) 153–159.

146. T. Guo, J. Zhao, J. Chang, Z. Ding, H. Hong, J. Chen, J. Zhang, Porous chitosan-gelatin scaffold containing plasmid DNA encoding transforming growth factor-beta1 for chondrocytes proliferation, Biomaterials 27 (2006) 1095–1103.

147. S.E. Kim, J.H. Park, Y.W. Cho, H. Chung, S.Y. Jeong, E.B. Lee, I.C. Kwon, Porous chitosan scaffold containing microspheres loaded with transforming growth factor-beta1: implications for cartilage tissue engineering, J. Control. Release 91 (2003) 365–374.

148. J.E. Lee, K.E. Kim, I.C. Kwon, H.J. Ahn, S.-H. Lee, H. Cho, H.J. Kim, S.C. Seong, M.C. Lee, Effects of the controlled-released TGF-beta1 from chitosan microspheres on chondrocytes cultured in a collagen/chitosan/ glycosaminoglycan scaffold, Biomaterials 25 (2004) 4163–4173.

149. A. Chevrier, C.D. Hoemann, J. Sun, M.D. Buschmann, Chitosan-glycerol phosphate/blood implants increase cell recruitment, transient vascularization and subchondral bone remodeling in drilled cartilage defects, Osteoarthr. Cartil. 15 (2007) 316–327.

150. M. Fujita, M. Ishihara, M. Simizu, K. Obara, T. Ishizuka, Y. Saito, H. Yura, Y. Morimoto, B. Takase, T. Matsui, M. Kikuchi, T. Maehara, Vascularization in vivo caused by the controlled release of fibroblast growth factor-2 from an injectable chitosan/non-anticoagulant heparin hydrogel, Biomaterials 25 (2004) 699–706.

151. M. Fujita, M. Ishihara, Y. Morimoto, M. Simizu, Y. Saito, H. Yura, T. Matsui, B. Takase, H. Hattori, Y. Kanatani, M. Kikuchi, T. Maehara, Efficacy of photocrosslinkable chitosan hydrogel containing fibroblast growth factor-2 in a rabbit model of chronic myocardial infarction, J. Surg. Res. 126 (2005) 27–33.

152. A. Goraltchouk, V. Scanga, C.M. Morshead, M.S. Shoichet, Incorpo¬ration of protein-eluting microspheres into biodegradable nerve guidance channels for controlled release, J. Control. Release 110 (2006) 400–407.

153. K. Obara, M. Ishihara, T. Ishizuka, M. Fujita, Y. Ozeki, T. Maehara, Y. Saito, H. Yura, T. Matsui, H. Hattori, M. Kikuchi, A. Kurita, Photocrosslinkable chitosan hydrogel containing fibroblast growth factor-2 stimulates wound healing in healing-impaired db/db mice, Biomaterials 24 (2003) 3437–3444.

154. W.R. Morrison, J. Karkalas, Starch, in: P.M. Dey (Ed.), Methods in Plant Biochemistry: Carbohydrates, vol. 2, Academic Press Limited, London, 1990, pp. 323–352.

155. K. Poutanen, P. Forssell, Modification of starch properties with plasticizers, Trends Polym. Sci. 4 (1996) 128–132.

156. P.A. Dell, W.G. Kohlman, Effects of water-content on the properties of starch poly(ethylene vinyl alcohol) blends, J. Appl. Polym. Sci. 52 (1994) 353–363.

157. C. Bastioli, A. Cerutti, I. Guanella, G.C. Romano, M. Tosin, Physical state and biodegradation behavior of starch–polycaprolactone systems, J. Environ. Polym. Degrad. 3 (1995) 81–95.

158. M.A. Villar, E.L. Thomas, R.C. Armstrong, Rheological properties of thermoplastic starch and starch poly(ethylene-co-vinyl alcohol) blends, Polymer 36 (1995) 1869–1876.

159. M.A. Kotnis, G.S. Obrien, J.L. Willett, Processing and mechanical properties of biodegradable poly(hydroxybutyrate-co-valerate)-starch compositions, J. Environ. Polym. Degrad. 3 (1995) 97–105.

160. J.M. Mayer, G.R. Elion, C.M. Buchanan, B.K. Sullivan, S.D. Pratt, D.L. Kaplan, Biodegradable blends of cellulose–acetate and starch: production and properties, J. Macromol. Sci., Part A, Pure Appl. Chem. 32 (1995) 775–785.

161. D. Trimnell, G.F. Fanta, Formulations prepared from polyacrylamide and starch, J. Polym. Mater. 11 (1994) 271–277.

162. J. Nakamatsu, F.G. Torres, O.P. Troncoso, M.L. Yuan, A.R. Boccaccini, Processing and characterization of porous structures from chitosan and starch for tissue engineering scaffolds, Biomacromolecules 7 (2006) 3345–3355.

163. A.K. Bajpai, J. Shrivastava, alpha-Amylase induced enhanced enzymatic degradation of binary polymeric blends of crosslinked starch and gelatin, J. Macromol. Sci., Part A, Pure Appl. Chem. 41 (2004) 949–969.

164. I. Pashkuleva, A.P. Marques, F. Vaz, R.L. Reis, Surface modification of starch based blends using potassium permanganate-nitric acid system and its effect on the adhesion and proliferation of osteoblast-like cells, J. Mater. Sci., Mater. Med. 16 (2005) 81–92.

165. K.M. Mostafa, Graft-polymerization of acrylic-acid onto starch using potassium-permanganate acid (redox system), J. Appl. Polym. Sci. 56 (1995) 263–269.

166. G. Williamson, N.J. Belshaw, D.J. Self, T.R. Noel, S.G. Ring, P. Cairns, V.J. Morris, S.A. Clark, M.L. Parker, Hydrolysis of A-type and B-type crystalline polymorphs of starch by alpha-Amylase, beta-Amylase and Glucoamylase-1, Carbohyd. Polym. 18 (1992) 179–187.

167. H.S. Azevedo, F.M. Gama, R.L. Reis, In vitro assessment of the enzymatic degradation of several starch based biomaterials, Biomacromolecules 4 (2003) 1703–1712.

168. L. Tuovinen, S. Peltonen, M. Liikola, M. Hotakainen, M. Lahtela-Kakkonen, A. Poso, K. Jarvinen, Drug release from starch–acetate microparticles and films with and without incorporated alpha-amylase, Biomaterials 25 (2004) 4355–4362.

169. R. Carter, T.G. Cooke, D. Hemingway, C.S. McArdle, W. Angerson, The combination of degradable starch microspheres and angiotensin-Ii in the manipulation of drug delivery in an animal-model of colorectal metastasis, Br. J. Cancer 65 (1992) 37–39.

170. C. Callens, J.P. Remon, Evaluation of starch–maltodextrin–Carbopol 974P mixtures for the nasal delivery of insulin in rabbits, J. Control. Release 66 (2000) 215–220.

171. C. Desevaux, V. Lenaerts, C. Girard, P. Dubreuil, Characterization of crosslinked high amylose starch matrix implants: 2. *in vivo* release of ciprofloxacin, J. Control. Release 82 (2002) 95–103.

172. C. Sturesson, L.D. Wikingsson, Comparison of poly(acryl starch) and poly(lactide-co-glycolide) microspheres as drug delivery system for a rotavirus vaccine, J. Control. Release 68 (2000) 441–450.

173. R.L. Reis, A.M. Cunha, Characterization of two biodegradable polymers of potential application within the biomaterials field, J. Mater. Sci., Mater. Med. 6 (1995) 786–792.

174. M.E. Gomes, A.S. Ribeiro, P.B. Malafaya, R.L. Reis, A.M. Cunha, A new approach based on injection moulding to produce biodegradable starch-based polymeric scaffolds: morphology, mechanical and degradation behaviour, Biomaterials 22 (2001) 883–889.

175. C.X.F. Lam,X.M.Mo, S.H. Teoh, D.W.Hutmacher, Scaffold development using 3D printing with a starch-based polymer, Mater. Sci. Eng., C, Biomim. Mater., Sens. Syst. 20 (2002) 49–56.

176. F.G. Torres, A.R. Boccaccini, O.P. Troncoso, Microwave processing of starch-based porous structures for tissue engineering scaffolds, J. Appl. Polym. Sci. 103 (2007) 1332–1339.

177. M.E. Gomes, J.S. Godinho, D. Tchalamov, A.M. Cunha, R.L. Reis, Alternative tissue engineering scaffolds based on starch: processing methodologies, morphology, degradation and mechanical properties, Mater. Sci. Eng., C, Biomim. Mater., Sens. Syst. 20 (2002) 19–26.

178. L.F. Boesel, R.L. Reis, The effect of water uptake on the behaviour of hydrophilic cements in confined environments, Biomaterials 27 (2006) 5627–5633.

179. I. Espigares, C. Elvira, J.F. Mano, B. Vazquez, J. San Roman, R.L. Reis, New partially degradable and bioactive acrylic bone cements based on starch blends and ceramic fillers, Biomaterials 23 (2002) 1883–1895.

180. P.B. Malafaya, F. Stappers, R.L. Reis, Starch-based microspheres produced by emulsion crosslinking with a potential media dependent responsive behavior to be used as drug delivery carriers, J. Mater. Sci., Mater. Med. 17 (2006) 371–377.

181. G.A. Silva, F.J. Costa, N.M. Neves, O.P. Coutinho, A.C.P. Dias, R.L. Reis, Entrapment ability and release profile of corticosteroids from starch-based particles, J. Biomed. Mater. Res. 73 (2005) 234–243.

182. G.A. Silva, O.P. Coutinho, P. Ducheyne, I.M. Shapiro, R.L. Reis. Starch-based microparticles as vehicles for the delivery of active platelet-derived growth factor. Tissue Eng. 13 (2007) 1259-1268.

183. A.P. Marques, R.L. Reis, J.A. Hunt, The biocompatibility of novel starch-based polymers and composites: in vitro studies, Biomaterials 23 (2002) 1471–1478.

184. A.J. Salgado, O.P. Coutinho, R.L. Reis, J.E. Davies, In vivo response to starch-based scaffolds designed for bone tissue engineering applications, J. Biomed. Mater. Res., A 80A (2007) 983–989.

185. M.I. Santos, S. Fuchs, M.E. Gomes, R.E. Unger, R.L. Reis, C.J. Kirkpatrick, Response of micro-and macrovascular endothelial cells to starch-based fiber meshes for bone tissue engineering, Biomaterials 28 (2007) 240–248.

186. G.A. Silva, O.P. Coutinho, P. Ducheyne, I.M. Shapiro, R.L. Reis, The effect of starch and starch-bioactive glass composite microparticles on the adhesion and expression of the osteoblastic phenotype of a bone cell line, Biomaterials 28 (2007) 326–334.

187. M.E. Gomes, R.L. Reis, A.G. Mikos, Bone tissue engineering constructs based on starch scaffolds and bone marrow cells cultured in a flow perfusion bioreactor, Adv. Mater. Forum 514–516 (2006) 980–984.

188. M.M. Stevens, H.F. Qanadilo, R. Langer, V. Prasad Shastri, A rapid-curing alginate gel system: utility in periosteum-derived cartilage tissue engineering, Biomaterials 25 (2004) 887–894.

189. B. Balakrishnan, A. Jayakrishnan, Self-cross-linking biopolymers as injectable in situ forming biodegradable scaffolds, Biomaterials 26 (2005) 3941–3951.

190. D. Tada, T. Tanabe, A. Tachibana, K. Yamauchi. Albumin-crosslinked alginate hydrogels as sustained drug release carrier. Mater. Sci. Eng., C, Biomim. Mater., Sens. Syst. 27(2007) 870-874.

191. K.I. Draget, G. Skjak-Braek, O. Smidsrod, Alginate based new materials, Int. J. Biol. Macromol. 21 (1997) 47–55.

192. J.L. Drury, R.G. Dennis, D.J. Mooney, The tensile properties of alginate hydrogels, Biomaterials 25 (2004) 3187–3199.

193. N.E. Simpson, C.L. Stabler, C.P. Simpson, A. Sambanis, I. Constantinidis, The role of the $CaCl_2$-guluronic acid interaction on alginate encapsulated betaTC3 cells, Biomaterials 25 (2004) 2603–2610.

194. D.M. Yoon, E.C. Hawkins, S. Francke-Carroll, J.P. Fisher, Effect of construct properties on encapsulated chondrocyte expression of insulin-like growth factor-1, Biomaterials 28 (2007) 299–306.

195. C.K. Kuo, P.X. Ma, Ionically crosslinked alginate hydrogels as scaffolds for tissue engineering: part 1. structure, gelation rate and mechanical properties, Biomaterials 22 (2001) 511–521.

196. T. Pongjanyakul, S. Puttipipatkhachorn, Xanthan-alginate composite gel beads: molecular interaction and in vitro characterization, Int. J. Pharm. 331 (2007) 61–71.

197. T. Grunder, C. Gaissmaier, J. Fritz, R. Stoop, P. Hortschansky, J. Mollenhauer, W.K. Aicher, Bone morphogenetic protein-2 enhances the expression of type II collagen and aggrecan in chondrocytes embedded in alginate beads, Osteoarthr. Cartil. 12 (2004) 559–567.

198. Y.M. Jenniskens, W. Koevoet, A.C.W. de Bart, H. Weinans, H. Jahr, J.A.N. Verhaar, J. DeGroot, G.J.V.M. van Osch, Biochemical and functional modulation of the cartilage collagen network by IGF1, TGF¬beta2 and FGF2, Osteoarthr. Cartil. 14 (2006) 1136–1146.

199. K. Masuda, B.E. Pfister, R.L. Sah, E.J.M.A. Thonar, Osteogenic protein-1 promotes the formation of tissue-engineered cartilage using the alginate-recovered-chondrocyte method, Osteoarthr. Cartil. 14 (2006) 384–391.

200. M.M. Stevens, R.P. Marini, I. Martin, R. Langer, V.P. Shastri, FGF-2 enhances TGF-beta1-induced periosteal chondrogenesis, J. Orthop. Res. 22 (2004) 1114–1119.

201. C. Kaps, C. Bramlage, H. Smolian, A. Haisch, U. Ungethum, G.R. Burmester, M. Sittinger, G. Gross, T. Haupl, Bone morphogenetic proteins promote cartilage differentiation and protect engineered artificial cartilage from fibroblast invasion and destruction, Arthritis Rheum. 46 (2002) 149–162.

202. C.M. Mierisch, S.B. Cohen, L.C. Jordan, P.G. Robertson, G. Balian, D.R. Diduch, Transforming growth factor-beta in calcium alginate beads for the treatment of articular cartilage defects in the rabbit, Arthrosc.-J. Arthrosc. Related Sur. 18 (2002) 892–900.

203. Y. Park, M. Sugimoto, A. Watrin, M. Chiquet, E.B. Hunziker, BMP-2 induces the expression of chondrocyte-specific genes in bovine synovium-derived progenitor cells cultured in three-dimensional alginate hydrogel, Osteoarthr. Cartil. 13 (2005) 527–536.

204. C. Gaissmaier, J. Fritz, T. Krackhardt, I. Flesch, W.K. Aicher, N. Ashammakhi, Effect of human platelet supernatant on proliferation and matrix synthesis of human articular chondrocytes in monolayer and three-dimensional alginate cultures, Biomaterials 26 (2005) 1953–1960.

205. K. Akeda, H.S. An, M. Okuma, M. Attawia, K. Miyamoto, E.J.M.A. Thonar, M.E. Lenz, R.L. Sah, K. Masuda, Platelet-rich plasma stimulates porcine articular chondrocyte proliferation and matrix biosynthesis, Osteoarthr. Cartil. 14 (2006) 1272–1280.

206. H. Huwer, J. Winning, B. Vollmar, J. Rissland, C. Welter, H.-J. Schafers, M.D. Menger, Microvascularization and ventricular function after local alginate-encapsulated angiogenic growth factor treatment in a rat cryothermia-induced myocardial infarction model, Microvasc. Res. 62 (2001) 211–214.

207. K.Y. Lee, M.C. Peters, D.J. Mooney, Comparison of vascular endothelial growth factor and basic fibroblast growth factor on angiogenesis in SCID mice, J. Control. Release 87 (2003) 49–56.

208. H. Keshaw, A. Forbes, R.M. Day, Release of angiogenic growth factors from cells encapsulated in alginate beads with bioactive glass, Biomaterials 26 (2005) 4171–4179.

209. H.K. Tilakaratne, S.K. Hunter, M.E. Andracki, J.A. Benda, V.G.J. Rodgers, Characterizing short-term release and neovascularization potential of multi-protein growth supplement delivered via alginate hollow fiber devices, Biomaterials 28 (2007) 89–98.

210. E. Vogelin, J.M. Baker, J. Gates, V. Dixit, M.A. Constantinescu, N.F. Jones, Effects of local continuous release of brain derived neurotrophic factor (BDNF) on peripheral nerve regeneration in a rat model, Exp. Neurol. 199 (2006) 348–353.

211. C.A. Simmons, E. Alsberg, S. Hsiong, W.J. Kim, D.J. Mooney, Dual growth factor delivery and controlled scaffold degradation enhance in vivo bone formation by transplanted bone marrow stromal cells, Bone 35 (2004) 562–569.

212. H. Gruber, E. Fisher, B. Desai, A. Stasky, G. Hoelscher, E. Hanley, Human intervertebral disc cells from the annulus: three-dimensional culture in agarose or alginate and responsiveness to TGF-beta1, Exp. Cell Res. 235 (1997) 13–21.

213. G.R. Erickson, J.M. Gimble, D.M. Franklin, H.E. Rice, H. Awad, F. Guilak, Chondrogenic potential of adipose tissue-derived stromal cells in vitro and in vivo, Biochem. Biophys. Res. Commun. 290 (2002) 763–769.

214. H.K. Heywood, D.L. Bader, D.A. Lee, Glucose concentration and medium volume influence cell viability and glycosaminoglycan synthesis in chondrocyte-seeded alginate constructs, Tissue Eng. 12 (2006) 3487–3496.

215. Y. Dausse, L. Grossin, G. Miralles, S. Pelletier, D. Mainard, P. Hubert, D. Baptiste, P. Gillet, E. Dellacherie, P. Netter, E. Payan, Cartilage repair using new polysaccharidic biomaterials: macroscopic, histological and biochemical approaches in a rat model of cartilage defect, Osteoarthr. Cartil. 11 (2003) 16–28.

216. W.J.C.M. Marijnissen, G.J.V.M. van Osch, J. Aigner, S.W. van der Veen, A.P. Hollander, H.L. Verwoerd-Verhoef, J.A.N. Verhaar, Alginate as a chondrocyte-delivery substance in combination with a non-woven scaffold for cartilage tissue engineering, Biomaterials 23 (2002) 1511–1517.

217. S.B. Cohen, C.M. Meirisch, H.A. Wilson, D.R. Diduch, The use of absorbable co-polymer pads with alginate and cells for articular cartilage repair in rabbits, Biomaterials 24 (2003) 2653–2660.

218. J.C. Pound, D.W. Green, J.B. Chaudhuri, S. Mann, H.I. Roach, R.O.C. Oreffo, Strategies to promote chondrogenesis and osteogenesis from human bone marrow cells and articular chondrocytes encapsulated in polysaccharide templates, Tissue Eng. 12 (2006) 2789–2799.

219. Y.H. Liao, S.A. Jones, B. Forbes, G.P. Martin, M.B. Brown, Hyaluronan: pharmaceutical characterization and drug delivery, Drug Deliv. 12 (2005) 327–342.

220. T.C. Laurent, U.B.G. Laurent, J.R.E. Fraser, Functions of hyaluronan, Ann. Rheum. Dis. 54 (1995) 429–432.

221. Y. Ji, K. Ghosh, B.Q. Li, J.C. Sokolov, R.A.F. Clark, M.H. Rafailovich, Dual-syringe reactive electrospinning of cross-linked hyaluronic acid hydrogel nanofibers for tissue engineering applications, Macromol. Biosci. 6 (2006) 811–817.

222. H.S. Nam, J. An, D.J. Chung, J.H. Kim, C.P. Chung, Controlled release behavior of bioactive molecules from photo-reactive hyaluronic acid-alginate scaffolds, Macromol. Res. 14 (2006) 530–538.

223. S. Cai, Y. Liu, X. Zheng Shu, G.D. Prestwich, Injectable glycosaminoglycan hydrogels for controlled release of human basic fibroblast growth factor, Biomaterials 26 (2005) 6054–6067.

224. D. Gupta, C.H. Tator, M.S. Shoichet, Fast-gelling injectable blend of hyaluronan and methylcellulose for intrathecal, localized delivery to the injured spinal cord, Biomaterials 27 (2006) 2370–2379.

225. J. Aigner, J. Tegeler, P. Hutzler, D. Campoccia, A. Pavesio, C. Hammer, E. Kastenbauer, A. Naumann, Cartilage tissue engineering with novel nonwoven structured biomaterial based on hyaluronic acid benzyl ester, J. Biomed. Mater. Res. 42 (1998) 172–181.

226. C. Chung, J. Mesa, G.J. Miller, M.A. Randolph, T.J. Gill, J.A. Burdick, Effects of auricular chondrocyte expansion on neocartilage formation in photocrosslinked hyaluronic acid networks, Tissue Eng. 12 (2006) 2665–2673.

227. M. Radice, P. Brun, R. Cortivo, R. Scapinelli, C. Battaliard, G. Abatangelo, Hyaluronan-based biopolymers as delivery vehicles for bone-marrow-derived mesenchymal progenitors, J. Biomed. Mater. Res. 50 (2000) 101–109.

228. Y.H. Yun, D.J. Goetz, P. Yellen, W.L. Chen, Hyaluronan microspheres for sustained gene delivery and site-specific targeting, Biomaterials 25 (2004) 147–157.

229. N.J. Turner, C.M. Kielty, M.G. Walker, A.E. Canfield, A novel hyaluronan-based biomaterial (Hyaff-11) as a scaffold for endothelial cells in tissue engineered vascular grafts, Biomaterials 25 (2004) 5955–5964.

230. E. Pianigiani, A. Andreassi, P. Taddeucci, C. Alessandrini, M. Fimiani, L. Andreassi, A new model for studying differentiation and growth of epidermal cultures on hyaluronan-based carrier, Biomaterials 20 (1999) 1689–1694.

231. J.S. Pieper, A. Oosterhof, P.J. Dijkstra, J.H. Veerkamp, T.H. van Kuppevelt, Preparation and characterization of porous crosslinked collagenous matrices containing bioavailable chondroitin sulphate, Biomaterials 20 (1999) 847–858.
232. L. Lippiello, Glucosamine and chondroitin sulfate: biological response modifiers of chondrocytes under simulated conditions of joint stress, Osteoarthr. Cartil. 11 (2003) 335–342.

233. C.T. Lee, P.H. Kung, Y.D. Lee, Preparation of poly(vinyl alcohol)chondroitin sulfate hydrogel as matrices in tissue engineering, Carbohydr. Polym. 61 (2005) 348–354.

234. C.T. Bassleer, J.P.A. Combal, S. Bougaret, M. Malaise, Effects of chondroitin sulfate and interleukin-1[beta] on human articular chondrocytes cultivated in clusters, Osteoarthr. Cartil. 6 (1998) 196–204.

235. C.M. Galtrey, J.W. Fawcett. The role of chondroitin sulfate proteoglycans in regeneration and plasticity in the central nervous system. Brain Res. Rev. 54 (2007) 1-18.

236. A. Sintov, N. Di-Capua, A. Rubinstein, Cross-linked chondroitin sulphate: characterization for drug delivery purposes, Biomaterials 16 (1995) 473–478.

237. S.C. Wang, B.H. Chen, L.F. Wang, J.S. Chen, Characterization of chondroitin sulfate and its interpenetrating polymer network hydrogels for sustained-drug release, Int. J. Pharmacogn. 329 (2007) 103–109.

238. Y.J. Park, Y.M. Lee, J.Y. Lee, Y.J. Seol, C.P. Chung, S.J. Lee, Controlled release of platelet-derived growth factor-BB from chondroitin sulfate–chitosan sponge for guided bone regeneration, J. Control. Release 67 (2000) 385–394.

239. C.H. Chang, H.C. Liu, C.C. Lin, C.H. Chou, F.H. Lin, Gelatin–chondroitin–hyaluronan tri-copolymer scaffold for cartilage tissue engineering, Biomaterials 24 (2003) 4853–4858.

240. H. Fan, Y. Hu, C. Zhang, X. Li, R. Lv, L. Qin, R. Zhu, Cartilage regeneration using mesenchymal stem cells and a PLGA-gelatin/chondroitin/hyaluronate hybrid scaffold, Biomaterials 27 (2006) 4573–4580.

241. T.C. Flanagan, B. Wilkins, A. Black, S. Jockenhoevel, T.J. Smith, A.S. Pandit, A collagen-glycosaminoglycan co-culture model for heart valve tissue engineering applications, Biomaterials 27 (2006) 2233–2246.

242. D.S. Keskin, A. Tezcaner, P. Korkusuz, F. Korkusuz, V. Hasirci, Collagen–chondroitin sulfate-based PLLA-SAIB-coated rhBMP-2 delivery system for bone repair, Biomaterials 26 (2005) 4023–4034.

243. M. Jensen, P. Birch Hansen, S. Murdan, S. Frokjaer, A.T. Florence, Loading into and electro-stimulated release of peptides and proteins from chondroitin 4-sulphate hydrogels, Eur. J. Pharm. Sci. 15 (2002) 139–148.

244. Y. Liu, H. Yang, K. Otaka, H. Takatsuki, A. Sakanishi, Effects of vascular endothelial growth factor (VEGF) and chondroitin sulfate A on human monocytic THP-1 cell migration, Colloids Surf., B Biointerfaces 43 (2005) 216–220.

245. W.F. Daamen, H.T.B. van Moerkerk, T. Hafmans, L. Buttafoco, A.A. Poot, J.H. Veerkamp, T.H. van Kuppevelt, Preparation and evaluation of molecularly-defined collagen–elastin–glycosaminoglycan scaffolds for tissue engineering, Biomaterials 24 (2003) 4001–4009.

246. C.-H. Chang, T.-F. Kuo, C.-C. Lin, C.-H. Chou, K.-H. Chen, F.-H. Lin, H.-C. Liu, Tissue engineering-based cartilage repair with allogenous chondrocytes and gelatin–chondroitin–hyaluronan tri-copolymer scaffold: a porcine model assessed at 18, 24, and 36 weeks, Biomaterials 27 (2006) 1876–1888.

247. J.L.C. van Susante, J. Pieper, P. Buma, T.H. van Kuppevelt, H. van Beuningen, P.M. van der Kraan, J.H. Veerkamp, W.B. van den Berg, R.P. H. Veth, Linkage of chondroitin-sulfate to type I collagen scaffolds stimulates the bioactivity of seeded chondrocytes in vitro, Biomaterials 22 (2001) 2359–2369.

248. M. Naessens, A. Cerdobbel, W. Soetaert, E.J. Vandamme, Leuconostoc dextransucrase and dextran: production, properties and applications, J. Chem. Technol. Biotechnol. 80 (2005) 845–860.

249. S. Arnott, A. Fulmer, W.E. Scott, I.C. Dea, R. Moorhouse, D.A. Rees, The agarose double helix and its function in agarose gel structure, J. Mol. Biol. 90 (1974) 269–284.

250. D.A. Rees, Structure, conformation and mechanism in the formation of polysaccharide gels and networks, Adv. Carbohydr. Chem. 24 (1969) 267–332.

251. M.R. Mangione, D. Giacomazza, D. Bulone, V. Martorana, G. Cavallaro, P.L. San Biagio, K+ and Na+ effects on the gelation properties of k-carrageenan, Biophys. Chemist. 113 (2005) 129–135.

252. A. Bartkowiak, D. Hunkeler, Carrageenan-oligochitosan microcapsules: optimization of the formation process, Colloid Surf., B Biointerfaces 21 (2001) 285–298.

253. H. Sjoberg, S. Persson, N. Caram-Lelham, How interactions between drugs and agarose–carrageenan hydrogels influence the simultaneous transport of drugs, J. Control. Release 59 (1999) 391–400.

254. C. Tapia, V. Corbalan, E. Costa, M.N. Gai, M. Yazdani-Pedram, Study of the release mechanism of diltiazem hydrochloride from matrices based on chitosan–alginate and chitosan–carrageenan mixtures, Biomacromolecules 6 (2005) 2389–2395.

255. P. Vlieghe, T. Clerc, C. Pannecouque, M. Witvrouw, E. De Clercq, J.P. Salles, J.L. Kraus, Synthesis of new covalently bound kappa-carrageen-an-AZT conjugates with improved anti-HIV activities, J. Med. Chem. 45 (2002) 1275–1283.

256. U.O. Ike-Nor, S.I. Ofoefule, A. Chukwu, Evaluation of gellan gum as a potential pharmaceutical adjuvant: binding properties in tablets containing a poorly water soluble and poorly compressible drug, J. Drug Deliv. Sci. Technol. 16 (2006) 397–401.

257. S.A. Agnihotri, S.S. Jawalkar, T.M. Aminabhavi, Controlled release of cephalexin through gellan gum beads: effect of formulation parameters on entrapment efficiency, size, and drug release, Eur. J. Pharm. Biopharm. 63 (2006) 249–261.

258. S. Suri, R. Banerjee, In vitro evaluation of in situ gels as short term vitreous substitutes, J. Biomed. Mater. Res., A 79A (2006) 650–664.

259. Y. Sultana, M. Aqil, A. Ali, Ion-activated, Gelrite-based in situ ophthalmic gels of pefloxacin mesylate: comparison with conventional eye drops, Drug Deliv. 13 (2006) 215–219.

260. R.M. Brown, Cellulose structure and biosynthesis: what is in store for the 21st century? J. Polym. Sci., A, Polym. Chem. 42 (2004) 487–495.

261. I.M. Saxena, R.M. Brown, Cellulose biosynthesis: current views and evolving concepts, Ann. Bot. 96 (2005) 9–21.

262. R.M. Brown, I.M. Saxena, K. Kudlicka, Cellulose biosynthesis in higher plants, Trends Plant Sci. 1 (1996) 149–156.

263. C. Somerville, Cellulose synthesis in higher plants, Annu. Rev. Cell Dev. Biol. 22 (2006) 53–78.

264. E. Entcheva, H. Bien, L.H. Yin, C.Y. Chung, M. Farrell, Y. Kostov, Functional cardiac cell constructs on cellulose-based scaffolding, Biomaterials 25 (2004) 5753–5762.

265. M. Martson, J. Viljanto, T. Hurme, P. Saukko, Biocompatibility of cellulose sponge with bone, Eur. Surg. Res. 30 (1998) 426–432.

266. F.A. Muller, L. Muller, I. Hofmann, P. Greil, M.M. Wenzel, R. Staudenmaier, Cellulose-based scaffold materials for cartilage tissue engineering, Biomaterials 27 (2006) 3955–3963.

267. H. Pulkkinen, V. Tiitu, E. Lammentausta, E.R. Hamalainen, I. Kiviranta, M.J. Lammi, Cellulose sponge as a scaffold for cartilage tissue engineering, Biomed. Mater. Eng. 16 (2006) S29–S35.

268. J. Holmbom, E. Ekholm, M. Martson, M. Liiho, J. Salonen, R. Penttinen, Cellulose and bioactive glass in bone tissue engineering, Bone 30 (2002) 5S-5S.

269. F.A. Muller, L. Jonasova, P. Cromme, C. Zollfrank, P. Greil, Biomimetic Apatite Formation on Chemically Modified Cellulose Templates, in: M.A. Barbosa, F.J. Monteiro, R. Correia, B. Leon (Eds.), Bioceramics 16, vol. 254–6, Trans Tech Publishers, Switzerland, 2004, pp. 1111–1114.

270. F.M. Chen, Z.F. Wu, Q.T. Wang, H. Wu, Y.J. Zhang, X. Nie, Y. Jin, Preparation of recombinant human bone morphogenetic protein-2 loaded dextran-based microspheres and their characteristics, Acta Pharmacol. Sin. 26 (2005) 1093–1103.

271. F.M. Chen, Y.M. Zhao, H. Wu, Z.H. Deng, Q.T. Wang, W. Zhou, Q. Liu, G.Y. Dong, K. Li, Z.F. Wu, Y. Jin, Enhancement of periodontal tissue regeneration by locally controlled delivery of insulin-like growth factor-I from dextran-co-gelatin microspheres, J. Control. Release 114 (2006) 209–222.

272. S.G. Levesque, M.S. Shoichet, Synthesis of cell-adhesive dextran hydro-gels and macroporous scaffolds, Biomaterials 27 (2006) 5277–5285.

273. R.S. Zhang, M.G. Tang, A. Bowyer, R. Eisenthal, J. Hubble, A novel pH-and ionic-strength-sensitive carboxy methyl dextran hydrogel, Biomaterials 26 (2005) 4677–4683.

274. K. Bloch, V.I. Lozinsky, I.Y. Galaev, K. Yavriyanz, M. Vorobeychik, D. Azarov, L.G. Damshkaln, B. Mattiasson, P. Vardi, Functional activity of insulinoma cells (INS-1E) and pancreatic islets cultured in agarose cryogel sponges, J. Biomed. Mater. Res., A 75A (2005) 802–809.

275. M. Alaminos, M.D. Sanchez-Quevdo, J.I. Munoz-Avila, D. Serrano, S. Medialdea, I. Carreras, A. Campos, Construction of a complete rabbit cornea substitute using a fibrin-agarose scaffold, Invest. Ophthalmol. Visual Sci. 47 (2006) 3311–3317.

276. I.K. Ko, H. Iwata, An Approach to Constructing Three-Dimensional Tissue, in: D. Hunkeler, A. Cherrington, A. Prokop, R. Rajotte (Eds.), Bioartificial Organs III: Tissue Sourcing, Immunoisolation, and Clinical Trials, vol. 944, The New York Academy of Sciences, New York, 2001, pp. 443–455.

277. A. Svensson, E. Nicklasson, T. Harrah, B. Panilaitis, D.L. Kaplan, M. Brittberg, P. Gatenholm, Bacterial cellulose as a potential scaffold for tissue engineering of cartilage, Biomaterials 26 (2005) 419–431.

278. I.L. Jung, K.H. Phyo, K.C. Kim, H.K. Park, I.G. Kim, Spontaneous liberation of intracellular polyhydroxybutyrate granules in Escherichia coli, Res. Microbiol. 156 (2005) 865–873.

279. G.Q. Chen, Q. Wu, The application of polyhydroxyalkanoates as tissue engineering materials, Biomaterials 26 (2005) 6565–6578.

280. S.F. Williams, D.P. Martin, D.M. Horowitz, O.P. Peoples, PHA applications: addressing the price performance issue in tissue engineering, Int. J. Biol. Macromol. 25 (1999) 111–121.

281. P.P. King, Biotechnology: an industrial view, J. Chem. Technol. Biotechnol. 32 (1982) 2–8.

282. G.Q. Chen, Q. Wu, J.Z. Xi, H.P. Yu, Microbial production of biopolyesters-polyhydroxyalkanoates, Prog. Nat. Sci. 10 (2000) 843–850.

283. C. Doyle, E.T. Tanner, W. Bonfield, In vitro and in vivo evaluation of polyhydroxybutyrate and of polyhydroxybutyrate reinforced with hydroxyapatite, Biomaterials 12 (1991) 841–847.

284. J.C.Knowles,G.W.Hastings, H. Ohta,S.Niwa, N. Boeree, Development of a degradable composite for orthopedic use-*in vivo* biomechanical and histological evaluation of 2 bioactive degradable composites based on the polyhydroxybutyrate polymer, Biomaterials 13 (1992) 491–496.

285. H.Y. Li, J. Chang, Fabrication and characterization of bioactive wollastonite/ PHBV composite scaffolds, Biomaterials 25 (2004) 5473–5480.

286. F. Koosha, R.H. Muller, Production of polyhydroxybutyrate (PHB) microparticles and nanoparticles, Arch. Pharm. 320 (1987) 913-913.

287. F. Koosha, R.H. Muller, S.S. Davis, Polyhydroxybutyrate as a drug carrier, Crit. Rev. Ther. Drug Carr. Syst. 6 (1989) 117–130.

288. R. Sodian, J.S. Sperling, D.P. Martin, A. Egozy, U. Stock, J.E. Mayer, J.P. Vacanti, Fabrication of a trileaflet heart valve scaffold from a polyhydroxyalkanoate biopolyester for use in tissue engineering, Tissue Eng. 6 (2000) 183–188.

SECTION 2.

CHAPTER II.

Materials and Methods

CHAPTER II.

Materials and Methods

This chapter intends to give an overview on the materials and experimental techniques behind the studies presented in this thesis. All the experimental work that support the achieved results described in Section 3 will be herein presented in detail. Additionally, in order to provide the reader with a better understanding of the research strategy, some considerations are made on the selection of the materials, production and characterization techniques, as well as on the underlying principles that sustain the proposed methodologies. This is expected to give the reader a more clear vision of the purpose of each study and the correspondent selected methodology.

1. MATERIALS

1.1. CHITOSAN

Chitosan is a cationic polymer obtained from chitin comprising copolymers of β(1→4)-glucosamine and *N*-acetyl-D-glucosamine [1] with a structure schematically represented in Figure 1 [2]. Chitin is a natural polysaccharide found particularly in the shell of crustacean, cuticles of insects and cell walls of fungi and is the second most abundant polymerized carbon found in nature. Chitosan, the fully or partially deacetylated form of chitin, due to its properties as attracted much attention in the tissue engineering and drug delivery fields with a wide variety of applications ranging from skin, bone, cartilage and vascular grafts to substrates for mammalian cell culture. It has been proved to be biologically renewable, biodegradable, biocompatible, non-antigenic, non-toxic and biofunctional [3].

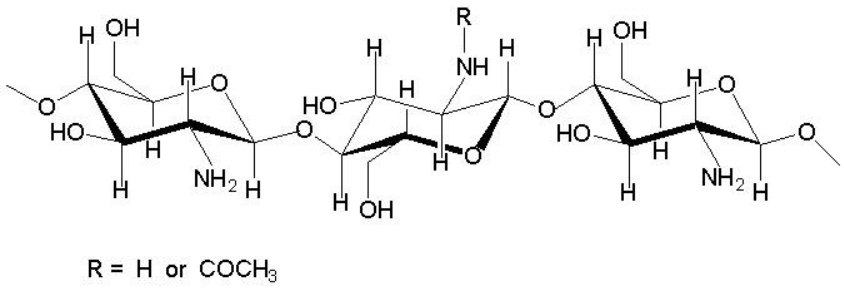

Figure 1. Schematic illustration of the structure of chitosan [2].

The adhesive properties of chitosan in a swollen state have been shown to persist well during repeated contacts of chitosan and the substrate [2-5] which implies that, in addition to the adhesion by hydration, many other mechanisms, such as hydrogen bonding and ionic interactions might also have be involved. This property is a key issue on what concerns to the production methodology proposed in this thesis, making possible to achieve the aggregation of chitosan particles in order to produced stable scaffolds. Moreover, chitosan exhibits a pH-sensitive behaviour as a weak poly-base due to the large quantities of amino groups on its chain [1-5]. Chitosan dissolves easily at low pH while it is insoluble at higher pH ranges. This property has held chitosan to be widely investigated as a delivery matrix.

Crosslinking is often used [4-8] to tailor chitosan-based materials properties. The most common crosslinkers used to crosslink chitosan are dialdehydes such as glyoxal [8] and glutaraldehyde [4] which was selected to be used in this thesis. The aldehyde groups form covalent imine bonds with the amino groups of chitosan due to the resonance established with adjacent double ethylinic bonds via a Schiff reaction [6]. Dialdehydes allow the crosslinking to happen by direct reaction in aqueous media and under mild conditions. Moreover, dihaldehydes such as glutaraldehyde stabilize the chitosan structure [7] retaining the biocompatibility of the polymer.

Porous chitosan matrices have been suggested [2,5,9-11] as a potential candidate as a bone regenerative material due to its proper biological and physical properties. Biological activity of chitosan on bone regeneration has been demonstrated in many reports [2,9-11]. Concerning cartilage engineering, chitosan is structurally similar to glycosaminoglycans (GAGs) found in extracellular matrices as in native articular cartilage and are very important in playing a key role in modulating chondrocytes morphology, differentiation and function [5]. This characteristic, together with the ones previously described, makes chitosan also an attractive natural-origin polymer to also engineered cartilage [4,12].

The chitosan used for production of the scaffolds developed in this thesis was purchased from Sigma-Aldrich. It is a chitosan with medium molecular weight with a deacetylation degree between 75-85%. This polymer was selected as polymeric matrix for the developed scaffolds described in this thesis due to the above discussed advantages.

1.2. HYDROXYLAPATITE

For the composites scaffolds production, the incorporation of a bioactive ceramic filler has been carried out with two main goals. In one hand, a bioactive ceramic has always the potential capability of inducing a bioactive behaviour in a polymeric matrix [13-15] . On the other, being a ceramic filler, it can potentially improve the mechanical performance of the polymeric matrix where it is incorporated [13,16,17].

Hydroxylapatite (HA) was selected as ceramic filler in this thesis due to its chemical composition which is similar to that of bone inducing a good biocompatibility in bone contact. The mineral phase of bone, which is around 60-70%wt of the bone can be described as a calcium phosphate with an apatitic structure and a composition close to HA [$Ca_{10}(PO_4)_6(OH)_2$, Ca/P =1.67] [18]. Hydroxylapatite is biocompatible and bioactive in the human body [19] and is compatible with various tissue types and can adhere directly to osseous, soft, and muscular tissue without an intermediate layer of modified tissue [20]. It also displays an osteoconductivity: a property of a material to encourage bone already being formed, to lie closely to, or adhere to, its surface [18]. Hydroxylapatite is the most stable calcium phosphate salt at normal temperatures and pH between 4 and 12 [19].

In this thesis, two types of hydroxylapatites were used: unsintered and sintered. Both are synthetic and commercial available hydroxylapatites. The unsintered hydroxylapatite (HA unsint) is a coating powder of CAMCERAM II grade and was purchased from CAM Implants BV, Leinden, The Netherlands. The sintered hydroxylapatite (HA sint) is a Captal's® HA grade and was purchased from Plasma Biotal Ltd, Tideswell, UK. This hydroxylapatite is subject to a sintering thermal cycle at 1250ºC for 2 hours. Sintered hydroxylapatite has high purity, crystalline, synthetic bone mineral which is chemically stable at 1330ºC in air, retaining is high crystalline structure.

Both unsintered and sintered hydroxylapatite (HA unsint and HA sint, respectively) were characterized by light scattering in order to assess the particle size distribution, as well as the mean particle size as presented in the following Figure 2. It was found that the used sintered hydroxylapatite has a more narrow particle size distribution with a mean particle size of around 6 μm. On its turn, unsintered hydroxylapatite has a broad range of particles sizes, being the mean particle size of 30.45 ± 15.35 μm as assessed by light scattering.

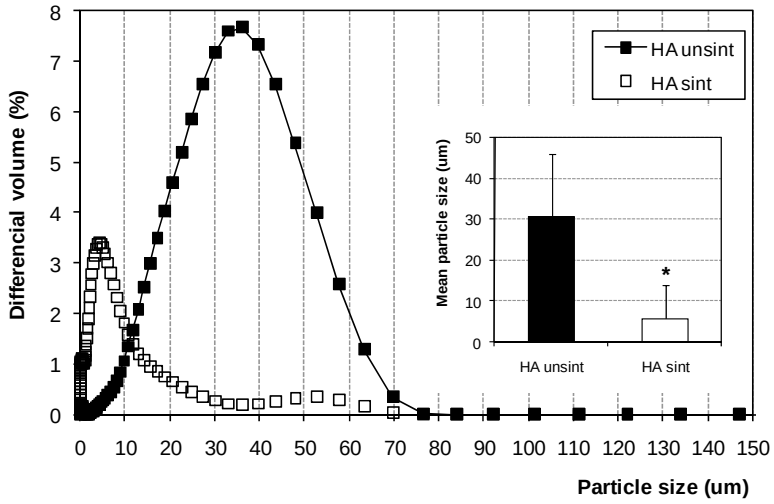

Figure 2. Particle size distribution of the sintered (HA sint) and unsintered hydroxylapatite (HA unsint) evaluated by light scattering. The onset graph shows the mean particle size of both hydroxylapatites.

1.3. INSULIN

Insulin was selected as active biomolecule to be incorporated in polymeric scaffolds in order to promote the chondrogenic differentiation. It is known that insulin has not only a great structural similarity to insulin growth factor-1 (IGF-1) but also a functional similarity and also elicits marked response in cartilage [21,22]. Among all the growth factors known to be involved in chondrogenesis, IGF-1 is considered to be the main anabolic growth factor of normal cartilage [9], playing an important role in the growth and differentiation of articular cartilage while also promoting chondrogenic differentiation of mesenchymal cells [23]. IGF-1 belongs to the IGF family of peptide hormones including relaxin and insulin and has a single polypeptide homologous to proinsulin [24]. It regulates many cellular functions by activating cell-surface receptors. Insulin was selected because it can also bind to IGF-1 and insulin receptors with a marked response in cartilage.

Insulin is routinely used in standard chondrogenic-inducing medium to induce differentiation at high concentration to activate the IGF-1 receptors [21,25,26]. The observed effects of insulin were shown to be similar to effects of the IGF-1 and are in agreement with the reported binding constants of IGF-1 and insulin at the IGF-1 receptors [26]. Furthermore, investigation of novel systems would benefit from a

readily cost model protein such as insulin, since the high costs of growth factors often limit a detailed and thorough investigation of new application systems.

The insulin used in this thesis, namely in Chapter V, is from bovine pancreas and was purchased from Sigma-Aldrich. It is a two-chain polypeptide hormone produced by the β-cells of pancreatic islets. The α chain contains an intrachain disulfide bond and both α and β chains are joined by two interchain disulfide bonds. The molecular formula is $C_{254}H_{377}N_{65}O_{75}S_6$ with a molecular weight of around 5800 Da.

1.4. REAGENTS

Unless otherwise stated, all the chemical reagents used in the experimental results described in Section 3 were purchased from Sigma-Aldrich. They presented analytical purity and were not submitted to further purification.

2. SCAFFOLDS PRODUCTION

In this thesis, the developed scaffolds for tissue engineering applications were produced by an innovative particle aggregation methodology which is based on the agglomeration of pre-fabricated microspheres. The technique is generally based on the random packing of microspheres with further aggregation by physical or thermal means to create a three dimensional porous structure. This technique is being used to construct scaffolds directly [27] or it can be proposed to be used indirectly by producing a negative structure which will serve as a reverse template to obtain the scaffolds.

For example, the research group of C.T. Laurencin [27-29] has been also applying this technique for the development of poly(lactide-co-glycolide) (PLAGA) microspheres-based matrices for bone repair. The researchers have tried different approaches by developing sintered microspheres based matrices [27,29] or gel microspheres matrices [28]. Composite microspheres containing hydroxyapatite were also used for the fabrication of polymer-ceramics 3D matrices for bone applications [30]. In the case of sintered microspheres matrices, the microspheres are first obtained by a solvent evaporation technique. The 3D structures are then further processed by heating the pre-fabricated PLAGA microspheres above

the glass transition temperature. The polymer chains are activated to interlink with neighbouring polymer chains and thus form contacts between neighbouring microspheres [28]. In the gel microspheres matrix methodology, the PLAGA gel microspheres are obtained by emulsion with poly(vinyl alcohol) (PVA). The following agglomeration is based on a multiple step production that includes air-drying, freeze-drying, rehydration with salt leaching and freeze-drying again. In general, microsphere based matrices show very interesting properties for a possible application in bone repair. Recently, this research group has also focused in the use of chitosan to be applied with the particle aggregation technique. First, by the development of 3D chitosan/poly(lactic acid-glycolic acid) (PLAGA) composite porous scaffolds by sintering together composite chitosan/PLAGA microspheres [10] and secondly, the production of 3D chitosan matrices based on microspheres with appropriate pore size, porosity and mechanical properties proposed for bone tissue engineering applications [9].

Another strategy that uses microspheres includes their embedding in a hydrogel matrix [31-33]. In that approach, the goal of incorporation of previously produced microspheres is to encapsulate either cells [34] or biologically active factors for either favouring the cell attachment and proliferation behaviour [12,31,35,36] or to enhance the vascularization [37].

In this thesis, polymeric scaffolds were produced by particle aggregation aiming at both bone and cartilage tissue engineering applications. On its turn, composite scaffolds were developed having in mind scaffolding for bone applications while bilayered materials were fabricated aiming at tissue engineer biphasic constructs to be applied in osteochondral defects. Furthermore, insulin-loaded scaffolds were also developed in order to promote chondrogenic differentiation. The following table (Table 1) intends to summarize the scaffolds nomenclature used in this thesis.

Table 1. Nomenclature used in the developed chitosan-based scaffolds described in this thesis.

ABBREVIATION	DESCRIPTION
C, Ch	Polymeric chitosan scaffolds
CHA	Composite chitosan-hydroxylapatite scaffolds
BiCCHA	Bilayered chitosan/chitosan-hydroxylapatite scaffolds
0.05	Polymeric chitosan scaffolds loaded with 0.05% of insulin
0.5	Polymeric chitosan scaffolds loaded with 0.5% of insulin
5	Polymeric chitosan scaffolds loaded with 5% of insulin

2.1. POLYMERIC CHITOSAN SCAFFOLDS

The chitosan particles-aggregated scaffolds were produced by particle aggregation methodology which is schematically represented in Figure 3. For that, chitosan was grinded and dissolved overnight in acetic acid (1%vv) to obtain a chitosan solution (2%wt). After complete dissolution and filtration, the prepared solutions were extruded through a syringe at a constant rate (10 ml/h) to form chitosan droplets into a NaOH (1M) precipitation bath, where particles with regular diameter were formed. The chitosan particles were collected and washed repeatedly with distilled water until neutral pH was reached. The particles were subsequently placed into cylindrical moulds and left to dry at 60ºC for 3 days. Cylindrical shaped scaffolds with 8 mm height and 5 mm diameter were produced for the morphological and morphometric characterization, mechanical and hydration behaviour, as well as for cytotoxicity tests. For the *in-vitro* cells tests and *in-vivo* studies, cylindrical shaped scaffolds with 3 mm height and 5 mm diameter were used.

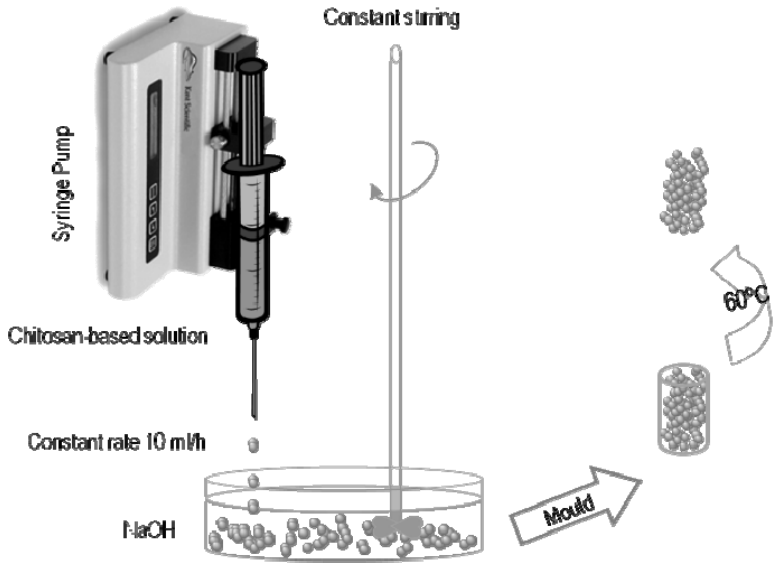

Figure 3. Schematic representation of the chitosan precipitation and particle aggregation methodologies.

2.2. COMPOSITE CHITOSAN-HYDROXYLAPATITE SCAFFOLDS

The composite scaffolds were developed having in mind the development of adequate bone tissue engineering 3D architectures. In order to increase the mechanical performance and induce a bioactive behaviour, hydroxylapatite as bioactive ceramic filler was incorporated. This strategy was firstly proposed by Bonfield [16] to produce hydroxylapatite-polyethylene bioactive composites and also applied afterwards to develop composites containing other bioactive phases, such as, bioactive glasses [38] and glass-ceramics [17], and a series of different polymers [16,28,38]. Furthermore, a crosslinking reaction was carried out in order to improve the mechanical performance of the developed composites.

In the preliminary composite particles production described in Chapter III, 20%wt of unsintered hydroxylapatite (HA unsint) (CAM Implants, UK) with an average particle size of 30 μm was homogeneously dispersed in the chitosan solution. The solution was kept under stirring overnight. Following the previously described methodology, after complete dissolution, dispersion and filtration, and, the prepared solutions were extruded through a syringe at a constant rate (10 ml/h) to form chitosan-HA droplets into a NaOH (1M) precipitation bath, where particles with regular diameter were formed. The chitosan particles were collected and washed repeatedly with distilled water until neutral pH was reached. The composite particles were then submitted to a crosslinking reaction with glutaraldehyde. For that, particles were immersed for 15 minutes in a 0.5%vv and, afterwards, washed repeatedly with distilled water until neutral pH was reached. The particles were subsequently placed into cylindrical moulds and left to dry at 60ºC for 3 days.

In Chapter IV, besides the unsintered hydroxylapatite, sintered hydroxylapatite (HA sint) (Captal's® HA, Plasma Biotal Ltd, UK) was also used in order to overcome the detected cytotoxicity behaviour of the composite scaffolds. Composite scaffolds were optimized according the following conditions. After the particles were formed as described previously, different glutaraldehyde concentrations (0.01%, 0.025%, 0.05% and 0.5% for 15min) were used. Scaffolds were further washed with glycine solution (0.2 and 1M for 15min) in order to block free aldehyde groups. After each step, scaffolds were washed with distilled water. Unless otherwise stated, composite scaffolds were crosslinked with 0.01% glutaraldehyde and washed with 1M glycine both for 15 minutes. After washing with distilled water, particles were placed into cylindrical moulds and left to dry at 60ºC for 3 days. Cylindrical shaped scaffolds with 8 mm height

and 5 mm diameter were produced for the morphological and morphometric characterization, mechanical and hydration behaviour, as well as for cytotoxicity and bioactivity tests.

2.3. BILAYERED CHITOSAN / CHITOSAN-HYDROXYLAPATITE SCAFFOLDS

Bilayered scaffold were developed aiming at osteochondral tissue engineering strategies. It has been more recently accepted [39-41] that a biphasic structure could be more challenging but more adequate to regenerate an osteochondral defect able to incorporate/induce different types of cells in a favourable environment requiring different chemical surroundings and mechanical requirements, leading the growth of two different tissues, with different biological requirements. The bilayered structures were fabricated by assembling polymeric and composite particles produced as described previously. Composite scaffolds were crosslinked with 0.01% glutaraldehyde and washed with 1M glycine both for 15 minutes. Cylindrical shaped scaffolds with 8 mm height and 5 mm diameter were produced for the morphological and morphometric characterization, mechanical behaviour, as well as for bioactivity tests, both in static and dynamic conditions.

2.4. INSULIN-LOADED CHITOSAN SCAFFOLDS

Osteochondral defects repair requires a tissue engineering approach which aims at mimicking the physiological properties and structure of two different tissues (cartilage and bone) using a scaffold-cell construct. One ideal approach is to engineer *in-vitro* a hybrid material using a single cell source. For that, the scaffold should be able to provide the adequate biochemical cues in order to promote the selective but simultaneous differentiation of both tissues.

In this thesis, attention was paid primarily to the chondrogenic differentiation by focusing on the development of polymeric systems that provide biomolecules release in order to induce chondrogenic differentiation, as described in Chapter V of Section 3. For that, different formulations of insulin-loaded chitosan particle aggregated scaffolds were developed as a potential model system for cartilage and osteochondral tissue engineering applications, using insulin as a potent substance to induce chondrogenic differentiation. Insulin was selected based in its previously described effects on

chondrogenic differentiation. Furthermore, release technologies are useful approaches to ensure local release of growth factors over a certain period of time, and are attractive alternatives to further improve the quality of the repaired tissue. This is due to the fact that a single dose application intraoperatively cannot guarantee a prolonged local protein concentration in order to achieve permanent stimuli on tissue differentiation.

Having always these considerations in mind, different formulations of insulin-loaded chitosan particle aggregated scaffolds were prepared. Insulin solutions were prepared in HCl (0.1M) for distinct theoretical protein loadings. The protein solution was mixed with the previously prepared chitosan solution in order to obtain a homogeneous distribution. Insulin theoretical loadings were 0.05, 0.5 and 5%wt relative to chitosan for each formulation. The prepared solutions were extruded through a syringe at a constant rate (10ml/h) to form chitosan droplets into a NaOH (1M) precipitation bath where particles with regular diameter were formed. The chitosan-based particles were quickly washed with distilled water until pH7. The particles were then placed into moulds and left to dry in an oven at 60ºC for 3 days. Cylindrical shape scaffolds with 3 mm height and 5 mm diameter were obtained and used as described in Chapter V.

3. MORPHOLOGICAL / MORPHOMETRIC CHARACTERIZATION

When developing scaffolds for tissue engineering, one of the key requirements is the adequate materials morphology. Besides the typical morphological characterization, the morphometric analysis has become a critical issue in scaffolding, since it allow for an accurate determination of the more relevant morphometric parameters such as porosity and interconnectivity, as following described.

3.1. SCANNING ELECTRON MICROSCOPY (SEM)

The chitosan-based scaffolds and particles morphology was analyzed by means of using scanning electron microscopy (SEM) equipment (S360, Leica Cambridge Ltd) equipped with V03.02A software. Previously to SEM analysis, sample surfaces were gold sputtered (Fisons Instruments, Sputter Coater SC502, UK).

3.2. MICRO-COMPUTED TOMOGRAPHY (MICRO-CT)

Micro-Computed Tomography (micro-CT) has been identified as having various key advantages over other techniques [42-45], such as its non-destructiveness and the possibility to assess many different parameters in a quantitative way. Porosity, surface area to volume ratio, cross-section area, pore size, strut/wall thickness, anisotropy and interconnectivity can be easily identified as important architectural and structural characteristics of scaffolds which can be assessed by micro-CT.

Micro-CT was first proposed to analyze trabecular samples [46] and since then has been used extensively in the study of trabecular architecture [47] and their applications in other areas are clearly increasing, namely in the tissue engineering field. The morphometric parameters for architectural analyses of scaffolds can be easily extrapolated based on the histomorphometric/structural indices usually measured for bone samples, such as bone surface (BS) and volume (BV), trabecular thickness (Tb.Th) and trabecular separation (Tb. Sp), structural degree of anisotropy (DA) or bone surface-to-volume ratio (BS/BV) [48].

The increasing use of this technique in tissue engineering can be attributed to micro-CT capacity to provide accurate quantitative and qualitative information on the 3D morphology of the sample. Another main advantage is that the interior of the object can be studied with great detail without physical sectioning or use of toxic chemicals. Moreover, after scanning, the integral samples can be subjected to other tests due to its non-destructive nature, therefore resolving the problem of sample scarcity.

In Chapter III, micro-CT evaluation of the polymeric scaffolds was carried out using a Scanco 20 equipment (Scanco Medicals, Switzerland). X-ray scans were performed in triplicate in high resolution mode (9 μm) and 240 slices of the scaffolds were obtained. The 2D morphometric analysis of the scaffolds was performed using a threshold 51 to identify the polymeric phase in order to determine the mean porosity, as well as the porosity distribution along the scaffold (from 0-2000 μm). Furthermore, with the micro-CT data import and MIMICS® (Materialise Interactive Medical Image Control System) image processing software (Materialise, Belgium), it was possible to build 3D virtual models representing the morphological structures of the scaffolds.

In Chapters IV and VI, chitosan-based particles-aggregated scaffolds (polymeric, composite and bilayered) were scanned in triplicate using a high-resolution micro-CT Skyscan 1072 scanner (Skyscan, Kontich, Belgium) (Figure 4) using a resolution of pixel size of 8.79 μm and integration time of 1.9 ms. The X-ray source was set at 40 keV of energy and 250 μA of current. Approximately 400 projections were acquired over a rotation range of 180° with a rotation step of 0.45°.

Figure 4. High-resolution micro-CT Skyscan 1072 scanner with a detailed view from the sample chamber. Adapted from reference [49].

Data sets were reconstructed using standardized cone-beam reconstruction software (NRecon v1.4.3, SkyScan). The output format for each sample was 850 serial 1024x1024 bitmap images. Representative data sets of 200 slices were segmented into binary images with a dynamic threshold of 40-255 (grey values) to identify the polymeric phase in order to calculate the porosity and 150-255 (grey values) to identify the ceramic phase. This data was used for morphometric analysis (CT Analyser v1.5.1.5, SkyScan) and to build 3D virtual models (ANT 3D creator v2.4, SkyScan).

The morphometric analysis included X-ray absorption histograms, porosity, scaffolds interconnectivity, ceramic content distribution, mean pore and particles size and respective distribution. 3D virtual models of representative regions in the bulk of the scaffolds were also created, visualized and registered using both image processing softwares (CT Analyser and ANT 3D creator). In order to fully characterize the porosity morphology of the scaffold, a threshold inversion technique was used to create a 3D model.

4. HYDRATION BEHAVIOUR

The hydration behaviour of polymeric scaffolds was assessed in media with different pH (5, 7.4 (physiological pH) and 9) in order to study the potential responsive behaviour of the developed systems. The assays were performed at physiological temperature (37º±1ºC) for pre-determined immersion periods up to 14 days. The swelling profile was characterized using the following equation 1:

$$\%\, Hydration\ degree = \frac{W_W - W_i}{W_i} * 100 \qquad (1)$$

where W_i is the initial weight and W_w is the wet weight at determined test period.

5. MECHANICAL CHARACTERIZATION

5.1. STATIC AND DRY CONDITIONS

The mechanical properties of the developed polymeric and composite scaffolds in dry state were tested on a compressive solicitation mode in an Instron Universal Mechanical Testing machine in a controlled environment (23ºC/55% RH). The cross-head speed used was 2 mm/min.

5.2. DYNAMIC AND WET CONDITIONS

Dynamic Mechanical Analysis (DMA) was conducted to characterize the mechanical behaviour of chitosan-based particles-aggregated scaffolds in wet state under dynamic compression solicitation. The scaffolds characterized by DMA were the following: (i) the developed polymeric, (ii) the composite and (iii) the bilayered materials. Cylindrical chitosan-based scaffolds were immersed in Phosphate Buffer Solution (PBS) at physiological pH and temperature (pH 7.4 and 37ºC) for 3 days for complete hydration. The scaffolds were then were subjected to compression cycles of increasing frequencies ranging from 0.1-40 Hz with constant amplitude displacements of 0.03 mm using a Tritec2000 DMA (Triton Technology, UK). Experiments were conducted at room temperature with n=5. The real (storage

modulus), E', and the imaginary component (loss modulus), E'', of the complex modulus, E*=E'+iE'' (with $i=(-1)^{1/2}$), were recorded against frequency. Reference values for the compression modulus were collected at a frequency of 1Hz.

6. *IN-VITRO* BIOACTIVITY STUDIES

Since the developed materials in this thesis are aiming to be used in osteochondral tissue engineering applications, *in-vitro* bioactivity tests were carried out with two main goals. In one hand, the aim was to assess if the composite constituent of the bilayered structures is able to induce an apatite formation on its surface in SBF (simulated body fluid) with ion concentration nearly equal to those of the human blood plasma, since this is useful for predicting the *in-vivo* bone bonding of the material. This method is widely used for screening bone bioactive materials before any other biological assay [13,38,50,51]. On the other hand, since we are endeavouring at an osteochondral application, ones need to assure that the polymeric component of the bilayered structure aimed at chondral part would not mineralized *in-vitro*. To preliminary screen this behaviour, SSF (simulated synovial fluid) was also used in order to mimic the chemical environment of a human joint.

For the dynamic bioactivity *in-vitro* tests, an innovative double-chamber bioreactor was designed. In spite of the ultimate goal of this bioreactor is to engineer bilayered hybrid constructs for osteochondral applications, we have used it in these assays as proof of concept mimicking future and ideal conditions for these applications.

6.1. STATIC CONDITIONS

To study the *in-vitro* bioactive behaviour in the static standard conditions, two different simulated solutions were used. A simulated body fluid (SBF) with ion concentrations (Na^+ 142.0, K^+ 5.0, Mg^{2+} 1.5, Ca^{2+} 2.5, Cl^- 103.0, HCO_3^{2-} 10.0,HPO_4^{2-} 1.0 and SO_4^{2-} 0.5 mM) [50,52] nearly equal to those of the human blood plasma was prepared as described elsewhere [50,52]. Simulated synovial fluid (SSF) was also used to approximate the chemical environment in a human joint. SSF, with ion concentration Na^+ 153.1, K^+ 4.2, Cl^- 139.6 and phosphate buffer 9.6 mM [53], was prepared by dissolving 0.3%wt

hyaluronic acid in phosphate buffered saline solution to obtain a pH of 7.4. Hyaluronic acid is a mucopolysaccharide composed of several thousand amino-sugar residues, and is the primary diffuse macromolecule that exists in human synovial fluid [53]. For the static bioactivity tests, samples (polymeric, composite and bilayered scaffolds) with n=3 were suspended and immersed in 50 ml of SBF and SSF separately at 37ºC and pH 7.4 (physiological conditions) for 0, 1, 3 and 14 days. After soaking, the samples were immediately washed with distilled water and dried at room temperature.

6.2. DYNAMIC CONDITIONS IN A SPECIALLY DESIGNED DOUBLE-CHAMBER BIOREACTOR

For the dynamic bioactivity tests, a double-chamber bioreactor was specially designed and set-up according Figure 5. As referred before, the ultimate goal is to use this bioreactor to engineer bilayered hybrid constructs for osteochondral applications. For that, the bioreactor was designed to allow simultaneous culturing of chondrocytes and osteoblasts or the same source of progenitor cells with different differentiation cell culture mediums within respective sections of a single-unit chamber. As represented in Figure 5, the scaffolds are supported by a transversal silicon membrane and both simulated solutions (SBF and SSF) have continuous and independent recirculation in the 6 interconnected chambers in each of respective part of the bilayered scaffolds. SBF has a flow circuit trough the composite parts of the bilayered structures and SSF is circulating through the polymeric part designed for the chondral constituent to approximate the chemical environment in a human joint.

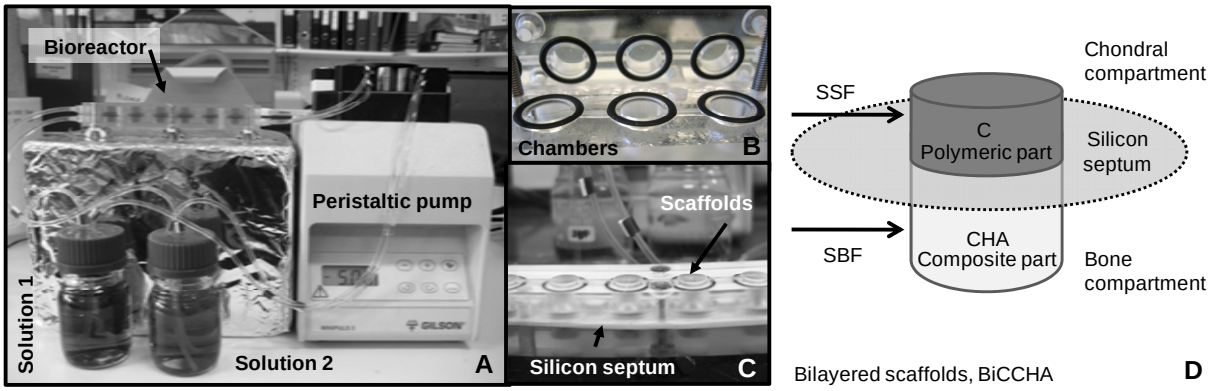

Figure 5. Double-chamber bioreactor set-up (A). The double-chamber bioreactor consists in 6 interconnected double-chambers (B) where the different solutions circulate in separated flow circuits. A silicon septum acts as scaffolds support (C,D). The schematically experimental conditions for the dynamic bioactivity assays are represented in (D).

For these assays which are described in Chapter IV, bilayered scaffolds (n=2) were assembled in the bioreactor using a silicon septum. The SBF and SSF, prepared as described previously, were continuously circulating in physiological conditions (pH 7.4 and 37ºC) using a peristaltic pump up to 14 days with an available volume of 50 ml of each solution. Scaffolds and solutions sampling was performed at 0, 3, 7 and 14 days.

6.3. CHARACTERIZATION

Scaffolds surface morphology, as well as the presence of calcium (Ca) and phosphorous (P) elements on the scaffolds surface were analyzed before and after soaking in SBF and SSF, for the different experimental conditions at the different immersion periods. This was carried out using scanning electron microscopy (SEM) equipment (S360, Leica Cambridge Ltd) and energy dispersive spectroscopy (EDS) equipment (Link EXL II, Oxford) coupled to the SEM. Previously to SEM and EDS analysis, sample surfaces were gold sputtered (Fisons Instruments, Sputter Coater SC502, UK) carbon coated (Fisons Instruments, Evaporation PSU CA508, UK) respectively. Microphotographs and spectra were registered for further analysis. Furthermore, the sample solutions were analyzed by inductively coupled plasma optical emission spectroscopy (ICP-OES JY70 plus, Jobin Yvon, France) in order to quantify the elemental concentrations as function of the immersion period of calcium (Ca), phosphorus (P), silicon (Si), magnesium (Mg) and sodium (Na) elements.

7. INSULIN-LOADED SYSTEMS CHARACTERIZATION

7.1. PROTEIN LOADING AND ENCAPSULATION EFFICIENCY

Protein loading and encapsulation efficiency were calculated by an indirect procedure. After the loaded-particles preparation (n=3) as described previously, particles were separated from the precipitation medium by filtration and the aqueous phase was sampled for insulin quantification. Non-loaded scaffolds were used as control. The particles were left to dry in a mould at 60ºC and weighed. The non-loaded free insulin was determined by Micro-BCA (Micro BCA™ Protein Assay Kit 23235, Pierce). This assay combines the well-known reduction of Cu^{2+} to Cu^{1+} by protein in an alkaline medium with the

highly sensitive and selective colorimetric detection of the cuprous cation (Cu^{1+}) by bicinchoninic acid. The quantification procedure was performed according to the supplier instructions.

Briefly, 150 µl of each of standards, controls and samples were placed in triplicate in a 96-well microplate with 150 µl of working reagent supplied in the kit was added to each well. The plate was then mixed thoroughly on a plate shaker for 30 seconds. The plate was covered and incubated at 37ºC for 2 hours, cooled to room temperature and the absorbance was measured at 562 nm on a microplate reader (Synergy HT, BioTek). The readings were then subtracted of the control (non-loaded scaffolds) and analysed with respective software (KC4 Microplate Data Analysis Software, BioTek). A standard-curve was then plotted with different insulin concentrations (0, 0.5, 1, 2.5, 5, 10, 20, 40, 200 µg/ml) to determine the insulin concentration of each unknown sample. Samples dilutions were used when necessary. Protein loading was defined as the mass of protein per unit mass of particles as shown in equation 2 and the encapsulation efficiency is calculated according equation 3.

$$Protein\ Loading\ (\%) = \frac{m_l - m_r}{m_p} * 100 \qquad (2)$$

and

$$Encapsulation\ Efficiency\ (\%) = \frac{m_l - m_r}{m_l} * 100 \qquad (3)$$

where m_l corresponds to the initially loaded weight of protein, m_r is the weight of protein in the precipitation solution and m_p is the weight of the dry particles prior to *in-vitro* release studies.

7.2. *IN-VITRO* INSULIN RELEASE STUDIES

In-vitro release studies were carried out mimicking the cell culture conditions described in the following section. Each insulin-loaded scaffold formulation was placed in a 24-well microplate with 1.5 ml of phosphate buffer solution (PBS). The in-vitro release studies were carried out in triplicate at physiological conditions (pH 7.4 and 37ºC). Non-loaded scaffolds were used as controls. At pre-determined periods and according to the medium replacement in cell culture studies, aliquots (1 ml) of

the supernatant were withdrawn and frozen at -20ºC for further protein quantification. The release medium was totally replaced by fresh PBS mimicking cell culture conditions for total medium replacement. The protein quantification was performed using Micro-BCA (Micro BCA™ Protein Assay Kit 23235, Pierce) according to the supplier instructions as described previously.

7.3. FOURIER-TRANSFORM INFRARED SPECTROSCOPY WITH ATTENUATED TOTAL REFLECTANCE (FTIR-ATR)

The surface chemical analysis was also performed by FTIR-ATR spectroscopy. Insulin-loaded scaffolds were characterized before and after the *in-vitro* release studies. The analysis was carried out using an IRPrestige 21 FTIR spectrophotometer with an attenuated total reflectance (ATR) device from Shimadzu. Spectra were recorded with a resolution of 4 cm^{-1} and averaged over 36 scans.

8. *IN-VITRO* BIOLOGICAL TESTING

8.1. CYTOTOXICITY ASSESSMENT (MTS)

To assess the possible cytotoxicity of the materials, the *in-vitro* cell viability was assessed using MTS assay (3-(4,5-dimethylthiazol-2-yl)-5-(3-carboxylmethoxyphenyl)-2-(4-sulfophenyl)-2H tetrazolium) (Cell Titer 96® AQueous Solution Cell Proliferation Assay, G3580, Promega, USA) according to ISO/EN 10993 part 5 guidelines, which determines whether cells are metabolically active. This cytotoxicity test is based on the bioreduction of the substrate (MTS) into a brown formazan product by dehydrogenase enzymes in metabolically active cells, directly related with cell viability. For this purpose, materials were incubated (n=3) in culture medium for 24 h at 37ºC with constant shaking after sterilization by ethylene oxide. Latex was also incubated as a positive control. A rat lung fibroblasts cell line (L929) acquired from the European Collection of Cell Cultures (ECACC) was used for the studies.

The cells were grown as monolayers in Dulbecco's modified Eagle's medium (DMEM) supplemented with 10% foetal bovine serum (Biochrom, Berlin, Germany; Heat Inactivated) and 1% of antibiotic-antimycotic mixture. Cultured L929 cells were trypsinised using trypsin-EDTA (Gibco, Invitrogen Corporation) and plated into 96-well micrometer plates (200 µl/well) at $6.6x10^4$ cells/well. The plates

were incubated, for 24 h, at 37ºC in a humidified atmosphere of 5% CO_2 in air. After that, the medium was replaced by the previous prepared materials extracts after sterilized by filtration (0.45 µm pore size) using culture medium by itself as a negative control. After 72 h incubation, cell culture was treated with MTS (in medium without phenol red) and incubated for further 3 h at 37ºC in a humidified atmosphere of 5% of CO_2 in air. At this stage, culture medium with MTS was transferred to new wells. The optical density (OD) which is directly proportional to the cellular activity (it reflects the mitochondrial activity) was read on a microplate reader (Synergy HT, BioTek Instruments) at 490 nm.

8.1.1. Analysis of elemental concentrations of materials extracts

In Chapter IV, the eventual cytotoxicity behaviour was detected for the composite scaffold materials produced with unsintered hydroxylapatite. In order to try to understand the cause of this behaviour, inductively coupled plasma (ICP) was carried out. Mimicking exactly the extract conditions performed in the MTS assay, the different sample extracts solutions were analyzed in order to determine the concentrations of calcium (Ca), phosphorus (P), silicon (Si), magnesium (Mg) and sodium (Na) elements. The element concentrations were measured by inductively coupled plasma-optical emission spectroscopy (ICP-OES JY70 plus, Jobin Yvon, France). Triplicate samples were analyzed for each condition. For this purpose, materials were incubated after sterilization with ethylene oxide in cell culture medium (DMEM) for 24h at 37ºC with constant shaking. After that, the elemental concentrations of the prepared materials extracts sterilized by filtration (0.45 µm pore) were measured, using cell culture medium itself as control.

8.2. HUMAN ADIPOSE STEM CELLS (ASCs) - CHONDROGENIC AND OSTEOGENIC DIFFERENTIATION

8.2.1. Cell culture

For the preliminary osteogenic and chondrogenic differentiation studies described in Chapter III, polymeric scaffolds were seeded with human mesenchymal stem cells (MSC) isolated from adipose tissue derived from liposuction procedures as previously described [54]. Briefly, the liposuction material was washed 3 times with phosphate buffered saline (PBS, purchased from PAA, Austria) to remove

most of the blood and tumescence solution. Afterwards, the tissue was digested in PBS buffered with 25 mM Hepes (PAA, Austria) containing 1.5 mg/mL collagenase (Biochrom, Germany) and 20 mg/mL bovine serum albumine (PAA, Austria) at 37°C under vigorous shaking for 1h. To eliminate red blood, cells the isolated fraction was incubated with erythrocyte lysis buffer consisting of 154 mM NH_4Cl, 10 mM $KHCO_3$ and 0.1 mM EDTA for 10 min at 37°C. After several washing and centrifugation steps, the cells were filtered through a 100 µm filter and cultured in DMEM/Ham´sF12 (1:1), 10% FCS, 2 mM L-glutamine, 100 U/mL penicillin and 100 µg/mL streptomycin at 37°C and 5% CO_2 in a water-saturated atmosphere. Subculturing was performed before the cells reached confluence. Cells from passages 2 to 4 were used for the cell seeding experiments.

For this purpose, $5x10^5$ cells were seeded onto each scaffold which were then cultured in control, osteogenic and chondrogenic medium, respectively. Osteogenic medium consisted of DMEM (1 g/L glucose), 10% FCS, 2 mM L-glutamine, 100 U/mL penicillin and 100 µg/mL streptomycin as well as 0.1 µM dexamethasone, 50 µM ascorbate-2-phosphate (Fluka, Switzerland), 10 mM β-glycerophosphate and 10 nM 1α,25-dihydroxyvitamin D3 (Fluka, Switzerland). Chondrogenic medium was comprised of DMEM (1 g/L glucose), 10% FCS, 2 mM L-glutamine, 100 U/mL penicillin and 100 µg/mL streptomycin as well as 0.1 µM dexamethasone, 0.15 µM ascorbate-2-phosphate, 1% insulin-transferrin-selenium supplement (100x, Invitrogen, Austria), 40 µM L-proline and 10 ng/ml TGF-β1 (PromoKine, Germany).

8.2.2. Histological analysis (Von Kossa and Alcian Blue stainings)

Additionally, seeded wells without scaffolds were also incubated for 2 weeks with control, osteogenic and chondrogenic medium, respectively and stained with Von Kossa or Alcian Blue to detect osteogenic and chondrogenic differentiation in a 2D environment. For Von Kossa staining, the cells were fixed for 30 min with 10% neutral-buffered formalin. After rinsing with distilled water, cells were overlaid with 5% silver nitrate for 30 min. Staining was performed with 5% sodium carbonate in 25% neutral-buffered formalin and fixed by a 5 min incubation with 5% sodium thiosulphate. For Alcian Blue staining, cells were rinsed with PBS and stained for 30 min at room temperature with 1% Alcian Blue in 3% acetic acid at pH 2.5.

8.2.3. Cell adhesion and morphology

After 2 weeks of incubation, cell-scaffolds constructs were prepared for scanning electron microscopy (SEM) observation by washing the seeded scaffolds 3 times in pre-warmed PBS, fixing them in 2.5% glutaraldehyde at 4°C for 30 min and washing them again 2 times with PBS. Then, the samples were dehydrated in increasing concentrations of ethanol (50, 70, 90 and 100%), each step lasting 30 min. After air-drying, the samples were incubated two times for 15 min in hexamethyldisilazane for critical point drying. Sample surfaces were then gold sputtered (Fisons Instruments, Sputter Coater SC502, UK) and analysed using scanning electron microscopy (SEM) (S360, Leica Cambridge Ltd).

8.2.4. ALP activity

The supernatant was harvested on day 7 and 14 for ALP activity determination using previously established protocols. In brief, 3 volumes of substrate solution consisting of 1 M diethanolamine-hydrochloric acid buffer with 0.2% p-nitrophenylphosphate at pH 9.8 were thoroughly mixed with the culture supernatant. After 45 to 60 min incubation at 37°C, 4 volumes of 2 M NaOH and 0.2 mM EDTA were added to stop the enzymatic reaction. Immediately, the samples, as well as serial dilutions of the standard *p*-nitrophenol ranging from 0 to 20 mmoL/L, were measured in triplicate in a microplate reader (Amersham Biosciences, UK) at 405 nm. Concentrations were calculated using a 4-parameter fit curve.

8.3. PRE-CHONDROGENIC ATDC5 CELLS STUDIES

8.3.1. Cell culture

These studies were performed with insulin-loaded scaffolds, as described in Chapter V, in order to assess the effect of these loaded-scaffolds in chondrogenic differentiation. Cells used in these experiments were a pre-chondrogenic murine mesenchymal cell line (ATDC5) purchased from the European Collection of Cell Cultures (ECACC) which differentiates into mature chondrocytes in the presence of insulin [24,55]. Cells were plated into tissue culture flasks and incubated at 37ºC in a humidified atmosphere of 5%CO_2 in air for expansion. ATDC5 cells were grown as monolayer cultures

in a culture medium consisting of 1:1 mixture of Dulbecco's Modified Eagle's Medium (DMEM) and Ham's F-12 Nutrient Mixture with 15 mM HEPES (F12), sodium bicarbonate, 10,000 units/ml penicillin/10,000 μg/ml streptomycin, 0.365 g/L L-glutamine and 5% (v/v) foetal bovine serum (FBS Heat Inactivated, Biochrom) (DMEM/F12).

When the adequate cell number was obtained, cells at passage 8 were trypsinized, centrifuged and ressuspended in cell culture medium. For the control group with non-loaded scaffolds, standard chondrogenic medium was used consisting in DMEM/F12 supplemented with 10 μg/ml of insulin (DMEM/F12/INS). Cells were seeded at a density of 100,000 cells/scaffold under static conditions using for this purpose aliquots of 100 μl loaded onto the top of the scaffolds, which had been previously placed in 24-well non-adherent tissue culture plates. Two hours after seeding, 1.5 ml of respective cell culture medium according to Table 2 was added to each well and the cell seeded scaffolds were cultured for 2 and 4 weeks, in a humidified atmosphere at 37ºC, containing 5% CO_2. The culture medium was changed every 3 to 4 days until the end of experiments.

Table 2. Scaffolds formulations and respective cell culture medium.

SCAFFOLDS	FORMULATION	CULTURE MEDIUM
C	Non-loaded (control group)	DMEM/F12/INS
0.05	Loaded with 0.05% (wt/wt) insulin	DMEM/F12
0.5	Loaded with 0.5% (wt/wt) insulin	DMEM/F12
5	Loaded with 5% (wt/wt) insulin	DMEM/F12

Abbreviations: DMEM - Dulbecco's Modified Eagle's Medium; F12 - Ham's F-12 Nutrient Mixture with 15 mM HEPES, INS - DMEM/F12 supplemented with 10μg/ml of insulin.

8.3.2. Cell adhesion and morphology

Cell adhesion, morphology and average distribution were observed by SEM analysis. Briefly, the cell-scaffold constructs were washed in PBS and fixed in 2.5% glutaraldehyde (in PBS). The constructs were then rinsed in PBS again, and subjected to 15 minutes immersion cycles into series of increasing ethanol concentrations (30, 50, 70, 90, 100% ethanol), each to dehydrate the samples. The samples

were finally subjected to critical point drying by double immersion into HMDS (hexamethyldisilazane reagent) for 15 minutes each, air dried and sputter coated with gold (JEOL JFC-1100) and analyzed with a Leica Cambridge S360 scanning electron microscope.

8.3.3. DNA quantification

DNA quantification was carried out using PicoGreen® dsDNA Quantitation reagent (Invitrogen, Barcelona, Spain) according to the supplier protocol. Briefly, the cell-scaffolds systems were collected at pre-defined time periods, placed into eppendorf tubes with 1ml ultrapure water, and kept at 37ºC for 1 hour. They were then subjected to 2-3 cycles of freezing-defrosting to assure that the entire DNA would be in solution. Standards of double stranded DNA were prepared using ultrapure water with the following concentrations: 0, 0.2, 0.5, 1 and 2 µg/ml. Chitosan scaffolds without cells were used as controls. Standards, controls and samples were placed in 96-well plates in triplicate according to kit instructions where each single well contained 200 µl of total mixture solution. The plates were submitted to a 10 minutes incubation cycle in the dark. Emitted fluorescence was read using a microplate reader (Synergy HT, BioTek) and the data was recorded for analysis with the software (KC4 Microplate Data Analysis Software, BioTek) (at excitation of 485/20 nm and emission of 528/20 nm).

8.3.4. Glycosaminoglycans (GAGs) quantification

Proteoglycans amount was determined by measuring the level of sulfated glcosaminoglycans (GAGs) using the dimethylmethylene blue metachromatic assay. GAG levels in solution can be quantified using the basic dye, 1,9-dimethylmethylene blue (DMB), which binds to glycosaminoglycans generating a metachromatic shift that peaks at A525-530 that can be measured spectrophotometrically. Briefly, the constructs (n=3) were immersed in a digestion solution with papain and N-acetyl cysteine and incubated at 60ºC overnight. After the digestion was completed, the tubes were centrifuged at 13,000 rpm for 10 minutes and the supernatant was collected. Chondroitin sulfate standard solutions were prepared with different concentrations (0, 2.5, 5, 10, 15, 20, 25, 30, 35, 40, 45 and 50 µg/ml) to establish the calibration curve for unknown samples quantification. Chitosan scaffolds without cells were used as controls. Standards, controls and samples (20 µl) were placed in triplicate in a 96 well plate and then

250 µl of DMB solution was added to each well. The optical density was measured at 530 nm using a microplate reader (Synergy HT, BioTek) and the data analysed with the software (KC4 Microplate Data Analysis Software, BioTek).

8.3.5. Histological analysis (hematoxylin-eosin and toluidine blue stainings)

Concerning the histological analysis, hematoxylin-eosin (H&E) and toluidine blue stainings were performed on 10 µm thickness sections of cells-scaffolds constructs (n=3) collected at different periods of culture. The samples were fixated by immersion for 30 minutes in glutaraldehyde 2.5%(v/v) at 4ºC, and washed in PBS. Histological processing was performed using Tecnhovit 7100® (Heraeus Kulzer GmbH) according to the supplier protocol and sections were sliced using a motorized rotary microtome (Leica RM2155, Leica Microsystems GmbH). H&E staining was performed using an automatic processor according to in-house methodology (Leica TP1020-1, Leica MicroSystems GmbH) and toluidine blue staining was performed as follows. Briefly, sections were hydrated in distilled water and stained in 1% toluidine blue working solution for 2-3 minutes. Afterwards, they were washed 3 times in distilled water and quickly dehydrated through 95% ethanol and 100% alcohol. Sections were then cleared in Histoclear® and mounted using Microscopy Entellan® (Merck) for observation.

8.3.6. Evaluation of gene expression by realtime-PCR

Samples were collected at the defined time periods, quickly frozen in liquid nitrogen, and stored at −80°C until further analysis. RNA was extracted using TRIzol® (Invitrogen, Barcelona, Spain) according to the supplier protocol. Briefly, samples of each condition (n=2) were grinded and mechanically homogenized with a mostar and pestle in TRIzol reagent. Afterwards, chloroform was added and the samples centrifuged to establish a three-phase composition in the tube. The aqueous phase was collected and put in a new tube where isopropanol was added. The samples were once again centrifuged, the supernatant discarded and the pellet washed with 75% ethanol. The samples were again centrifuged, let to air-dry, and suspended in ultrapure water for posterior analysis. The amount of isolated RNA and A260/280 ratio was determined using Nanodrop ND-1000 Spectrophotometer (NanoDrop Technologies). After these determinations, 1 µg of RNA of each sample was reverse

transcribed into cDNA using the IScriptTM cDNA synthesis kit (Biorad, California, USA) in a MJ MiniTM Personal Thermal Cycler (Biorad, California, USA). Cartilage related markers were chosen to evaluate the chondrogenic phenotype of the cultured systems. These included collagen type I, collagen type II, Sox-9 and aggrecan, using GAPDH as the housekeeping gene for normalization. The expression of each gene was normalized to the GAPDH value in that sample. All the primer sequences were generated using Primer3 software and acquired from MWG Biotech. More details can be found in Table 3. Realtime-PCR was performed using SYBR Green IQTM Supermix (Biorad, California, USA) to detect amplification variations in a MJ MiniTM Personal Thermal Cycler (Biorad, California, USA) machine. The analysis of the results was performed with MJ Opticon Monitor 3.1 software (Biorad, California, USA).

Table 3. Primers used for realtime-PCR evaluation of ATDC-5 gene expression.

GENE	ACCESSION	LEFT PRIMER	RIGHT PRIMER
Collagen type I	NM_007742	GAGCGGAGAGTACTGGATCG	GCTTCTTTTCCTTGGGGTTC
Collagen type II	NM_001113515	GCCAAGACCTGAAACTCTGC	GCCATAGCTGAAGTGGAAGC
Sox-9	NM_011448	AGCTCACCAGACCCTGAGAA	TCCCAGCAATCGTTACCTTC
Aggrecan	NM_007424	TGGCTTCTGGAGACAGGACT	TTCTGCTGTCTGGGTCTCCT
GAPDH	NM_008084	AACTTTGGCATTGTGGAAGG	ACACATTGGGGGTAGGAACA

9. *IN-VIVO* BIOCOMPATIBILITY STUDY

It is critical to evaluate the scaffolds' performance in an *in-vivo* environment when proposing materials to be used in biomedical applications, namely tissue engineering. *In-vivo* parameters such as inflammatory response, tissue ingrowth, vascularization potential and overall host response give the correct evidence to consider the biofunctionality of scaffolds. This is one of the obvious key requirements for tissue engineering applications. In Chapter VI, the experimental results are described for the *in-vivo* performance in a rat muscle-pockets model for different implantation periods, where scaffolds interconnectivity shown to be favourable to the connective tissues ingrowth and to promote the neo-vascularization even in early stages of implantation.

9.1. SURGICAL PROCEDURE

Four male Sprague Dawley rats, weighing 350-380 g were used for intramuscular implantation of the chitosan aggregated scaffolds. Each animal was anaesthetized (induction with 3-3.5% isofluorane and 7 L/minute of air for 2-3 minutes; maintenance with intramuscular injection of 90 mg/kg of ketamin combined with 5 mg/kg xylazine) and subjected to local tricotomy for adequate surgical procedure. The skin was disinfected and under surgical sterile conditions, four lumbar paravertebral incisions of approximately 2 cm length were performed through the cutis, subcutis and the *panniculus carnosus* (smooth skin muscle). After incising the fascia of the *latissimus dorsi* muscle, craniolateral oriented muscle-pockets were created by blunt dissection. Into these pockets, the scaffolds were inserted and the fascia carefully sutured, as well as the *panniculus carnosus* and finally the skin. As an analgesic treatment, animals received Metamizol (200 μg/g of body weight per day in drinking water *ad libitum*). At 1, 2 and 12 weeks post-implantation, the animals were anaesthetized (see above) and sacrificed by an intracardial overdose of pentobarbital. The scaffolds and surrounding tissue were explanted for further evaluation. The animal experiment was approved by the local ethical authorities for animal experimentation.

9.2. EXPLANTS MORPHOLOGICAL CHARACTERIZATION

At 1, 2 and 12 weeks post-implantation, explants were registered using stereolight microscopy. Furthermore, micro-Computed Tomography (micro-CT) of the explants was carried out using the Skyscan equipment, as described previously. Two-dimensional (2D) X-ray photographs were registered from the bulk of the explants.

9.3. HISTOLOGICAL EVALUATION

After explantation at 1, 2 and 12 weeks, samples were fixed in 4.7% formalin for 24 hours and then kept in 70% ethanol. After fixation, samples were dehydrated in graded ethanol (50, 70, 95 and 100%), embedded in xylene and then, in paraffin. Afterwards, samples were sectioned in 2-4 μm sections and

stained with haematoxylin/eosin (H&E). The stained microscope slides were observed by, at least, two independent observers.

9.3.1. Immunohistochemistry

In order to perform immunohistochemistry, paraffin was removed from the samples slides upon heating. They were hydrated in descending ethanol concentrations (100, 95, 70 and 50%) and incubated in Phosphate Buffer Saline (PBS). The antigen retrieval was performed with microwave incubation in citrate buffer (pH=6) at 800W for 20 minutes and the slides were washed with PBS. The endogenous peroxidase was blocked with 1% hydrogen peroxide (H_2O_2) in methanol, at room temperature (RT) for 15 minutes. After washing, the slides were incubated with the primary antibodies at RT for 1 hour (see Table 4) and washed at the end of the incubation period. Subsequently, the samples were incubated with the secondary antibody (Polyclonal Swine Anti-Goat, Mouse, Rabbit Immunoglobulins/Biotinylated – DakoCytomation, Denmark; dilution 1:100) at RT, for 30 minutes. After washing with PBS, the samples were incubated with the ABComplex (StreptABComplex/HRP, DakoCytomation, Denmark) at RT for 30 minutes and washed again after the incubation period.

Visualisation of the bound antibodies in the samples was revealed by incubation with AEC substrate (Dako RealTM EnVisionTM Detection System, Peroxidase/DAB+, Rabbit/Mouse; DakoCytomation, Denmark) until the colour could be detected. The revelation of the labelling was stopped with PBS and the samples were stained with Mayer's Haematoxylin for nuclear contrast, at RT, for 2 minutes. After this, the samples were washed with distilled water, dehydrated in graded ethanol (50, 70, 95 and 100%), cleared with xylene substitute, permanently mounted with Clarion™ Mounting Medium, and observed in the light microscope by, at least, two independent observers.

Table 4. Primary antibodies used in the immunohistochemistry evaluation of the explants.

ANTIBODY	RECOGNIZES	DILUTION	INCUBATION/TEMPERATURE	COMPANY	COUNTRY
CD18	Rat β2 integrins (βchain of LFA-1)	1:100	1 hour/RT	Serotec	UK
CD3	T lymphocytes	1:30	1 hour/RT	DakoCytomation	Denmark
vWF	von Willebrand Factor	1:200	1 hour/RT	DakoCytomation	Denmark
SMA	Smooth Muscle Actin	1:5000	1 hour/RT	Sigma	USA

10. STATISTICAL ANALYSIS

The statistical analysis of values obtained with the several relevant characterization techniques was carried out using Student's two-tailed *t*-test with a confidence level of 99.5%. All statistical calculations were performed with Analysis ToolPak software. ρ-Values below 0.05 were considered statistically significant.

REFERENCES

1. P.B. Malafaya, G.A. Silva, R.L. Reis. Natural-origin polymers as carriers and scaffolds for biomolecules and cell delivery in tissue engineering applications. Advanced Drug Delivery Reviews, 59 (2007) 207-233.

2. A.D. Martino, M. Sittinger, M.V. Risbud. Chitosan: a versatile biopolymer for orthopaedic tissue-engineering. Biomaterials, 26 (2005) 5983-5990.

3. E. Khor, L.Y. Lim. Implantable applications of chitin and chitosan. Biomaterials, 24 (2003) 2339-2349.

4. P.B. Malafaya, A. Pedro, A. Peterbauer, C. Gabriel, H. Redl, R.L. Reis. Chitosan particles agglomerated scaffolds for cartilage and osteochondral tissue engineering approaches with adipose tissue derived stem cells. Journal of Materials Science: Materials in Medicine, 16 (2005) 1077.

5. I.Y. Kim, S.J. Seo, H.S. Moon, M.K. Yoo, I.Y. Park, B.C. Kim, C.S. Cho. Chitosan and its derivatives for tissue engineering applications. Biotechnology Advances, 26 (2008) 1-21.

6. M. George, T.E. Abraham. Polyionic hydrocolloids for the intestinal delivery of protein drugs: alginate and chitosan - a review. Journal of Controlled Release, 114 (2006) 1-14.

7. M. Julien, D.R. Letouneau, Y. Marois, A. Cardou, M.W. King, R. Guidoin, D. Chachra, J.M. Lee. Shelf-life of bioprosthetic heart valves: a structural and mechanical study. Biomaterials, 18 (1997).

8. V.R. Patel, M.M. Amiji. Preparation and characterization of freezedried chitosan-poly(ethylene oxide) hydrogels for site-specific antibiotic delivery in the stomach. Pharmaceutical Research, 13 (1996) 588-593.

9. W.I. Abdel-Fattah, T. Jiang, G.E.T. El-Bassyouni, C.T. Laurencin. Synthesis, characterization of chitosans and fabrication of sintered chitosan microsphere matrices for bone tissue engineering. Acta Biomaterialia, 3 (2007) 503-514.

10. T. Jiang, W.I. Abdel-Fattah, C.T. Laurencin. In vitro evaluation of chitosan/poly(lactic acid-glycolic acid) sintered microsphere scaffolds for bone tissue engineering. Biomaterials, 27 (2006) 4894-4903.

11. J.Y. Lee, S.H. Nam, S.Y. Im, Y.J. Park, Y.M. Lee, Y.J. Seol, C.P. Chung, S.J. Lee. Enhanced bone formation by controlled growth factor delivery from chitosan-based biomaterials. Journal of Controlled Release, 78 (2002) 187-197.

12. S.E. Kim, J.H. Park, Y.W. Cho, H. Chung, S.Y. Jeong, E.B. Lee, I.C. Kwon. Porous chitosan scaffold containing microspheres loaded with transforming growth factor-beta1: implications for cartilage tissue engineering. Journal of Controlled Release, 91 (2003) 365-74.

13. R.A. Sousa, R.L. Reis, A.M. Cunha, M.J. Bevis. Bi-Composite Sandwich Mouldings: Processing, Mechanical Performance and Bioactive Behaviour. Journal of Materials: Materials in Medicine, 14 (2003) 385-397.

14. I.B. Leonor, A.I. A, K. Onuma, N. Kanzaki, R.L. Reis. In-vitro bioactivity of starch thermoplastic/hydroxylapatite composite biomaterials: an in-situ study using atomic force microscopy Biomaterials, 24 (2003) 579-585.

15. D.A. Wahl, J.T. Czernuszka. Collagen-hydroxyapatite composites for hard tissue repair. European Cells and Materials, 11 (2006) 43-56.

16. W. Bonfield, M.D. Grynpas, A.E. Tully. Hydroxyapatite reinforced polyethylene - a mechanically compatible implant material for bone replacement. Biomaterials, 2 (1981) 185-186.

17. J.A. Juhasz, S.M. Best, R. Brooks, M. Kawashita, N. Miyata, T. Kokubo, T. Nakamura, W. Bonfield. Mechanical properties of glass-ceramic A-W-polyethylene composites: Effect of filler content and particle size. Biomaterials, 25 (2004) 949-955.

18. I. Sopyan, M. Mel, S. Ramesh, K.A. Khalid. Porous hydroxyapatite for artificial bone applications. Science and Technology of Advanced Materials, 8 (2007) 116-123.

19. J.H. Kim, S.H. Kim, H.K. Kim, T. Akaike, S.C. Kim. Synthesis and characterization of hydroxyapatite crystals: A review study on the analytical methods. Journal of Biomedical Materials Research, 62 (2002) 600-612.

20. J.W. Frame. Hydroxyapatite as a biomaterial for alveolar ridge augmentation. International journal of oral and maxillofacial surgery, 16 (1987) 642-655.

21. C. Phornphutkul, K.Y. Wu, X. Yang, Q. Chen, P.A. Gruppuso. Insulin-like growth factor-I signaling is modified during chondrocyte differentiation. Journal of Endocrinology, 183 (2004) 477-486.

22. C. Schmid. Insulin-like growth factors. Cell Biology International, 19 (1995) 445-457.

23. H. Madry, G. Kaul, M. Cucchiarini, U. Stein, D. Zurakowski, K. Remberger, M.D. Menger, D. Kohn, S.B. Trippel. Enhanced repair of articular cartilage defects in vivo by transplanted chondrocytes overexpressing insulin-like growth factor I (IGF-I). Gene Therapy, 12 (2005) 1171-1179.

24. Z. Lin, C. Willers, J. Xu, M.-H. Zheng. The Chondrocyte: Biology and Clinical Application. Tissue Engineering, 12 (2006) 1971-1984.

25. K.H. Chua, B.S. Aminuddin, N.H. Fuzina, B.H.I. Ruszymah. Insulin-Transferrin-Selenium prevent human chondrocyte dedifferentiation and promote the formation of high quality tissue engineered human hyaline cartilage. European Cells and Materials, 9 (2005) 58-67.

26. K. Kellner, M.B. Schulz, A. Gopferich, T. Blunk. Insulin in tissue engineering of cartilage: A potential model system for growth factor application. Journal of Drug Targeting, 9 (2001) 439-448.

27. M. Borden, S.F. El-Amin, M. Attawia, C.T. Laurencin. Structural and human cellular assessment of a novel microsphere-based tissue engineered scaffold for bone repair. Biomaterials, 24 (2003) 597-609.

28. M. Borden, M. Attawia, Y. Khan, C.T. Laurencin. Tissue engineered microsphere-based matrices for bone repair: design and evaluation. Biomaterials, 23 (2002) 551-559.

29. M. Borden, M. Attawia, C.T. Laurencin. The sintered microsphere matrix for bone tissue engineering: In vitro osteoconductivity studies. Journal of Biomedical Materials Research, 61 (2002) 421-429.

30. J.E. Devin, M.A. Attawia, C.T. Laurencin. Three-dimensional degradable porous polymer-ceramic matrices for use in bone repair. Journal of Biomaterials Science-Polymer Edition, 7 (1996) 661-669.

31. T.A. Holland, Y. Tabata, A.G. Mikos. *In vitro* release of transforming growth factor-b1 from gelatin microparticles encapsulated in biodegrabable, injectable oligo(poly(ethylene glycol) fumarate) hydrogels. Journal of Controlled Release, 91 (2003) 299-313.

32. D.H.R. Kempen, C.W. Kim, L. Lu, W.J.A. Dhert, B.L. Currier, M.J. Yaszemski. Controlled release from poly(lactic-co-glycolic acid) microspheres embedded in an injectable, biodegradable scaffold for bone tissue engineering. Thermec'2003, Pts 1-5, 426-4 (2003) 3151-3156.

33. R.G. Payne, J.S. McGonigle, M.J. Yaszemski, A.W. Yasko, A.G. Mikos. Development of an injectable, in situ crosslinkable, degradable polymeric carrier for osteogenic cell populations. Part 3. Proliferation and differentiation of encapsulated marrow stromal osteoblasts cultured on crosslinking poly(propylene fumarate). Biomaterials, 23 (2002) 4381-7.

34. R.G. Payne, M.J. Yaszemski, A.W. Yasko, A.G. Mikos. Development of an injectable, in situ crosslinkable, degradable polymeric carrier for osteogenic cell populations. Part 1. Encapsulation of marrow stromal osteoblasts in surface crosslinked gelatin microparticles. Biomaterials, 23 (2002) 4359-71.

35. E.L. Hedberg, A. Tang, R.S. Crowther, D.H. Carney, A.G. Mikos. Controlled release of an osteogenic peptide from injectable biodegradable polymeric composites. Journal of Controlled Release, 84 (2002) 137-50.

36. T.M. Meese, Y. Hu, R.W. Nowak, K.G. Marra. Surface studies of coated polymer microspheres and protein release from tissue-engineered scaffolds. J Biomater Sci Polym Ed, 13 (2002) 141-51.

37. A. Perets, Y. Baruch, F. Weisbuch, G. Shoshany, G. Neufeld, S. Cohen. Enhancing the vascularization of three-dimensional porous alginate scaffolds by incorporating controlled release basic fibroblast growth factor microspheres. Journal of Biomedical Materials Research, 65A (2003) 489-97.

38. I.B. Leonor, R.A. Sousa, A.M. Cunha, R.L. Reis, Z.P. Zhong, D. Greenspan. Novel starch thermoplastic/Bioglass® composites: Mechanical properties, degradation behavior and in-vitro bioactivity. Journal of Materials Science: Materials in Medicine, 13 (2002) 939-945.

39. J.F. Mano, R.L. Reis. Osteochondral defects: present situation and tissue engineering approaches. Journal of Tissue Engineering and Regenerative Medicine 1(2007) 261-273.

40. I. Martin, S. Miot, A. Barbero, M. Jakob, D. Wendt. Osteochondral tissue engineering. Journal of Biomechanics, 40 (2007) 750-765.

41. W. Swieszkowski, B.H.S. Tuan, K.J. Kurzydlowski, D.W. Hutmacher. Repair and regeneration of osteochondral defects in the articular joints. Biomolecular Engineering, 24 (2007) 489-495.

42. S.T. Ho, D.W. Hutmacher. A comparison of micro-CT with other techniques used in the characterization of scaffolds. Biomaterials, 27 (2006) 1362-1376.

43. A.C. Jones, B. Milthorpe, H. Averdunk, A. Limaye, T.J. Senden, A. Sakellariou, A.P. Sheppard, R.M. Sok, M.A. Knackstedt, A. Brandwood, D. Rohner, D.W. Hutmacher. Analysis of 3D bone ingrowth into polymer scaffolds via micro-computed tomography imaging. Biomaterials, 25 (2004) 4947-4954.

44. B. Otsuki, M. Takemoto, S. Fujibayashi, M. Neo, T. Kokubo, T. Nakamura. Novel micro-CT based 3-dimentional structural analyses of porous biomaterials. Key Engineering Materials, 330-332 II (2007) 967-970.

45. F. Peyrin, M. Mastrogiacomo, R. Cancedda, R. Martinetti. SEM and 3D synchrotron radiation micro-tomography in the study of bioceramic scaffolds for tissue-engineering applications. Biotechnology and Bioengineering, 97 (2007) 638-648.

46. L.A. Feldkamp, S.A. Goldstein, A.M. Parfitt, G. Jesion, M. Kleerekoper. The direct examination of three-dimensional bone architecture in vitro by computed tomography. Journal of Bone and Mineral Research, 4 (1989) 3-11.

47. T. Hildebrand, A. Laib, R. Muller, J. Dequeker, P. Ruegsegger. Direct three-dimensional morphometric analysis of human cancellous bone: Microstructural data from spine, femur, iliac crest, and calcaneus. Journal of Bone and Mineral Research, 14 (1999) 1167-1174.

48. L.M. Mathieu, T.L. Mueller, P.-E. Bourban, D.P. Pioletti, R. Muller, J.-A.E. Manson. Architecture and properties of anisotropic polymer composite scaffolds for bone tissue engineering. Biomaterials, 27 (2006) 905-916.

49. http://www.skyscan.be/ (2008).

50. T. Kokubo, H. Takadama. How useful is SBF in predicting in vivo bone bioactivity? Biomaterials, 27 (2006) 2907-2915.

51. H. Takadama, M. Hashimoto, M. Mizuno, K. Ishikawa, T. Kokubo. Newly Improved Simulated Body Fluid. Key Engineering Materials, 254-256 (2004) 115-118.

52. A. Oyane, H.-M. Kim, T. Furuya, T. Kokubo, T. Miyazaki, T. Nakamura. Preparation and assessment of revised simulated body fluids. Journal of Biomedical Materials Research Part A, 65A (2003) 188-195.

53. S.D. Conzone, R.F. Brown, D.E. Day, G.J. Ehrhardt. In vitro and in vivo dissolution behavior of a dysprosium lithium borate glass designed for the radiation synovectomy treatment of rheumatoid arthritis. Journal of Biomedical Materials Research, 60 (2002) 260-268.

54. P.A. Zuk, M. Zhu, P. Ashjian, D.A. De Ugarte, J.I. Huang, H. Mizuno, Z.C. Alfonso, J.K. Fraser, P. Benhaim, M.H. Hedrick. Human adipose tissue is a source of multipotent stem cells. Mol Biol Cell, 13 (2002) 4279-4295.

55. C. Phornphutkul, K.-Y. Wu, P.A. Gruppuso. The role of insulin in chondrogenesis. Molecular and Cellular Endocrinology, 249 (2006) 107-115.

SECTION 3.

CHAPTER III.

Chitosan particles agglomerated scaffolds for cartilage and osteochondral tissue engineering approaches with adipose tissue derived stem cells

CHAPTER III.

Chitosan particles agglomerated scaffolds for cartilage and osteochondral tissue engineering approaches with adipose tissue derived stem cells *

ABSTRACT

It is well accepted that natural tissue regeneration is unlikely to occur if the cells are not supplied with an extracellular matrix (ECM) substitute. With this goal, several different methodologies have been used to produce a variety of 3D scaffolds as artificial ECM substitutes suitable for bone and cartilage tissue engineering. Furthermore, osteochondral tissue engineering presents new challenges since the combination of scaffolding and co-culture requirements from both bone and cartilage applications is required in order to achieve a successful osteochondral construct.

In this paper, an innovative processing route based on a chitosan particles aggregation methodology for the production of cartilage and osteochondral tissue engineering scaffolds is reported. An extensive characterization is presented including a morphological evaluation using Micro-Computed Tomography (μ-CT) and 3D virtual models built with an image processing software. Mechanical and water uptake characterizations were also carried out, evidencing the potential of the developed scaffolds for the proposed applications. Cytotoxicity tests show that the developed chitosan particles agglomerated scaffolds do not exert toxic effects on cells. Furthermore, osteochondral bilayered scaffolds could also be developed. Preliminary seeding of mesenchymal stem cells isolated from human adipose tissue was performed aiming at developing solutions for chondrogenic and osteogenic differentiation for osteochondral tissue engineering applications.

---

* This chapter is based in the following publication:

PB Malafaya, AJ Pedro, A. Peterbauer, C. Gabriel, H. Redl, RL Reis. Chitosan particles agglomerated scaffolds for cartilage and osteochondral tissue engineering approaches with adipose tissue derived stem cells. Journal of Materials Science: Materials in Medicine (2005) 16:1077-1085

---

1. INTRODUCTION

Tissue engineering has developed into a multi-disciplinary field using both the state of the art and breakthrough research of several different areas. It uses biological, chemical and materials engineering principles towards the repair, restoration or regeneration of living tissues combining biomaterials, cells and biologically active factors. This now well accepted concept leads to the basis of one of the three key issues in tissue engineering which is clearly the scaffolding that should provide an ideal site for cell attachment and proliferation leading to further tissue regeneration. The extracellular matrix (ECM) that surrounds cells in the body not only physically supports cells but also regulates their proliferation and differentiation. Consequently, scaffolds need to be developed for sustaining *in-vitro* tissue reconstruction, as well as for *in-vivo* cell-mediated tissue regeneration. It is almost impossible to repair tissue defects if the cells are not supplied with such kind of an ECM substitute.

Bearing this in mind, several different methodologies have been used to produce a variety of three dimensional synthetic or naturally based scaffolds suitable for tissue engineering applications. Researchers have been using, for instance, injection moulding with blowing agents [1], solvent casting and salt leaching techniques [2] or the latter combined with compression moulding [3] or gas foaming [4,5]. In the salt leaching technique, the pre-incorporated salt in the polymeric matrix is dissolved creating the pores. Fibre bonding [6] has also been used to produce successfully fibre meshed 3D structures with high interconnectivity. Other techniques, such as freeze-drying [7-9] and rapid prototyping technologies [10-12] have also been used to produce interesting scaffolds. Nevertheless, further research on the scaffold design is still needed because the chemical nature and structure of the 3D constructs significantly affect the success of tissue engineering approaches both *in-vitro* and *in-vivo*. Moreover, an optimal scaffold has not been identified yet.

Towards this goal, an innovative methodology is being developed in several groups, based on the agglomeration of prefabricated microspheres. The technique is generally based on the random packing of microspheres with further aggregation by physical or thermal means to create a three dimensional porous structure. This technique is being used to construct scaffolds directly [13] or it can be proposed to be used indirectly by producing a negative structure which will serve as a reverse template to obtain the scaffolds.

The research group of C.T. Laurencin [13-15] has been applying this technique for the development of poly(lactide-co-glycolide) (PLAGA) microspheres-based matrices for bone repair. The researchers have tried different approaches by developing sintered microspheres based matrices [13,14] or gel microspheres matrices [15]. Composite microspheres containing hydroxyapatite were also used for the fabrication of polymer-ceramics 3D matrices for bone applications [16]. In the case of sintered microspheres matrices, the microspheres are first obtained by a solvent evaporation technique. The 3D structures are then further processed by heating the pre-fabricated PLAGA microspheres above the glass transition temperature. The polymer chains are activated to interlink with neighbouring polymer chains and thus form contacts between neighbouring microspheres [15]. In the gel microspheres matrix methodology, the PLAGA gel microspheres are obtained by emulsion with poly(vinyl alcohol) (PVA). The following agglomeration is based on a multiple step production that includes air-drying, freeze-drying, rehydration with salt leaching and freeze-drying again. In general, microsphere based matrices show very interesting properties for a possible application in bone repair.

Another strategy that uses microspheres includes their embedding in a hydrogel matrix [17-19]. In that approach, the goal of incorporation of previously produced microspheres is to encapsulate either cells [20] or biologically active factors for either favouring the cell attachment and proliferation behaviour [18,21-23] or to enhance the vascularization [24].

Several million people worldwide suffer from severe joint pain and related dysfunction, such as loss of motion as a result of injury or osteoarthritis [25-28]. In particular, loss of function of the knees can severely reduce mobility and thus the patient's quality of life [29]. The biological basis of joint problems is the deterioration of articular cartilage which covers the bone at the joint surface [30]. Current treatments most widely used are based on autologous strategies such as mosaicplasty [31]. Abrasion arthroscopy, subchondral bone drilling and microfracture typically result in fibrocartilage filling the defect site [29]. Allogenic transplantation of osteochondral grafts has had clinical success, but its supply is limited and has a risk of infection or even rejection [26,28]. Therefore, besides bone and cartilage tissue engineering approaches, a combination of both as osteochondral constructs is needed in clinical practice.

To create constructs with more favourable integrative properties, several researchers are exploring the development of tissue engineered osteochondral composite constructs [26,27,32,33]. However,

osteochondral tissue engineering presents new interesting challenges because the combination of scaffolding and co-culture requirements, from both bone and cartilage applications, in an efficient way is required to achieve a successful osteochondral approach.

A few approaches have been proposed based on the development of bilayered 3D materials [25,26,32-35]. Osteochondral scaffolds based on collagen gels and calcium phosphate ceramics were proposed by Tagushi *et al.* [33]. The processing methodology consists of the formation of a calcium phosphate gradient into cartilage-like matrices containing type II collagen using a modified alternate soaking process. It was shown that, after a number of soaking cycles, calcium phosphate crystals were gradiently formed from the top to the middle of gels [33].

A very interesting work was presented by Sherwood *et al.* [26] in 2002 where a three-dimensional printing process was used to build a one-piece bilayered osteochondral scaffold. The upper, cartilage region was 90% porous and composed of D,L-PLGA/L-PLA, with macroscopic staggered channels to facilitate homogenous cell seeding. The lower, cloverleaf-shaped bone portion was 55% porous and consisted of a L-PLGA/TCP composite, designed to maximize bone ingrowth while maintaining critical mechanical properties [26].

A different approach was used by Lu *et al.* [25,34,35]. They based their studies on chondrocyte encapsulation in agarose hydrogels for the cartilage component, and composites microspheres (PLAGA and Bioactive Glass®) prepared by a water-oil-water emulsion and further sintered to produce the 3D scaffolds for the bone component. These studies showed that chondrocytes maintained their phenotype and developed a functional extracellular matrix. In addition, the osteochondral construct was found to be capable to simultaneously support the growth of multiple matrix zones. Recently, this research group has also presented a multi-phased composite scaffold for soft tissue-to-bone interface [34] using 3 different phases composed by PLAGA woven mesh, PLAGA microspheres and PLAGA - Bioactive Glass® microspheres. Studies were undertaken with osteoblasts and fibroblasts to evaluate the potential of supporting multiple cell types and the scaffold was used as a model system to regenerate soft tissue to bone interface.

In the present paper, a new processing route based on chitosan particles aggregation is described for the production of cartilage and osteochondral tissue engineering scaffolds. The described method uses

previously prepared chitosan-based particles. For the osteochondral approach, bilayered scaffolds were developed in order to achieve an improved integrative bone and cartilage interface needed for these applications. Preliminary cell tests were performed by seeding mesenchymal stem cells isolated from human adipose tissue on the scaffolds and trying to promote them both in chondrogenic and osteogenic differentiation. This is a prerequisite for cartilage and osteochondral tissue engineering applications.

2. MATERIALS AND METHODS

2.1. SCAFFOLDS PRODUCTION

Chitosan (from Sigma-Aldrich, medium molecular weight and 87.8 % of deacetylation degree) was grinded and dissolved overnight in acetic acid (1%vv) to obtain a chitosan solution (2%wt). Unless otherwise stated, all chemicals were bought from Sigma-Aldrich and used as received. In composite particles production for the osteochondral bilayered scaffolds, 20%wt of non-sintered hydroxylapatite (HA) (CAM Implants, UK) with an average particle size of 30 μm [36] was homogeneously dispersed in the chitosan solution. After complete dissolution and filtration, the prepared solutions were extruded trough a syringe at constant rate (10 ml/h) to form chitosan droplets into a NaOH (1M) precipitation bath where particles with regular diameter were formed. The chitosan particles were left overnight in the precipitation bath and then repeatedly washed with distilled water. For the production of the bilayered scaffolds, the composite particles were submitted to a crosslinking reaction with glutaraldehyde. Further information on this can be found elsewhere [37,38]. The particles were subsequently pressed into moulds and left to dry in an oven at 50ºC for 3 days. Cylinder shaped scaffolds with 8 mm height and 5 mm in diameter were obtained. A schematic representation of the used methodologies is shown in Figure 1.

→

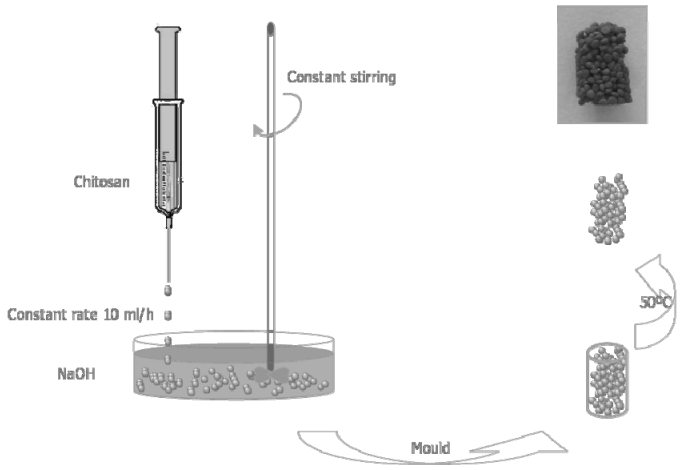

Figure 1. Schematic representation of the chitosan precipitation and particle aggregation methodologies.

2.2. SCAFFOLDS CHARACTERIZATION

The scaffolds morphology was analyzed by Scanning Electron Microscopy (SEM) in a Leica-Cambridge S-360 (Leica-Cambridge, UK) microscope equipped with V03.02A software. Micro-Computed Tomography (μ-CT) evaluation of the scaffolds was carried out using a Scanco 20 equipment (Scanco Medicals, Switzerland). X-ray scans were performed in high resolution mode (9 μm) and 240 slices of the scaffolds were obtained. The 2-D histomorphometric analysis of the scaffolds was performed using a threshold 51 to identify the polymeric phase in order to determine the mean porosity as well as the porosity distribution along the scaffold (from 0-2000 μm). Furthermore, with the μ-CT data import and MIMICS® (Materialise Interactive Medical Image Control System) image processing software (Materialise, Belgium), it was possible to build 3D virtual models representing the morphological structures of the scaffolds.

The mechanical properties of the developed scaffolds were tested on a compressive solicitation mode in an Instron Universal Mechanical Testing machine in a controlled environment (23ºC/55% RH). The cross-head speed used was 2 mm/min.

The hydration behaviour was assessed in media with different pH (5, 7.4 (physiological pH) and 9) in order to study the potential responsive behaviour of the developed systems. The assays were

performed at physiological temperature (37º±1ºC) for predetermined immersion periods up to 14 days. The swelling profile was characterized using the following equation:

$$\%\, Hydration\ degree = \frac{W_W - W_i}{W_i} * 100 \qquad (1)$$

where W_i is the initial weight and W_w is the wet weight at determined test period.

2.3. *IN-VITRO* BIOLOGICAL TESTING

The cytotoxicity of the material was assessed by evaluating cellular viability using MTS assay (3-(4,5-dimethylthiazol-2-yl)-5-(3-carboxylmethoxyphenyl)-2-(4-sulfophenyl)-2H tetrazolium) (Cell Titer 96® AQueous Solution Cell Proliferation Assay, G3580, Promega, USA). For this purpose, materials were incubated in culture medium for 24h at 37ºC with constant shaking. Latex was also incubated as a positive control. Cultured cells (L929 fibroblasts cell line) were plated (200 µl/well) into 96-well micrometer plates at $6.6x10^4$ cells/well. The plates were incubated for 24h at 37ºC in a humidified atmosphere of 5% CO_2 in air. After that, the medium was replaced by the previously prepared material extracts, using culture medium as a negative control. After a 72h incubation, the cell culture was treated with MTS (in medium without phenol red) and incubated for further 3 h at 37ºC in a humidified atmosphere of 5% of CO_2 in air. At this stage, culture medium with MTS was transferred to new wells. The optical density (OD) which is directly proportional to the cellular activity (it reflects the mitochondrial activity) was read on a multiwell microplate reader (Synergy HT, BioTek Instruments) at 490 nm.

For the preliminary osteogenic and chondrogenic differentiation studies, the scaffolds were seeded with mesenchymal stem cells (MSC) isolated from adipose tissue derived from liposuction procedures as previously described [39]. Briefly, the liposuction material was washed 3 times with phosphate buffered saline (PBS purchased from PAA, Austria) to remove most of the blood and tumescence solution. Afterwards, the tissue was digested in PBS buffered with 25 mM Hepes (PAA, Austria) containing 1.5 mg/mL collagenase (Biochrom, Germany) and 20 mg/mL bovine serum albumine (PAA, Austria) at 37°C under vigorous shaking for 1h. To eliminate red blood cells, the isolated fraction was incubated with erythrocyte lysis buffer consisting of 154 mM NH_4Cl, 10 mM $KHCO_3$ and 0.1 mM EDTA for 10 min at 37°C. After several washing and centrifugation steps, the cells were filtered through a 100 µm filter

and cultured in DMEM/Ham´sF12 (1:1), 10% FCS, 2 mM L-glutamine, 100 U/mL penicillin and 100 µg/mL streptomycin at 37°C and 5% CO_2 in a water-saturated atmosphere. Subculturing was performed before the cells reached confluence. Cells from passages 2 to 4 were used for the cell seeding experiments.

For this purpose, $5x10^5$ cells were seeded onto each scaffold which were then cultured in control, osteogenic and chondrogenic medium, respectively. Osteogenic medium consisted of DMEM (1 g/L glucose), 10% FCS, 2 mM L-glutamine, 100 U/mL penicillin and 100 µg/mL streptomycin as well as 0.1 µM dexamethasone, 50 µM ascorbate-2-phosphate (Fluka, Switzerland), 10 mM β-glycerophosphate and 10 nM 1α,25-dihydroxyvitamin D3 (Fluka, Switzerland). Chondrogenic medium was comprised of DMEM (1 g/L glucose), 10% FCS, 2 mM L-glutamine, 100 U/mL penicillin and 100 µg/mL streptomycin as well as 0.1 µM dexamethasone, 0.15 µM ascorbate-2-phosphate, 1% insulin-transferrin-selenium supplement (100x, Invitrogen, Austria), 40 µM L-proline and 10 ng/ml TGF-β1 (PromoKine, Germany). After 2 weeks of incubation, samples were prepared for SEM observation by washing the seeded scaffolds 3 times in pre-warmed PBS, fixing them in 2.5% glutaraldehyde at 4°C for 30 min and washing them again 2 times with PBS. Then, the samples were dehydrated in increasing concentrations of ethanol (50, 70, 90 and 100%), each step lasting 30 min. After air-drying, the samples were incubated two times for 15 min in hexamethyldisilazane.

The supernatant was harvested on day 7 and 14 for ALP activity determination using previously established protocols. In brief, 3 volumes of substrate solution consisting of 1 M diethanolamine-hydrochloric acid buffer with 0.2% p-nitrophenylphosphate at pH 9.8 were thoroughly mixed with the culture supernatant. After 45 to 60 min incubation at 37°C, 4 volumes of 2 M NaOH and 0.2 mM EDTA were added to stop the enzymatic reaction. Immediately, the samples as well as serial dilutions of the standard *p*-nitrophenol ranging from 0 to 20 mmoL/L were measured in triplicate in a microplate reader (Amersham Biosciences, UK) at 405 nm. Concentrations were calculated using a 4-parameter fit curve.

Additionally, seeded wells without scaffolds were also incubated for 2 weeks with control, osteogenic and chondrogenic medium, respectively and stained with Von Kossa or Alcian Blue to detect osteogenic and chondrogenic differentiation in a 2D environment. For Von Kossa staining, the cells were fixed for 30 min with 10% neutral-buffered formalin. After rinsing with distilled water, cells were overlaid with 5% silver nitrate for 30 min. Staining was performed with 5% sodium carbonate in 25% neutral-buffered

formalin and fixed by a 5 min incubation with 5% sodium thiosulphate. For Alcian Blue staining, cells were rinsed with PBS and stained for 30 min at room temperature with 1% Alcian Blue in 3% acetic acid at pH 2.5.

3. RESULTS AND DISCUSSION

3.1. SCAFFOLDS MORPHOLOGICAL AND MECHANICAL CHARACTERIZATION

Using the particle aggregation method, it was possible to obtain chitosan-based scaffolds with very interesting properties. The obtained chitosan particles are characterized by a smooth surface and uniform spherical shape with a mean diameter of 500-800 μm confirmed by SEM microphotographs (Fig. 2A). After press-fitting into specific moulds and drying, chitosan scaffolds could be obtained with a mean pore diameter ranging from 100 to 400 μm with a typical pore morphology shown in Fig. 2B. However, the overall random packing of the chitosan particles into the 3D scaffold structures shown in the cross-section (Fig.2C) clearly influenced the nature of the pores.

Fig. 2C shows the interconnectivity and three-dimensional structure of the developed chitosan scaffolds. The bonding of the chitosan particles was achieved due to the bioadhesive character of the chitosan polymer that resulted in the union of adjacent particles at their contact points to form the chitosan porous matrices (Fig. 2D). The scaffold´s cross-sections (Fig. 2C) indicate the bonding areas by the flat planes on the particle surfaces. This chitosan particle bonding leads to a very stable interface between the particles which assure the mechanical integrity of the developed scaffolds. Concerning the compressive properties, scaffolds have shown a very good mechanical behaviour compared to the typical mechanical properties obtained for chitosan based porous materials. For the polymeric scaffolds, a high compressive modulus of 132 ± 7 MPa was obtained. Furthermore, it is important to keep in mind that the mechanical properties may be further increased when the scaffolds are crosslinked or a ceramic filler is incorporated.

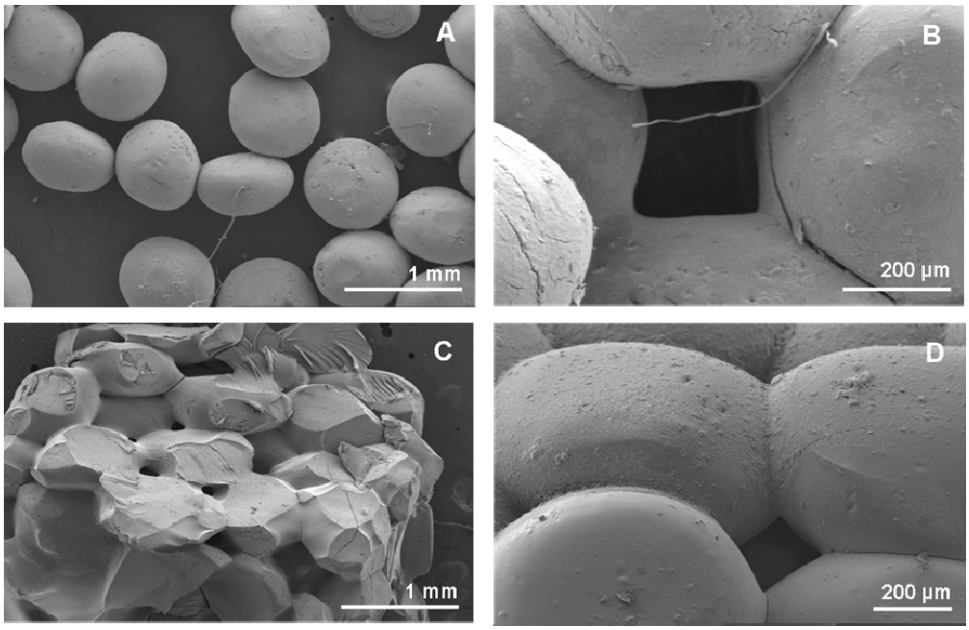

Figure 2. SEM micrographs of chitosan particles obtained by precipitation method (A); pore morphology in the chitosan scaffolds (B); cross-section of chitosan scaffolds obtained by the particle aggregation method (C); and interface between the chitosan particles after production of the scaffolds (D).

SEM of relevant cross-sections (Fig. 2C) and µ-CT analysis confirmed the formation of pores in the bulk of chitosan porous materials evidencing the scaffolds interconnectivity. The 2D histomorphometric analysis allowed for the characterization of the degree of porosity and pore distribution throughout the developed scaffolds as presented in Fig. 3. The developed scaffolds presented a mean porosity of about 30% (well distributed throughout the scaffold). In spite of the fact that many researchers are looking for scaffolds with much higher pore volumes, there is a compromise between the porosity and mechanical properties. In fact, for particles/microspheres agglomerated scaffolds it has been demonstrated that interconnected structures with a pore volume of at least 30% and a pore size of at least 100 µm are appropriate for cell ingrowth [13-15]. The main issue seems to be to assure a proper interconnectivity.

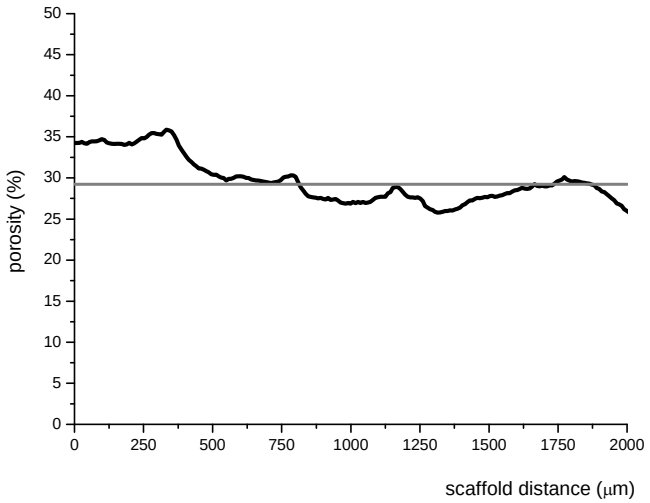

Figure 3. 2D histomorphometric analysis of mean porosity (——) and pore distribution throughout the developed scaffolds.

MIMICS® (Materialise Interactive Medical Image Control System) is an image processing software and, in spite of being designed as an interface software for CT/MRI data and rapid prototyping machines, it can be very useful for the morphological characterization of scaffolds. MIMICS® enables μ-CT data import and with the segmentation, thresholding and visualization tools allows for the construction of accurate 3D virtual models of the developed scaffolds as shown in Fig. 4.

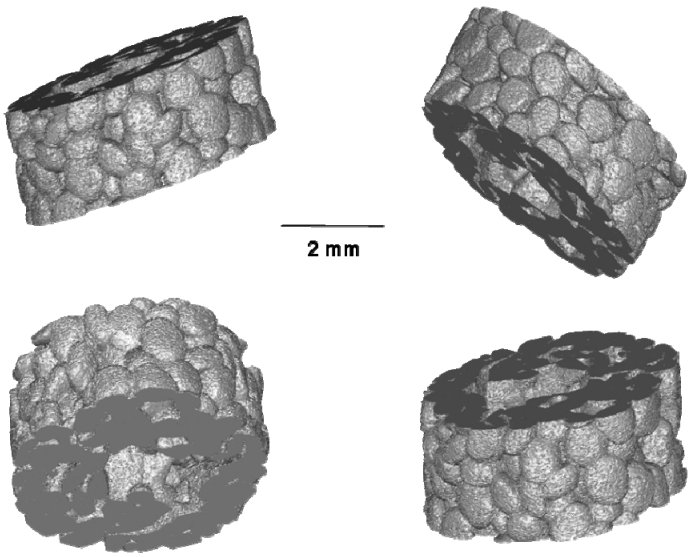

Figure 4. Different perspectives of 3D virtual models of the developed chitosan scaffolds produced by particle aggregation.

3.2. WATER UPTAKE BEHAVIOUR AT DIFFERENT PH

Concerning the water uptake, we observed a pH dependent behaviour of the developed scaffolds. In general, the degree of swelling of chitosan based materials is very high at pH 5 compared to pH 7.4 and 9. This is due to the inherent hydrophobicity of chitosan dominating at high pH values. In polymeric scaffolds, a hydration equilibrium of 160-175% (depending on the pH of the medium) was reached after 8 days of immersion in different aqueous media as shown in Fig. 5.

The swelling degree curve at pH 5 begins to decline after day 3, showing that the dissolution tendency exceeds the swelling degree (Fig. 5). This may be due to the protonation of the NH_2 groups in the acidic medium. However, and if desirable, this behaviour can be controlled by means of a crosslinking reaction where the dissolution is prevented by the reaction of the reactive NH_2 groups with glutaraldehyde. This pH dependent behaviour will be very useful in a scaffold that should also exhibit controlled release of a desired biologically active agent at the implantation site, especially when considering the decrease of pH that is observed *in-vivo* due to the inflammatory response. Therefore, it might be very useful that the main mechanism which controls the release observed for chitosan based materials is their respective water uptake behaviour.

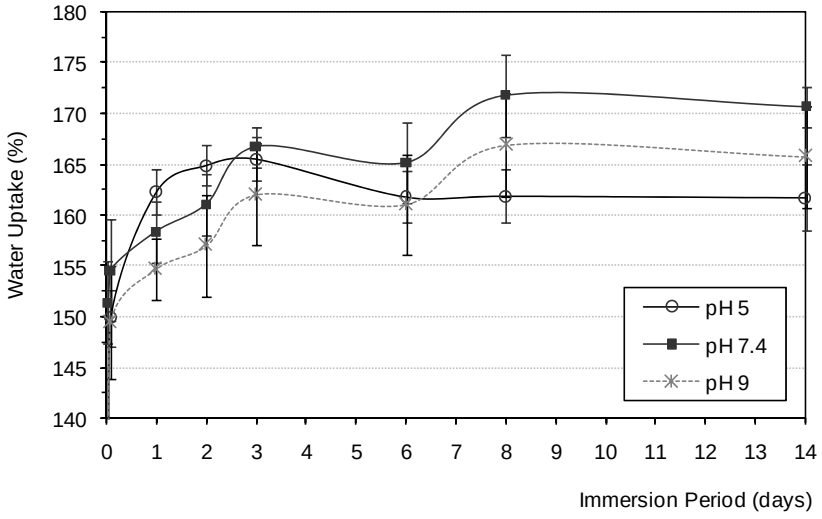

Figure 5. Water uptake behaviour of the chitosan porous scaffolds at different pH.

3.3. CYTOTOXICITY TESTS

MTS tests were performed in order to assess the potential cytotoxicity of the developed scaffolds. It was verified that extracts from the chitosan based scaffolds shown did not affect the cellular viability, since a similar cellular viability was obtained in the controls (culture medium). The MTS results are plotted in Fig. 6.

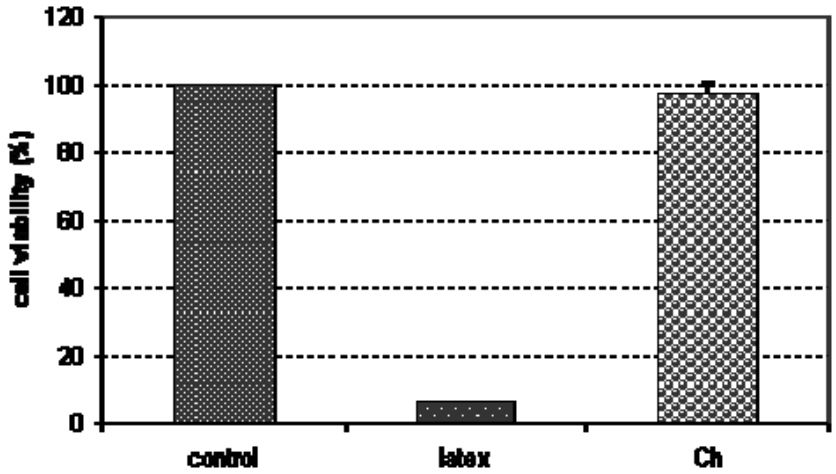

Figure 6. Cytotoxicity of the developed chitosan (Ch) scaffolds evaluated by MTS assay of $6.6x10^4$ cells incubated with extracts of the scaffolds.

3.4. OSTEOCHONDRAL BILAYERED SCAFFOLDS

To create constructs having more favourable integration properties that might be used for osteochondral tissue engineering applications, we have also investigated osteochondral composite porous materials development. Bilayered scaffolds were successfully developed by means of aggregating polymeric and composite chitosan-based particles. Fig. 7 shows the typical scaffolds obtained with this methodology.

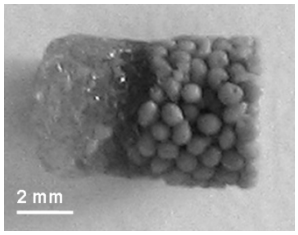

Figure 7. Photograph showing the developed bilayered chitosan scaffolds.

Furthermore, the simplest strategy to obtain osteochondral constructs, especially when aiming at minimizing complex co-culture procedures seems to be to culture both components of the scaffolds in their own separated differentiation media and, at a later stage, try to bond the polymeric (cartilage part) and composite (bone part) chitosan-based layers by using e.g. a tissue adhesive. The most widely used tissue sealant is fibrin glue due to its biocompatibility and adhesive properties [40,41]. Furthermore, this material was already successfully used in the repair of chondral and osteochondral injuries [42]. Studies were carried out using different concentrations of thrombin in order to achieve appropriate viscosity and coagulation time. The adequate thrombin concentration was found to be 4 IU/ml accomplishing the bonding of both scaffold components in aqueous solution for short immersion periods. The fibrin glue approach has shown to be effective in the bonding of chitosan particles as demonstrated in Fig. 8A. The bridging created by fibrin allows indeed this particle-linking. Particles exhibit a high compatibility with this sealant. However, for longer immersion periods or after drying, the linkage stability was found to be rather poor leading to the dissociation of both components as shown in Fig. 8B.

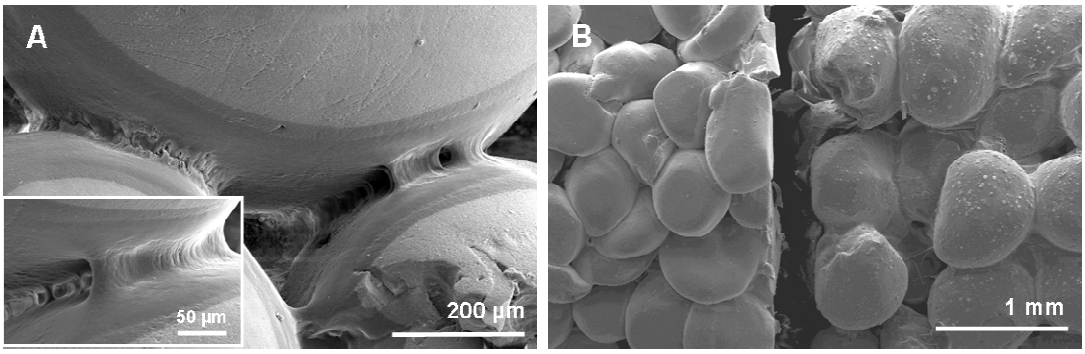

Figure 8. SEM micrographs showing the interface between chitosan particles (A) and scaffolds components (B) obtained using fibrin glue.

In order to solve this problem, another bonding strategy was followed using a highly viscous chitosan solution as an adhesive layer. As it was already referred, chitosan polymers present very good bioadhesive properties. In fact, with this approach it was possible to accomplish the bonding between both particles and components with additional high material compatibility. By SEM observation it was not possible to detect the chitosan glue which reveals the high compatibility between the glue and the scaffolds. Stereolight microscopy was used to identify the scaffolds interface when using the chitosan glue. The chitosan glue can be identified by the brighter area in the interface of the scaffolds as shown

in Fig. 9. One interesting feature is that this approach does not compromise the scaffolds interconnectivity at the interface, since the bonding sites are still the contact points of adjacent particles where the adhesive is present. This strategy does not create any interface barrier area allowing further cell migration and nutrients flow. One can conclude that a successful adhesion was achieved by means of using a chitosan glue to assemble the polymeric and composite layers in order to fabricate an osteochondral scaffold.

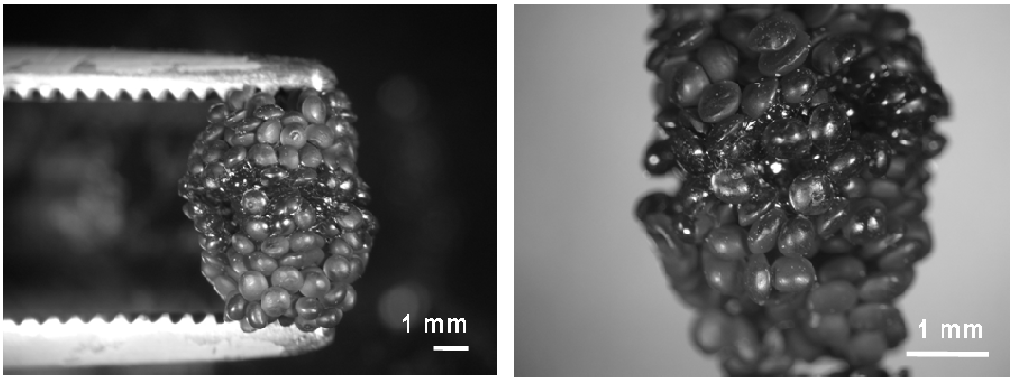

Figure 9. Stereolight photographs showing the interface between both scaffolds components using chitosan glue (brighter area).

3.5. CELL SEEDING AND DIFFERENTIATION

Such tissue engineered constructs may provide an alternative clinical option for the currently used autologous transplantation of mature tissue which is associated with high donor site morbidity. For this purpose, a suitable cell source would likely have to be incorporated into the construct design. First experiments of seeding porous chitosan scaffolds with mesenchymal stem cells isolated from adipose tissue were performed. The preliminary results obtained are very promising as in the seeded scaffolds some events occurred which may indicate an osteogenic and chondrogenic differentiation. In contrast, no events of osteogenic or chondrogenic differentiation in the control wells without the scaffolds (2D cultures) were detected in this short time frame, as confirmed also by Von Kossa and Alcian Blue staining, respectively (data not shown). This may propose an influence of the 3D support provided by the scaffolds on the differentiation ability of the cells indicated by a change in cell morphology shown by SEM analysis (Fig. 10). Hence, mesenchymal stem cells isolated from adipose tissue, seeded on the scaffolds and cultured with chondrogenic medium had a rounded shape which is a morphological

prerequisite for chondrogenic differentiation (Fig. 10A and 10B). The ones cultured with osteogenic medium had a flattened morphology and showed bridging between the chitosan particles which might suggest a differentiation along the osteogenic lineage (Fig. 10C and 10D). Similar attachment behaviour has been observed by Borden *et al.* [13] who seeded primary human osteoblasts in PLAGA-based microspheres sintered scaffolds. The assumption that the cells had in fact differentiated into mature cell types might be corroborated by ALP activity measurements which showed very low levels when cultured in chondrogenic medium (data not shown). On the contrary, scaffolds seeded with cells and incubated in osteogenic medium showed a very high ALP activity compared to the controls cultured without osteogenic supplements (data not shown). However, future work will focus on the detection of specific markers on the molecular as well as the protein level to confirm these results.

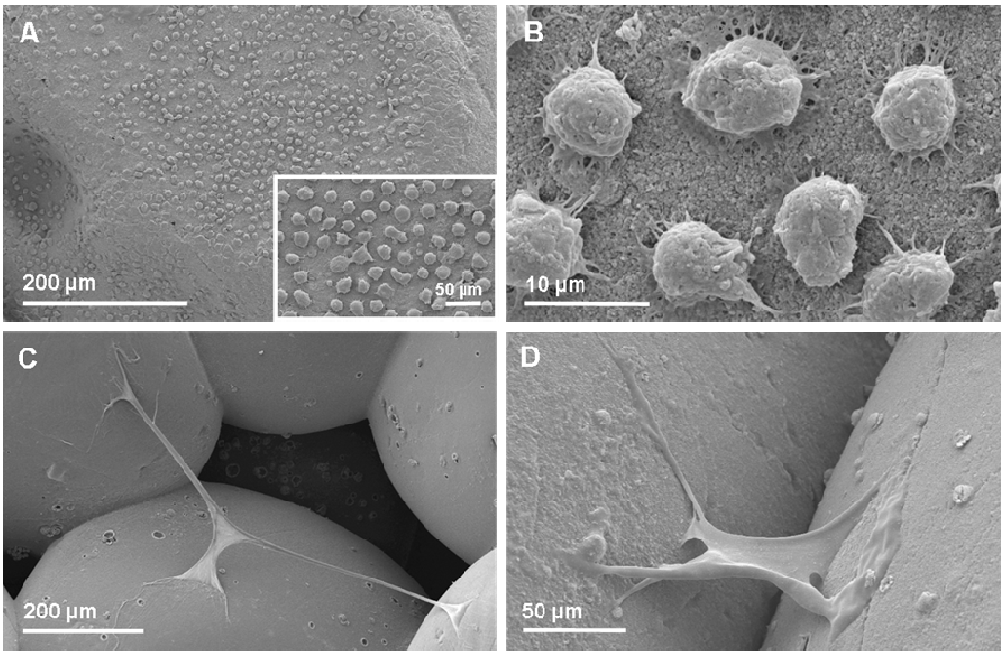

Figure 10. SEM microphotographs showing the morphological difference of cells isolated from adipose tissue, seeded on chitosan particle agglomerated scaffolds and cultured for 2 weeks under chondrogenic (A, B) and osteogenic (C, D) conditions, respectively.

4. CONCLUSIONS

By means of using a particle aggregation method, it was possible to obtain chitosan-based scaffolds with very promising properties for the use in cartilage and osteochondral applications. µ-CT and

MIMICS® could be successfully used for the morphological characterization of the developed scaffolds. Scaffolds have a mean porosity of 30% with pores ranging from 100 to 400 μm well distributed throughout the scaffolds and clearly interconnected. The developed scaffolds seem to be very adequate for cell ingrowth. In addition, and due to its low pore volume, there is no compromise of the typical mechanical properties of the particle-based scaffolds. The developed scaffolds demonstrate no cytotoxicity as evaluated by the MTS assay. Furthermore, very promising osteochondral bilayered scaffolds could also be developed. A simple strategy is also presented based on the use of an adhesive material for obtaining bilayered scaffolds. Preliminary cell seeding and differentiation tests with mesenchymal stem cells isolated from adipose tissue were carried out, indicating the presence of cells with osteogenic and chondrogenic morphology in the 3D particle agglomerated scaffolds. Although this needs to be further investigated it is a very promising indicator for the use of the developed scaffolds in the proposed osteochondral applications.

REFERENCES

1. M.E. Gomes, A.S. Ribeiro, P.B. Malafaya, R.L. Reis, and A.M. Cunha, A new approach based on injection moulding to produce biodegradable starch-based polymeric scaffolds: morphology, mechanical and degradation behaviour. Biomaterials 22 (2001) 883-889.

2. Y. Deng, K. Zhao, X.-f. Zhang, P. Hu, and G.-Q. Chen, Study on the three-dimensional proliferation of rabbit articular cartilage-derived chondrocytes on polyhydroxyalkanoate scaffolds. Biomaterials 23 (2002) 4049.

3. Q. Hou, D.W. Grijpma, and J. Feijen, Porous polymeric structures for tissue engineering prepared by a coagulation, compression moulding and salt leaching technique. Biomaterials 24 (2003) 1937.

4. M. Nof, and L.D. Shea, Drug-releasing scaffolds fabricated from drug-loaded microspheres. Journal of Biomedical Materials Research 59 (2002) 349-356.

5. H.S. Yoo, E.A. Lee, J.J. Yoon, and T.G. Park, Hyaluronic acid modified biodegradable scaffolds for cartilage tissue engineering. Biomaterials 26 (2005) 1925.

6. M.E. Gomes, V.I. Sikavitsas, E. Behravesh, R.L. Reis, and A.G. Mikos, Effect of flow perfusion on the osteogenic differentiation of bone marrow stromal cells cultured on starch-based three-dimensional scaffolds. Journal of Biomedical Materials Research 67A (2003) 87-95.

7. S.V. Madihally, and H.W.T. Matthew, Porous chitosan scaffolds for tissue engineering. Biomaterials 20 (1999) 1133.

8. P.B. Malafaya, and R.L. Reis, Porous bioactive composites from marine origin based in chitosan and hydroxylapatite particles. in: B. Ben-Nissan, D. Sher, and W. Walsh, (Eds.), Bioceramics 15, Trans Tech Publications, Zurich, 2003, pp. 39-42.

9. S. Zmora, R. Glicklis, and S. Cohen, Tailoring the pore architecture in 3-D alginate scaffolds by controlling the freezing regime during fabrication. Biomaterials 23 (2002) 4087-94.

10. K.F. Leong, C.M. Cheah, and C.K. Chua, Solid freeform fabrication of three-dimensional scaffolds for engineering replacement tissues and organs. Biomaterials 24 (2003) 2363-2378.

11. E. Sachlos, N. Reis, C. Ainsley, B. Derby, and J.T. Czernuszka, Novel collagen scaffolds with predefined internal morphology made by solid freeform fabrication. Biomaterials 24 (2003) 1487-97.

12. I. Zein, D.W. Hutmacher, K.C. Tan, and S.H. Teoh, Fused deposition modeling of novel scaffold architectures for tissue engineering applications. Biomaterials 23 (2002) 1169-85.

13. M. Borden, S.F. El-Amin, M. Attawia, and C.T. Laurencin, Structural and human cellular assessment of a novel microsphere-based tissue engineered scaffold for bone repair. Biomaterials 24 (2003) 597-609.

14. M. Borden, M. Attawia, and C.T. Laurencin, The sintered microsphere matrix for bone tissue engineering: In vitro osteoconductivity studies. Journal of Biomedical Materials Research 61 (2002) 421-429.

15. M. Borden, M. Attawia, Y. Khan, and C.T. Laurencin, Tissue engineered microsphere-based matrices for bone repair: design and evaluation. Biomaterials 23 (2002) 551-559.

16. J.E. Devin, M.A. Attawia, and C.T. Laurencin, Three-dimensional degradable porous polymer-ceramic matrices for use in bone repair. Journal of Biomaterials Science-Polymer Edition 7 (1996) 661-669.

17. D.H.R. Kempen, C.W. Kim, L. Lu, W.J.A. Dhert, B.L. Currier, and M.J. Yaszemski, Controlled release from poly(lactic-co-glycolic acid) microspheres embedded in an injectable, biodegradable scaffold for bone tissue engineering. Thermec'2003, Pts 1-5 426-4 (2003) 3151-3156.

18. T.A. Holland, Y. Tabata, and A.G. Mikos, *In vitro* release of transforming growth factor-β1 from gelatin microparticles encapsulated in biodegrabable, injectable oligo(poly(ethylene glycol) fumarate) hydrogels. Journal of Controlled Release 91 (2003) 299-313.

19. R.G. Payne, J.S. McGonigle, M.J. Yaszemski, A.W. Yasko, and A.G. Mikos, Development of an injectable, in situ crosslinkable, degradable polymeric carrier for osteogenic cell populations. Part 3. Proliferation and differentiation of encapsulated marrow stromal osteoblasts cultured on crosslinking poly(propylene fumarate). Biomaterials 23 (2002) 4381-7.

20. R.G. Payne, M.J. Yaszemski, A.W. Yasko, and A.G. Mikos, Development of an injectable, in situ crosslinkable, degradable polymeric carrier for osteogenic cell populations. Part 1. Encapsulation of marrow stromal osteoblasts in surface crosslinked gelatin microparticles. Biomaterials 23 (2002) 4359-71.

21. T.M. Meese, Y. Hu, R.W. Nowak, and K.G. Marra, Surface studies of coated polymer microspheres and protein release from tissue-engineered scaffolds. J Biomater Sci Polym Ed 13 (2002) 141-51.

22. E.L. Hedberg, A. Tang, R.S. Crowther, D.H. Carney, and A.G. Mikos, Controlled release of an osteogenic peptide from injectable biodegradable polymeric composites. Journal of Controlled Release 84 (2002) 137-50.

23. S.E. Kim, J.H. Park, Y.W. Cho, H. Chung, S.Y. Jeong, E.B. Lee, and I.C. Kwon, Porous chitosan scaffold containing microspheres loaded with transforming growth factor-beta1: implications for cartilage tissue engineering. Journal of Controlled Release 91 (2003) 365-74.

24. A. Perets, Y. Baruch, F. Weisbuch, G. Shoshany, G. Neufeld, and S. Cohen, Enhancing the vascularization of three-dimensional porous alginate scaffolds by incorporating controlled release basic fibroblast growth factor microspheres. Journal of Biomedical Materials Research 65A (2003) 489-97.

25. C.T. Hung, E.G. Lima, R.L. Mauck, E. Taki, M.A. LeRoux, H.H. Lu, R.G. Stark, X.E. Guo, and G.A. Ateshian, Anatomically shaped osteochondral constructs for articular cartilage repair. Journal of Biomechanics 36 (2003) 1853-64.

26. J.K. Sherwood, S.L. Riley, R. Palazzolo, S.C. Brown, D.C. Monkhouse, M. Coates, L.G. Griffith, L.K. Landeen, and A. Ratcliffe, A three-dimensional osteochondral composite scaffold for articular cartilage repair. Biomaterials 23 (2002) 4739-51.

27. P. Angele, R. Kujat, M. Nerlich, J. Yoo, V. Goldberg, and B. Johnstone, Engineering of osteochondral tissue with bone marrow mesenchymal progenitor cells in a derivatized hyaluronan-gelatin composite sponge. Tissue Engineering 5 (1999) 545-54.

28. J.S. Temenoff, and A.G. Mikos, Review: tissue engineering for regeneration of articular cartilage. Biomaterials 21 (2000) 431-40.

29. R.K. Sanders, and J.R. Crim, Osteochondral injuries. Seminars in Ultrasound, CT, and MRI 22 (2001) 352-370.

30. J.A. Buckwalter, S.L. Woo, V.M. Goldberg, E.C. Hadley, F. Booth, T.R. Oegema, and D.R. Eyre, Soft-tissue aging and musculoskeletal function. Journal of Bone and Joint Surgery American 10 (1993) 1533-1548.

31. L. Hangody, P. Feczko, L. Bartha, G. Bodo, and G. Kish, Mosaicplasty for the treatment of articular defects of the knee and ankle. Clinical Orthopaedics and Related Research (2001) S328-336.

32. J. Gao, J.E. Dennis, L.A. Solchaga, V.M. Goldberg, and A.I. Caplan, Repair of osteochondral defect with tissue-engineered two-phase composite material of injectable calcium phosphate and hyaluronan sponge. Tissue Engineering 8 (2002) 827-37.

33. T. Taguchi, Y. Sawabe, H. Kobayashi, Y. Moriyoshi, K. Kataoka, and J. Tanaka, Preparation and charaterization of osteochondral scaffold. Materials Science and Engineering C 24 (2004) 881-885.

34. J.P. Spalazzi, K.L. Moffat, S.B. Doty, and H.H. Lu, Novel multi-phased composite scaffold for soft tissue-to-bone interface tissue engineering, Society for Biomaterials 30th Annual Meeting Transactions, 2005, pp. 253.

35. J. Jiang, C.T. Hung, X.E. Guo, G.A. Ateshian, and H.H. Lu, Multi-phase polymer-ceramic-hydrogel scaffold for osteochondral repair, 7th World Biomaterials Congress, 2004, pp. 7.

36. R.A. Sousa, R.L. Reis, A.M. Cunha, and M.J. Bevis, Structure Development and Interfacial Interactions in High-Density Polyethylene/Hydroxyapatite (HDPE/HA) Composites Molded with Preferred Orientation. Journal of Applied Polymer Science 86 (2002) 2873-2886.

37. P.B. Malafaya, and R.L. Reis, Development and characterization of pH responsive chitosan and chitosan/HA scaffolds processed by a microsphere-based aggregation route, 7th World Biomaterials Congress, Sydney, Australia, 2004, pp. 1285.

38. P.B. Malafaya, and R.L. Reis, Chitosan-based particle agglomerated scaffolds developed for bone, cartilage and osteochondral tissue engineering applications, 6th International Symposium on Frontiers in Biomedical Polymers - FBPS'05, Granada, Spain 2005, pp. O19.

39. P.A. Zuk, M. Zhu, P. Ashjian, D.A. De Ugarte, J.I. Huang, H. Mizuno, Z.C. Alfonso, J.K. Fraser, P. Benhaim, and M.H. Hedrick, Human adipose tissue is a source of multipotent stem cells. Mol Biol Cell 13 (2002) 4279-4295.

40. L.J. Currie, J.R. Sharpe, and R. Martin, The use of fibrin glue in skin grafts and tissue-engineered skin replacements: a review. Plast Reconstr Surg 108 (2001) 1713-26.

41. H. Redl, History of tissue adhesives. in: R. Saltz, and D.M. Toriumi, (Eds.), Tissue Glues in Cosmetic Surgery, Quality Medical Publishing Inc., St.Louis, Missouri, 2004, pp. 4-27.

42. G. Kaplonyi, I. Zimmerman, A.D. Frenyo, T. Farkas, and G. Nemes, The use of fibrin adhesive in the repair of chondral and osteochondral injuries. Injury 19 (1988) 267.

CHAPTER IV.

Bilayered chitosan-based scaffolds for osteochondral tissue engineering: influence of hydroxylapatite on *in vitro* cytotoxicity and dynamic bioactivity studies in a specific double chamber bioreactor

CHAPTER IV.

Bilayered chitosan-based scaffolds for osteochondral tissue engineering: influence of hydroxylapatite on *in vitro* cytotoxicity and dynamic bioactivity studies in a specific double chamber bioreactor *

ABSTRACT

Osteochondral tissue engineering presents a challenge to the present research due to the combination of both bone and cartilage tissue engineering principles. In the present study, bilayered chitosan scaffolds are introduced being based in the optimization of both polymeric and composite scaffolds. A particle aggregation methodology is proposed in order to achieve an improved integrative bone and cartilage parts' interface needed for this application, since any discontinuity is likely to cause long-term device failure.

Cytotoxicity was evaluated by MTS with L929 fibroblast cell line for different conditions. Surprisingly, in composite scaffolds using unsintered hydroxylapatite, an *in vitro* cytotoxicity was observed. This work reports the investigation that was conducted to overcome and explain this behaviour. It is suggest that the uptake of divalent cations may be inducing the cytotoxic behaviour. Sintered hydroxylapatite was consequently used, showing no cytotoxicity when compared to the controls.

Micro-Computed Tomography (micro-CT) was carried out for accurate morphometric characterization to quantify porosity, interconnectivity, ceramic content, particles and pores size. The results exhibited that the developed scaffolds are highly interconnected and present ideal pore size range, being morphometrically adequate for the proposed applications. Dynamical mechanical analysis (DMA) has demonstrated that scaffolds are mechanically stable in the wet state even under dynamic compression solicitation. The obtained elastic modulus was respectively 4.21±1.04 MPa, 7.98±1.77 MPa and 6.26±1.04 MPa at 1Hz frequency for polymeric, composite and bilayered scaffolds.

Bioactivity studies using both a simulated body fluid (SBF) and a simulated synovial fluid (SSF) were conducted in order to assure that the polymeric component for chondrogenic part would not mineralize

as confirmed by SEM, ICP and EDS for different immersion periods. The assays were carried out also in dynamic conditions using, for this purpose, a specifically designed double-chamber bioreactor, aiming at a future osteochondral application.

It was concluded that chitosan-based bilayered scaffolds produced by particle aggregation overcome any risk of delamination of both polymeric and composite parts designed respectively for chondrogenic and osteogenic components being mechanically stable. Moreover, the proposed bilayered scaffolds could serve as alternative, biocompatible, and safe biodegradable scaffolds for osteochondral tissue engineering applications.

---

* This chapter is based in the following publication:

PB Malafaya, RL Reis. Bilayered chitosan-based scaffolds for osteochondral tissue engineering: influence of hydroxylapatite on *in vitro* cytotoxicity and dynamic bioactivity studies in a specific double chamber bioreactor. Acta Biomaterialia (2008) submitted

---

1. INTRODUCTION

Osteochondral defects are lesions of the articular cartilage where the underlying bone tissue is also damaged. Currently, osteochondral defects are mostly treated by either osteochondral autograft transfer taken from an outer region of the joint [1], or by filling the lesion with autologous, precultured chondrocytes (autologous chondrocyte transplantation, ACT) [2] or matrix-induced autologous chondrocyte implantation [3]. Although some studies have achieved success in repairing small cartilage defects, no accepted method for complete repair of osteochondral defects exists [4]. Large osteochondral defects are associated with mechanical instability and are accepted indications for surgical intervention to prevent development of degenerative joint disease. Ideally, a large osteochondral defect should be repaired with a graft that can provide mechanical stability and allow early postoperative function under physiologic loading conditions [5]. In addition, the graft should structurally and functionally integrate with the host tissue, since any discontinuity can incite a long-term device failure [6].

The requirements for an osteochondral graft could potentially be met by using a tissue-engineered osteochondral (bone-cartilage) composite of predefined size and shape, generated in vitro using autologous cells. Such a graft would provide a mechanical stability from the time of implantation, minimize donor site morbidity by using cell expansion techniques, and eliminate complications related to the use of allografts and/or mechanical devices. The bone region of the engineered osteochondral composite may further help anchor the graft within the defect, since a bone-to-bone interface integrates better and faster than a cartilage-to-cartilage interface [6].

The overall objective of tissue engineering is the restoration of normal tissue function. Ideally, a lost or damaged tissue should be replaced by an engineered graft that can re-establish appropriate structure, composition, cell signalling and function(s) of the native tissue [7]. The clinical utility of tissue engineering likely depends on our ability to replicate the site-specific properties of the tissue being replaced across different size scales, and provide the continuity and strength of the interface with the neighbouring host tissues [8]. Therefore, for an osteochondral defect, one should consider the need for a simultaneous regeneration of both cartilage and subchondral bone, making osteochondral tissue engineering a challenge to the present research due to this combination of both bone and cartilage tissue engineering principles.

In the literature [5,9-11], there are several possible strategies for developing hybrid constructs for osteochondral tissue engineering, namely: (i) the cell culturing is performed independently in two sides, that are integrated before implantation; (ii) two different cell sources are seeded in the two sides of a single- or double-phase scaffold, and cultivated in a special bioreactor with two separated chambers; and ideally (iii) common progenitor cells are seeded in the two sides of a biphasic scaffold that contains different differentiation agents and then cultivated in a bioreactor with one/two chambers. For these, several bioreactors have been described as reviewed [8,12] and proposed [13] by different authors. Bioreactor systems can provide the technological means to reveal fundamental mechanisms of cell function in a 3D environment and the potential to improve the quality of engineered tissues, providing environmental control, biochemical and mechanical cues. Several bioreactors systems such as rotating bioreactors, perfused cartridges or chambers have been used. Nevertheless, it is the author's opinion that double-chamber bioreactors [12,13] consisting in one chamber for culture of chondrogenic part and the other chamber for osteogenic part seem to be more adequate for osteochondral applications. The double-chamber bioreactor should allow for either culture of chondrocytes or osteoblasts or common progenitor cells with two different cell culture mediums.

Many tissue engineering scaffolding strategies dealing with osteochondral repair engage the design of bilayered scaffolds that could regenerate both cartilage and subchondral bone involving different combinations of materials, morphologies and properties in both parts of the scaffold. Nevertheless, some researchers suggest that osteochondral defects could be regenerated from single-layer scaffolds by seeding autologous chondrocytes in the top of the 3D scaffold to create a cell-scaffold construct for *in vivo* implantation [14,15] or engineering complex tissue grafts with gradients of molecular, structural, and functional properties. Several strategies with single-layer materials can be followed as recently reviewed by Mano *et al* [9]. Nevertheless, it has been more accepted that a bilayered structure could be more challenging but more adequate to regenerate an osteochondral defect able to incorporate/induce different types of cells in a favourable environment requiring different chemical surroundings and mechanical requirements, leading the growth of two different tissues, with different biological requirements.

Bearing this in mind, different approaches have been reported. Swieszkowski *et al* [4] propose two different systems using bone marrow-derived mesenchymal cells cultured in chondrogenic and

osteogenic favourable conditions. The biphasic scaffolds consists of fibrin and polycaprolactone (PCL) and PCL and PCL/β-tricalcium phosphate (TCP) where the PCL-based scaffolds were fabricated via fused deposition modelling (rapid prototyping system). Both phases are fabricated and seeded separately and then integrated into one construct by using fibrin glue. The results demonstrated the potential of the porous PCL and PCL-TCP scaffolds in promoting bone healing. Scotti *et al* [16] reported a biphasic composite made of expanded chondrocytes-fibrin glue gel composite with a calcium-phosphate scaffold. This paper focused mainly in the problem of the neocartilage-to-bone integration, so no cells are used in the osteogenic part of the biphasic scaffold. Hence, the bilayered construct showed a tri-phasic structure with a cartilaginous zone, an intermediate zone with the chondrocytes-fibrin glue complex penetrating the calcium-phosphate and a zone free from cells, made of the remaining part of the calcium-phosphate scaffold [16].

In the present study, particle aggregation methodology is proposed to fabricate bilayered scaffolds for osteochondral tissue engineering in order to achieve an improved integrative bone and cartilage interface needed for this application. Chitosan was chosen due to its structural similarity to glycosaminoglycans (GAGs) found in extracellular matrices as in native articular cartilage playing a key role in modulating chondrocytes morphology, differentiation and function [17, 18]. For the osteogenic part, composites with hydroxylapatite were developed to mimic the bony structure. Glutaraldehyde was used as crosslinking agent to further improve the mechanical performance. An extensive characterization is reported including *in vitro* cytotoxicity, morphometric analysis and dynamic-mechanical behaviour in hydrated state. Furthermore, dynamic bioactivity assays were carried out in specific designed double-chamber bioreactor.

2. MATERIALS AND METHODS

2.1. SCAFFOLDS PRODUCTION

The scaffolds were produced as described elsewhere [19]. Briefly, chitosan (medium molecular weight and ≈ 85% of deacetylation degree) was grinded and dissolved overnight in acetic acid (1%vv) to obtain a chitosan solution (2%wt). Unless otherwise stated, all chemicals were bought from Sigma-Aldrich and used as-received. In composite particles production, 20%wt of non-sintered hydroxylapatite (HA unsint)

(Camceram II, coating powder, CAM Implants BV, Leiden, The Netherlands) or sintered hydroxylapatite (HA sint) (Captal's® HA, Plasma Biotal Ltd, Tideswell, UK) was homogeneously dispersed in the chitosan solution. After complete dissolution and filtration, the prepared solutions were extruded trough a syringe at constant rate (10 ml/h) to form chitosan droplets into a NaOH (1M) precipitation bath where particles with regular diameter were formed. The chitosan particles were left in the precipitation bath until complete precipitation and then repeatedly washed with distilled water until pH 7.

For composite and bilayered scaffolds production, the composite particles were submitted to a crosslinking reaction with glutaraldehyde. For scaffolds production optimization, different glutaraldehyde concentrations (0.01%, 0.025%, 0.05% and 0.5% for 15min) were used. Scaffolds were further washed with glycine solution (0.2 and 1M for 15min) in order to block free aldehyde groups. After each step, scaffolds were washed with distilled water. Unless otherwise stated, composite scaffolds were crosslinked with 0.01% glutaraldehyde and washed with 1M glycine both for 15 minutes as described in Table 1. The particles were then pressed into moulds and left to dry in an oven at 60ºC for 3 days. Scaffolds with cylinder shape with 8mm height and 5mm diameter were obtained.

Table 1. Summary of scaffolds' abbreviation and composition.

ABBREVIATION	SCAFFOLDS	COMPOSITION		
		CHITOSAN:HA RATIO	GLUTALDEHYDE (%VV)	GLYCINE [M]
C	Polymeric	100:0	-	-
CHA	Composite	80:20	0.01%, 15 min	1M, 15 min
BiCCHA	Bilayered structures (polymeric + composite)			

2.2. CELL VIABILITY EVALUATION (MTS)

To assess the possible cytotoxicity of the developed scaffolds, the *in vitro* cell viability was assessed using MTS assay (3-(4,5-dimethylthiazol-2-yl)-5-(3-carboxylmethoxyphenyl)-2-(4-sulfophenyl)-2H tetrazolium) (Cell Titer 96® AQueous Solution Cell Proliferation Assay, G3580, Promega, USA) according to ISO/EN 10993 part 5 guidelines, which determines whether cells are metabolically active. This cytotoxicity test is based on the bioreduction of the substrate (MTS) into a brown formazan product by dehydrogenase enzymes in metabolically active cells, directly related with cell viability. For this

purpose, materials (n=3) were incubated in culture medium for 24h at 37ºC with constant shaking after sterilization by ethylene oxide (EtO) in conditions that have been described previously [20].

Latex was also incubated as a positive control for cell death. A rat lung fibroblasts cell line (L929) acquired from the European Collection of Cell Cultures (ECACC) was used for the studies. The cells were grown as monolayers in Dulbecco's modified Eagle's medium (DMEM) supplemented with 10% foetal bovine serum (Biochrom, Berlin, Germany; Heat Inactivated) and 1% of antibiotic-antimycotic mixture. Cultured L929 cells were trypsinised using trypsin-EDTA (Gibco, Invitrogen Corporation) and plated into 96-well micrometer plates (200 µl/well) at $6.6x10^4$ cells/well. The plates were incubated, for 24 h, at 37ºC in a humidified atmosphere of 5% CO_2 in air.

After that, the medium was replaced by the previous prepared materials extracts after sterilized by filtration (0.45 µm pore size) using culture medium by itself as a negative control. After 72 h incubation, cell culture was treated with MTS (in medium without phenol red) and incubated for further 3 h at 37ºC in a humidified atmosphere of 5% of CO_2 in air. At this stage, culture medium with MTS was transferred to new wells. The optical density (OD) which is directly proportional to the cellular activity (it reflects the mitochondrial activity) was read on a microplate reader (Synergy HT, BioTek Instruments) at 490 nm.

2.2.1. Inductively Coupled Plasma Optical Emission Spectroscopy (ICP)

Following the protocol for materials extracts performed in the MTS assay, the different sample extracts solutions were further analyzed in order to determine the concentrations of calcium (Ca), phosphorus (P), silicon (Si), magnesium (Mg) and sodium (Na) elements. The element concentrations were measured by inductively coupled plasma-optical emission spectroscopy (ICP-OES JY70 plus, Jobin Yvon, France). Triplicate samples were analyzed for each condition. For this purpose, materials were incubated in cell culture medium (DMEM) for 24 h at 37ºC with constant shaking, after sterilization by ethylene oxide (EtO) in conditions that have been described previously [20]. After that, the elemental concentrations of the prepared materials extracts sterilized by filtration (0.45 µm pore) were measured, using cell culture medium itself as control.

2.3. MICRO-COMPUTED TOMOGRAPHY (MICRO-CT)

The scaffolds (n=3) were analysed using micro-Computed Tomography (micro-CT). Micro-CT was carried out with a high-resolution μ-CT Skyscan 1072 scanner (Skyscan, Kontich, Belgium) using a resolution of pixel size of 7.53μm and integration time of 1.7ms. The X-ray source was set at 40 keV of energy and 250 μA of current. Approximately 400 projections were acquired over a rotation range of 180° with a rotation step of 0.45°. Data sets were reconstructed using standardized cone-beam reconstruction software (NRecon v1.4.3, SkyScan). The output format for each sample was 300 serial 1024x1024 bitmap images. Representative data sets of 200 slices were segmented into binary images with a dynamic threshold of 40-255 to access the porosity and 150-255 to identify the ceramic phase (grey values). The same representative volume of interest (VOI) was analysed for all the samples. These data sets were used for morphometric analysis (CT Analyser, v1.5.1.5, SkyScan) and to build 3D models (ANT 3D creator, v2.4, SkyScan). The morphometric analysis included histogram, scaffolds' porosity and interconnectivity, mean pore and particle size, pore size and ceramic phase distribution. 3D virtual models of representative regions in the bulk of the scaffolds were created, visualized and registered using both image processing softwares (CT Analyser and ANT 3D creator).

2.4. DYNAMICAL MECHANICAL ANALYSIS (DMA)

Dynamic Mechanical Analysis (DMA) was conducted in order to characterize the mechanical behaviour of chitosan particle-aggregated scaffolds in wet state, under dynamic compression solicitation. Cylindrical chitosan-based scaffolds were immersed in phosphate buffer solution (PBS) at physiological pH and temperature (pH 7.4 and 37ºC) for 3 days for complete hydration. The scaffolds were then were subjected to compression cycles of increasing frequencies ranging from 0.1-40 Hz with constant dynamic displacements of 0.03 mm using a Tritec2000 DMA (Triton Technology, UK). Experiments were conducted at room temperature and five points were measured within each decade. For each individual scaffold, the data is averaged over three consecutive runs. Five samples were measured for each type of scaffolds. The real (storage modulus), E', and the imaginary component (loss modulus), E'', of the complex modulus, $E^*=E'+iE''$ (with $i=(-1)^{1/2}$), were recorded against frequency. Reference values for comparison of the compression modulus were collected at a frequency of 1 Hz.

2.5. STATIC AND DYNAMIC BIOACTIVITY STUDIES IN A DOUBLE-CHAMBER BIOREACTOR

To study the *in vitro* bioactive behaviour (*in vitro* bone-bonding ability [21]), two different simulated solutions were used. A simulated body fluid (SBF) with ion concentrations (Na^+ 142.0, K^+ 5.0, Mg^{2+} 1.5, Ca^{2+} 2.5, Cl^- 103.0, HCO_3^{2-} 10.0,HPO_4^{2-} 1.0 and SO_4^{2-} 0.5 mM) [21,22] nearly equal to those of the human blood plasma was prepared as described elsewhere [21,22]. A simulated synovial fluid (SSF) was also used to approximate the chemical environment in a human joint. SSF, with ion concentration Na^+ 153.1, K^+ 4.2, Cl^- 139.6 and phosphate buffer 9.6 mM [23], was prepared by dissolving 0.3%wt hyaluronic acid in phosphate buffered saline solution to obtain a pH of 7.4. Hyaluronic acid is a mucopolysaccharide composed of several thousand amino-sugar residues, and is the primary diffuse macromolecule that exists in human synovial fluid [23].

For the static bioactivity tests, samples (polymeric, composite and bilayered scaffolds) with n=3 were suspended and immersed in 50 ml of SBF and SSF separately at 37ºC and pH 7.4 (physiological conditions) for 0, 1, 3 and 14 days. After soaking, the samples were immediately washed with distilled water and dried at room temperature. For the dynamic bioactivity tests, a double-chamber bioreactor was specially designed and set-up according Figure 1. For these assays, bilayered scaffolds (n=2) were assembled in the bioreactor using a silicon septum. The SBF and SSF were continuously circulating in physiological conditions (pH 7.4 and 37ºC) using a peristaltic pump up to 14 days with an available volume of 50 ml of each solution. Scaffolds and solutions sampling was performed at 0, 3, 7 and 14 days.

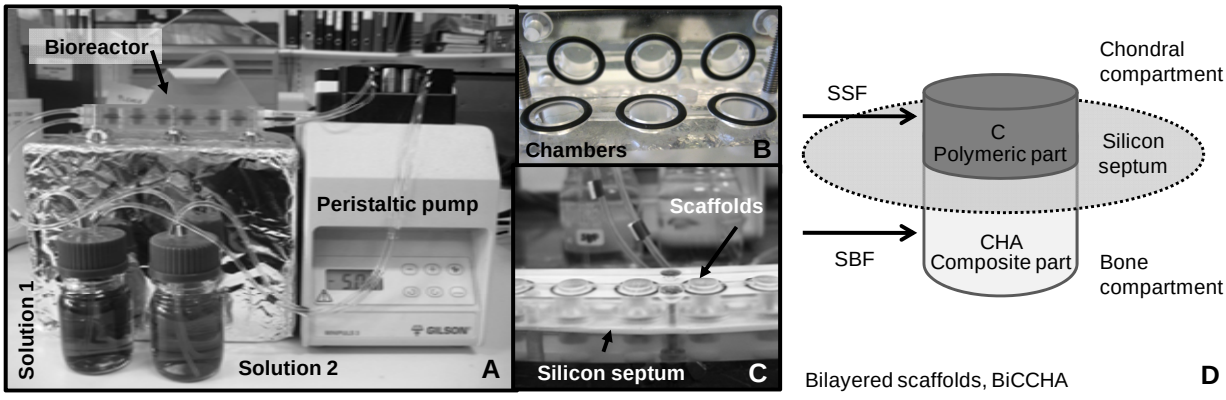

Figure 1. Double-chamber bioreactor set-up (A). The double-chamber bioreactor consists in 6 interconnected double-chambers (B) where the different solutions circulate in separated flow circuits. A silicon septum acts as scaffolds support (C,D). The schematically experimental conditions for the dynamic bioactivity assays are represented in (D).

The scaffolds surface morphology, as well as the presence of calcium (Ca) and phosphorous (P) elements on the scaffolds surface were both analyzed before and after soaking in SBF and SSF, for the different experimental conditions at the different immersion periods. This was carried out using scanning electron microscopy (SEM) equipment (S360, Leica Cambridge Ltd) and energy dispersive spectroscopy (EDS) equipment (Link EXL II, Oxford) coupled to the SEM. Sample surfaces were carbon coated for EDS (Fisons Instruments, Evaporation PSU CA508, UK) or gold sputtered for SEM (Fisons Instruments, Sputter Coater SC502, UK). Microphotographs and spectra were registered for further analysis. Furthermore, the sample solutions were analyzed by inductively coupled plasma optical emission spectroscopy (ICP-OES JY70 plus, Jobin Yvon, France) in order to quantify the elemental concentrations as function of the immersion period of calcium (Ca), phosphorus (P), silicon (Si), magnesium (Mg) and sodium (Na) elements.

2.6. STATISTICAL ANALYSIS

When applicable, statistical analysis of values obtained with the characterization techniques was carried out using Student's two-tailed t-test with a confidence level of 99.5%. All statistical calculations were performed with Analysis ToolPak software. ρ-Values below 0.05 were considered statistically significant.

3. RESULTS AND DISCUSSION

For osteochondral tissue engineering scaffolding, it is the authors' opinion that a bilayered structure will be more favourable to achieve a successful approach, as it was previously discussed in the introduction. For that, chitosan was chosen as natural origin and biodegradable polymeric matrix since it is know that this polymer has a structural similarity to glycosaminoglycans (GAGs) found in extracellular matrices as in native articular cartilage playing a key role in modulating chondrocytes morphology, differentiation and function [17,18]. For the composite component aiming at the osteogenic part, hydroxylapatite was selected as filler since this it is the main mineral present in bone composition approaching the bone composite structure. In this way, it is expected that both chitosan as chondrogenic component and the presence of hydroxylapatite for osteogenic part will provide adequate biochemical cues up to a certain extent.

3.1. CYTOTOXICITY ASSESSMENT

Indirect contact tests such as cytotoxicity tests with MTS are widely used as a preliminary screening for biomaterials. These biological tests allow to assure that the leachables from the materials will not induce any in vitro cytotoxic effect on the cells. MTS tests were performed in order to screen eventual cytotoxicity of the developed polymeric and composite scaffolds, by means of assessing the cell viability of L929 cells cultured with extracts for 72 h. All the cell viability percentages plotted in the following graphs are values relative to the control (100% considered for L929 cells cultured with cell culture medium). It was verified that extracts from the polymeric chitosan scaffolds (C) did not affect the cellular viability, since a similar cellular viability was obtained as in the controls, as shown in Figure 2.

However, and quite surprisingly, it was found that composite scaffolds produced with unsintered hydroxylapatite and crosslinked with glutaraldehyde reduced significantly the cell viability even for low glutaraldehyde concentrations (Figure 2.A). Lower glutaraldehyde concentrations were used since it was previously reported that residual glutaraldehyde may induce a decrease in cell viability due to free aldehyde groups [24]. Nevertheless, crosslinking is desirable to improve the mechanical performance. To try to overcome this problem, composite scaffolds with unsintered hydroxylapatite crosslinked with 0.01% of glutaraldehyde were treated with different glycine concentrations in order to block any residual free aldehyde groups that could be potentially inducing this cytotoxic behaviour. The cell viability increased after the treatment with higher concentration of glycine (1M) independently of the treatment time, even though was found to be low (around 40%) as shown in Figure 2.B.

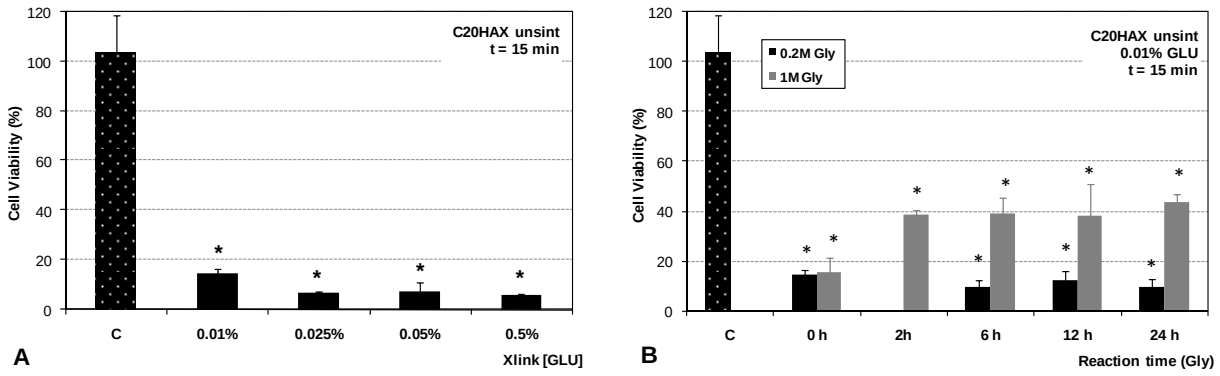

Figure 2. Cell viability evaluated by MTS assays of composite chitosan particle aggregated scaffolds showing the influence of glutaraldehyde concentration (A) and glycine treatment (B) when using unsintered hydroxylapatite. C stands for the polymeric scaffolds. Statistically significant difference (*) as compared to controls and polymeric scaffolds (C).

From these results, one could conclude that the cytotoxicity effect of the composite scaffolds was not being provoked by the glutaraldehyde and, therefore, the unsintered hydroxylapatite was replaced by sintered hydroxylapatite which is more chemically stable. The effect of both hydroxylapatites was studied with no crosslinking as function of its concentrations. It it was found that sintered hydroxylapatite did show a significant increase on cell viability even for higher concentrations as 20% with no statistical difference with the control and polymeric scaffolds for this concentration. These MTS results are plotted in Figure 3.A.

The influence of glutaraldehyde concentration on composite scaffolds with sintered hydroxylapatite was further investigated. No significant decrease in cell viability was observed for the majority of the conditions when compared to the controls and to the polymeric scaffolds as shown in Figure 3.B. In general, when using sintered HA, the obtained values for cell viability for all formulations were completely acceptable for the proposed applications. From these results, composite scaffolds with 20%wt of sintered hydroxylapatite crosslinked with 0.01% glutaraldehyde and treated with 1M glycine both for 15 minutes were selected and used for further characterization studies, since they have shown the higher cell viability with no statistical difference to that of the controls and polymeric scaffolds.

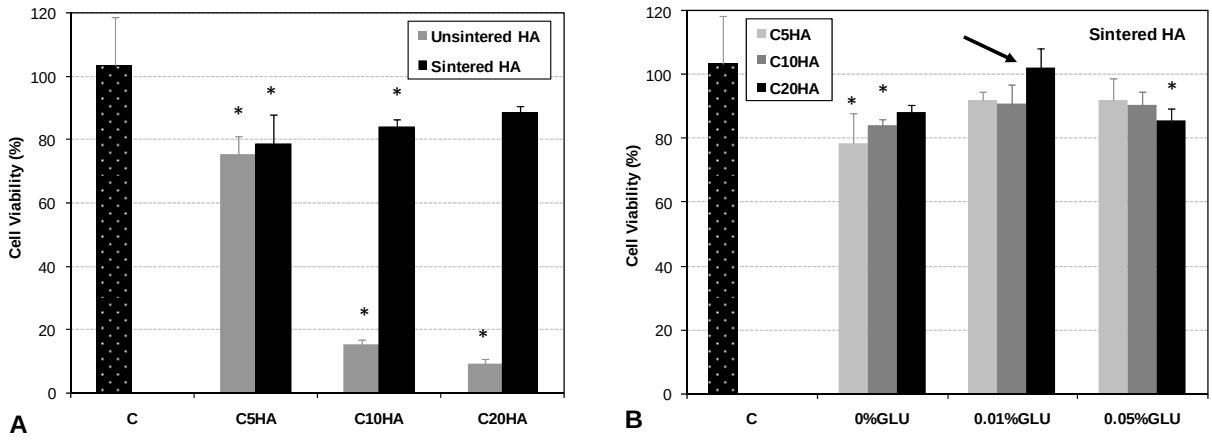

Figure 3. Influence of unsintered and sintered hydroxylapatite (A) and glutaraldehyde concentrations with glycine 1M treatment when using sintered hydroxylapatite (B) on cell viability evaluated by MTS assays of composite chitosan particle aggregated scaffolds. Statistically significant difference (*) as compared to controls and polymeric scaffolds (C).

In order to try to understand the cytotoxic behaviour induced by composite scaffolds with unsintered HA, ICP was used to study the extracts from the materials after 24 h immersion in cell culture medium following the MTS protocol and using the culture medium as control. ICP results obtained for Ca, Mg, Si and P elemental concentrations are shown in Figure 4. Interestingly, it was found that in composite scaffolds when using unsintered hydroxylapatite, the Ca and Mg elemental concentrations were statistically lower when compared to that of composite scaffolds with sintered hydroxylapatite. When both HAs are incorporated in a chitosan matrix, these ions are uptaken by the materials indicating also the formation of an apatite like layer as discussed later. It is known that apatites formed in a solution often replace the Ca^{2+} ion site with small amounts of Mg^{2+}, Na^{+} or K^{+} ions [25]. Thus, from both ICP and MTS results one can say that this uptake of Ca^{2+} and Mg^{2+} ions reached critical low values for the composites scaffolds with unsintered HA inducing a cytotoxic behaviour of these materials. It is known that divalent cations including Ca^{2+} and Mg^{2+} are active in cell adhesion mechanisms, as further discussed [26-28].

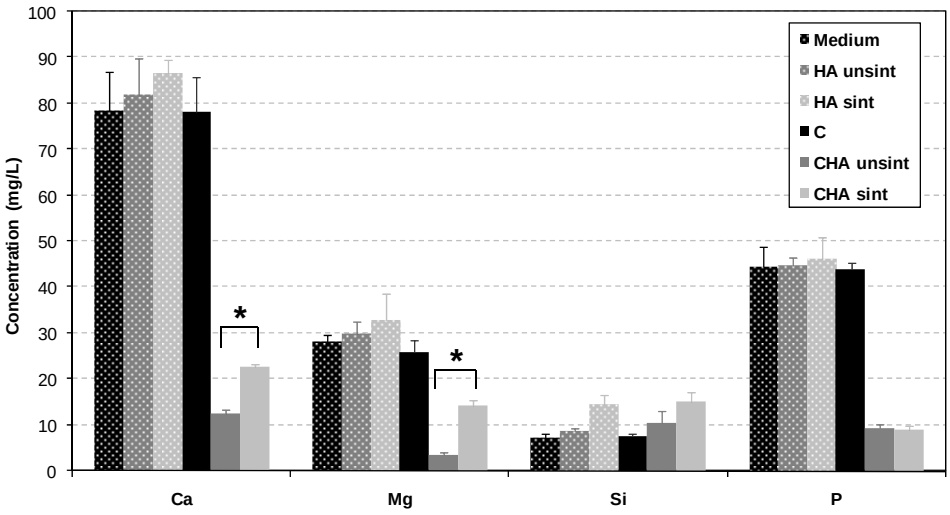

Figure 4. Calcium (Ca), magnesium (Mg), silicon (Si) and phosphorous (P) elemental concentrations of materials extracts after 24 h immersion in cell culture medium. Statistically significant difference (*) between conditions. Respectively, HA unsint and HA sint stands for unsintered and sintered hydroxylapatite. C stands for chitosan polymeric scaffolds, CHA for chitosan/ hydroxylapatite composite scaffolds, while BiCCHA stands for chitosan-chitosan/hydroxylapatite bilayered scaffolds. Medium is the control DMEM culture medium.

Fibroblast like many other cell types such as osteoblasts, chondrocytes or endothelial cells are anchorage-dependent cells [29] meaning that they need to adhere in order to maintain their function and viability. Furthermore, it is known that the cell-cell, cell-extracellular matrix or cell-substrate interactions

are mediated by integrins which are cell adhesion receptors [30]. The extracellular domains of these receptors possess binding sites for a diverse range of protein ligands. Ligand binding is divalent cation dependent and involves well-defined motifs in the ligand [31]. Integrins can dynamically regulate their affinity for ligands which is a key issue to their involvement in processes such as cell adhesion or cell migration [31]. The cation composition of the extracellular milieu is a potential regulatory factor as the binding of divalent cations to extracellular domains has been shown to activate integrins [27] activating the intracellular signaling pathways. This divalent cations dependence for integrins activation might explain why composite scaffolds produced with unsintered hydroxylapatite showed a cytotoxic behaviour. The divalent cations uptake led to critical low values present in the materials extracts, thereby compromising cell adherence to the substrate.

In addition to integrins, cells express another Ca^{2+}-dependent molecule responsible for cell-cell adhesion. The Ca^{2+}-dependent group consists largely of a class of transmembrane glycoproteins called cadherins that mediate cell-cells adhesion by homotypic protein-protein interactions through their extracellular domain by forming Ca^{2+} binding sites regulating cell adhesion [32]. In the presence of Ca^{2+}, E-cadherin (one subclass of cadherins) resides principally in the areas of cell-cell contacts. In reduced Ca^{2+}, however, E-cadherin becomes susceptible to proteolytic cleavage and rapidly loses function [33].

There are several studies [26,28,34] reporting these divalent cations dependence behaviours. Paul *et al* [28] have investigated the behaviour of MG63 osteoblast-like cells when cultured in porous ceramic matrices from nanoparticles of calcium phosphate containing zinc and magnesium. The study showed that the presence of calcium and magnesium in ceramic scaffolds encourages the cell adhesion and spreading and of osteoblasts cells onto the bioceramic matrices. In another study by Fugii *et al* [26], the sensitivity to serine proteinases of cellular proteins involved in cell-matrix adhesion was investigated using C32 melanoma cells. The treatment of cells with serine proteinases can effect integrin-mediated attachment to matrix proteins in a manner moderated by Ca^{2+}. The study showed that in the absence of Ca^{2+} a reduced cell attachment was observed and that the presence of this divalent cation had an additional effect [26]. Furthermore, the divalent cation dependence of fibroblastic cell adhesion to non cellular substrate was also demonstrated by Ueda *et al* [34] where Ca^{2+}, Mg^{2+}, Mn^{2+}, and Co^{2+} were effective in promoting the aggregation of fibroblastic cells as well as their adhesion to non cellular substrate.

As conclusion, one may say that the adhesion proteins and their receptors together constitute a versatile recognition system providing cells with anchorage, traction for migration, and signals for polarity, position, differentiation, and possibly growth [30]. Since these integrins require divalent cations for ligand binding, one may justify the cytotoxic behaviour of composite scaffolds produced with unsintered hydroxylapatite based in the uptake of these divalent ions to a critical low value. The low concentration of Ca^{2+} and Mg^{2+} may be compromising the integrins activation affecting the fibroblasts adhesion and therefore, the cell viability when cultured with the materials extracts. However, and as mentioned before, this problem could be overcome by using sintered hydroxylapatite that showed the cell viability similar to that of the control and to the polymeric scaffolds.

3.2. MORPHOMETRIC ANALYSIS

When aiming at osteochondral applications, the graft should structurally and functionally integrate itself and with the host tissue, since any discontinuity is likely to cause long-term device failure. To create constructs having more favourable integration properties that might be used as osteochondral tissue engineering scaffolds, we have successfully designed and produced bilayered structures combining polymeric and composite chitosan-based particles by promoting their aggregation.

In order to assess the morphometric characterization of the developed scaffolds, micro-CT was carried out. The 3D micro-CT technique provides a better understanding of the scaffolds standard properties, thereby allowing for the optimization of their design and a better fulfilment of tissue engineering scaffolding needs, being in this way is a valuable instrument to support new fabrication technologies. It provides accurate quantitative 3D information at a micro-level and in a non-destructive fashion. This justifies why micro-CT has become a very popular technique for characterizing porous scaffolds. Relevant morphometric parameters such as porosity, interconnectivity, pore and particle size, as well as the ceramic and pore size distribution, can be retrieved from this analysis.

The scaffolds porosity and interconnectivity were quantified as shown in Figure 5.A. The mean total porosity values of 27.78 ± 2.80 %, 22.41 ± 2.79% and 31.49 ± 3.04 % were obtained with an interconnectivity degree of about 94.97 ± 1.40, 91.77 ± 1.91 and 94.05 ± 2.43 % for the proposed polymeric, composite and bilayered scaffolds, respectively. It is important to stress out that

interconnectivity was calculated with a limit in pore size of 53 μm as minimum value for interconnected pores, meaning that interconnection diameters lower that this value were considered as closed pores.

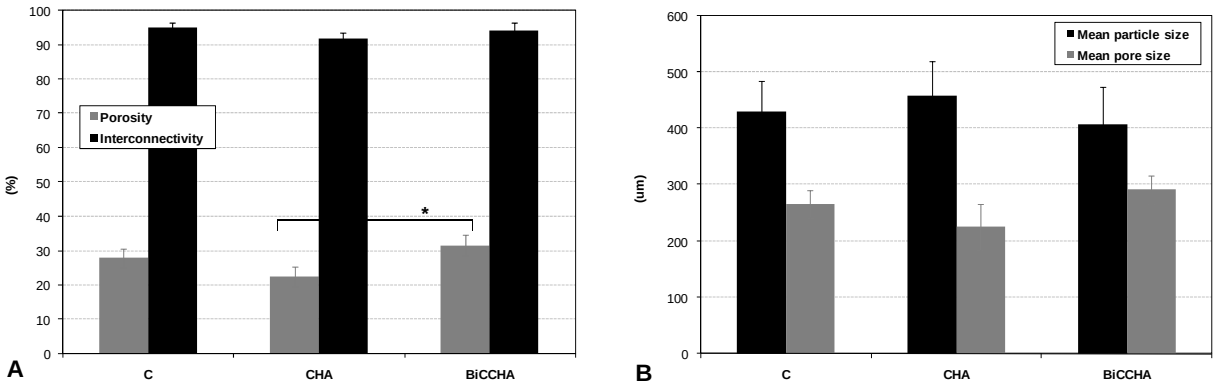

Figure 5. Porosity and interconnectivity (A) and mean particle and pore size (B) of polymeric, composite and bilayered chitosan particles-aggregated scaffolds measured by micro-CT. Statistically significant difference (*) between both formulations. C stands for chitosan polymeric scaffolds, CHA for chitosan/ hydroxylapatite composite scaffolds, while BiCCHA stands for chitosan-chitosan/hydroxylapatite bilayered scaffolds.

One interesting feature of the particles aggregation methodology is that it does not compromise the scaffolds interconnectivity, even at the interface (Figure 5.A). Since this methodology is based on the random assembly of particles, the bonding sites are the contact points of adjacent particles, thereby creating a highly interconnected network. As a result, this strategy does not create any interface barrier area allowing further cell migration and nutrients flow that might avoid some potential necrotic central regions. Moreover, the values of porosity (Figure 5.A) that might be considered low for tissue engineering applications [7,35] are responsible for the high mechanical performance of the materials, which is a critical issue when aiming at load bearing tissue engineering applications.

Furthermore, pore size is another important morphological factor for tissue ingrowth and the developed scaffolds present a wide 3D pore size distribution in the range of the optimal pore size, as indicated by different authors [36-38]. These results are demonstrated in Figure 6 which represents the number of pores in each given size range for the different scaffolds formulations. The mean values of pore diameter and particle size (pore wall thickness) were found to vary between 225-290 μm and 410-460 μm, respectively as shown previously in Figure 5.B.

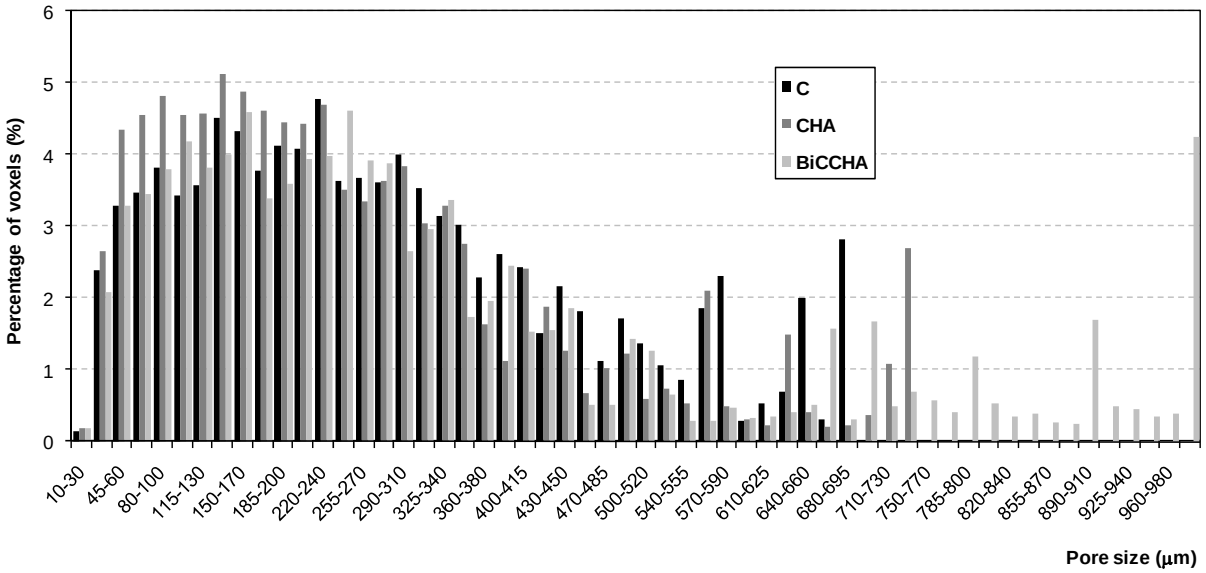

Figure 6. Distribution of pore size of polymeric, composite and bilayered chitosan particle aggregated scaffolds measured by micro-CT. C stands for chitosan polymeric scaffolds, CHA for chitosan/ hydroxylapatite composite scaffolds, while BiCCHA stands for chitosan-chitosan/hydroxylapatite bilayered scaffolds.

The different polymeric and ceramic phases present in the samples are characterized by different values of the linear attenuation coefficient for X-ray. To obtain quantitative data for each analyzed scaffold, a histogram was generated plotting the frequency of a given number of voxels as a function of the X-ray absorption coefficient, as presented in Figure 7.A. In the X-ray absorption histograms of the polymeric and composite scaffolds, only one peak was observed for each formulation corresponding to the chitosan polymeric phase and to the chitosan-hydroxylapatite phase, respectively. The mean of the peak related to the composite phase shifted to higher values of linear attenuation coefficient due to the presence of hydroxylapatite. In the case of the bilayered structure samples, both peaks were observed at lower and higher X-ray absorption values as expected, matching both polymeric and composite phases that comprise this biphasic structure.

Furthermore, the ceramic phase content profile in the scaffolds was also assessed and plotted against scaffolds thickness. These results allow to evaluate the ceramic distribution along the scaffold including in the interface of the bilayered structures (Figure 7.B). The steady increase of the ceramic phase in the interface is a clear evidence of the gradual transition from the polymeric phase to the composite structure.

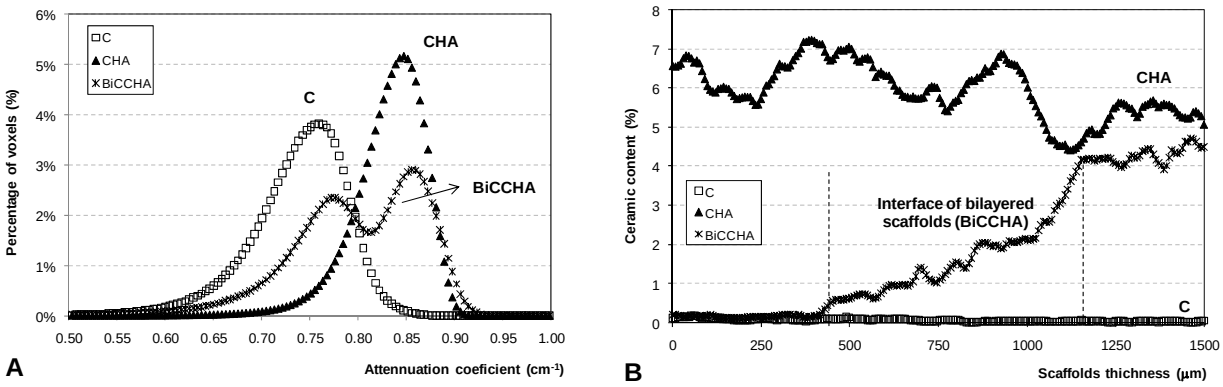

Figure 7. Representative X-ray absorption histogram (A) and ceramic content distribution (B) obtained for polymeric, composite and bilayered chitosan particles-aggregated scaffolds. C stands for chitosan polymeric scaffolds, CHA for chitosan/hydroxylapatite composite scaffolds, while BiCCHA stands for chitosan-chitosan/hydroxylapatite bilayered scaffolds.

The 3D virtual models represented in Figure 8 allowed for the visualization of the scaffolds' interface using different threshold disclosing the spatial distribution of both polymeric and ceramic matrix in the central part of the scaffolds. From these images, we can observe the good integration of both phases accomplished by using chitosan as polymeric matrix with this processing methodology without any need of extra joining approach. This is due to the bioadesive properties of chitosan [39]. One can conclude that a successful approach was achieved by means of assembling polymeric and composite chitosan-based particles, in order to fabricate an integrated two-phase scaffold for osteochondral tissue engineering.

→

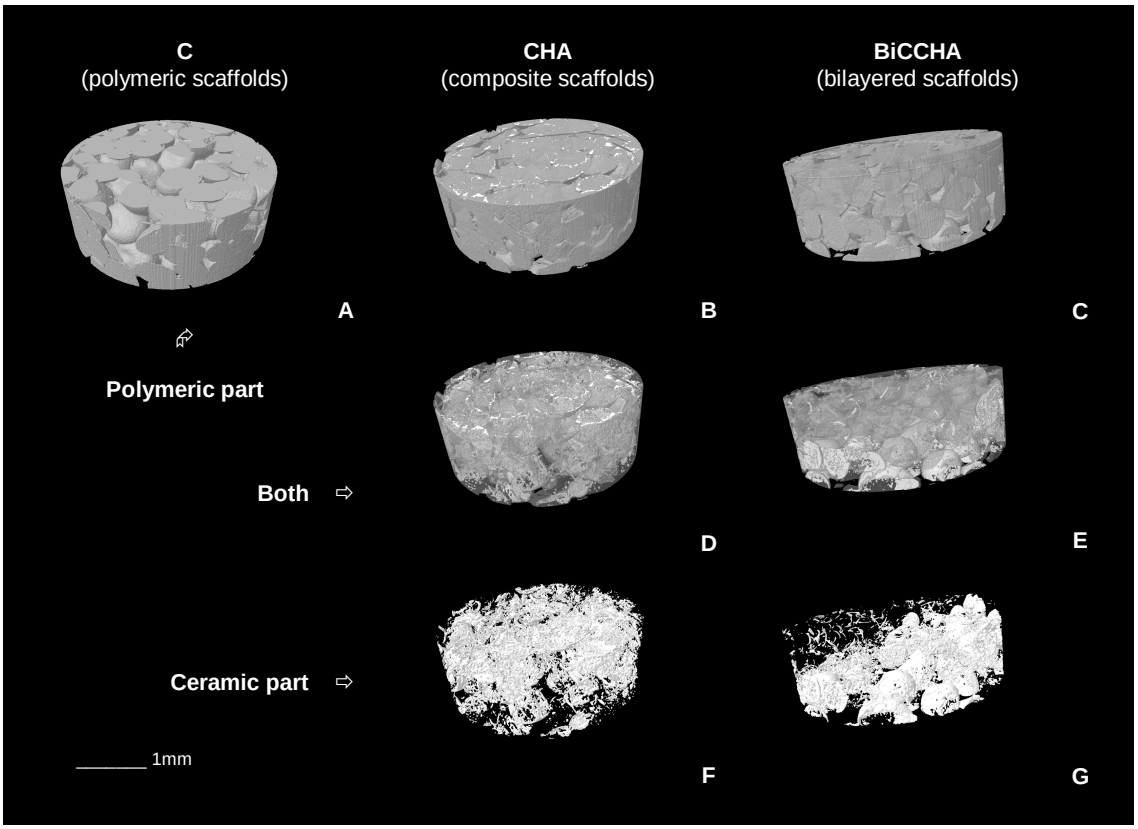

Figure 8. 3D virtual models of chitosan particles-aggregated scaffolds: polymeric, C (A), composite, CHA (B, D, F) and bilayered, BiCCHA (C, E, G) showing the gradual transition (D,E) evidencing the ceramic phase distribution (F,G).

3.3. Dynamical-Mechanical Behaviour

As previously discussed, large osteochondral defects are associated with mechanical instability [5]. Therefore, the mechanical properties of the scaffold or engineered tissue before implantation into an osteochondral defect are key determinants of its posterior success or eventual failure. Furthermore, the mechanical properties of a scaffold will influence the mechanical environment of the seeded cells [40].

When designing a complex osteochondral construct, it is desirable that heterogeneous structures should be built in a way on which one of the sides should promote cartilage regeneration and the other region, exhibiting different properties, is designed to support bone integration. For example, the cartilage-side layer should be more ductile and should have much more fluid uptake capability [9]. However, it is predicted that increasing the stiffness of the scaffold up to a certain limit, increases the amount of cartilage formation and reduces the amount of fibrous tissue formation in the defect [40]. The bone-side

layer should exhibit higher stiffness, should preferably have a good affinity to the ceramic constituent of bone and, ideally, should be able to induce vascularization, especially for large defects [9].

In the present study, the bilayered structures were designed having these considerations in mind. For the chondrogenic part, chitosan polymeric particles were assembled while for the osteogenic constituent composite particles were used with hydroxylapatite as ceramic filler further crosslinked with glutaraldehyde in order to improve the stiffness of this component. The assessment of scaffolds mechanical behaviour is essential to demonstrate the mechanical stability, namely in dynamic conditions and in hydrated state resembling the in vivo condition where physiological fluids are present. For that purpose, chitosan-based scaffolds were fully hydrated in PBS for 3 days in physiological conditions based in previous hydration studies where after this time period the hydration plateau was achieved (data not shown). Chitosan-based particles aggregated scaffolds in wet state were then characterized under dynamic compression solicitation over a range of physiological frequency range in load-bearing applications, such as articular cartilage or bone [14, 41].

The values at a frequency of 1Hz considered as reference values for comparison of elastic (storage) and viscous (loss) components of the complex modulus are shown in Figure 9.A. From the this results, the first conclusion that comes out is that the scaffolds showed a very good mechanical behaviour when compared to the typical mechanical properties obtained for chitosan based porous materials [42,43], even if only considering the polymeric formulation. The mean values for the elastic component (E') were found to be 4.21 ± 1.04 MPa, 7.98 ± 1.77 MPa and 6.26 ± 1.04 MPa, for polymeric, composite and bilayered scaffolds, respectively. The high mechanical properties obtained by the particle aggregation methodology are further supported by other works, namely the work by Jiang *et al* [44] when using chitosan microspheres in this case with poly(lactic acid-glycolic acid) sintered together to obtain the final 3D structure. The compressive modulus (E') was further increased for the composite scaffolds by incorporating the hydroxylapatite and crosslinking the polymeric matrix allowing to obtain a scaffold with higher stiffness, as envisioned for the osteogenic component. A two-fold increase in the elastic modulus (E') was accomplished and, as expected, the bilayered materials present an intermediate value between the polymeric and composite scaffolds since they are both the basis of its structure.

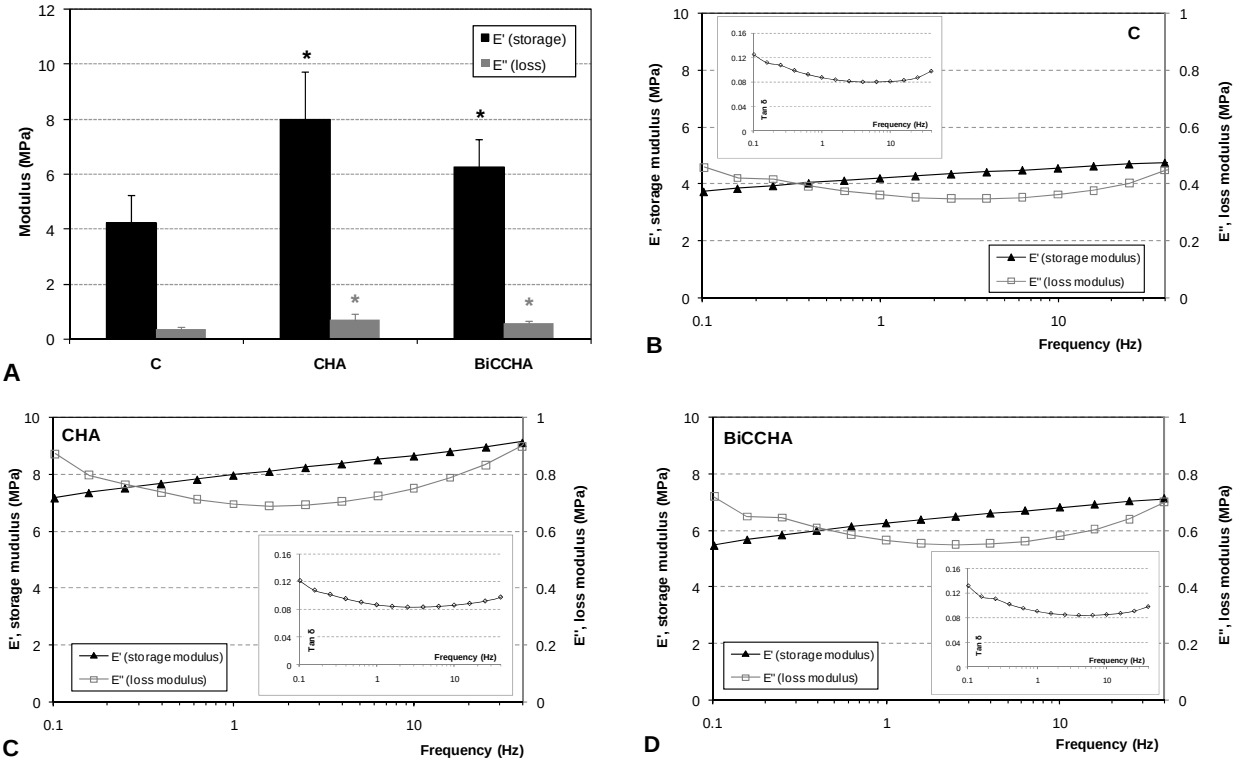

Figure 9. Storage (E') and loss (E'') modulus under dynamic compression solicitation at 1Hz frequency (A) and behaviour for increasing frequencies (B, C, D) of polymeric (C), composite (CHA) and bilayered (BiCCHA) chitosan particle-aggregated scaffolds in wet state. The inset graphs show the frequency dependence of the loss factor (tan δ). Statistically significant difference (*) as compared to the polymeric scaffolds.

In addition, the storage (E') and loss (E'') modulus behaviours for increasing frequencies are presented in Figures 9.B-D and the frequency dependences of the loss factor (tanδ) are shown in the inset graphs. As it is possible to observe, the developed materials shown the same profile for storage (E') and loss (E'') modulus with increasing frequencies. The elastic modulus (E') increases with increasing frequency, being typically between 4 and 9 MPa while the viscous modulus (E'') shows the inverse trend with an increasing for higher frequencies, being this behaviour more obvious for composite materials. As a consequence, there is a decrease of the loss factor, (tanδ=E''/E') with increasing frequency with a slight increase for higher frequencies, as shown in the inset graphs. This factor measures the proportion of the imposed mechanical stress that is dissipated in the form of heat. As tan δ is typically above 0.08 for f<1 Hz, one may conclude that the scaffolds possesses significant damping capability that may be useful to dissipate some cyclic mechanical energy that is imposed in an implantation scenario. Nevertheless,

there is an increase in E'' for high frequencies, which suggests that the material exhibits some dissipation capability for high frequencies.

By dynamically testing the bilayered scaffolds in wet conditions in a physiological range of frequencies, we were able to demonstrate that these biphasic materials are mechanically stable even for higher frequencies, showing once again the high integration between both components.

3.4. STATIC AND DYNAMIC *IN VITRO* BIOACTIVITY STUDIES

The *in vitro* bioactivity studies were performed to address two hypotheses, since we are discussing the potential application in osteochondral tissue engineering. By one hand, one should assure that the polymeric component designed for the chondrogenic part will not mineralize even with the extra supply of Ca and P from the composite component. To preliminary screen this behaviour, SSF (simulated synovial fluid) was also used in order to mimic the chemical environment of a human joint. On the other hand, we needed to evaluate the ability for the composite component designed for the osteogenic part to form per se an apatite layer on its surface. This can predict, in a certain way, the bone-bonding ability of the material which is often evaluated in a simulated body fluid (SBF) with ion concentrations nearly equal to those of human blood plasma [21].

For that, the osteogenic component was designed as a polymer composite, which includes a bioactive ceramic phase (HA) as the source of both bioactivity and reinforcement incorporated into the polymeric matrix. Thereby, the composite component has potentially the capability of combining bioactive behaviour with improved mechanical performance, as discussed previously. This strategy was firstly used to produce hydroxylapatite-polyethylene bioactive composites [45] and was also applied to develop composites containing other bioactive phases, such as, bioactive glasses [46] and glass-ceramics [47], and a series of different polymers [45,46,48]. To address both hypotheses, *in vitro* bioactivity studies were carried out using two different simulated solutions (SBF and SSF) used both in static, as well as in dynamic conditions. The aim of the dynamic strategy was to approach the ideal scenario required to engineer *in vitro* an osteochondral construct.

The SEM microphotographs for static conditions are disclosed in Figure 10, where it is possible to analyse the scaffolds surface before and after 14 days immersion in both SBF and SSF. From these images, one can say that no significant morphological changes were observed in the scaffolds surface, even for 14 days of immersion in both simulated solutions. In the case of composite components, this may be due to the presence of HA already in the surface which makes it already very irregular and might be masking any apatite formation.

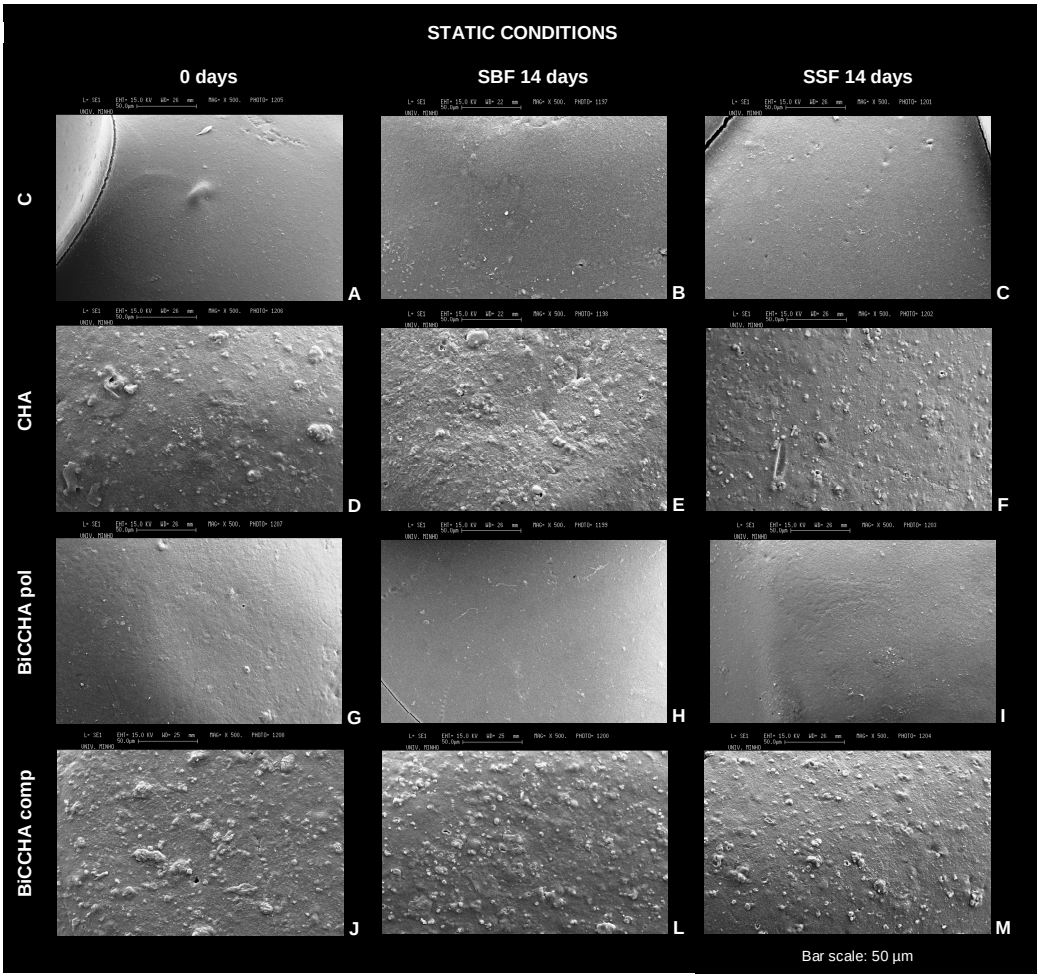

Figure 10. SEM microphotographs of scaffolds surface before (A, D, G, J) and after 14 days immersion in SBF (B, E, H, L) and SSF (C, F, I, M) in static conditions. C stands for polymeric scaffolds (A, B, C), CHA for composite scaffolds (D, E, F), BiCCHA pol for the surface of the polymeric part (G, H, I) while BiCCHA comp for the surface of the composite part (J, L, M) of the bilayered scaffolds. Bar scale represent 50 µm.

However, from the ICP results (Figure 11) there is a clear evidence of the Ca and P concentration decrease in the solution from both composite and bilayered scaffolds indicating that these materials are

consuming these ions for an apatite formation. As can be seen, a sharp decrease in the Ca concentration of SBF (Figure 11.A) takes place in the first 7 days of immersion for composite and bilayered samples, stabilizing at a certain value up to 14 days. The same trend is observed for P concentration (Figure 11.B) becoming stable after 3 and 7 days for SSF and SBF, respectively.

Interestingly, ICP reveal a selective absorption of Ca and P for the bilayered structures, since these materials show a higher profile of both Ca and P present in solution when compared to composite samples. This selective absorption was further confirmed by EDS (Figure 12) where no Ca and P were detected at the surface of the polymeric component after 14 days of immersion in both solutions (Figure 12.B). In addition, an increase of Ca and P peaks intensity for the composite constituent can be observed, becoming more clear when immersed in SBF (Figure 12.C).

From these results together, one can conclude that both hypotheses were addressed, since in static conditions the polymeric component designed for the chondrogenic part did not mineralized in vitro, and the composite part is consuming both Ca and P from the simulated solutions to form an apatite layer.

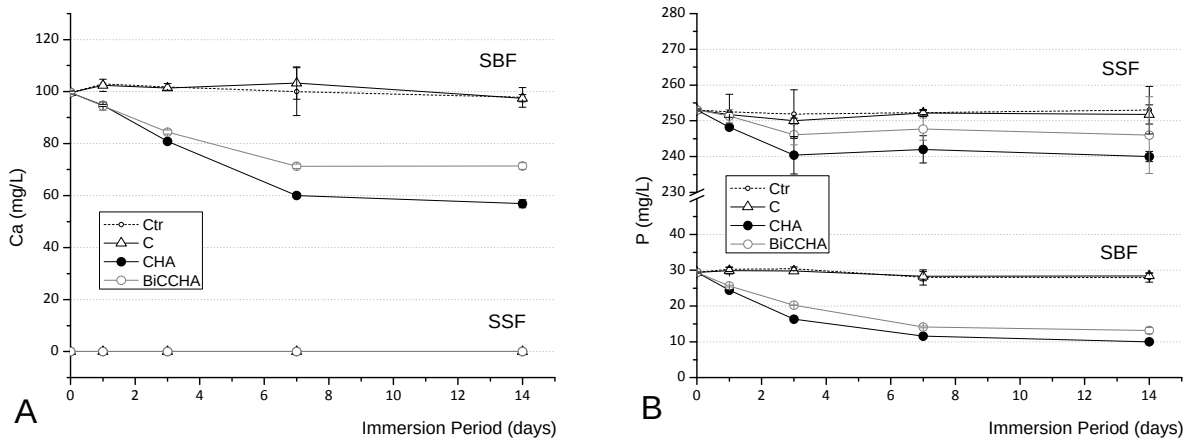

Figure 11. Calcium (A) and phosphorous (B) concentration profile of SBF and SSF as function of immersion time of polymeric (C), composite (CHA) and bilayered (BiCCHA) scaffolds in static conditions.

→

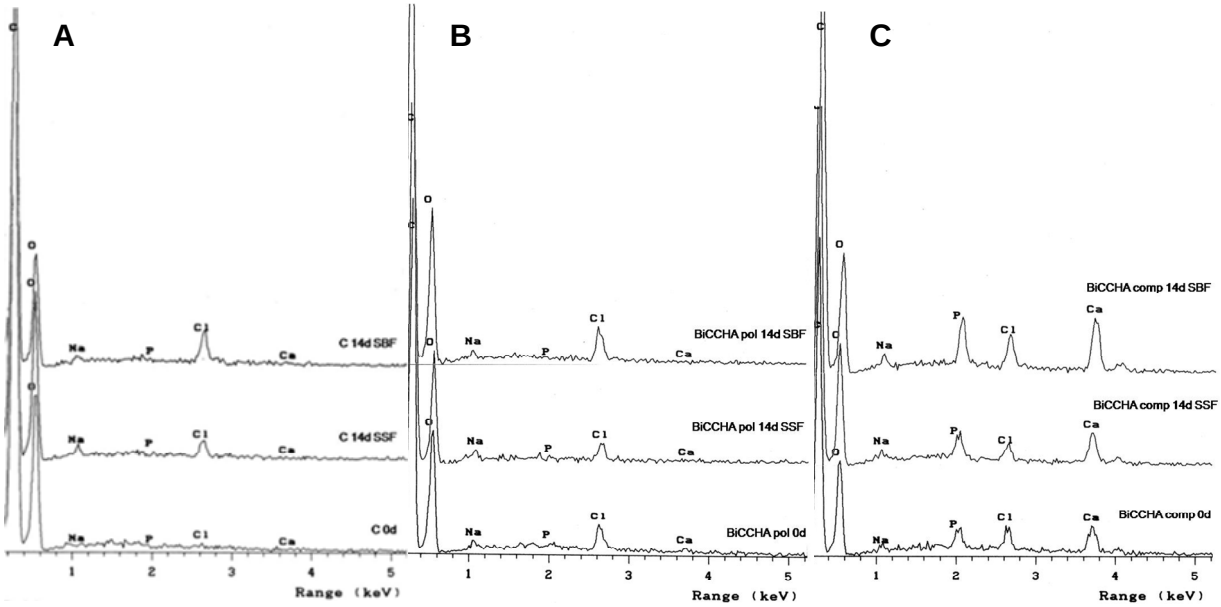

Figure 12. EDS spectra showing the presence of calcium and phosphorous in the surface of polymeric scaffolds (A), polymeric part of bilayered scaffolds, BiCCHA pol (B) and ceramic part of bilayered scaffolds, BiCCHA comp (C) before and after 14 days of immersion in SBF and SSF in static conditions.

To study the *in vitro* bioactivity in dynamic conditions, we have designed a specific double-chamber bioreactor (see Figure 1). The ultimate goal of the design of this specific bioreactor is to be used in future studies to engineer bilayered hybrid constructs for osteochondral applications. For that, the bioreactor was designed to allow the simultaneous culturing of chondrocytes and osteoblasts in the respective sections of a single-unit chamber.

The scaffolds are supported by a transversal silicon membrane and both simulated solutions (SBF and SSF) have continuous recirculation in the 6 interconnected chambers in each of respective part of the bilayered scaffolds. This will also promote a dynamic perfusion and laminar flow in each of the bioreactor compartments, and thereby contribute for an enhanced cells distribution and mass transfer of nutrients avoiding some potential necrotic central regions. SBF has a flow circuit through the composite parts of the bilayered structures while SSF is circulating through the polymeric part designed for the chondral constituent to approximate the chemical environment in a human joint.

Similarly to static conditions, SEM microphotographs of dynamic assays did not show any significant morphological change in both polymeric and composite surfaces of the bilayered scaffolds as shown in Figure 13.

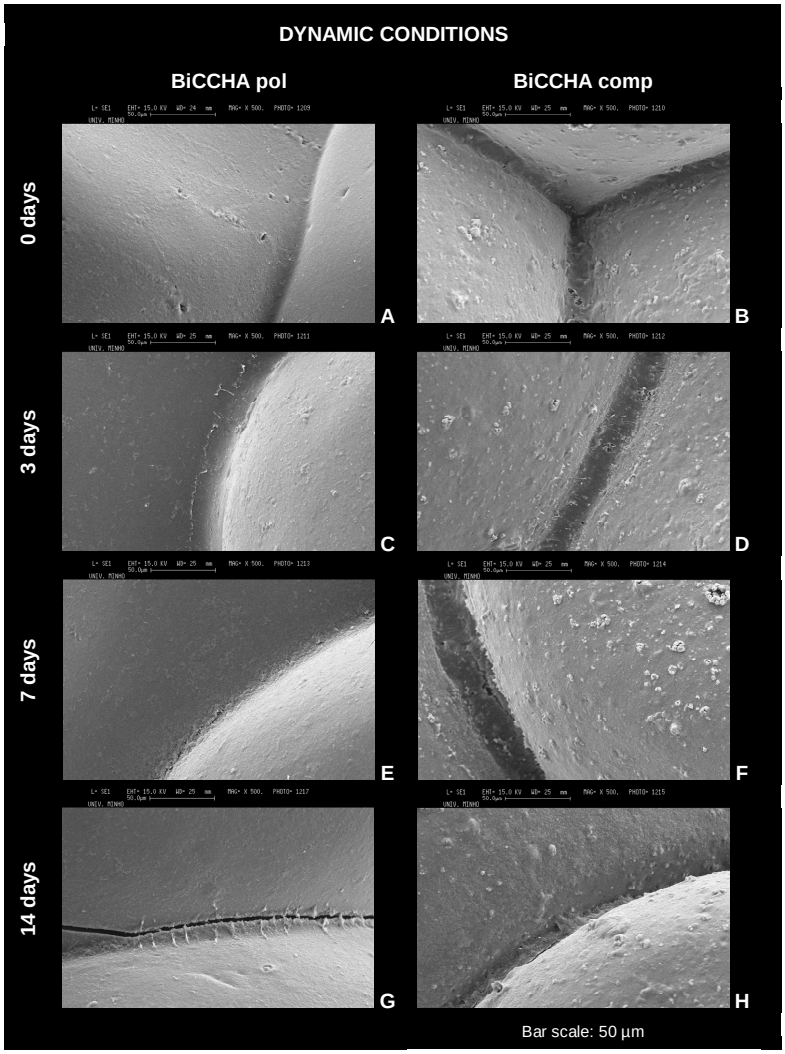

Figure 13. SEM microphotographs of scaffolds surface before (A, B) and after 3 (C, D), 7 (E, F) and 14 days (G, H) of dynamic bioactivity assay in the double-chamber bioreactor where SBF and SSF were circulating. BiCCHA pol stands for the surface of the polymeric part (A, C, E, G) while BiCCHA comp the surface of the composite part (B, D, F, H) of the bilayered scaffolds. Bar scale represent 50 µm.

The concentration profiles of Ca and P of both simulated solutions (SBF and SSF) in the double-chamber bioreactor assessed by ICP analysis are shown in Figure 14. Through the first 7 days, the Ca

concentration of SBF decreased significantly from 100 to around 40 mg/L (Figure 14.A). The Ca concentration seems then to stabilize. The inversed profile is observed for the Ca concentration of SSF with a clear increase within the first 3 days becoming less attenuated for longer periods. Exactly the same trend profile is observed for P concentration (Figure 14.B), only in this case is the SSF solution that is supplying P to SBF. This is an indication of ion exchange between both simulated solutions in the double-chamber bioreactor.

However, we have calculated and compared the consumption of Ca and P of the bilayered structures by subtracting the constant initial value from the total concentration at a given time period (dash grey line (--) in Figure 13). It is possible to observe that the consumption of Ca experiences a gradual increase up to 7 days, stabilizing at a certain value after this period of time. The same trend is observed for the P concentration profile, with a slight increasing tendency after 3 days of immersion period. This consumption data clearly indicates that the CaP is being captured by the materials, which is one of the criteria for the evaluation of the in vitro bioactivity of materials.

These results were further complemented by EDS analysis (Figure 15) which disclosed that both Ca and P were not detected at the surface of the polymeric component after 14 days in the double-chamber bioreactor and showed an increase of Ca and P peaks intensity for the composite part even after only 3 days. This is a clear evidence that these ions are being selectively consumed by the composite part of the bilayered structures.

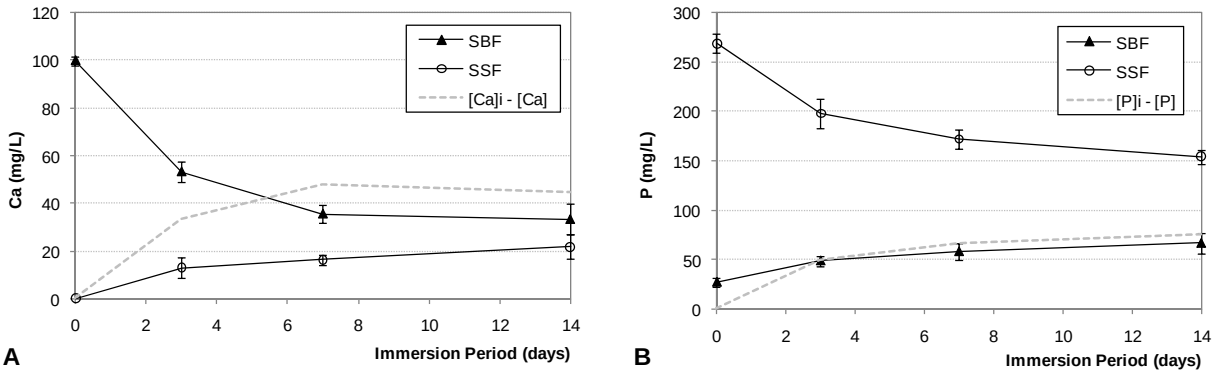

Figure 14. Calcium (A) and phosphorous (B) concentration profile of SBF and SSF as function of time in the double-chamber bioreactor with the bilayered chitosan-based scaffolds. [Ca]i - [Ca] and [P]i - [P] represent the initial total concentration of each element minus the concentration of each element at a given time period.

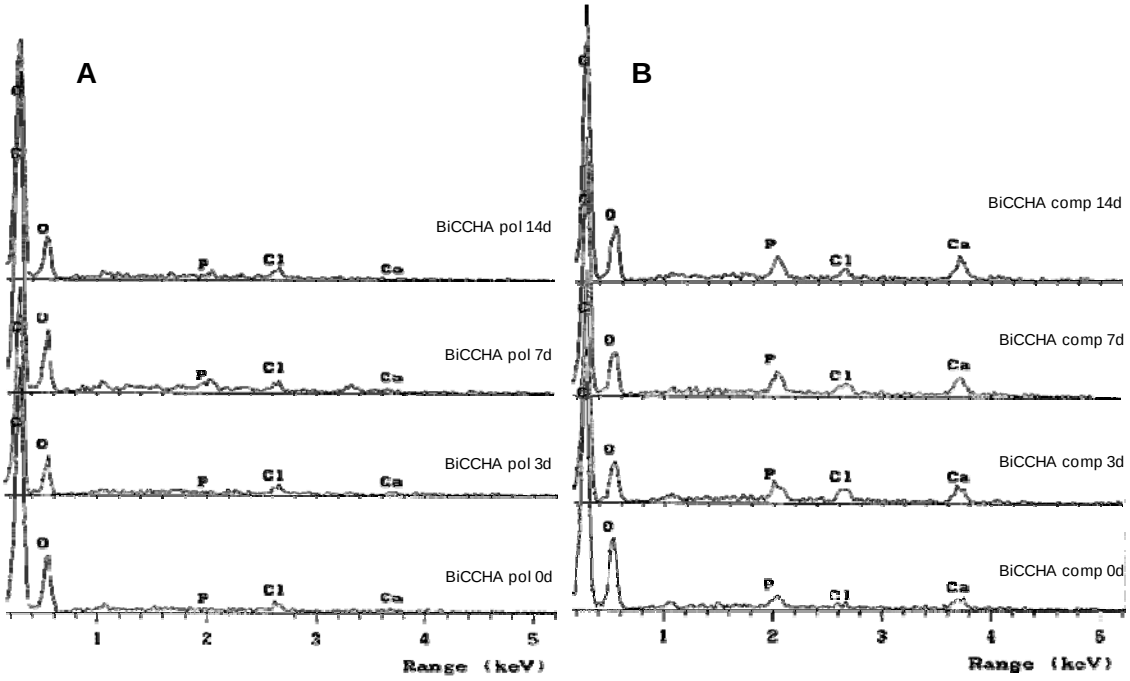

Figure 15. EDS spectra showing the presence of calcium and phosphorous in the surface of polymeric part of bilayered scaffolds, BiCCHA pol (A) and ceramic part of bilayered scaffolds, BiCCHA comp (B) for 0, 3, 7 and 14 days in the double chamber bioreactor.

The studies with the double-chamber bioreactor showed its potential since the scaffolds were able to withstand the perfusion rates. With the proposed design, the medium flow direction can be inverted at certain interval periods, in order to promote increased homogeneity and charge distribution. The ions exchange between both simulated solutions was observed due to the high interconnectivity of the developed scaffolds that allowed the solutions exchange with time. This can be considered as a disadvantage to have in mind when aiming at engineering an osteochondral hybrid construct using the same source of progenitor cells with different differentiation cell culture mediums or the simultaneous but independent culturing of chondrocytes and osteoblasts.

Nevertheless, we have to consider that in cell culture assays, the culture mediums are frequently mixed to supply the adequate concentration of nutrients. Furthermore, if desirable, the materials can be designed with a physical barrier between both chondrogenic and osteogenic components without compromising the integration of the scaffolds. In the case of chitosan-based materials, a chitosan membrane can be assembled when producing the materials since this polymer is known to be

bioadhesive [39]. Furthermore, as one of the ongoing strategies with the chitosan-based particle aggregated scaffolds, the physical barrier can be accomplished using a hydrogel for the chondrogenic component where chondrocytes can be encapsulated.

Alternatively, there are authors [8,49,50] that defend the application of a single-phase material but with gradients of molecular, structural and functional properties to engineer complex tissue grafts, as discussed in the introduction. As an example, Vunjak-Novakovic *et al* [8] proposes a single-phase silk-based scaffold which is functionalized by covalently binding growth factors with spatial concentration gradients, with opposing gradients of a chondrogenic factors (IGF-I) and osteogenic factors (BMP-2) for tissue engineering of osteochondral grafts. The opposite gradients of these two different growth factors in the same scaffold are proposed in order to mimic an 'ideal' concentration of IGF-I for cartilage at one end and an 'ideal' concentration of BMP-2 for bone at the other end [8].

One can say that, if desirable, the double-chamber bioreactor or the materials to be used within it can be further optimized when used in future studies for engineer osteochondral hybrid constructs. Nevertheless, for the present study, the double-chamber bioreactor was successfully designed to study the *in vitro* bioactivity behaviour in dynamic conditions.

4. CONCLUSIONS

By means of using a simple particle aggregation method, it was possible to obtain bilayered chitosan-based scaffolds that exhibit very promising properties for osteochondral applications. The risk of possible delamination between both polymeric and composite components designed for chondrogenic and osteogenic constituents, respectively, could be avoided since the materials showed an integrated interface assessed by micro-CT, as well as mechanical stability in wet state under compression dynamic solicitation. It is suggested that the unexpected cytotoxic behaviour of composite materials produced with unsintered hydroxylapatite could be explained by the low critical concentrations of Ca and Mg found in the extracts. This low divalent cations concentration might by affecting integrins activation, compromising the cell adhesion and, therefore, the cell viability. This unexpected result was overcome by means of using sintered hydroxylapatite that showed no cytotoxic behaviour. From the overall results of the *in vitro* bioactivity assays, both addressed hypothesis were corroborated, since in static conditions

the polymeric component designed for the chondrogenic part did not mineralized *in vitro* and the composite part is consuming selectively both Ca and P from the simulated solutions for an apatite layer formation. Furthermore, a specific double-chamber bioreactor was successfully designed for *in vitro* bioactivity tests in dynamic conditions, aimed also to be used in future studies to engineer osteochondral hybrid constructs.

REFERENCES

1. Marcacci M, Kon E, Delcogliano M, Filardo G, Busacca M, Zaffagnini S. Arthroscopic autologous osteochondral grafting for cartilage defects of the knee: Prospective study results at a minimum 7-year follow-up. American Journal of Sports Medicine 2007;35(12):2014-2021.

2. Lee CY, Liu X, Hsu HC, Wang DY, Luo ZP. A modified cell culture method for autologous chondrocyte transplantation. Connective Tissue Research 2005;46(2):93-99.

3. Ait Si Selmi T, Neyret P, Verdonk PCM, Barnouin L. Autologous chondrocyte transplantation in combination with an alginate-agarose based hydrogel (Cartipatch). Techniques in Knee Surgery 2007;6(4):253-258.

4. Swieszkowski W, Tuan BHS, Kurzydlowski KJ, Hutmacher DW. Repair and regeneration of osteochondral defects in the articular joints. Biomolecular Engineering 2007;24(5):489-495.

5. Schaefer D, Martin I, Jundt G, Seidel J, Heberer M, Grodzinsky A, et al. Tissue-engineered composites for the repair of large osteochondral defects. Arthritis and Rheumatism 2002;46(9):2524-2534.

6. Schaefer D, Martin I, Shastri P, Padera RF, Langer R, Freed LE, et al. In vitro generation of osteochondral composites. Biomaterials 2000;21(24):2599-2606.

7. Hollister SJ. Porous scaffold design for tissue engineering. Nature Materials 2005;4(7):518-524.

8. Vunjak-Novakovic G, Meinel L, Altman G, Kaplan D. Bioreactor cultivation of osteochondral grafts. Orthodontics and Craniofacial Research 2005;8(3):209-218.

9. Mano JF, Reis RL. Osteochondral defects: present situation and tissue engineering approaches. Journal of Tissue Engineering and Regenerative Medicine 2007;1(4):261-273.

10. Martin I, Miot S, Barbero A, Jakob M, Wendt D. Osteochondral tissue engineering. Journal of Biomechanics 2007;40(4):750-765.

11. Huang X, Yang D, Yan W, Shi Z, Feng J, Gao Y, et al. Osteochondral repair using the combination of fibroblast growth factor and amorphous calcium phosphate/poly(l-lactic acid) hybrid materials. Biomaterials 2007;28(20):3091-3100.

12. Wendt D, Jakob M, Martin I. Bioreactor-based engineering of osteochondral grafts: From model systems to tissue manufacturing. Journal of Bioscience and Bioengineering 2005;100(5):489-494.

13. Chang CH, Lin CC, Chou CH, Lin FH, Liu HC. Novel bioreactors for osteochondral tissue engineering. Biomedical Engineering - Applications, Basis and Communications 2005;17(1):38-43.

14. Munirah S, Samsudin OC, Chen HC, Sharifah Salmah SH, Aminuddin BS, Ruszymah BHI. Articular cartilage restoration in load-bearing osteochondral defects by implantation of autologous chondrocyte-fibrin constructs: An experimental study in sheep. Journal of Bone and Joint Surgery - Series B 2007;89(8):1099-1109.

15. Robertson WB, Fick D, Wood DJ, Linklater JM, Zheng MH, Ackland TR. MRI and clinical evaluation of collagen-covered autologous chondrocyte implantation (CACI) at two years. Knee 2007;14(2):117-127.

16. Scotti C, Buragas MS, Mangiavini L, Sosio C, Di Giancamillo A, Domeneghini C, et al. A tissue engineered osteochondral plug: An in vitro morphological evaluation. Knee Surgery, Sports Traumatology, Arthroscopy 2007;15(11):1363-1369.

17. Malafaya PB, Silva GA, Reis RL. Natural-origin polymers as carriers and scaffolds for biomolecules and cell delivery in tissue engineering applications. Advanced Drug Delivery Reviews 2007;59(4-5):207-233.

18. Mano JF, Silva GA, Azevedo HS, Malafaya PB, Sousa RA, Silva SS, et al. Natural origin biodegradable systems in tissue engineering and regenerative medicine: Present status and some moving trends. Journal of the Royal Society Interface 2007;4(17):999-1030.

19. Malafaya PB, Pedro A, Peterbauer A, Gabriel C, Redl H, Reis RL. Chitosan particles agglomerated scaffolds for cartilage and osteochondral tissue engineering approaches with adipose tissue derived stem cells. Journal of Materials Science: Materials in Medicine 2005;16(12):1077.

20. Reis RL, Mendes SC, Cunha AM, Bevis MJ. Processing and In-Vitro Degradation of Starch/EVOH Thermoplastic Blends. Polymer International 1997;43:347-353

21. Kokubo T, Takadama H. How useful is SBF in predicting in vivo bone bioactivity? Biomaterials 2006;27(15):2907-2915.

22. Oyane A, Kim H-M, Furuya T, Kokubo T, Miyazaki T, Nakamura T. Preparation and assessment of revised simulated body fluids. Journal of Biomedical Materials Research Part A 2003;65A(2):188-195.

23. Conzone SD, Brown RF, Day DE, Ehrhardt GJ. In vitro and in vivo dissolution behavior of a dysprosium lithium borate glass designed for the radiation synovectomy treatment of rheumatoid arthritis. Journal of Biomedical Materials Research 2002;60(2):260-268.

24. Zhang YZ, Venugopal J, Huang ZM, Lim CT, Ramakrishna S. Crosslinking of the electrospun gelatin nanofibers. Polymer 2006;47(8):2911-2917.

25. Oliveira AL, Malafaya PB, Reis RL. Sodium silicate gel as a precursor for the in vitro nucleation and growth of a bone-like apatite coating in compact and porous polymeric structures. Biomaterials 2003;24(15):2575-2584.

26. Fujii K, Lazarus GS, Schechter NM. Modification of Integrin-Mediated Cell Attachment to Substrata by Serine Proteinases in the Presence and Absence of Divalent Cations. Experimental Cell Research 1993;208(1):94-103.

27. Hughes PE, Pfaff M. Integrin affinity modulation. Trends in Cell Biology 1998;8(9):359-364.

28. Paul W, Sharma CP. Effect of calcium, zinc and magnesium on the attachment and spreading of osteoblast like cells onto ceramic matrices. Journal of Materials Science: Materials in Medicine 2007;18(5):699-703.

29. Lopez-Perez PM, Marques AP, Silva RMPD, Pashkuleva I, Reis RL. Effect of chitosan membrane surface modification via plasma induced polymerization on the adhesion of osteoblast-like cells. Journal of Materials Chemistry 2007;17(38):4064-4071.

30. Ruoslahti E, Pierschbacher M. New perspectives in cell adhesion: RGD and integrins Science 1987;238(4826):491-497.

31. Tozer EC, Hughes PE, Loftus JC. Ligand binding and affinity modulation of integrins. Biochemistry and Cell Biology 1996;74(6):785-798.

32. Tuan RS. Molecular basis of cell-cell interaction and signalling in mesenchymal chondrogenesis. In: Massaro EJ, Rogers JM, editors. The Skeleton: Biochemical, Genetic, and Molecular Interactions in Developement and Homeostasis. New Jersey: Humana Press, 2004. p. 3-15.

33. Grzesiak JJ, Pierschbacher MD. Shifts in the concentrations of magnesium and calcium in early porcine and rat wound fluids activate the cell migratory response. Journal of Clinical Investigation 1995;95(1):227-233.

34. Ueda MJ, Takeichi M. Two mechanisms in cell adhesion revealed by effects of divalent cations. Cell Structure and function 1976;1(4):377-388.

35. Hutmacher DW. Scaffolds in tissue engineering bone and cartilage. Biomaterials 2000;21(24):2529-2543.

36. Otsuki B, Takemoto M, Fujibayashi S, Neo M, Kokubo T, Nakamura T. Pore throat size and connectivity determine bone and tissue ingrowth into porous implants: Three-dimensional micro-CT based structural analyses of porous bioactive titanium implants. Biomaterials 2006;27(35):5892-5900.

37. Bobyn JD, Pilliar RM, Cameron HU, Weatherly GC. The optimum pore size for the fixation of porous surfaced metal implants by the ingrowth of bone. Clinical Orthopaedics and Related Research 1980;150:263-270.

38. Whang K, Elenz DR, Nam EK, Tsai DC, Thomas CH, Nuber GW, et al. Engineering bone regeneration with bioabsorbable scaffolds with novel microarchitecture. Tissue Engineering 1999;5(1):35-51.

39. Kim IY, Seo SJ, Moon HS, Yoo MK, Park IY, Kim BC, et al. Chitosan and its derivatives for tissue engineering applications. Biotechnology Advances 2008;26(1):1-21.

40. Kelly DJ, Prendergast PJ. Prediction of the optimal mechanical properties for a scaffold used in osteochondral defect repair. Tissue Engineering 2006;12(9):2509-2519.

41. Garner E, Lakes R, Lee T, Swan C, Brand R. Viscoelastic dissipation in compact bone: Implications for stress- induced fluid flow in bone. Journal of Biomechanical Engineering 2000;122(2):166-172.

42. Huang Y, Onyeri S, Siewe M, Moshfeghian A, Madihally SV. In vitro characterization of chitosan-gelatin scaffolds for tissue engineering. Biomaterials 2005;26(36):7616-7627.

43. Wan Y, Fang Y, Wu H, Cao X. Porous polylactide/chitosan scaffolds for tissue engineering. Journal of Biomedical Materials Research - Part A 2007;80A(4):776-789.

44. Jiang T, Abdel-Fattah WI, Laurencin CT. In vitro evaluation of chitosan/poly(lactic acid-glycolic acid) sintered microsphere scaffolds for bone tissue engineering. Biomaterials 2006;27(28):4894-4903.

45. Bonfield W, Grynpas MD, Tully AE. Hydroxyapatite reinforced polyethylene - a mechanically compatible implant material for bone replacement. Biomaterials 1981;2(3):185-186.

46. Leonor IB, Sousa RA, Cunha AM, Reis RL, Zhong ZP, Greenspan D. Novel starch thermoplastic/Bioglass® composites: Mechanical properties, degradation behavior and *in-vitro* bioactivity. Journal of Materials Science: Materials in Medicine 2002;13(10):939-945.

47. Juhasz JA, Best SM, Brooks R, Kawashita M, Miyata N, Kokubo T, et al. Mechanical properties of glass-ceramic A-W-polyethylene composites: Effect of filler content and particle size. Biomaterials 2004;25(6):949-955.

48. Borden M, Attawia M, Khan Y, Laurencin CT. Tissue engineered microsphere-based matrices for bone repair: Design and evaluation. Biomaterials 2002;23(2):551-559.

49. Guo X, Wang C, Duan C, Descamps M, Zhao Q, Dong L, et al. Repair of osteochondral defects with autologous chondrocytes seeded onto bioceramic scaffold in sheep. Tissue Engineering 2004;10:1830-1840.

50. Solchaga LA, Temenoff JS, Gao J, Mikos AG, Caplan AL, Goldberg VM. Repair of osteochondral defects with hyaluronan- and polyester-based scaffolds. Osteoarthritis and Cartilage 2005;13:297-309.

CHAPTER V.

The effect of insulin-loaded chitosan particle aggregated scaffolds in chondrogenic differentiation

CHAPTER V.

The effect of insulin-loaded chitosan particle aggregated scaffolds in chondrogenic differentiation*

ABSTRACT

Osteochondral defects repair requires a tissue engineering approach which aims at mimicking the physiological properties and structure of two different tissues (cartilage and bone) using a scaffold-cell construct. One ideal approach would be to engineer *in vitro* a hybrid material using a single cell source. For that purpose, the scaffold should be able to provide the adequate biochemical cues in order to promote the selective but simultaneous differentiation of both tissues.

In this work, attention was paid primarily to the chondrogenic differentiation by focusing on the development of polymeric systems that provide biomolecules release in order to induce chondrogenic differentiation. For that, different formulations of insulin-loaded chitosan particle aggregated scaffolds were developed as a potential model system for cartilage and osteochondral tissue engineering applications using insulin as a potent bioactive substance known to induce chondrogenic differentiation. The insulin encapsulation efficiency was shown to be high with values of 70.37%±0.8, 84.26%±1.76 and 87.23%±1.58 for loadings of 0.05%, 0.5 and 5%, respectively. The *in vitro* release profiles were assessed in physiological conditions mimicking the cell culture procedures and quantified by Micro-BCA™ protein assay. Different release profiles were obtained that shown to be dependent on the loading amount.

Furthermore, the effect on pre-chondrogenic ATDC5 cells was investigated for periods up to 4 weeks by studying the influence of these release systems on cells morphology, DNA and GAGs content, histology and gene expression of collagen type I and II, Sox-9 and aggrecan assessed by realtime-PCR. When compared to control conditions (unloaded scaffolds cultured with standard chondrogenic-inducing medium), insulin-loaded scaffolds upregulated the Sox-9 and aggrecan expression after 4 weeks of culture.

From the overall results, it is reasonable to conclude that the developed loaded scaffolds when seeded with ATDC5 can provide biochemical cues for chondrogenic differentiation. Among the tested formulations, the higher insulin loaded system (5%) was the most effective in promoting chondrogenic differentiation.

---

* This chapter is based in the following publication:

PB Malafaya, JT Oliveira, RL Reis. The effect of insulin-loaded chitosan particle aggregated scaffolds in chondrogenic differentiation. Biomaterials (2008) submitted

---

1. INTRODUCTION

Osteochondral defects affect both the articular cartilage and the underlying subchondral bone in the joint area and may inflict pain and thereby limited mobility compromising life quality. The requirements for a successful regeneration of an osteochondral defect could potentially be met by using a tissue-engineered osteochondral (bone-cartilage) composite of predefined size and shape, generated *in vitro* using autologous cells. In this sense, various strategies have been reported which result from the use of one or more cell types cultured into single-component or more complex scaffolds in a broad spectrum of compositions and biomechanical properties as recently reviewed [1,2]. The most attractive approach seems to be the design of a suitable scaffold that will provide differentiated and adequate conditions for guiding the growth of the two tissues, satisfying in this way their different biological and functional requirements. Ideally, the final hybrid construct will be accomplished with the same cell source and, in this case, the scaffold must be able to provide the different and appropriate differentiation cues in order to promote an adequate development of both cartilage and bone tissues.

Several works [3-7] can be found reporting the use of different biomolecules in order to promote the cell differentiation either as supplements of culture medium or loaded in the scaffolds. For instances, Martin *et al* [7] have applied specific regulatory molecules to selectively differentiate bone marrow stromal cells into either cartilaginous or bone-like tissues in conjunction with 3D porous polymeric structures. The work shows that using appropriate chondrogenic (dexamethasone, insulin, transforming growth factor (TGF)-β1) or osteogenic (dexamethasone, β-glycerophosphate) medium supplements, the generated extracellular matrix (ECM) was cartilaginous (containing collagen type II and sulfated glycosaminoglycans) or bone-like (containing osteocalcin, osteonectin, and mineralized foci) after 4 weeks of culture [7].

Nevertheless, several studies [4,8,9] address the osteochondral defects regeneration by promoting the repair of articular cartilage that can be further enhanced with controlled release technology approaches. Chondrogenic cells arise from pluripotential mesenchymal stem cells (MSCs) through a series of differentiation pathways, which are being extensively studied. Subsequently, it has been shown that a number of cytokines and transcription factors are involved in chondrocyte maturation and cartilage formation; however, the specific mechanisms regulating these processes remain unclear [10]. Cell culture is a basic experimental approach used in cellular and molecular biological studies of

chondrocytes [10-14]. The manipulation of the culture environment for chondrocytes presents the most feasible mechanism for optimizing cell behaviour and phenotype. Various studies have illustrated the benefits of growth factor integration in establishing and maintaining the phenotype during *in vitro* cultivation [10,12].

Among all the growth factors known to be involved in chondrogenesis, insulin-like growth factor (IGF)-1 is considered to be the main anabolic growth factor of normal cartilage [12], playing an important role in the growth and differentiation of articular cartilage while also promoting chondrogenic differentiation of mesenchymal cells [15]. IGF-1 belongs to the IGF family of peptide hormones including relaxin and insulin and has a single polypeptide homologous to proinsulin [10]. It regulates many cellular functions by activating cell-surface receptors. Insulin has not only a great structural similarity to IGF-1 but also a functional similarity and also elicits marked response in cartilage [13,16]. It has been demonstrated that in cartilage, the insulin receptor is distinct from the IGF-1 receptors, but that both proteins interact with other's receptors although they do so with significantly lower affinity than they display for their own cognate receptors [13].

While several studies [12,14,17] have demonstrated the biological effect of IGF-1 on chondrocytes, the physiological effect of insulin on these cells has not been fully demonstrated. Doing so, is quite complicated by the potential for the combined presence of insulin receptors, IGF-1 receptors and hybrid receptors containing both insulin receptors and IGF-1 receptors components. In addition, insulin and IGF-1 can bind each other's receptors and hybrid receptors can bind both growth factors. However, the biological effects of hybrid receptor activation are similar to those seen in response to IGF-1 receptors activation. The ATDC5 cell line, a well-characterized chondrogenic cell line, is routinely induced to differentiate into chondrocytes by exposing the cells to high concentrations of insulin [18]. This concentration is presumed to exert its effects through the IGF-1 receptors with approximately 100-fold lower affinity that IGF-1 [18,19]. Phornphutkul *et al* [13] have reported that insulin is indeed a physiological regulator of chondrogenesis, and that its actions are also mediated by the insulin receptor. From this study, the authors have arisen to the conclusion that insulin is a potent differentiating agent, but not as potent mitogen as IGF-1 for chondrocytes [13]. In addition, both proliferating and differentiating ATDC5 cells express insulin receptors at the protein level [13].

Insulin is routinely used at high concentration to activate the IGF-1 receptors in standard chondrogenic-inducing medium to induce differentiation [13,19,20]. The observed effects of insulin were shown to be similar to effects of the IGF-1 and are in agreement with the reported binding constants of IGF-1 and insulin at the IGF-1 receptors [19]. Furthermore, investigation of novel systems would benefit from a readily cost model protein such as insulin since the high costs of growth factors often limit a detailed and thorough investigation of new application systems. Its incorporation in the scaffolds as controlled release system appears as an attractive strategy since it will further allow for selective differentiation required for osteochondral tissue engineering.

Since active biomolecules are normally used as medium supplements [7] or administrated together at implantation site [21], its incorporation in the scaffolds as controlled release systems has become a commonly used strategy [4,22,23]. This is due to the fact that a single dose application intraoperatively cannot guarantee a prolonged local protein concentration in order to achieve permanent stimuli on tissue differentiation, as demonstrated by Gotterbarm *et al* [21]. They observed that additional local deposition of liquid growth factors improved the cartilage repair tissue quality at 12 weeks but had not significantly influenced the outcome at 52 weeks. Therefore, release technologies are useful approaches to ensure local release of growth factors over a certain period of time and are attractive alternatives to further improve the quality of the cartilage repair tissue.

For most tissue engineering applications, a scaffold material is required in order to provide not only a temporary three-dimensional framework to form the designed tissues, but also space filling and the possibility of acting as a carrier for controlled release of signal molecules. From the variety of materials that were already investigated, natural materials appear as key candidates due to their properties [23-26]. Among them, chitosan is being extensively studied [9,27-29] namely for cartilage tissue engineering due to its structural similarity with various glycosaminoglycans (GAGs) found in articular cartilage making it an elite scaffolding material for this application. Chitosan structurally resembles GAGs consisting of long chain, unbranched, repeating disaccharide units, regarded to play a key role in regulating the expression of the chondrocytic phenotype and in supporting chondrogenesis *in vitro* as well as *in vivo* [30]. The cationic nature of chitosan also allows for electrostatic interactions with anionic GAGs and proteoglycans distributed widely throughout the body and other negatively charged species [31]. This property is one of the important elements for tissue engineering applications because numbers of cytokines/growth factors are known to be bound and modulated by GAG including heparin

and heparan sulfate [28]. Furthermore, it has been applied as a controlled release system mostly for TGF-β1 in cartilage tissue engineering [30-32]. Chitosan has adequate properties such as biocompatibility, biodegradability, antibacterial, and wound-healing activity [28]. It is a promising candidate owing to their porous structure, gel forming properties, ease of chemical modification and high affinity to *in vivo* macromolecules.

The present work describes the development and characterization of insulin-loaded chitosan particle aggregated scaffolds as controlled release systems for chondrogenic differentiation to be further applied in osteochondral tissue engineering. The *in vitro* assessment of the release profiles of the different formulations was carried out in physiological conditions mimicking the cell culture procedures. Furthermore, the effect on pre-chondrogenic ATDC5 cells was investigated for periods of 2 and 4 weeks by studying the influence of these controlled release systems on cells morphology, DNA and GAGs content, histology and gene expression of collagen type I and II, Sox-9 and aggrecan assessed by realtime-PCR.

2. MATERIALS AND METHODS

2.1. SCAFFOLDS PRODUCTION

The scaffolds were produced as described elsewhere [27]. Briefly, chitosan (medium molecular weight and of deacetylation degree ≈85%) was grinded and dissolved overnight in acetic acid (1%v/v) to obtain a chitosan solution (2%wt). After complete dissolution, the chitosan solution was filtered. Unless otherwise stated, all chemicals were bought from Sigma-Aldrich and used as-received. For preparation of insulin-loaded chitosan scaffolds, insulin (from bovine pancreas with molecular weight ~5800 Da) solutions were prepared in HCl (0.1M) for distinct theoretical protein loadings. The protein solution was mixed with the chitosan solution in order to obtain a homogeneous distribution. Insulin theoretical loadings were 0.05, 0.5 and 5%wt relative to chitosan for each formulation. The prepared solutions were extruded through a syringe at a constant rate (10 ml/h) to form chitosan droplets into a NaOH (1M) precipitation bath where particles with regular diameter were formed. The chitosan particles were quickly washed with distilled water until pH 7. The particles were then placed into moulds and left to dry

in an oven at 60ºC for 3 days. Scaffolds with 3 mm height and 5 mm diameter cylindrical shape were obtained.

2.2. INSULIN-LOADED SYSTEMS CHARACTERIZATION:

2.2.1. Protein loading and encapsulation efficiency

Protein loading and encapsulation efficiency were calculated by an indirect procedure. After the loaded-particles preparation (n=3) as described previously, particles were separated from the precipitation medium by filtration and the aqueous phase was sampled for insulin quantification. Non-loaded scaffolds were used as control. The particles were left to dry in a mould at 60ºC and weighed. The non-loaded free insulin was determined by Micro-BCA™ (Micro BCA™ Protein Assay Kit 23235, Pierce). This assay combines the well-known reduction of Cu^{2+} to Cu^{1+} by protein in an alkaline medium with the highly sensitive and selective colorimetric detection of the cuprous cation (Cu^{1+}) by bicinchoninic acid.

The quantification procedure was performed according to the supplier instructions. Briefly, 150 µl of each of standards, controls and samples were placed in triplicate in a 96-well microplate with 150 µl of working reagent supplied in the kit was added to each well. The plate was then mixed thoroughly on a plate shaker for 30 seconds. The plate was covered and incubated at 37ºC for 2 hours, cooled to room temperature and the absorbance was measured at 562nm on a microplate reader (Synergy HT, BioTek). The readings were then subtracted of the control (non-loaded scaffolds) and analysed with respective software (KC4 Microplate Data Analysis Software, BioTek). A standard-curve was then plotted with different insulin concentrations (0, 0.5, 1, 2.5, 5, 10, 20, 40, 200 µg/ml) to determine the insulin concentration of each unknown sample. Samples dilutions were used when necessary. Protein loading was defined as the mass of protein per unit mass of particles as shown in the following equation 1 and the encapsulation efficiency is calculated according equation 2.

→

$$Protein\ Loading\ (\%) = \frac{m_l - m_r}{m_p} * 100 \qquad (1)$$

and

$$Encapsulation\ Efficiency\ (\%) = \frac{m_l - m_r}{m_l} * 100 \qquad (2)$$

where m_l corresponds to the initially loaded weight of protein, m_r is the weight of protein in the precipitation solution and m_p is the weight of the dry particles prior to *in vitro* release studies.

2.2.2. *In vitro* insulin release studies

In vitro release studies were carried out mimicking the cell culture conditions described in the following section. Each insulin-loaded scaffold formulation was placed in a 24-well microplate with 1.5 ml of phosphate buffer solution (PBS). The *in vitro* release studies were carried out in triplicate at physiological conditions (pH 7.4 and 37ºC). Non-loaded scaffolds were used as controls. At pre-determined periods and according to the medium replacement in cell culture studies, aliquots (1 ml) of the supernatant were withdrawn and frozen at -20ºC for further protein quantification. The release medium was totally replaced by fresh PBS mimicking cell culture conditions for total medium replacement. The protein quantification was performed using Micro-BCA (Micro BCA™ Protein Assay Kit 23235, Pierce) according to the supplier instructions as described previously.

2.2.3. Fourier-transform infrared spectroscopy with attenuated total reflectance

The surface chemical analysis was also performed by Fourier-Transform Infrared Spectroscopy with attenuated total reflectance (FTIR-ATR) spectroscopy. Insulin-loaded scaffolds were characterized before and after the *in vitro* release studies. The analysis was carried out using an IRPrestige 21 FTIR spectrophotometer with attenuated total reflectance (ATR) device from Shimadzu. Spectra were recorded with a resolution of 4 cm^{-1} and averaged over 36 scans.

2.3. ATDC5 CELLS CULTURE IN INSULIN-LOADED SCAFFOLDS

2.3.1. Cell culture

Cells used in these experiments were a pre-chondrogenic murine mesenchymal cell line (ATDC5) purchased from the European Collection of Cell Cultures (ECACC) which differentiates into mature chondrocytes in the presence of insulin [33]. Cells were plated into tissue culture flasks and incubated at 37ºC in a humidified atmosphere of 5%CO_2 in air for expansion. ATDC5 cells were grown as monolayer cultures in a culture medium consisting of 1:1 mixture of Dulbecco's Modified Eagle's Medium and Ham's F-12 Nutrient Mixture with 15 mM HEPES, sodium bicarbonate, 10,000 units/ml penicillin/10,000 µg/ml streptomycin, 0.365 g/L L-glutamine and 5% (v/v) foetal bovine serum (FBS Heat Inactivated, Biochrom) (DMEM/F12).

When the adequate cell number was obtained, cells at passage 8 were trypsinized, centrifuged and ressuspended in cell culture medium. For the control group with non-loaded scaffolds, standard chondrogenic medium was used consisting in DMEM/F12 supplemented with 10µg/ml of insulin (DMEM/F12/INS). Cells were seeded at a density of 100,000 cells/scaffold under static conditions using for this purpose aliquots of 100 µl loaded onto the top of the scaffolds that had been previously placed in 24-well non-adherent tissue culture plates. Two hours after seeding, 1.5 ml of respective cell culture medium according to Table 1 was added to each well and the cell seeded scaffolds were cultured for 2 and 4 weeks, in a humidified atmosphere at 37ºC, containing 5% CO_2. The culture medium was changed every 3 to 4 days until the end of experiments.

Table 1. Scaffolds formulations and respective cell culture medium.

SCAFFOLDS	FORMULATION	CULTURE MEDIUM
C	Non-loaded (control group)	DMEM/F12/INS
0.05	Loaded with 0.05% (wt/wt) insulin	DMEM/F12
0.5	Loaded with 0.5% (wt/wt) insulin	DMEM/F12
5	Loaded with 5% (wt/wt) insulin	DMEM/F12

Abbreviations: DMEM - Dulbecco's Modified Eagle's Medium; F12 - Ham's F-12 Nutrient Mixture with 15 mM HEPES, INS - DMEM/F12 supplemented with 10µg/ml of insulin.

2.3.2. Cell adhesion and morphology

Cell adhesion, morphology and average distribution were observed by scanning electron microscopy (SEM) analysis. Briefly, the cell-scaffold constructs were washed in PBS and fixed in 2.5% glutaraldehyde (in PBS). The constructs were then rinsed in PBS again, and subjected to 15 minutes immersion cycles into series of increasing ethanol concentrations (30, 50, 70, 90, 100% ethanol), each to dehydrate the samples. The samples were finally subjected to critical point drying by double immersion into HMDS (hexamethyldisilazane reagent) for 15 minutes each, air dried and sputter coated with gold (JEOL JFC-1100) and analyzed with a Leica Cambridge S360 scanning electron microscope.

2.3.3. DNA quantification

DNA quantification was carried out using PicoGreen® dsDNA Quantitation reagent (Invitrogen, Barcelona, Spain) according to the supplier protocol. Briefly, the cell-scaffolds systems were collected at pre-defined time periods, placed into eppendorf tubes with 1 ml ultrapure water, and kept at 37ºC for 1 hour. They were then subjected to 2-3 cycles of freezing-defrosting to assure that the entire DNA would be in solution. Standards of double stranded DNA were prepared using ultrapure water with the following concentrations: 0, 0.2, 0.5, 1 and 2 µg/ml. Chitosan scaffolds without cells were used as controls. Standards, controls and samples were placed in 96-well plates in triplicate according to kit instructions where each single well contained 200 µl of total mixture solution. The plates were submitted to a 10 minutes incubation cycle in the dark. Emitted fluorescence was read using a microplate reader (Synergy HT, BioTek) and the data was recorded for analysis with the software (KC4 Microplate Data Analysis Software, BioTek) (at excitation of 485/20 nm and emission of 528/20 nm).

2.3.4. Glycosaminoglycans (GAGs) quantification

Proteoglycans amount was determined by measuring the level of sulfated glcosaminoglycans (GAGs) using the dimethylmethylene blue metachromatic assay. GAG levels in solution can be quantified using the basic dye, 1,9-dimethylmethylene blue (DMB) which binds to glycosaminoglycans generating a metachromatic shift that peaks at A525-530 that can be measured spectrophotometrically.

Briefly, the constructs (n=3) were immersed in a digestion solution with papain and N-acetyl cysteine and incubated at 60ºC overnight. After the digestion was completed, the tubes were centrifuged at 13,000 rpm for 10 minutes and the supernatant was collected. Chondroitin sulfate standard solutions were prepared with different concentrations (0, 2.5, 5, 10, 15, 20, 25, 30, 35, 40, 45 and 50 μg/ml) to establish the calibration curve for unknown samples quantification. Chitosan scaffolds without cells were used as controls. Standards, controls and samples (20 μl) were placed in triplicate in a 96 well plate and then 250 μl of DMB solution was added to each well. The optical density was measured at 530 nm using a microplate reader (Synergy HT, BioTek) and the data analysed with the software (KC4 Microplate Data Analysis Software, BioTek).

2.3.5. Histological analysis

Concerning the histological analysis, hematoxylin-eosin (H&E) and toluidine blue stainings were performed on 10 μm thickness sections of cells-scaffolds constructs (n=3) collected at different periods of culture. The samples were fixated by immersion for 30 minutes in glutaraldehyde 2.5%(v/v) at 4ºC, and washed in PBS. Histological processing was performed using Tecnhovit 7100® (Heraeus Kulzer GmbH) according to the supplier protocol and sections were sliced using a motorized rotary microtome (Leica RM2155, Leica Microsystems GmbH). H&E staining was performed using an automatic processor according to in-house methodology (Leica TP1020-1, Leica MicroSystems GmbH) and toluidine blue staining was performed as follows. Briefly, sections were hydrated in distilled water and stained in 1% toluidine blue working solution for 2-3 minutes. Afterwards, they were washed 3 times in distilled water and quickly dehydrated through 95% ethanol and 100% alcohol. Sections were then cleared in Histoclear® (National Diagnostics) and mounted using Microscopy Entellan® (Merck) for observation.

2.3.6. Evaluation of gene expression by realtime-PCR

Samples were collected at the defined time periods, quickly frozen in liquid nitrogen, and stored at −80°C until further analysis. RNA was extracted using TRIzol® (Invitrogen, Barcelona, Spain) according to the supplier protocol. Briefly, samples of each condition (n=2) were grinded and mechanically

homogenized with a mostar and pestle in TRIzol® reagent. Afterwards, chloroform was added and the samples centrifuged to establish a three-phase composition in the tube. The aqueous phase was collected and put in a new tube where isopropanol was added. The samples were once again centrifuged, the supernatant discarded and the pellet washed with 75% ethanol. The samples were again centrifuged, let to air-dry, and suspended in ultrapure water for posterior analysis.

The amount of isolated RNA and A260/280 ratio was determined using Nanodrop ND-1000 Spectrophotometer (NanoDrop Technologies). After these determinations, 1 µg of RNA of each sample was reverse transcribed into cDNA using the IScriptTM cDNA synthesis kit (Biorad, California, USA) in a MJ MiniTM Personal Thermal Cycler (Biorad, California, USA). Cartilage related markers were chosen to evaluate the chondrogenic phenotype of the cultured systems. These included collagen type I, collagen type II, Sox-9 and aggrecan, using GAPDH as the housekeeping gene for normalization. The expression of each gene was normalized to the GAPDH value in that sample. All the primer sequences were generated using Primer3 software and acquired from MWG Biotech. More details can be found in Table 2. Realtime-PCR was performed using SYBR Green IQTM Supermix (Biorad, California, USA) to detect amplification variations in a MJ MiniTM Personal Thermal Cycler (Biorad, California, USA) machine. The analysis of the results was performed with MJ Opticon Monitor 3.1 software (Biorad, California, USA).

Table 2. Primers used for realtime-PCR evaluation of ATDC-5 gene expression.

GENE	ACCESSION	LEFT PRIMER	RIGHT PRIMER
Collagen type I	NM_007742	GAGCGGAGAGTACTGGATCG	GCTTCTTTTCCTTGGGGTTC
Collagen type II	NM_001113515	GCCAAGACCTGAAACTCTGC	GCCATAGCTGAAGTGGAAGC
Sox-9	NM_011448	AGCTCACCAGACCCTGAGAA	TCCCAGCAATCGTTACCTTC
Aggrecan	NM_007424	TGGCTTCTGGAGACAGGACT	TTCTGCTGTCTGGGTCTCCT
GAPDH	NM_008084	AACTTTGGCATTGTGGAAGG	ACACATTGGGGGTAGGAACA

2.4. STATISTICAL ANALYSIS

When applicable, the statistical analysis of values obtained with the several characterization techniques was carried out using Student's two-tailed t-test with a confidence level of 99.5%. All statistical

calculations were performed with Analysis ToolPak software. ρ-Values below 0.05 were considered statistically significant.

3. RESULTS

3.1. INSULIN-LOADED CHITOSAN SCAFFOLDS

3.1.1. Protein loading and encapsulation efficiency

The developed insulin-loaded scaffolds were characterized by assessing the encapsulation efficiency and protein loading as shown in Figure 1. Insulin loadings of the scaffolds were 0.0297% ± 0.0001, 0.3843% ± 0.0118, and 3.9911% ± 0.1159, as determined by Micro-BCA™, and correlated well with the intended and designed insulin theoretical loadings of 0.05%, 0.5%, and 5%, respectively. The obtained encapsulation efficiencies were high with values of 70.37% ± 0.80, 84.26% ± 1.76 and 87.23% ± 1.58 for insulin loadings of 0.05%, 0.5%, and 5%, respectively.

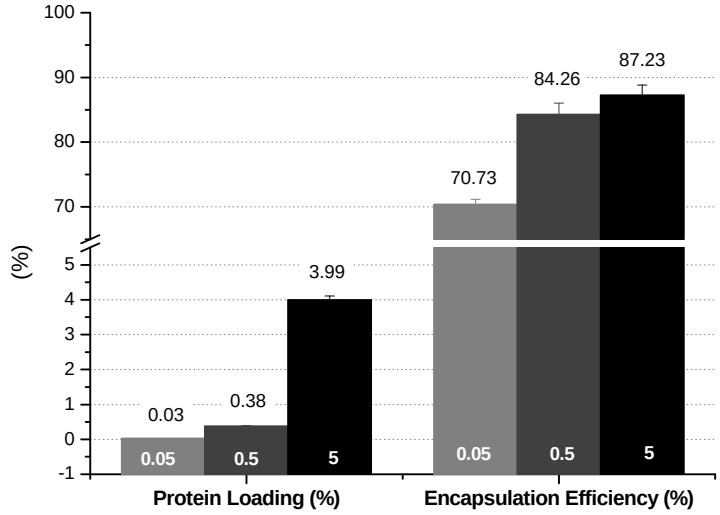

Figure 1. Protein loading and encapsulation efficiency of chitosan particle aggregated scaffolds loaded with 0.05, 0.5 and 5% of insulin. Numbers in white represent the theoretical loading value. Data are expressed as mean ± standard deviation with n=3.

3.1.2. *IN VITRO* RELEASE STUDIES

The release of insulin from chitosan particle aggregated scaffolds under physiological conditions was investigated with total medium replacement at the same intervals of cell culture medium replacement (3 or 4 days). The assays were performed in this way in order to mimic exactly the cell culture conditions. The obtained release profiles represented in Figure 2 were characterized by an initial rapid release within the first 4 days with values around 80% and 60% of released insulin for 0.05% and 0.5% formulations, respectively. This burst effect was less pronounced for the 5% insulin-loaded scaffolds with a 40% release in the same initial immersion period. The cumulative release profile shown to be dependent on the initial scaffolds loading, being the release rate slower for higher initial insulin concentrations. For the 0.05% formulation, the remaining 20% insulin was almost totally released until day 11. Furthermore, the release behaviour of the 0.5% appeared similar since more than 60% of the insulin was released within the first 3 days and the remaining 40% insulin was almost released up within 18 days. When insulin content increased to 5%, the release rate decreased and only around 85% insulin was released until the end of the experiment at 28 days, most likely due to its high initial concentration.

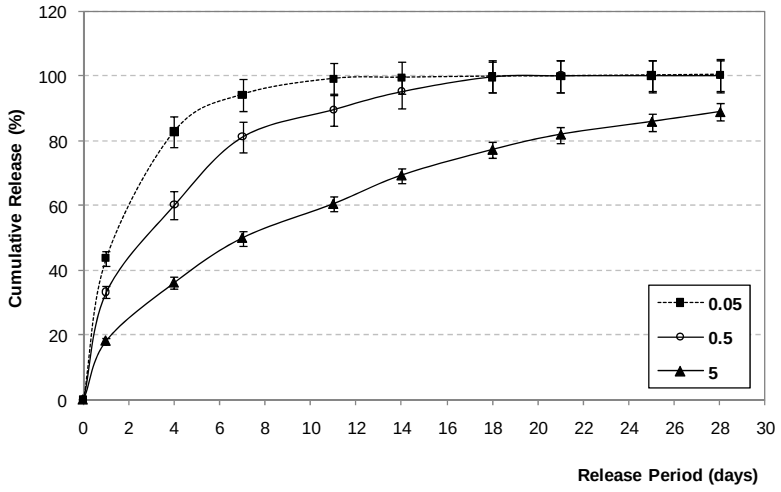

Figure 2. Cumulative insulin release profile for the different formulations of insulin-loaded chitosan scaffolds after immersion in PBS for periods up to 28 days (4 weeks) with total medium replacement at determined time points mimicking the cell culture conditions. Data are expressed as mean ± standard deviation with n=3.

The insulin release was also plotted considering the insulin concentrations in the release medium as represented in Figure 3 which is an important data, considering the further cell culture studies. The insulin concentrations released to the medium were, as expected, well correlated with the initial loading

in the respective order of magnitude. The insulin released to the medium was below 1 μg/ml after day 11 and day 21 for 0.05% and 0.5% formulations, respectively. After these times periods and for these formulations, lower amounts of insulin were released and were always below 0.1 μg/ml until the end of the experiments. In contrast, for higher initial insulin loading, protein concentrations were kept always above 80 μg/ml even at the last day of these studies (day 28).

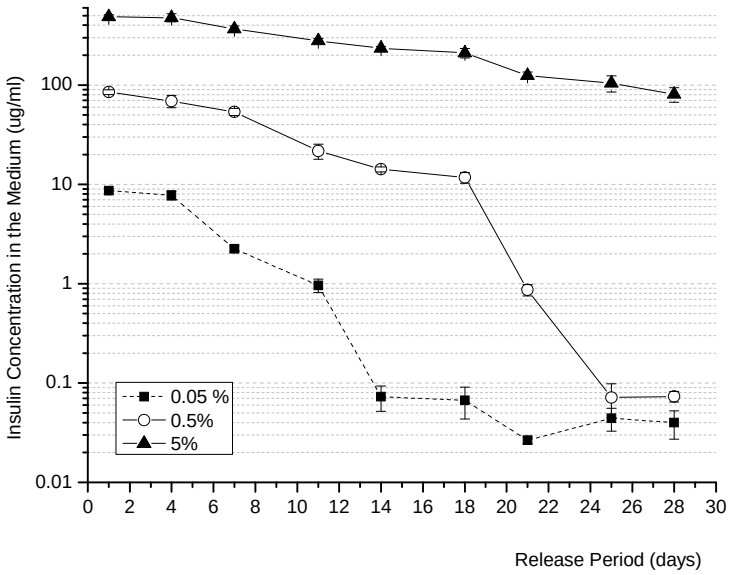

Figure 3. Insulin concentration in the release medium for chitosan loaded scaffolds with 0.05%, 0.5% and 5% of insulin immersed in PBS for periods up to 28 days (4 weeks) with total medium replacement every 3 or 4 days mimicking the cell culture conditions. Data are expressed as mean ± standard deviation with n=3.

3.1.3. FTIR-ATR

The incorporation of insulin into scaffolds was also investigated by FTIR-ATR analysis before and after the *in vitro* release studies of insulin-loaded scaffolds. The obtained spectra with the representative signals assigned are represented in Figure 4 where insulin and non-loaded scaffolds were also plotted as controls. The characteristic peaks of chitosan can be observed. The broad band at 3400-3200 cm^{-1} (§) is attributed to the stretching vibration of hydroxyl groups (-OH), primary (-NH_2) and secondary amide (-NH-) [34]. The peaks appearing at 1650 cm^{-1} (*) can be assigned to the primary amide NH_2 bending and at 1550 cm^{-1} (+) to the secondary amide N-H bending. The bands at 1000-1200 cm^{-1} (¥) are attributed to the saccharide structure of chitosan [35]. Concerning insulin, the main representative signals are also observed and revealed two sharp shoulders on the absorption bands in the primary and

secondary amide bending at 1650 cm^{-1} (*) and 1550 cm^{-1} (+), respectively, which are characteristic of protein spectra [36]. In the FTIR spectra of insulin-loaded scaffolds, no band shifts could be detected due to the overlapping of the main characteristics peaks.

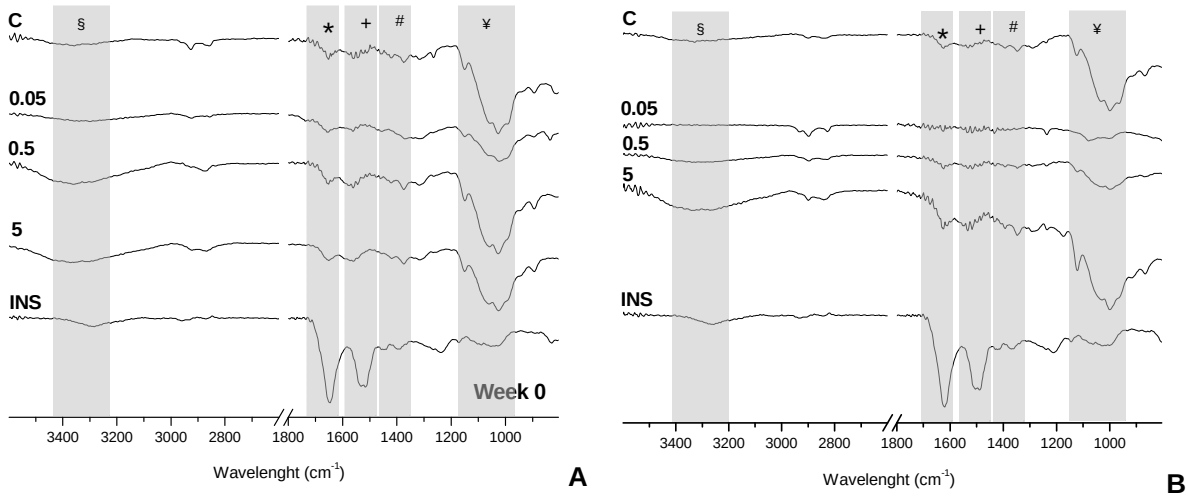

Figure 4. FTIR spectra of insulin (INS) and scaffolds loaded with 0% (C), 0.05%, 0.5% and 5% of insulin before (A) and after 4 weeks (B) of *in vitro* release in PBS at physiological conditions. The scale was adjusted for better observation in the most representative regions.

3.2. BIOLOGICAL ASSESSMENT OF ATDC5 CHONDROGENIC DIFFERENTIATION BY INSULIN-LOADED SCAFFOLDS

3.2.1. Cell Morphology

In order to study the effect of insulin-loaded scaffolds on chondrogenic differentiation, the performance of the scaffolds was investigated in a long-term cell culture with a pre-chondrogenic cell line (ATDC5) for up to four weeks. This study allowed also to assess the bioactivity of incorporated and released insulin from the scaffolds. The results were always compared with standard culture conditions, i.e., unloaded scaffolds cultured with standard chondrogenic medium. Cells morphology was qualitatively evaluated by SEM after 2 and 4 weeks of culture as shown in Figure 5. After 2 weeks of culture, cells had adhered to the chitosan particle aggregated scaffolds. Chondrocyte cells seeded on insulin-loaded chitosan scaffolds proliferated, possessing a rounded typical chondrocytic morphology which is an indication of chondrocytes differentiation (Figures 5.C, 5.E and 5.G). Cell condensation and formation of extracellular matrix (ECM) was detected as well, since it is also possible to observe the formation of collagen fibrils [37]. In contrast, for the control group, cells presented a flattened and spread morphology still showing a fibroblast like phenotype with some cytoplasmic extensions (Figure 5.A). However, for 4 weeks of

culture, in all the studied formulations, the cells maintained a rounded shape morphology and remained aggregated, being this more clear for the 5% formulation (Figures 5.B, 5.D, 5.F and 5.H). Nevertheless, it was noticeable that, for 0.05% and 0.5% insulin loading, the cell distribution over the scaffolds was lower. The formation of extracellular matrix (ECM) including collagen fibrils was also detected being more evident for the control and for the 5% insulin formulation where the cells clustering is also visible (Figure 5.B and 5.H).

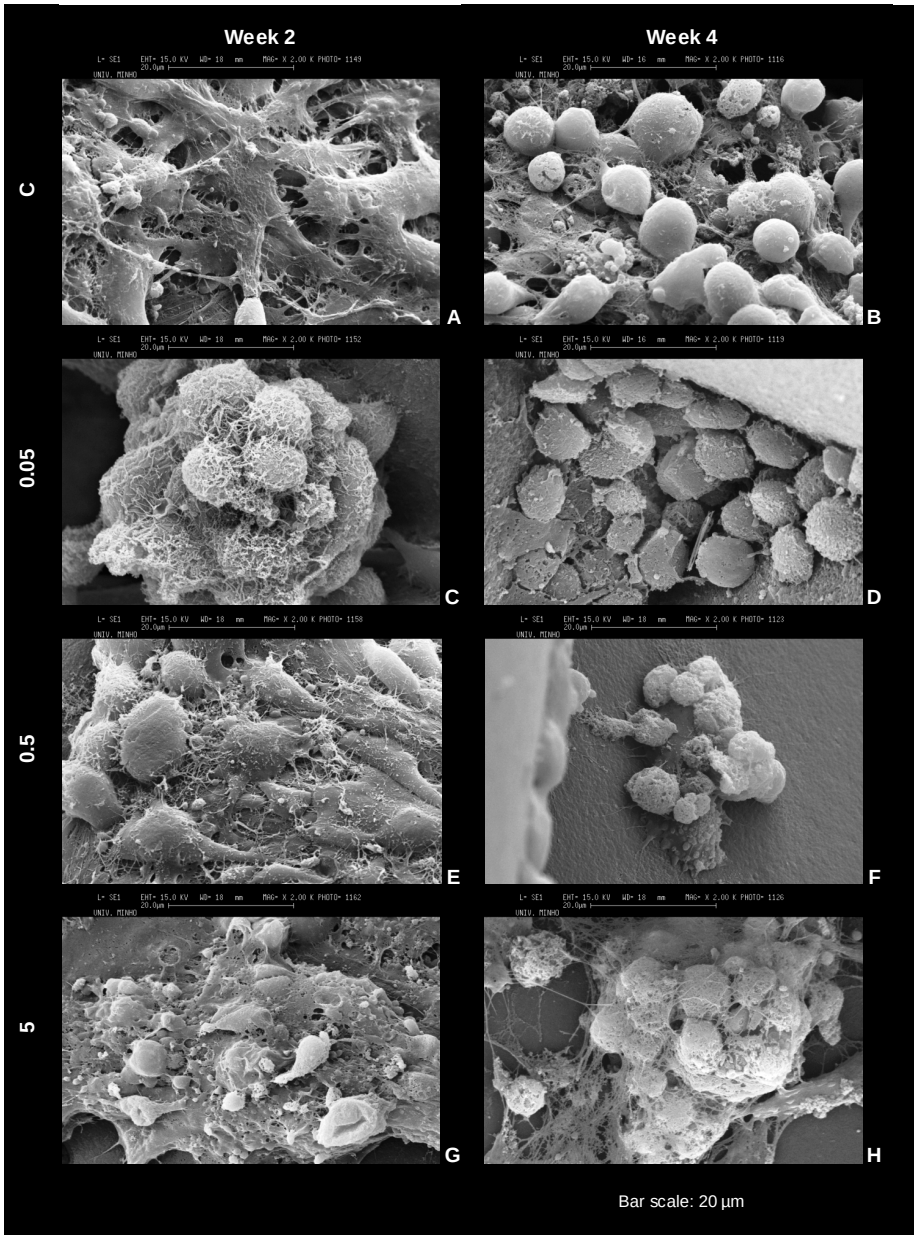

Figure 5. Scanning electron microscopy microphotographs of chitosan scaffolds loaded with 0% (A, B), 0.05% (C, D), 0.5% (E, F) and 5% (G, H) of insulin seeded with ATDC5 cells and cultured for 2 weeks (A, C, E, G) and 4 weeks (A, D, F, H). Magnification: 2000x.

3.2.2. Cell Proliferation

For all the developed formulations, cell proliferation was investigated by DNA quantification after 2 and 4 weeks and the obtained results are plotted in Figure 6. After 2 weeks in culture, the total amount of DNA in each group was 0.042 ± 0.029 µg/sample in the control group, 0.026 ± 0.002 µg/sample in the 0.05% group, 0.063 ± 0.002 µg/sample in the 0.5% group, and 0.091 ± 0.008 µg/sample in the 5% group. The amount of DNA presented a clear increase trend for higher insulin loadings with the higher insulin-loading scaffolds (5%) being significantly higher than that in the other formulations and the control. This increasing tendency for higher values of insulin loading was maintained after 4 weeks with all DNA values statistically different, except between 0.5% and 0.05% formulation. At 4 weeks, the obtained values were 0.533 ± 0.033 µg/sample for the control, 0.029 ± 0.007 µg/sample for 0.05%, 0.040 ± 0.011 µg/sample for 0.5% and 0.084 ± 0.002 µg/sample for the 5%insulin loading group. At this time period, there was a clear significant increase of the DNA content for the control condition.

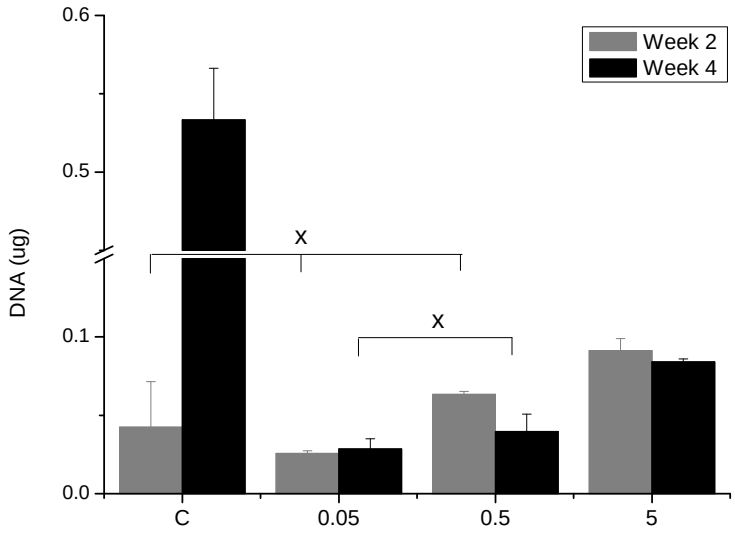

Figure 6. DNA quantification for chitosan scaffolds (C) loaded with 0.05%, 0.5% and 5% of insulin cultured with ATDC5 cells for 2 and 4 weeks. The indicated conditions (x) were found to be not statistically significant different. Statistically significant difference was found between the other conditions ($\rho<0.05$). Scale was adjusted for better observation of tendencies.

3.2.3. GAGs quantification

Glycosaminoglycans (GAGs) are important components of proteoglycans and are typically present in the cartilaginous extracellular matrix (ECM) being aggrecan the most relevant in terms of mechanical functionality. GAGs content was determined to assess the formation of newly formed ECM and thus if occur the differentiation of ATDC5 into chondrocytes in these insulin-loaded cell-scaffold constructs, at weeks 2 and 4 (Figure 7). The GAGs content was calculated per DNA content of each formulation. The biochemical analysis demonstrated that the content of GAGs per DNA increased from week 2 to 4 for the higher insulin initial loadings (0.5% and 5%). Comparing the results for 2 weeks of culture, one can say that there is a decreasing tendency with increasing insulin concentrations, in spite of no statistically difference found when compared to that of the control. In contrast, for 4 weeks this tendency is inverted with higher GAGs contents for higher insulin concentrations. The values for GAGs contents were 54.22 ± 5.62 μg/μg DNA for control group, 37.08 ± 25.08 μg/μg DNA for 0.05%, 287.57 ± 86.04 μg/μg DNA for 0.5% and 188.99 ± 22.55 μg/μg DNA for the 5% formulation after 4 weeks of culture with ATDC5 cells.

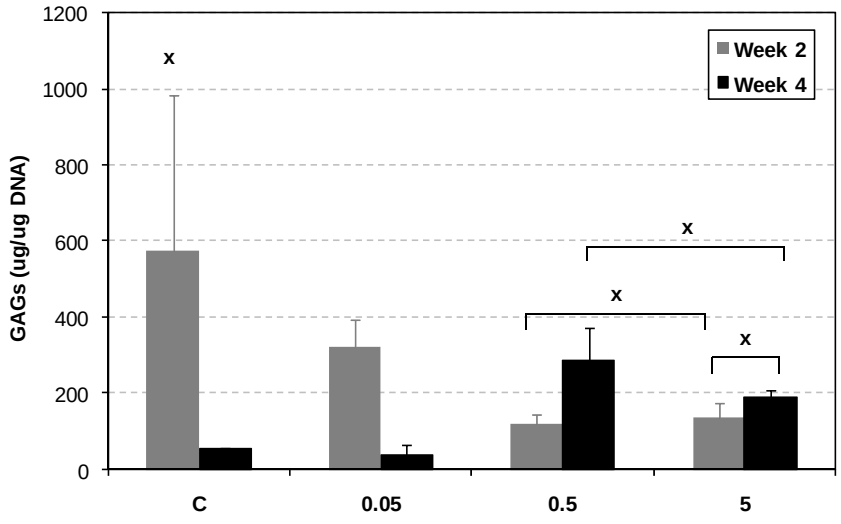

Figure 7. GAGs quantification for chitosan scaffolds (C) loaded with 0.05%, 0.5% and 5% of insulin cultured with ATDC5 cells for 2 and 4 weeks. The indicated conditions (x) were found to be not statistically significant different. Statistically significant difference was found between the other conditions ($p<0.05$).

3.2.4. Histological examination

Chondrocytes were seeded onto loaded and unloaded chitosan scaffolds and the morphologies were observed histologically upon hematoxylin-eosin (H&E) and toluidine blue staining of sections from the bulk of the scaffolds. Representative sections obtained after 2 and 4 weeks of culture are shown in Figure 8 and 9 for the standard condition and higher insulin-loading formulation (5%). Histological examination of the sections indicated that the chondrocytes were evenly distributed throughout the scaffold and that the chondrocytes were able to infiltrate, adhere and proliferate into the inner pores of the scaffolds. Analysing the sections stained with H&E (Figure 8), one can say that cells seeded in the insulin-loaded scaffolds have similar morphology when compared to the control condition after 2 and 4 weeks. The cell-constructs were composed of viable chondrocytes as detected by the H&E-positive staining. The clustering of chondrocytes was evident after 4 weeks, being more clear for 5% insulin loading.

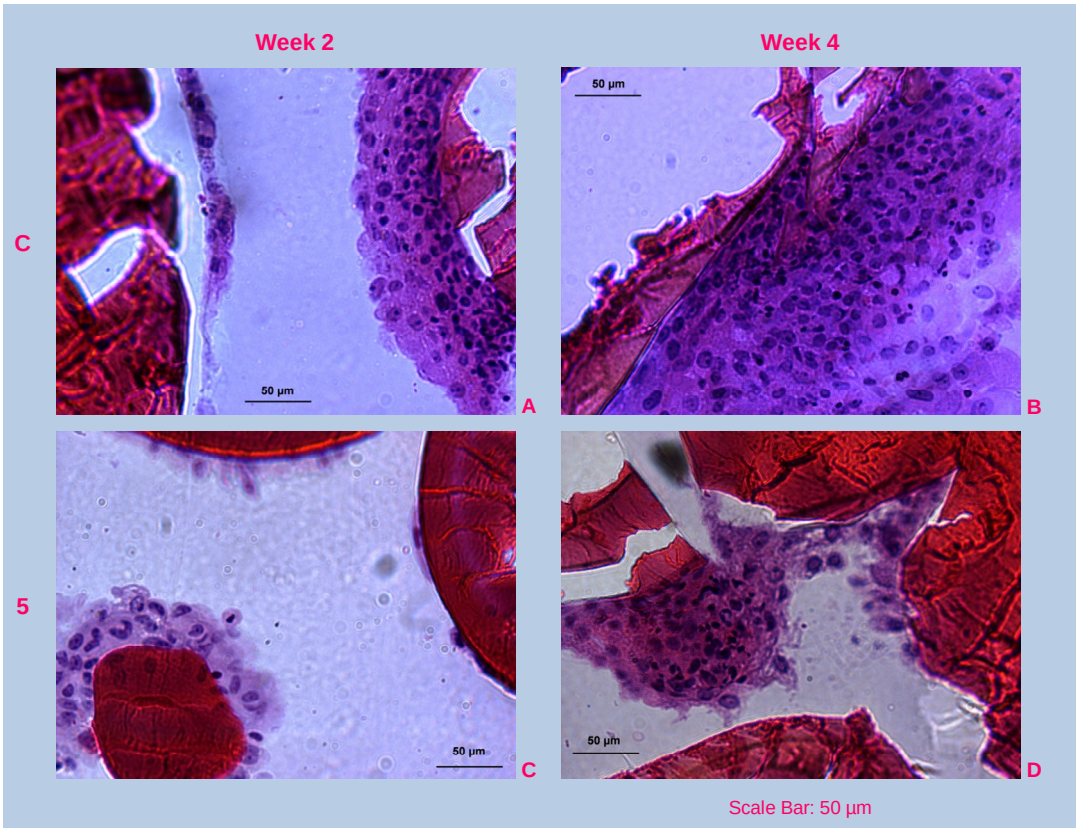

Figure 8. Representative histological sections stained with H&E of chitosan-based scaffolds (A, B) and chitosan-based scaffolds loaded with 5% insulin (C, D) after 2 (A, C) and 4 weeks (B, D) of culture with ATDC5 cells. Magnification: 400x.

Toluidine blue staining showed evidence of viable chondrocytes embedded in a newly synthesized ECM as shown in Figure 9. The histological sections stained mainly metachromatic (purple) indicative of sulphated proteoglycan deposition at 4 weeks of culture. Some orthochromatic areas (blue) were also identified, but these were found primarily at 2 weeks of culture [31]. The central matrix stained positively with toluidine blue, thereby indicating the presence of a cartilaginous matrix composed of proteoglycans. The formation of cell aggregates is once more evident with characteristic lacunae of differentiated chondrocytes that were invested with intense metachromatic matrix as shown in Figure 9.B and 9.D, suggesting the active deposition of proteoglycan after 4 weeks.

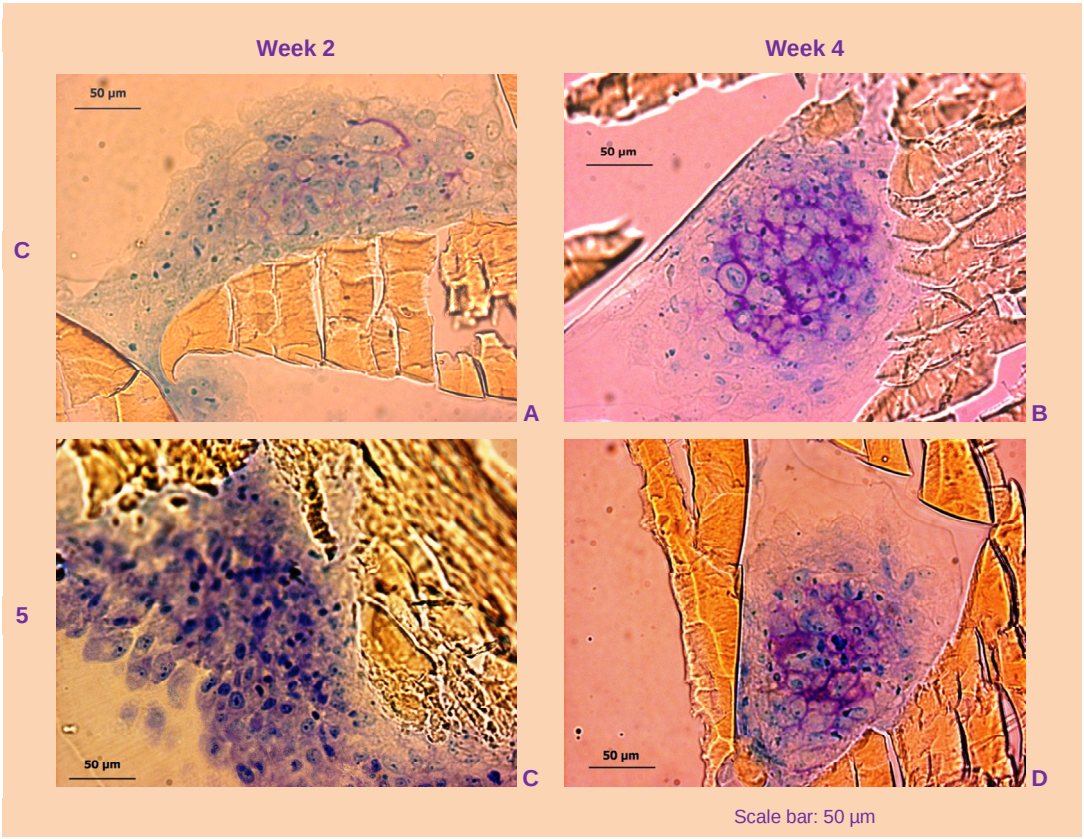

Figure 9. Representative histological sections stained with toluidine blue of chitosan-based scaffolds (A,B) and chitosan-based scaffolds loaded with 5% insulin (C,D) after 2 (A,C) and 4 weeks (B,D) of culture with ATDC5 cells. Magnification: 400x.

→

3.2.5. Gene expression

The gene expression of type I collagen, type II collagen, Sox-9 and aggrecan in the loaded constructs after 4 weeks of culture with ATDC5 cells was examined by realtime-PCR and normalized for the control condition (ratio=1). The obtained normalized expression ratios for each gene are shown in Figure 10. The cells in the constructs expressed genes encoding collagen type I, Sox-9 and aggrecan after 4 weeks of culture, except for Sox-9 that was not detected for the 0.05% insulin-loaded formulation. No expression of collagen type II was identified in all the groups, including the standard condition. The normalized ratio of Sox-9 gene expression of the insulin loaded scaffolds with 5% group significantly increased, as compared to the standard condition. The same tendency is observed for aggrecan expression that is also increasing for the higher insulin loading constructs with a 9.6-fold higher ratio. Concerning the values for type I collagen expression, there is no statistically significant difference between the control and the 5% formulation.

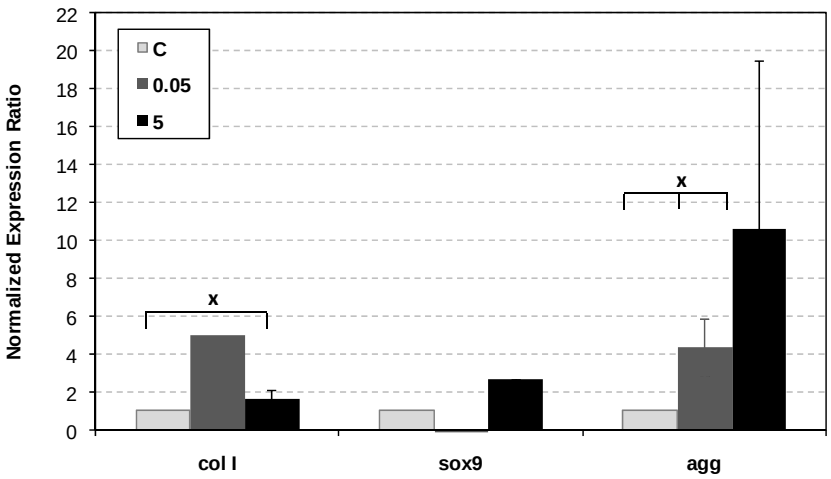

Figure 10. Normalized gene expression ratio of collagen type I (col I), Sox-9 (sox9) and aggrecan (agg) assessed by realtime-PCR of chitosan-based scaffolds loaded with 0% (C), 0.05% and 5% of insulin cultured with ATDC5 cells for a 4 weeks period. The ratios were normalized relative to the control (ratio=1, non-loaded scaffolds cultured with chondrogenic medium). The indicated conditions (x) were not statistically significant different. Statistically significant difference was found between the other conditions ($p<0.05$).

→

4. DISCUSSION

4.1. INSULIN-CHITOSAN SYSTEMS CHARACTERIZATION AND *IN VITRO* RELEASE STUDIES

Chondrocytes experience biochemical and mechanical stimulation *in vivo* that are integral to the development and maintenance of cartilage. Growth factors aid in signalling and regulating cartilage development and ECM maintenance. Growth factors are present in serum, synovial fluid or may be stored in the cartilage matrix for immediate release when needed. Among these, IGF-1 is considered to be the main anabolic growth factor of normal cartilage [12,16]. In addition, it is known that insulin has a great structural and functional similarity to IGF-1 and can bind to IGF-1 and insulin receptors with a marked response in cartilage [13,16]. Furthermore, local delivery of biochemical active substances is ideal, since these proteins often have short half-lives and multiple biological effects with potential systemic toxicity.

Investigation of novel experimental application systems for growth factors or other bioactive substances in tissue engineering is often limited by high costs of substances and would benefit from a defined and easily controllable model system, namely using insulin as a differentiation biomolecule since it is a readily available protein. In addition, release technology approaches can further improve the function of active biomolecules, namely in an *in vivo* situation where a single dose application cannot guarantee a prolonged local protein concentration. Furthermore, when aiming at osteochondral applications, systems loaded with different adequate differentiation agents can be assembled in a biphasic construct, allowing for selective but simultaneous differentiation of a single source of stem cells into both chondrogenic and osteogenic pathways.

Having this in mind, the purpose of this work was to incorporate insulin in a chitosan particle aggregated scaffold to aid in cartilage tissue engineering. The future final goal will involve the incorporation of these insulin-systems in osteochondral biphasic constructs in order to selectively but simultaneously differentiate the same cell source into the chondrogenic and osteogenic lineages. For that purpose, insulin was successfully incorporated at different concentrations in chitosan matrices as shown by the obtained high encapsulation efficiencies and protein loadings.

It is known that chitosan is positively charged due to the protonation of the amino groups, and insulin is negatively charged at pH above its isoelectric point. Consequently, electrostatic interactions between both materials can be used as a driving force for insulin incorporation into chitosan matrices [38]. This is one key issue that explains why chitosan has been widely investigated as carrier for insulin delivery for other than tissue engineering applications, such as oral insulin delivery [39,40] or self-assembled polyelectrolyte nanocomplexes for intranasal absorption [38] or oral delivery [41].

The obtained real protein loading values correlated well with the intended insulin theoretical loadings, in spite of the slight insulin loss that can be attributed to the washing procedure required for the particle aggregated scaffolds production. In the same way, the encapsulation efficiencies were also high. These values shown to be dependent on the insulin content, increasing for higher initial insulin concentrations in the scaffolds. The same dependence was observed for the release profiles that correlated well in terms of order of magnitude with the initial insulin loading.

For lower initial insulin contents, there was a burst release on the first days of immersion. Nevertheless, insulin levels in the release medium were above 1 μg/ml until day 11 for 0.05% formulation and day 21 for 0.5%. This burst effect was less evident for the higher insulin-loaded scaffolds that, in general, presented best performance in the biological tests. For the higher initial loading, insulin concentration in the medium was above 80 μg/ml until the end of the experiment. The insulin monomer contains many ionizable groups, due to six amino acid residues capable of attaining a positive charge and 10 amino acid residues capable of attaching a negative charge [42]. These properties are, therefore, possibly responsible for the entrapment of insulin into chitosan matrices due to the electrostatic interaction between the protein and the polyanion that might also favour the retention of insulin within the chitosan matrix [43].

Concerning the FTIR analysis, in the insulin-loaded scaffolds no band shifts could be detected due to the overlapping of the main characteristic peaks of both chitosan and insulin. Nevertheless, it seems that this overlapping resulted in a widening of the primary and secondary amide bending at 1650 cm^{-1} (*) and 1550 cm^{-1} (+) more evident for higher insulin concentrations (5%). This band widening is in agreement with other reported works [44]. In addition, the change of the three small bands at wavenumbers about 1400–1500 cm^{-1} (#) to two bands of insulin was observed. These observations show the possibility of a weak interaction between insulin and chitosan and clear influence of the protein

on final formulation as an entrapped biomolecule. After the 4 weeks *in vitro* release in PBS at physiological conditions, only for the higher insulin loading concentration (5%) it was possible to detect this band widening which is in agreement with the obtained release profiles. At this immersion period, the total release has been already achieved for the 0.05% and 0.5% formulations.

4.2. BIOLOGICAL ASSESSMENT OF ATDC5 CHONDROGENIC DIFFERENTIATION BY INSULIN-LOADED SCAFFOLDS

4.2.1. Cell Morphology

There are several studies [7,19] reporting the use of insulin for cartilage tissue engineering. The most typical approach is obviously the use of insulin as a differentiating agent in the cell culture medium and it is used nowadays as a standard condition in chondrogenic differentiation medium. The group of Göpferich [19,45,46] has been working in different strategies including this standard approach [19], but also going from the incorporation of insulin-loaded microspheres into fibrin hydrogels with encapsulated chondrocytes [46] to the development of lipidic cylinders that are placed together with the seeded scaffolds for insulin controlled release [45]. The reported studies show, in a general way, that insulin is able to promote cartilage formation improving the quality of the cartilaginous constructs, since it increases the collagen content and promotes glycosaminoglycan deposition [45,46]. Nevertheless, to the best of our knowledge this is the first study with direct insulin encapsulation into tissue engineering scaffolds.

In the present study, the bioactivity of the released insulin as well as its influence on chondrogenic differentiation was studied with long term culture of ATDC5 cells for a period up to 28 days. ATDC5 cells are an example of a prechondrogenic stem cell line and reproduce the differentiation stages of chondrocytes [10]. In monolayer culture and only in presence of insulin (or other chondrogenic differentiation agent), ATDC5 cells retain the properties of chondroprogenitor cells that are at the early phase of differentiation and form cartilage nodules when cells reach condensation [18]. The cartilage nodules enlarge while chondrocytes proliferate, for about 2 weeks in culture. The ATDC5 cell line is the first example to display the entire spectrum of chondrocyte differentiation [10].

Our results showed that ATDC5 cells were able to attach and were dispersed throughout the scaffolds after 2 weeks of culture. Cellular condensation was observed for the insulin-loaded scaffolds, which is one of the key events in chondrogenesis [47]. The capability of chondrocytes to synthesize and retain their matrix in close cell proximity is the basis of the chondrocyte phenotype and is vitally important in maintaining their rounded cell shape [3]. After 2 weeks of culture in the insulin-loaded scaffolds, the majority of cells presented a rounded morphology while in the control condition some flattened elongated cells could be detected. After 4 weeks of culture, the cells were already with the typical round chondrocytic morphology in all the studied groups. The deposition of newly formed ECM was possible to be observed microscopically and collagen fibrils were also detected [37].

4.2.2. Cell Proliferation

Concerning cell proliferation after 2 weeks, insulin highest concentration (5%) showed to have a positive effect on DNA content. This effect was not maintained for longer culture periods which can be related with the differentiation stage, since chondrogenesis results from a complex equilibrium between chondrocyte proliferation and differentiation [48]. This may also be related with the higher concentration of insulin present in the medium. In the standard condition, cell-scaffolds constructs are exposed to 10 μg/ml of insulin, while in the higher concentration of insulin-loaded scaffolds (5%), the concentration is always above 80 μg/ml. It is know that insulin is a potent differentiating agent, but not a potent mitogen for chondrocytes [13] and this higher concentration may be inhibiting its proliferative capacity.

4.2.3. GAGs quantification

The biochemical analysis demonstrated that the content of GAGs increased from week 2 to 4 for higher insulin-loading scaffolds, indicating that typical ECM components were being deposited occur biosynthesis thereby confirming the differentiation of the ATDC5 cells towards the chondrogenic lineage. The GAGs production is higher for control condition at 2 weeks and 0.5% at 4 weeks when compared to the 5% formulation, due to the lower DNA content at the respective time periods. On the other hand, in the control condition, GAGs content decreased substantially from 2 to 4 weeks of culture due to the substantial increase in cell proliferation in unloaded scaffolds.

4.2.4. Histological examination

Histologically, it was also possible to observe that the chondrocytes were able to infiltrate, adhere and proliferate into the inner pores of the scaffolds. This reflects the advantageous structural design of these scaffolds which present a high interconnectivity degree as characterized in previous works [49,50]. Furthermore, toluidine blue staining demonstrated the typical metachromasia of the articular cartilage matrix both to the control condition and 5% insulin-loaded scaffolds after 4 weeks of culture. Toluidine blue dyes form complexes with anionic glycoconjugates such as proteoglycans and glycosaminoglycans (GAGs) and its positive staining is therefore an evidence of proteoglycan deposition for extracellular matrix production [51]. Furthermore, the observed morphology is consistent to that observed with mature chondrocytes which are predominantly round cells located in matrix cavities called lacunae [10].

4.2.5. Gene expression

The results of the realtime-PCR confirmed the mRNA expression of genes encoding the specific extracellular matrix (ECM) markers for cartilaginous tissue, such as Sox-9 and aggrecan. The transcription factor Sox-9 is considered to be a crucial factor in chondrocyte differentiation and cartilage formation and is required to maintain the chondrocytes phenotype [10]. Aggrecan is a large chondroitin sulphate proteoglycan and one of the main macromolecules constituting the cartilaginous ECM being responsible for the tissues compressive resistance [10]. The cells seeded in high insulin content scaffolds revealed a higher expression of these genes suggesting the development of phenotypic characteristics consistent with chondrocytes. The insulin-loaded scaffolds with 5% showed a 1.7-fold change significantly higher up-regulation for Sox-9 and 9.6-fold higher for aggrecan when compared with the standard condition after 4 weeks of culture.

Sox-9 is known to promote chondrocyte differentiation in part by activating chondrocyte-specific enhancer elements in aggrecan [52]. This finding is supported by our results which showed that insulin-loaded scaffolds induced an increase in Sox-9 in association with a substantial up-regulation of aggrecan mRNA. However, Sox-9 is also known to regulate the expression of collagen type II [10, 52]. In the present study, no expression of collagen type II was detected for any group. It is known that chondrocytes can dedifferentiate with change in shape, production of collagen type I, and changes in

the metabolic pattern of their proteoglycan synthesis [37, 48]. Nevertheless, in the higher insulin content scaffolds, the typical round chondrocytic morphology was maintained after 4 weeks, the proteoglycan synthesis was increasing as detected by toluidine blue and GAGs quantification and the gene expression of Sox-9 and aggrecan was also higher. Moreover, no significant up-regulation in collagen type I was measured. Further studies would be necessary to identify the causes for the absence of collagen type II expression in all the studied groups.

Cell culture and tissue culture systems have long been known to display insulinase activity, which can rapidly and markedly reduce the effective insulin concentration [13]. This is particularly relevant to the studies in which the long-term effects on ATDC5 cell differentiation are investigated, such as the one describe herein. This is a possible explanation why, from the overall results, the higher insulin concentration was more effective on promoting chondrogenic differentiation. Nevertheless, there are studies that report that the insulin receptor can initiate and sustain a differentiation promoting signal in chondrocytes [13] explaining the slight biochemical effects of lower insulin content formulations (0.05% and 0.5%) after 4 weeks, even though the release was complete.

As an overall remark, one can mention that the most promising results were obtained with ATDC5 cells seeded in the higher insulin-loaded scaffolds (5%) that showed a typical chondrocytic round morphology with visible cell condensation. Cells were positively stained by toluidine blue, presented a high GAGs production, and expressed genes encoding cartilaginous markers such as Sox-9 and aggrecan which suggests the formation of cartilaginous tissue. Furthermore, in the developed insulin-release systems, the insulin retained its bioactivity for at least 28 days which is in agreement with other reported studies [45, 53].

5. CONCLUSIONS

The present work reports the possibility to incorporate insulin as a potent substance for cartilage tissue engineering in a chitosan particle aggregated scaffold. It is an easily controllable *in vitro* release system using insulin as a model protein, since its potent differentiating capacity in chondrocytes is well known. In addition, this approach opens the possibility to assemble the developed systems in bilayered constructs in order to promote selective differentiation of cartilage and bone in osteochondral

applications. The results showed high encapsulation efficiencies, well correlated protein loadings as well as adequate release profiles. The chondro-inductive effect of the insulin-loaded scaffolds was further investigated with long term ATDC5 cell culture. The cells seeded in the higher insulin-loaded scaffolds (5%) showed a round morphology and were able to synthesize GAGs. ATDC5 stained positively stained for proteoglycans and evidenced an up-regulation of the expression profiles of cartilaginous genes Sox-9 and aggrecan when compared with the standard condition. Therefore, the results of this study demonstrate the ability of insulin-loaded chitosan scaffolds to support chondrocyte attachment and differentiation as well as cartilaginous matrix biosynthesis in a dose-dependent manner, opening interesting prospects for their use in therapeutical approaches to treat osteochondral lesions.

REFERENCES

1. Martin I, Miot S, Barbero A, Jakob M, Wendt D. Osteochondral tissue engineering. Journal of Biomechanics 2007;40(4):750-765.

2. Mano JF, Reis RL. Osteochondral defects: present situation and tissue engineering approaches. Journal of Tissue Engineering and Regenerative Medicine 2007;1(4):261-273.

3. Chaipinyo K, Oakes BW, van Damme MP. Effects of growth factors on cell proliferation and matrix synthesis of low-density, primary bovine chondrocytes cultured in collagen I gels. Journal of Orthopaedic Research 2002 Sep;20(5):1070-1078.

4. Cucchiarini M, Sohier J, Mitosch K, Kaul G, Zurakowski D, Bezemer JM, et al. Effect of transforming growth factor-beta 1 (TGF-ß1) released from a scaffold on chondrogenesis in an osteochondral defect model in the rabbit. Central European Journal of Biology 2006;1(1):43-60.

5. Elisseeff J, McIntosh W, Fu K, Blunk BT, Langer R. Controlled-release of IGF-I and TGF-beta1 in a photopolymerizing hydrogel for cartilage tissue engineering. Journal of Orthopaedic Research 2001 Nov;19(6):1098-1104.

6. Fukumoto T, Sperling JW, Sanyal A, Fitzsimmons JS, Reinholz GG, Conover CA, et al. Combined effects of insulin-like growth factor-1 and transforming growth factor-beta1 on periosteal mesenchymal cells during chondrogenesis *in vitro*. Osteoarthritis Cartilage 2003 Jan;11(1):55-64.

7. Martin I, Shastri VP, Padera RF, Yang J, Mackay AJ, Langer R, et al. Selective differentiation of mammalian bone marrow stromal cells cultured on three-dimensional polymer foams. Journal of Biomedical Materials Research 2001;55(2):229-235.

8. Swieszkowski W, Tuan BHS, Kurzydlowski KJ, Hutmacher DW. Repair and regeneration of osteochondral defects in the articular joints. Biomolecular Engineering 2007;24(5):489-495.

9. Frenkel SR, Bradica G, Brekke JH, Goldman SM, Ieska K, Issack P, et al. Regeneration of articular cartilage - Evaluation of osteochondral defect repair in the rabbit using multiphasic implants. Osteoarthritis and Cartilage 2005;13(9):798-807.

10. Lin Z, Willers C, Xu J, Zheng M-H. The Chondrocyte: Biology and Clinical Application. Tissue Engineering 2006;12(7):1971-1984.

11. Bohme K, Conscience-Egli M, Tschan T, Winterhalter KH, Bruckner P. Induction of proliferation or hypertrophy of chondrocytes in serum-free culture: the role of insulin-like growth factor-I, insulin, or thyroxine. Journal of Cell Biology 1992 February 1, 1992;116(4):1035-1042.

12. van der Kraan PM, Buma P, van Kuppevelt T, van den Berg WB. Interaction of chondrocytes, extracellular matrix and growth factors: relevance for articular cartilage tissue engineering. Osteoarthritis Cartilage 2002 Aug;10(8):631-637.

13. Phornphutkul C, Wu K-Y, Gruppuso PA. The role of insulin in chondrogenesis. Molecular and Cellular Endocrinology 2006;249(1-2):107-115.

14. Phornphutkul C, Wu KY, Yang X, Chen Q, Gruppuso PA. Insulin-like growth factor-I signaling is modified during chondrocyte differentiation. Journal of Endocrinology 2004;183(3):477-486.

15. Madry H, Kaul G, Cucchiarini M, Stein U, Zurakowski D, Remberger K, et al. Enhanced repair of articular cartilage defects *in vivo* by transplanted chondrocytes overexpressing insulin-like growth factor I (IGF-I). Gene Therapy 2005;12(15):1171-1179.

16. Schmid C. Insulin-like growth factors. Cell Biology International 1995;19(5):445-457.

17. Darling EM, Athanasiou KA. Growth factor impact on articular cartilage subpopulations. Cell and Tissue Research 2005;322(3):463-473.

18. Shukunami C, Shigeno C, Atsumi T, Ishizeki K, Suzuki F, Hiraki Y. Chondrogenic differentiation of clonal mouse embryonic cell line ATDC5 *in vitro*: differentiation-dependent gene expression of parathyroid hormone (PTH)/PTH-related peptide receptor. Journal of Cell Biology 1996 April 1, 1996;133(2):457-468.

19. Kellner K, Schulz MB, Gopferich A, Blunk T. Insulin in tissue engineering of cartilage: A potential model system for growth factor application. Journal of Drug Targeting 2001;9(6):439-448.

20. Chua KH, Aminuddin BS, Fuzina NH, Ruszymah BHI. Insulin-Transferrin-Selenium prevent human chondrocyte dedifferentiation and promote the formation of high quality tissue engineered human hyaline cartilage. European Cells and Materials 2005;9:58-67.

21. Gotterbarm T, Richter W, Jung M, Berardi Vilei S, Mainil-Varlet P, Yamashita T, et al. An *in vivo* study of a growth-factor enhanced, cell free, two-layered collagen-tricalcium phosphate in deep osteochondral defects. Biomaterials 2006;27(18):3387-3395.

22. Holland TA, Bodde EWH, Cuijpers VMJI, Baggett LS, Tabata Y, Mikos AG, et al. Degradable hydrogel scaffolds for *in vivo* delivery of single and dual growth factors in cartilage repair. Osteoarthritis and Cartilage 2007;15(2):187-197.

23. Mierisch CM, Cohen SB, Jordan LC, Robertson PG, Balian G, Diduch DR. Transforming growth factor-beta in calcium alginate beads for the treatment of articular cartilage defects in the rabbit. Arthroscopy 2002;18(8):892-900.

24. Tuzlakoglu K, Bolgen N, Salgado AJ, Gomes ME, Piskin E, Reis RL. Nano- and micro-fiber combined scaffolds: A new architecture for bone tissue engineering. Journal of Materials Science: Materials in Medicine 2005;16(12):1099-1104.

25. Gomes ME, Bossano CM, Johnston CM, Reis RL, Mikos AG. *In vitro* localization of bone growth factors in constructs of biodegradable scaffolds seeded with marrow stromal cells and cultured in a flow perfusion bioreactor. Tissue Engineering 2006;12(1):177-188.

26. Marques AP, Reis RL, Hunt JA. An *in vivo* study of the host response to starch-based polymers and composites subcutaneously implanted in rats. Macromolecular Bioscience 2005;5(8):775-785.

27. Malafaya PB, Pedro A, Peterbauer A, Gabriel C, Redl H, Reis RL. Chitosan particles agglomerated scaffolds for cartilage and osteochondral tissue engineering approaches with adipose tissue derived stem cells. Journal of Materials Science: Materials in Medicine 2005;16(12):1077.

28. Kim IY, Seo SJ, Moon HS, Yoo MK, Park IY, Kim BC, et al. Chitosan and its derivatives for tissue engineering applications. Biotechnology Advances 2008;26(1):1-21.

29. Cai DZ, Zeng C, Quan DP, Bu LS, Wang K, Lu HD, et al. Biodegradable chitosan scaffolds containing microspheres as carriers for controlled transforming growth factor-beta1 delivery for cartilage tissue engineering. Chinese Medical Journal 2007;120(3):197-203.

30. Kim SE, Park JH, Cho YW, Chung H, Jeong SY, Lee EB, et al. Porous chitosan scaffold containing microspheres loaded with transforming growth factor-beta1: Implications for cartilage tissue engineering. Journal of Controlled Release 2003;91(3):365-374.

31. Lee JE, Kim KE, Kwon IC, Ahn HJ, Lee SH, Cho H, et al. Effects of the controlled-released TGF-beta1 from chitosan microspheres on chondrocytes cultured in a collagen/chitosan/glycosaminoglycan scaffold. Biomaterials 2004;25(18):4163-4173.

32. Jong EL, Seoung EK, Ick CK, Hyun JA, Cho H, Lee SH, et al. Effects of a chitosan scaffold containing TGF-beta1 encapsulated chitosan microspheres on *in vitro* chondrocyte culture. Artificial Organs 2004;28(9):829-839.

33. Uchihashi T, Kimata M, Tachikawa K, Koshimizu T, Okada T, Ihara-Watanabe M, et al. Involvement of nuclear factor I transcription/replication factor in the early stage of chondrocytic differentiation. Bone 2007;41(6):1025-1035.

34. Da Silva RMP, Elvira C, Mano JF, Roman JS, Reis RL. Influence of beta-Radiation Sterilization in Properties of New Chitosan/Soybean Protein Isolate Membranes for Guided Bone Regeneration. Journal of Materials Science - Materials in Medicine 2004;15:523-528.

35. Mincheva R, Manolova N, Sabov R, Kjurkchiev G, Rashkov I. Hydrogels from chitosan crosslinked with poly(ethylene glycol) diacid as bone regeneration materials. E-Polymers 2004.

36. Bouchard M, Zurdo J, Nettleton EJ, Dobson CM, Robinson CV. Formation of insulin amyloid fibrils followed by FTIR simultaneously with CD and electron microscopy. Protein Science 2000;9(10):1960-1967.

37. Kino-Oka M, Yashiki S, Ota Y, Mushiaki Y, Sugawara K, Yamamoto T, et al. Subculture of Chondrocytes on a Collagen Type I-Coated Substrate with Suppressed Cellular Dedifferentiation. Tissue Engineering 2005;11(3-4):597-608.

38. Mao S, Bakowsky U, Jintapattanakit A, Kissel T. Self-assembled polyelectrolyte nanocomplexes between chitosan derivatives and insulin. Journal of Pharmaceutical Sciences 2006;95(5):1035.

39. Ubaidulla U, Sultana Y, Ahmed FJ, Khar RK, Panda AK. Chitosan phthalate microspheres for oral delivery of insulin: Preparation, characterization, and *in vitro* evaluation. Drug Delivery 2007;14(1):19-23.

40. Sajeesh S, Sharma CP. Interpolymer complex microparticles based on polymethacrylic acid-chitosan for oral insulin delivery. Journal of Applied Polymer Science 2006;99(2):506-512.

41. Sarmento B, Martins S, Ribeiro A, Veiga F, Neufeld R, Ferreira D. Development and comparison of different nanoparticulate polyelectrolyte complexes as insulin carriers. International Journal of Peptide Research and Therapeutics 2006;12(2):131-138.

42. Wang LY, Gu YH, Su ZG, Ma GH. Preparation and improvement of release behavior of chitosan microspheres containing insulin. International Journal of Pharmaceutics 2006;311(1-2):187.

43. Boonsongrit Y, Mitrevej A, Mueller BW. Chitosan drug binding by ionic interaction. European Journal of Pharmaceutics and Biopharmaceutics 2006;62(3):267.

44. Boonsongrit Y, Mueller BW, Mitrevej A. Characterization of drug-chitosan interaction by 1H NMR, FTIR and isothermal titration calorimetry. European Journal of Pharmaceutics and Biopharmaceutics 2008;in press:doi:10.1016/j.ejpb.2007.1011.1008.

45. Appel B, Maschke A, Weiser B, Sarhan H, Englert C, Angele P, et al. Lipidic implants for controlled release of bioactive insulin: Effects on cartilage engineered *in vitro*. International Journal of Pharmaceutics 2006;314(2):170-178.

46. Maschke A, Becker C, Eyrich D, Kiermaier J, Blunk T, Gopferich A. Development of a spray congealing process for the preparation of insulin-loaded lipid microparticles and characterization thereof. European Journal of Pharmaceutics and Biopharmaceutics 2007;65(2):175-187.

47. Fujita T, Fukuyama R, Enomoto H, Komori T. Dexamethasone inhibits insulin-induced chondrogenesis of ATDC5 cells by preventing PI3K-Akt signaling and DNA binding of Runx2. Journal of Cellular Biochemistry 2004;93(2):374-383.

48. Spagnoli A, Hwa V, Horton WA, Lunstrum GP, Roberts Jr CT, Chiarelli F, et al. Antiproliferative effects of insulin-like growth factor-binding protein-3 in mesenchymal chondrogenic cell line RCJ3.1C5.18. Relationship to differentiation stage. Journal of Biological Chemistry 2001;276(8):5533-5540.

49. Malafaya PB, Reis RL. Bilayered chitosan-based scaffolds for osteochondral tissue engineering: influence of hydroxylapatite on *in vitro* cytotoxicity and dynamic bioactivity studies in a specific double chamber bioreactor. Acta Biomaterialia 2008: submitted.

50. Malafaya PB, Santos TC, Griensven Mv, Reis RL. Morphometric, mechanical characterization and *in vivo* neo-vascularization of novel chitosan particle aggregated tissue engineering scaffolding architectures. Tissue Engineering 2008: submitted.

51. Wenger R, Hans MG, Welter JF, Solchaga LA, Sheu YR, Malemud CJ. Hydrostatic pressure increases apoptosis in cartilage-constructs produced from human osteoarthritic chondrocytes. Frontiers in Bioscience 2006;11(2 P.1591-2006):1690-1695.

52. Robins JC, Akeno N, Mukherjee A, Dalal RR, Aronow BJ, Koopman P, et al. Hypoxia induces chondrocyte-specific gene expression in mesenchymal cells in association with transcriptional activation of Sox9. Bone 2005;37(3):313-322.

53. Ibrahim MA, Ismail A, Fetouh MI, Gopferich A. Stability of insulin during the erosion of poly(lactic acid) and poly(lactic-co-glycolic acid) microspheres. Journal of Controlled Release 2005;106(3):241-252.

CHAPTER VI.

Morphometric, mechanical characterization and *in vivo* neo-vascularization of novel chitosan particle aggregated tissue engineering scaffolding architectures

CHAPTER VI.

Morphometric, mechanical characterization and *in vivo* neo-vascularization of novel chitosan particle aggregated tissue engineering scaffolding architectures *

ABSTRACT

In tissue engineering, scaffolds development presents, in our opinion, three major key requirements, for an ideal design: (i) the need for a porous structure with adequate morphological characteristics, (ii) a suitable mechanical behaviour, and (iii) an indisputable *in vivo* functional biocompatibility. The aim of the present study was to evaluate the performance of chitosan-based scaffolds produced by an innovative particle aggregation method that are aimed to be used in tissue engineering applications addressing all those key issues. It is claimed that the particle aggregation methodology may present several advantages, such to combine simultaneously a high interconnectivity with high mechanical properties that are both critical for an *in vivo* successful application.

In order to evaluate these properties, micro-Computed Tomography (micro-CT) was applied, allowing for an accurate morphometric characterization and Dynamical Mechanical Analysis (DMA) was performed, in order to study the scaffolds behaviour while in wet state under dynamic compression solicitation. Micro-CT provides valuable knowledge for scaffold design allowing for the quantification of scaffolds porosity, interconnectivity, particles and pores size. The herein proposed scaffolds present an interesting morphology that generally seems to be adequate for the proposed applications. At a mechanical level, DMA has shown that chitosan scaffolds have an elastic behaviour, being simultaneously mechanically stable in the wet state and exhibiting a storage modulus of 4.21 ± 1.04 MPa at 1Hz frequency.

Furthermore, chitosan scaffolds were evaluated *in vivo* using a rat muscle-pockets model for different implantation periods (1, 2 and 12 weeks). The histological and immunohistochemistry results have demonstrated that chitosan scaffolds are clearly biocompatible, and can provide the required *in vivo*

functionality. In addition, the scaffolds interconnectivity shown to be favourable to the connective tissues ingrowth into the scaffolds and to promote the neo-vascularization even in early stages of implantation.

It is concluded that chitosan scaffolds produced by this particle aggregation method are suitable alternatives, being simultaneously mechanical stable and functional biocompatible scaffolds that might be used in load-bearing tissue engineering applications, including bone and cartilage regeneration.

---

* This chapter is based in the following publication:

PB Malafaya, TC Santos, M van Griensven, RL Reis. Morphometric, mechanical characterization and *in vivo* neo-vascularization of novel chitosan particle aggregated tissue engineering scaffolding architectures. Tissue Engineering: Part A (2008) submitted

---

1. INTRODUCTION

In tissue engineering, scaffolds are typically needed, both as carriers for cells or biochemical factors, or as constructs providing appropriate mechanical conditions. In general, the term scaffold is used to describe all structures that are used to restore functionality of an organ either permanently or temporarily [1]. An ideal scaffold should have several characteristics as it has been comprehensively reviewed in several papers [1-4]: (i) three-dimensional (3D) and porous supports with an interconnected pore network for cell growth and flow transport of nutrients and metabolic waste; (ii) biocompatibility and biodegradability with a controllable degradation and resorption rate to match cell/tissue growth *in vitro* and *in vivo*; (iii) suitable surface chemistry for cell attachment, proliferation, and differentiation and (iv) mechanical properties adequate to the tissues at the site of implantation.

When considering the main aimed applications, it is not surprising that there is a wide range of scaffolds, including porous scaffolds that allow for cell adhesion, and provide biological functions [5-9]. In fact, from a mechanical point of view, scaffolds vary widely from soft gels, mainly serving as carriers for cells [10-12] to stiff biodegradable calcium phosphate scaffolds [13-15]. Another criterion to be fulfilled is the biocompatibility or *in vivo* biofunctionality. All implant materials must be non-toxic to the body and prove to interact properly with the host tissue.

Another quite important requirement is that the scaffold must act as a three-dimensional (3D) template for *in vitro* and *in vivo* tissue growth, i.e. the scaffold must consist of an interconnected macroporous network allowing for cell/tissue growth and flow transport of nutrients. In the case of bone tissue engineering, it was shown [16,17] that the interconnections for bone ingrowth larger than 50 μm were favourable for mineralized bone formation. The interconnectivity of the pores dominates the flow properties, which are important to ensure adequate delivery of cells during seeding and nutrients during subsequent culture/implantation. Several investigators [14,16,18-20] have also studied bone ingrowth into porous material with different pore sizes and the consensus seems to be that the optimal pore size for bone ingrowth is 100-400 μm [14-17,21-23]. Therefore, an ideal scaffold would have interconnects of at least 50 μm in diameter between its macropores of 100-400 μm pore size range. It is thus important to be able to quantify both the pores and interconnects to optimize tissue scaffolds.

Effective scaffold assessment techniques are then required right at the initial stages of research and development to select or design scaffolds with suitable properties. Reliable methods to quantify the morphology and properties of tissue scaffold are required to enable standards for their regulatory approval to be developed. Furthermore, the measurements should also be quantitative since quantitative results have become an important factor for success in basic research and the development of novel tissue engineering approaches. Micro-Computed Tomography (micro-CT) appears to be such a measurement technique.

Micro-CT was identified as having various key advantages over other techniques, such as its non-destructiveness and the possibility to assess many different morphometric parameters [15,22,24-26]. Micro-CT was first proposed to analyze trabecular samples [27] and, since then, has been used extensively in the study of trabecular architecture [28] and their applications in other areas are clearly increasing, namely in the tissue engineering field. The morphometric parameters for architectural analyses of scaffolds can be easily extrapolated based on the histomorphometric/structural indices usually measured for bone samples, such as bone surface (BS) and volume (BV), trabecular thickness (Tb.Th) and trabecular separation (Tb. Sp), structural degree of anisotropy (DA) or bone surface-to-volume ratio (BS/BV) [29].

The increasing use of this technique in tissue engineering [15,22,24-26] can be attributed to micro-CT capacity to provide for accurate quantitative and qualitative information on the 3D morphology of the sample. Another main advantage is that the interior of the object can be studied with great detail without physical sectioning or use of toxic chemicals. Moreover, after scanning, the integral samples can be subjected to other tests due to its non-destructive nature, thereby resolving the problem of sample scarcity. This is a very important characteristic allowing, for instance, to the accurate study of bone ingrowth which has being widely used by the group of Cancedda [14,20].

The recent use of micro-CT in scaffolds research allowed for significant morphological and morphometric studies to be carried out, yielding comprehensive data sets on scaffolding strategies [15,26,29,30]. For example, in a study by Peyrin *et al* [15], 3D synchrotron radiation micro-CT was used to have information on the geometry of two hydroxyapatite bioceramics with identical chemical composition obtained with two different procedures (sponge matrix embedding and foaming) with different micro-porosity, pore size distribution, and pore interconnection pathway. The results allowed to

conclude that foaming methodology produced scaffolds that appeared to be superior regarding the interconnection of pores, surface on which the new bone could be deposited, and percentage of volume available to bone deposition. In conclusion, the aforementioned advantages of micro-CT for the characterization of scaffolds architecture makes it a useful tool to characterize, compare and optimize scaffold production techniques [15,26,31].

Different materials have been proposed to be used as both 3D porous scaffolds and hydrogel matrices for distinct tissue engineering strategies. It is often beneficial for the scaffolds to mimic certain advantageous characteristics of the natural extracellular matrix, or developmental or wound healing programs [32]. Ideally, scaffolds would be made of biodegradable polymers whose properties closely resemble those of the extracellular matrix (ECM), a soft, tough, and elastomeric protein-rich network, that provides mechanical stability and structural integrity to tissues and organs [33]. Polymers of natural origin are one of the most attractive options, mainly due to their similarities with the extracellular matrix, chemical versatility, as well as typically good biological performance [6,8,9,33,34].

Among them, chitosan appears to be an excellent alternative due its interesting and versatile properties [6,35,36]. Studies on chitosan as a potential candidate for tissue engineering scaffolding demonstrate this, as those have been clearly intensified as during the past years [30,35-37]. Chitosan is a natural polymer obtained from renewable resources, obtained from the shell of shellfish, and the wastes of seafood industry. It has attractive properties such as biocompatibility, biodegradability, antibacterial, and wound-healing activity [36]. Furthermore, recent studies suggested that chitosan and its derivatives are promising candidates to be used as supporting materials for tissue engineering applications, owing to their porous structure, gel forming properties, ease of chemical modification, high affinity to *in vivo* macromolecules, and so on [5,6,35,36,38,39].

Bearing all these considerations in mind, the aim of the present study was to evaluate the performance of chitosan-based scaffolds produced by a particle aggregation method that has been proposed for tissue engineering applications [30,40,41]. Those systems should try to meet the three key requirements for an ideal design: a porous structure with adequate morphological characteristics, adequate mechanical behaviour and an *in vivo* biocompatibility. To evaluate these properties, micro-computed tomography (micro-CT) was carried out for accurate morphometric characterization and dynamical mechanical analysis (DMA) was performed to study the scaffolds behaviour in wet state under

compression solicitation. Chitosan scaffolds were also evaluated *in vivo* using a rat muscle-pockets model for different implantation periods (1, 2 and 12 weeks) with subsequent characterization, including histological and immunohistochemical evaluation.

2. MATERIALS AND METHODS

2.1. SCAFFOLDS PRODUCTION

The chitosan particle aggregated scaffolds were produced as described elsewhere [30]. Briefly, chitosan (medium molecular weight and deacetylation degree ≈85%) was grinded and dissolved overnight in acetic acid (1%vv) to obtain a chitosan solution (2%wt). Unless otherwise stated, all chemicals were bought from Sigma-Aldrich and used as received. After complete dissolution and filtration, the prepared solutions were extruded through a syringe at a constant rate (10 ml/h) to form chitosan droplets into a NaOH (1M) precipitation bath where particles with regular diameter were formed. The chitosan particles were collected and washed repeatedly with distilled water until neutral pH was reached. The particles were subsequently placed into cylindrical moulds and left to dry at 60ºC for 3 days. Cylindrical shaped scaffolds with 8 mm height and 5 mm diameter were obtained. For the *in vivo* studies, cylindrical shaped scaffolds with 3 mm height and 5 mm diameter were used. Cross-sections of 10 μm were also obtained from the scaffolds' bulk and stained with eosin for visual evaluation of the interface between the particles.

2.2. MICRO-COMPUTED TOMOGRAPHY (MICRO-CT)

Chitosan particle aggregated scaffolds (n=3) were scanned using micro-Computed Tomography (micro-CT) for morphological and morphometric characterization. Micro-CT was carried out with a high-resolution micro-CT Skyscan 1072 scanner (Skyscan, Kontich, Belgium) using a resolution of pixel size of 8.79 μm and integration time of 1.9 ms. The X-ray source was set at 70 keV of energy and 145 μA of current. Approximately 400 projections were acquired over a rotation range of 180° with a rotation step of 0.45°. Data sets were reconstructed using standardized cone-beam reconstruction software (NRecon v1.4.3, SkyScan). The output format for each sample was 850 serial 1024x1024 bitmap images.

Representative data sets of 200 slices were segmented into binary images with a dynamic threshold of 60-255 (grey values). This data was used for morphometric analysis (CT Analyser v1.5.1.5, SkyScan) and to build 3D virtual models (ANT 3D creator v2.4, SkyScan). The morphometric analysis included porosity, scaffolds interconnectivity, mean pore and particles size and respective distribution. 3D virtual models of representative regions in the bulk of the scaffolds were created, visualized and registered using both image processing softwares (CT Analyser and ANT 3D creator). In order to characterize the porosity morphology of the scaffold, threshold inversion was used to create a 3D model.

2.3. DYNAMIC MECHANICAL ANALYSIS (DMA)

Dynamic Mechanical Analysis (DMA) was conducted in order to characterize the dynamic mechanical behaviour of chitosan particle aggregated scaffolds in wet state under dynamic compression solicitation. Chitosan cylindrical scaffolds were immersed in phosphate buffer solution (PBS) at physiological pH for 3 days for complete hydration. The scaffolds were then were subjected to compression cycles of increasing frequencies ranging from 0.1-40 Hz with constant amplitude displacements of 0.03 mm using a Tritec2000 DMA (Triton Technology, UK). Experiments were conducted at room temperature and five points were measured within each decade. For each individual scaffold, the data is averaged over three consecutive runs. Five samples were measured for each type of scaffolds. The real (storage modulus), E', and the imaginary component (loss modulus), E'', of the complex modulus, $E^*=E'+iE''$ (with $i=(-1)^{1/2}$), were recorded against frequency. Reference values for the compression modulus were collected at a frequency of 1Hz.

2.4. *IN VIVO* BIOCOMPATIBILITY STUDY

2.4.1. Surgical Procedure

Four male Sprague Dawley rats, weighing 350-380 g were used for intramuscular implantation of the chitosan aggregated scaffolds. Each animal was anaesthetized (induction with 3-3.5% isofluorane and 7 L/minute of air for 2-3 minutes; maintenance with intramuscular injection of 90 mg/kg of ketamin combined with 5 mg/kg xylazine) and subjected to local tricotomy for adequate surgical procedure. The

skin was disinfected and under surgical sterile conditions, four lumbar paravertebral incisions of approximately 2 cm length were performed through the cutis, subcutis and the *panniculus carnosus* (smooth skin muscle). After incising the fascia of the *latissimus dorsi* muscle, craniolateral oriented muscle-pockets were created by blunt dissection. Into these pockets, the scaffolds were inserted and the fascia carefully sutured, as well as the *panniculus carnosus* and finally the skin. As an analgesic treatment, animals received Metamizol (200 μg/g of body weight per day in drinking water *ad libitum*). At 1, 2 and 12 weeks post-implantation, the animals were anaesthetized (see above) and sacrificed by an intracardial overdose of pentobarbital. The scaffolds and surrounding tissue were explanted for further evaluation. The animal experiment was approved by the local ethical authorities responsible for animal experimentation.

2.4.2. Explants Morphological Characterization

At 1, 2 and 12 weeks post-implantation, explants were registered using stereolight microscopy. Furthermore, micro-computed tomography (micro-CT) of the explants was carried out as described previously. Two-dimensional X-ray photographs were registered from the bulk of the explants.

2.4.3. Histological Evaluation

After explantation at 1, 2 and 12 weeks, samples were fixed in 4.7% formalin for 24 hours and then kept in 70% ethanol. After fixation, samples were dehydrated in graded ethanol (50, 70, 95 and 100%), embedded in xylene and then, in paraffin. Afterwards, samples were sectioned in 2-4 μm sections and stained with haematoxylin/eosin (H&E). The stained microscope slides were observed by, at least, two independent observers.

2.4.3.1. Immunohistochemistry

In order to perform immunohistochemistry, paraffin was removed from the samples slides upon heating. They were hydrated in descending ethanol concentrations (100, 95, 70 and 50%) and incubated in phosphate buffer saline (PBS). The antigen retrieval was performed with microwave incubation in citrate

buffer (pH=6) at 800 W for 20 minutes and the slides were washed with PBS. The endogenous peroxidase was blocked with 1% hydrogen peroxide (H_2O_2) in methanol, at room temperature (RT) for 15 minutes. After washing, the slides were incubated with the primary antibodies at RT for 1 hour (see Table 1) and washed at the end of the incubation period. Subsequently, the samples were incubated with the secondary antibody (Polyclonal Swine Anti-Goat, Mouse, Rabbit Immunoglobulins/Biotinylated - DakoCytomation, Denmark; dilution 1:100) at RT, for 30 minutes. After washing with PBS, the samples were incubated with the ABComplex (StreptABComplex/HRP, DakoCytomation, Denmark) at RT for 30 minutes and washed again after the incubation period.

Visualisation of the bound antibodies in the samples was revealed by incubation with AEC substrate (Dako RealTM EnVisionTM Detection System, Peroxidase/DAB+, Rabbit/Mouse; DakoCytomation, Denmark) until the colour could be detected. The revelation of the labelling was stopped with PBS and the samples were stained with Mayer's Haematoxylin for nuclear contrast, at RT for 2 minutes. After this, the samples were washed with distilled water, dehydrated in graded ethanol (50, 70, 95 and 100%), cleared with xylene substitute, permanently mounted with Clarion™ Mounting Medium, and observed in the light microscope by, at least, two independent observers.

Table 1. Primary antibodies used in the immunohistochemistry evaluation of the explants.

ANTIBODY	RECOGNIZES	DILUTION	INCUBATION/TEMPERATURE	COMPANY	COUNTRY
CD18	Rat β2 integrins (βchain of LFA-1)	1:100	1 hour/RT	Serotec	UK
CD3	T lymphocytes	1:30	1 hour/RT	DakoCytomation	Denmark
vWF	von Willebrand Factor	1:200	1 hour/RT	DakoCytomation	Denmark
SMA	Smooth Muscle Actin	1:5000	1 hour/RT	Sigma	USA

3. RESULTS

3.1. MORPHOMETRIC ANALYSIS

With the emerging of the advances on computer technology, micro-CT has become a powerful tool for analyzing porous materials based on 3D geometrical considerations. Micro-CT can provide virtual representations and accurate morphometric parameters of structural characteristics in a non-destructive and reproducible way that generates precise three-dimensional (3D) measurements of scaffold

architecture [15,26]. One of the key parameters of micro-CT that one as to define is the threshold that is the basis for an adequate morphometric analysis. In Figure 1, we represent a characteristic histogram for chitosan particle aggregated scaffolds that allows us to define the dynamic threshold used for further morphometric analysis and 3D models generation.

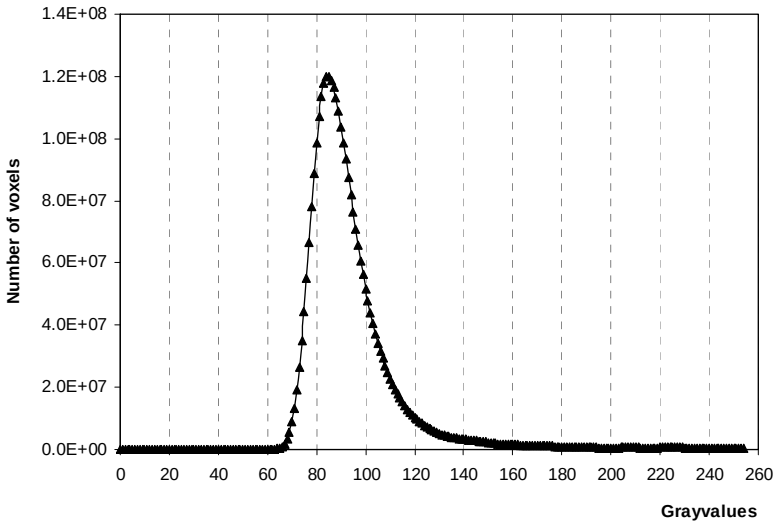

Figure 1. Representative histogram obtained for chitosan particle aggregated scaffolds used to define the dynamic threshold (greyvalues).

Quantitative analysis of the scaffolds architecture such as porosity or pore size distribution can be obtained by micro-CT based on the structural indexes usually measured for bone samples [28]. Scaffold (bone) volume (BV) is calculated using tetrahedrons corresponding to the enclosed volume of the triangulated surface [29]. Total volume (TV) is the overall volume of the scanned scaffold. Scaffolds porosity (%) can therefore be calculated as (1-BV/TV). Particle size (trabecular thickness) or pore diameter (trabecular separation) as well as their distribution can also be computed. Furthermore, interconnectivity can also be calculated using an appropriate pore size limit. The referred values can be computed as an average of all the 2D measurements giving information of the parameters behaviour along the scaffolds (such as porosity distribution) or more accurately in 3D analysis.

Porosity and interconnectivity of the chitosan particle aggregated scaffolds were computed and are shown in Figure 2. Percentages values of 27.78 ± 2.80% and 94.99 ± 1.41% were found for both

parameters, respectively. It is important to stress out that interconnectivity was calculated with a limit in pore size of 53 μm as minimum value for interconnected pores, meaning that interconnection diameters lower that this value were consider as closed pores.

The average particle size was 430.72 ± 54.42 μm and the average pore diameter was 265.46 ± 24.27 μm and their distribution is disclosed in Figure 3. By analysing the pore size distribution, one can observe that the chitosan based scaffolds present a heterogeneous range of pore size covering the optimal pore size reported as consensus for tissue engineering applications [14-17, 21-23].

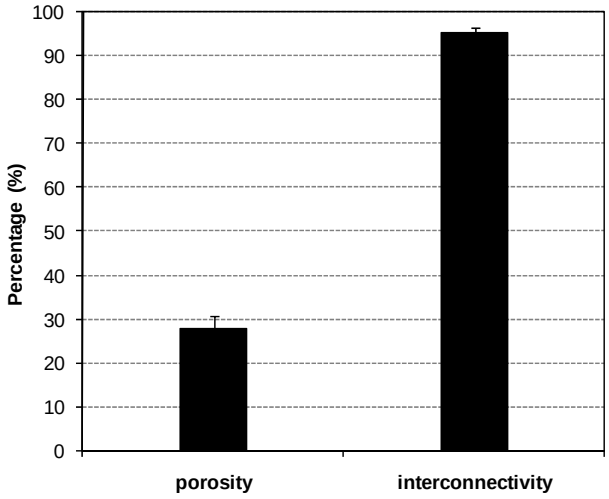

Figure 2. Porosity and interconnectivity of chitosan particle aggregated scaffolds measured by micro-CT.

→

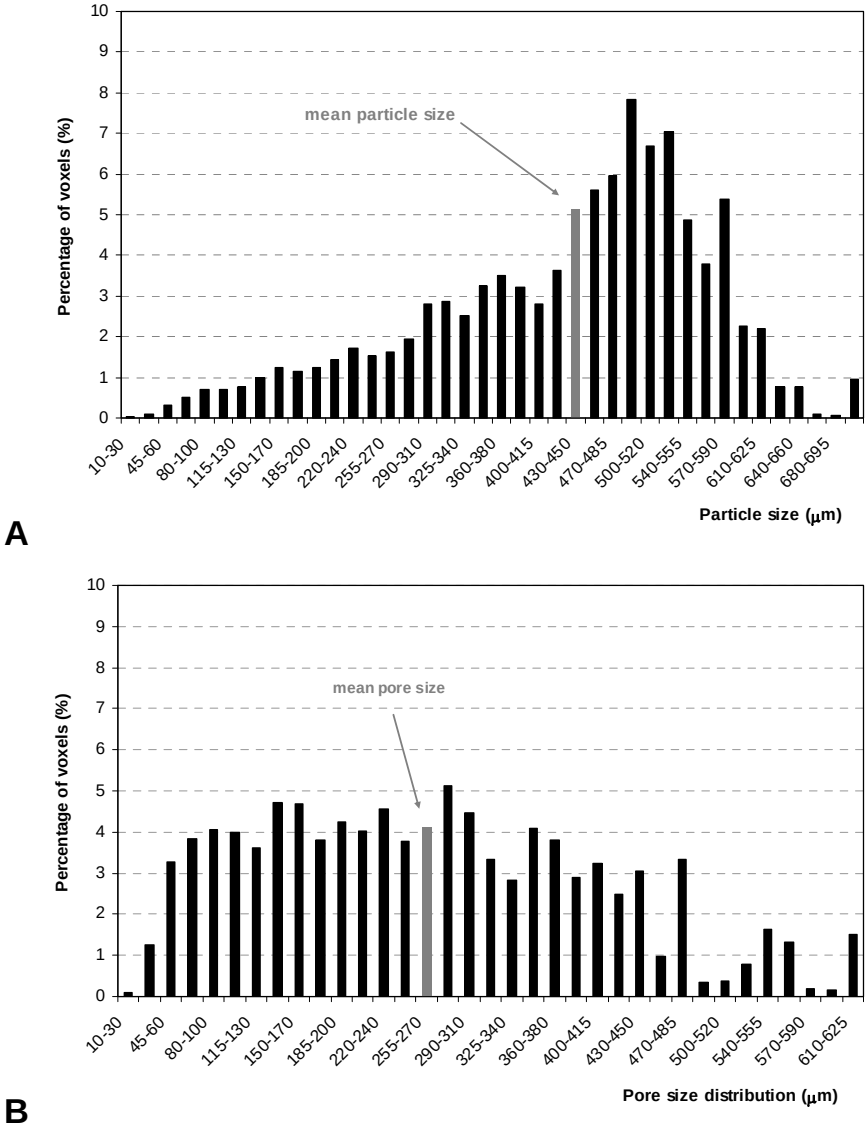

Figure 3. Particle (A) and pore (B) size distribution of chitosan particle aggregated scaffolds accessed by μ-CT.

3.2. DYNAMIC MECHANICAL ANALYSIS (DMA)

As previously discussed, one of the key issues of scaffolds design for tissue engineering is their mechanical performance. Therefore, the assessment of scaffolds mechanical behaviour is essential to ensure the mechanical stability, namely in hydrated state approaching the *in vivo* condition where physiological fluids are present. In the present paper, chitosan particle aggregated scaffolds were characterized in the wet state over a range of physiological frequency range in load-bearing

applications, such as articular cartilage or bone [42,43]. The reference values at a frequency of 1Hz for elastic (storage) and viscous (loss) components of the complex modulus are shown in Figure 4. At this frequency, the elastic and viscous moduli of the scaffolds were 4.21 ± 1.04 MPa and 0.36 ± 0.07 MPa respectively.

The storage (E') and loss (E'') modulus behaviour for increasing frequencies is presented in Figure 5 and the frequency dependence of the loss factor (tanδ) is shown in the inset graph. As it is possible to observe, the elastic modulus (E') increases with increasing frequency, being typically above 4 MPa, while the viscous modulus (E'') shows the inverse trend with a slight increasing for higher frequencies. As a consequence, there is an obvious decrease of the loss factor, (tanδ=E''/E') with increasing frequency with a slight increase for higher frequencies as shown in the inset graph.

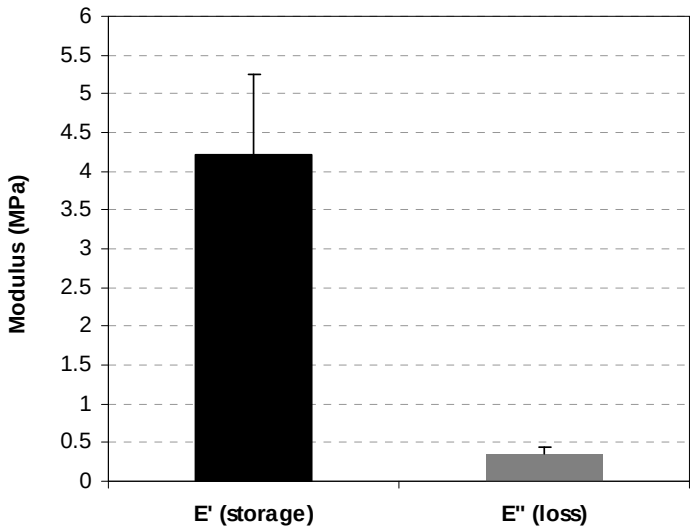

Figure 4. Storage (E') and loss (E'') modulus under dynamic compression solicitation at 1Hz frequency of chitosan particle aggregated scaffolds in wet state.

→

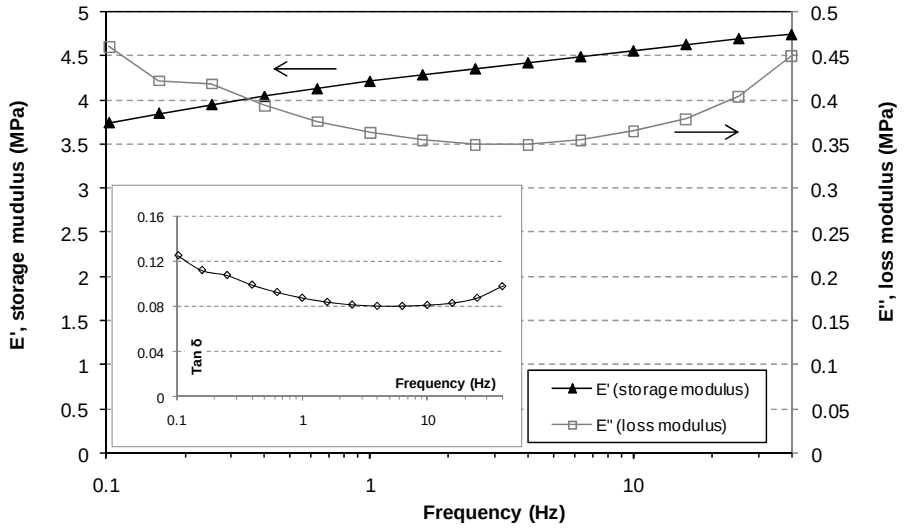

Figure 5. Dynamic mechanical analysis of chitosan particle aggregated scaffolds in wet state showing the storage (E') and loss (E'') modulus behaviour for increasing frequencies under dynamic compression solicitation. The inset graph shows the frequency dependence of the loss factor.

3.3. *IN VIVO* BIOCOMPATIBILITY

No systemic or regional surgical complications were seen for any of the rats in the post-operative period. A morphological characterization of the explants, after the different implantation periods, showed connective tissue ingrowth into the chitosan-scaffolds even after 1 week of implantation (Figure 6). This tissue ingrowth becomes more pronounced with increasing time periods of implantation. This was further confirmed by micro-CT. The 2D X-Ray evaluation of the cross-sections in the explants' bulk is presented in Figure 7 where it is possible to identify the increase of the host tissue inside the scaffolds pores with the implantation time. Furthermore, there is a macroscopic indication of vascularization of the implants after 12 weeks of implantation (Figure 6.E and 6.F).

→

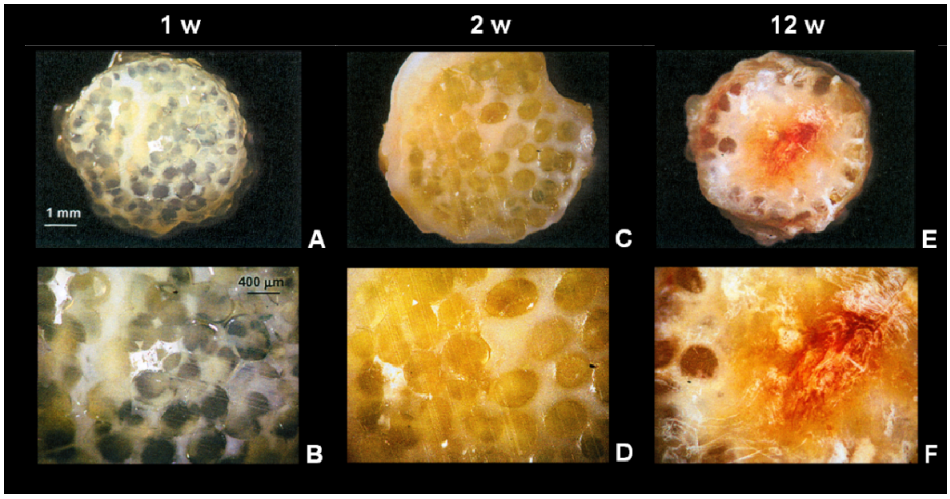

Figure 6. Chitosan particle aggregated explants after 1, 2 and 12 weeks after implantation using stereolight microscopy at different magnifications.

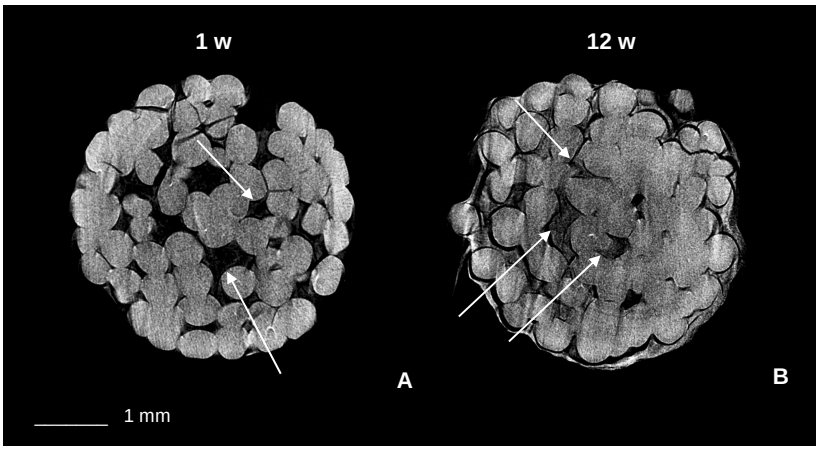

Figure 7. Representative 2D X-ray microphotographs obtained by micro-CT of the bulk chitosan particle aggregated explants after 1 (A) and 12 (B) weeks after implantation clearly showing the tissue ingrowth.

Histological, including immunohistochemistry analysis, was performed after the different implantation periods, and the obtained results are disclosed in the following Figures 8 to 12. After 1 week implantation of the chitosan particle aggregated scaffolds, the predominant inflammatory cell type found was the polymorphonuclear neutrophil (PMNs) recruited from the circulation in response to the implanted material (Figures 8.A and 8.B). Some other inflammatory cells, such as lymphocytes and macrophages can also be observed, but in a less extent compared with the PMNs. In addition, the recruited PMNs were labelled by anti-CD18, which has affinity with the integrins, binding to the surface of recruited leukocytes (Figures 9.C and 9.D). The lymphocytes present in the histological samples were labelled by anti-CD3 (specific for the T lymphocytes subset) and shown to be residual when compared

to PMNs (Figures 10.C and 10.D). Few new blood vessels could be found at this stage (Figure 11.C, 11.D, 12.C and 12.D), in spite of the expression of vWF at this time of implantation which is a common endothelial marker during the angiogenic process [44]. In addition, it is possible to identify a rudimentary extracellular matrix produced in the pores of the chitosan particle aggregated scaffolds, although it is still much disorganized (Figures 8.A, 8.B, 12.C and 12.D).

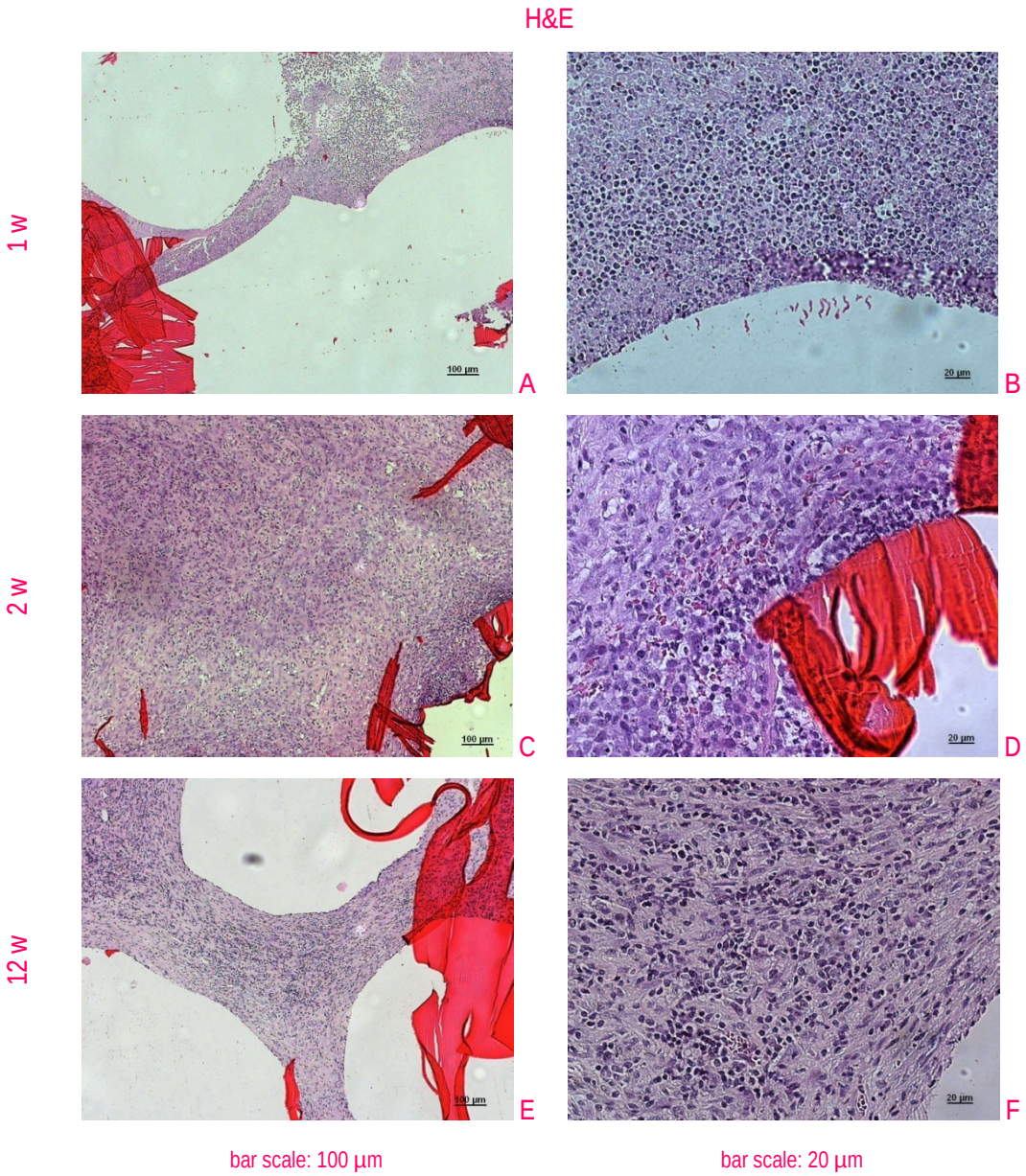

Figure 8. Representative H&E stained histological sections of tissues surrounding chitosan-based implants after 1 week (A) and (B), 2 weeks (C) and (D), and 12 weeks (E) and (F) of intramuscular implantation. Magnification: (A) (C) and (E) 100x; (B), (D), and (F) 400x.

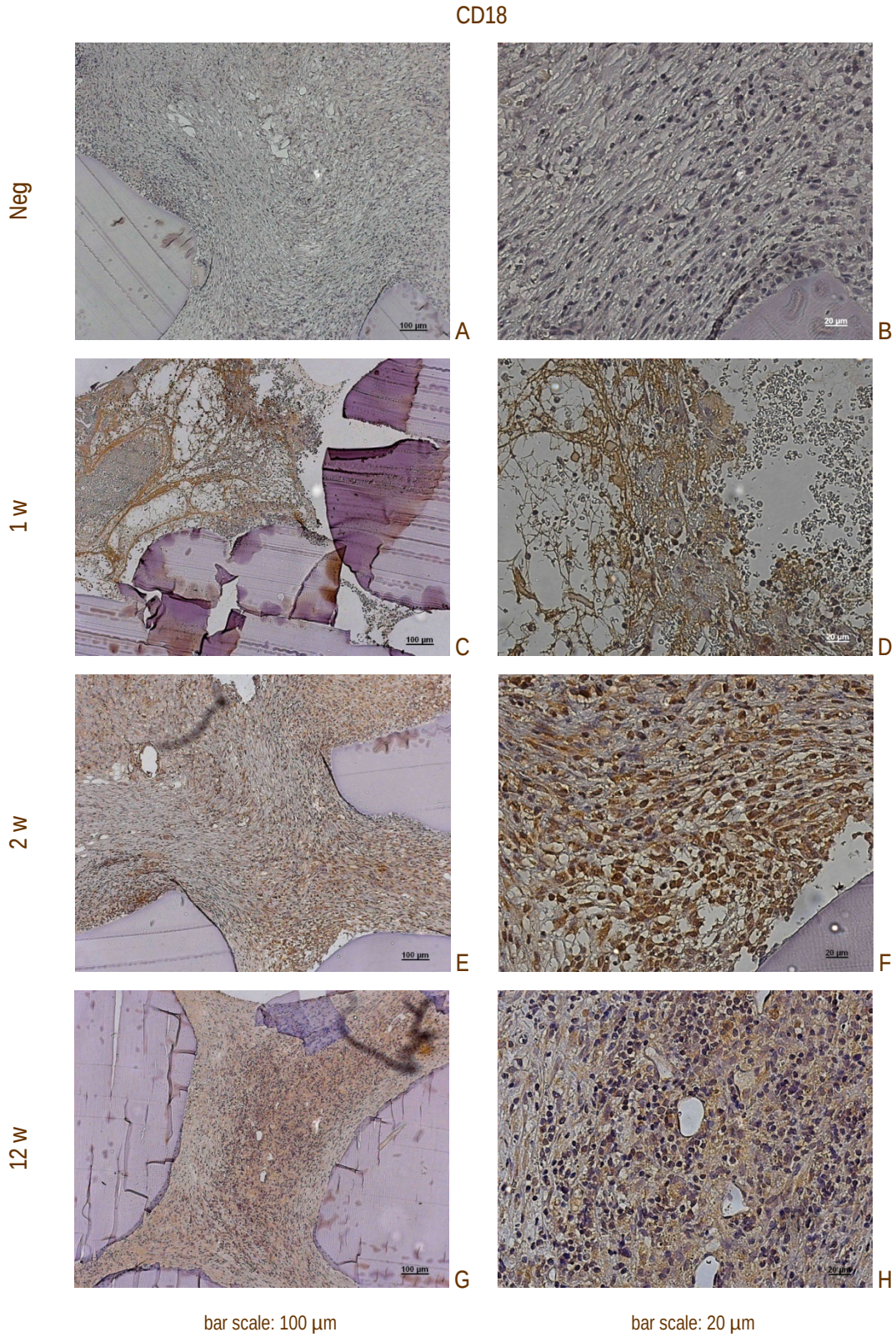

Figure 9. Representative CD18 immunostained sections of tissues surrounding chitosan-based implants after 1 week (C) and (D), 2 weeks (E) and (F), and 12 weeks (G) and (H) of intramuscular implantation. Negative control (A) and (B). Magnification: (A) (C) (E) and (G) 100x; (B), (D), (F) and (H) 400x.

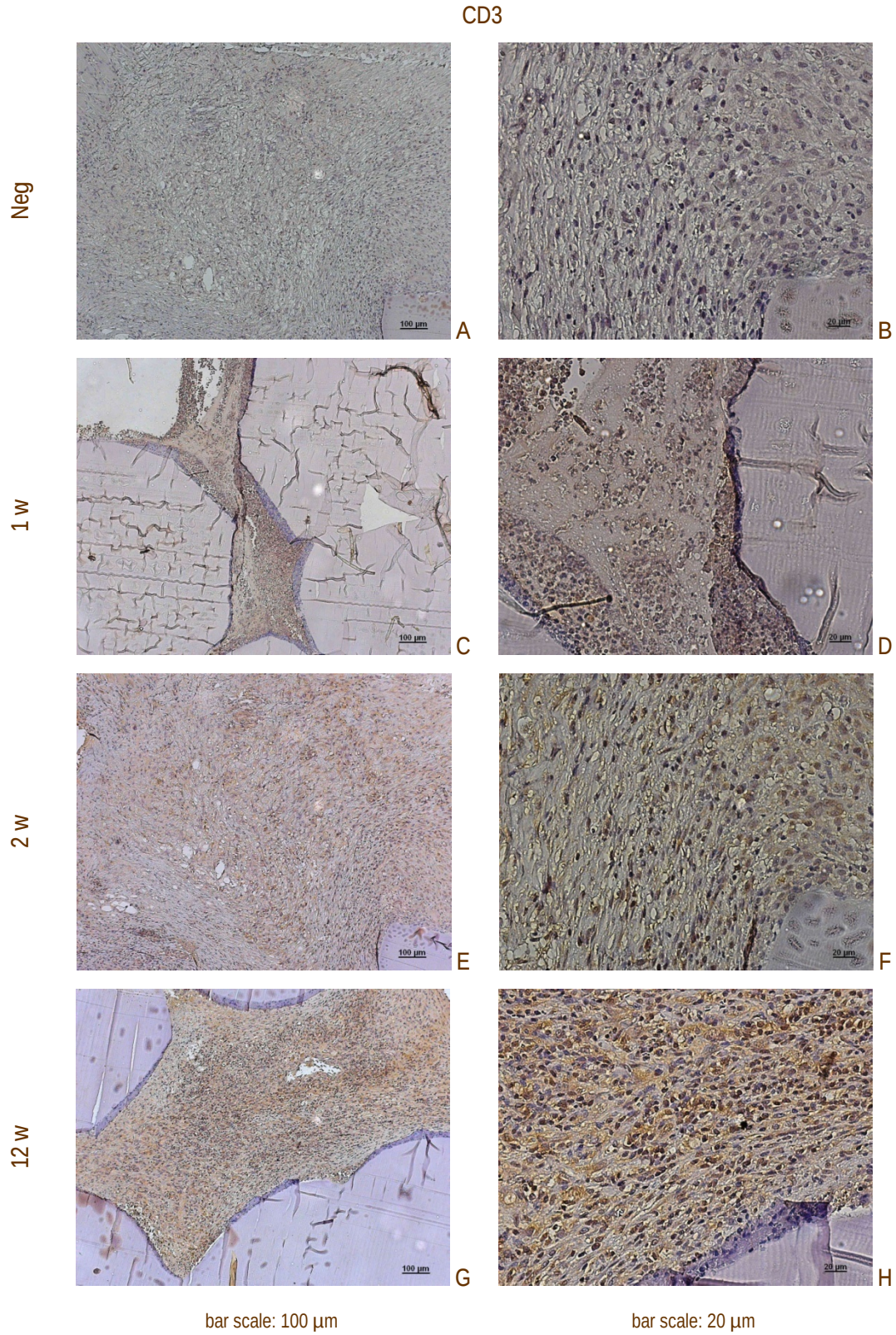

Figure 10. Representative CD3 immunostained sections of tissues surrounding chitosan-based implants after 1 week (C) and (D), 2 weeks (E) and (F), and 12 weeks (G) and (H) of intramuscular implantation. Negative control (A) and (B). Magnification: (A) (C) (E) and (G) 100x; (B), (D), (F) and (H) 400x.

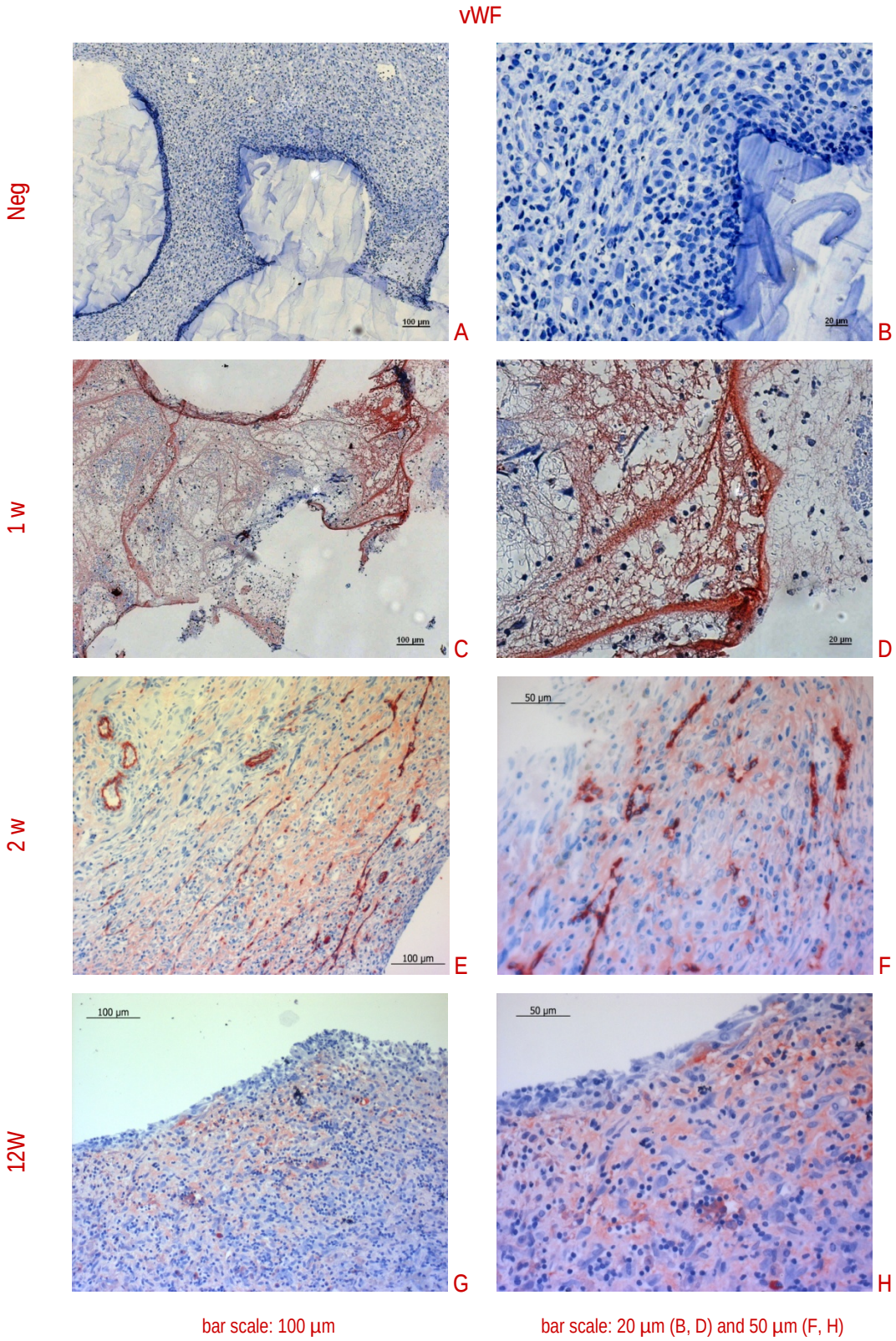

Figure 11. Representative vWF immunostained sections of tissues surrounding chitosan-based implants after 1 week (C) and (D), 2 weeks (E) and (F), and 12 weeks (G) and (H) of intramuscular implantation. Negative control (A) and (B). Magnification: (A) (C) (E) and (G) 100x; (B), (D), (F) and (H) 400x.

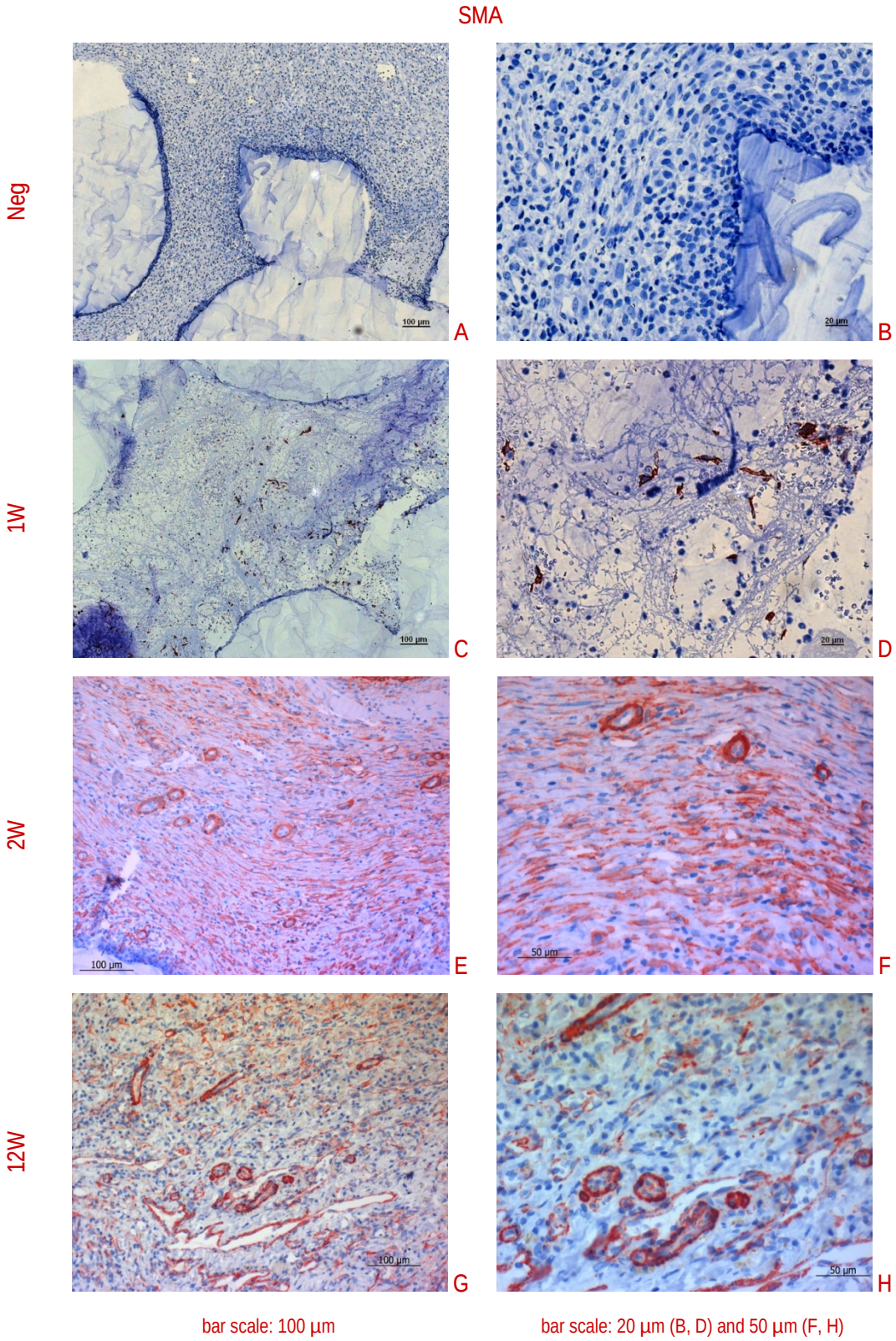

Figure 12. Representative SMA immunostained sections of tissues surrounding chitosan-based implants after 1 week (C) and (D), 2 weeks (E) and (F), and 12 weeks (G) and (H) of intramuscular implantation. Negative control (A) and (B). Magnification: (A) (C) (E) and (G) 100x; (B), (D), (F) and (H) 400x.

After 2 weeks of implantation, the main inflammatory cells present were shown to be lymphocytes (Figures 8.C and 8.D), which was confirmed with their specific labelling (Figures 10.E and 10.F). Some remaining PMNs could still be observed (Figures 9.E and 9.F), as well as some foreign body giant cells, resulting from the fusion of macrophages trying to phagocyte the implant (Figures 8.C and 8.D). Although some necrosis can be observed in the periphery of the implant (Figures 8.C and 8.D), it can be neglected if compared with the amount of extracellular matrix formed around the particles of the scaffold (Figures 8.C, 8.D, 12.E and 12.F), which shows a more organized structure compared with 1 week of implantation.

Furthermore, the presence of smooth muscle actin is more evident (Figures 12.E and 12.F), and allows to say that, both the connective tissue is growing and the neo-vascularization is also increasing between the particles of the scaffold. This fact is further supported by the expression of vWF at this implantation period (Figures 11.E and 11.F).

Three months after the implantation of the chitosan particle aggregated scaffolds, some of the remaining PMNs showed to be apoptotic (Figures 8.E and 8.F) and the spaces between the particle of the scaffolds are, in this stage, filled with connective tissue cells (Figures 8.E and 8.F). It was possible to observe that the PMNs appeared in much less amount compared with the other implantation times (Figures 9.G and 9.H). Some lymphocytes are, as well, still present in the infiltrate (Figures 10.G and 10.H). Furthermore, the general expression of vWF observed at 1 week of implantation due to the initially formed clot is now less evident, being much more restricted to the vascularized tissue (Figures 11.E and 11.F).

At this stage of implantation it is clear that the extracellular matrix shows to be much more organized along and between the particles of the scaffold (Figures 8.E, 8.F, 12.E and 12.F). Furthermore, the neo-vascularization already observed in earlier times of implantation increased as the SMA labelling shows in the newly formed blood vessels (Figures 12.E and 12.F). These features demonstrate that the scaffolds were well tolerated by the host and the ingrowth of host connective tissue into the scaffolds structure is an evidence of good integration.

4. DISCUSSION

4.1. MORPHOMETRIC ANALYSIS

For tissue engineering applications, it is important to ensure that the scaffold has an adequate architecture in order to allow for optimal cell migration and nutrients supply to assure optimal tissue growth in an in vivo situation. In order to be able to assess these morphometric requirements, micro-CT has becoming a powerful tool to compare scaffold production techniques [25,26,45]. Direct micro-CT based imaging analysis is non-destructive and non-invasive and allows precise 3D measurements of scaffold architecture quantifying scaffold porosity, surface area, and 3D measures such as interconnectivity, pore size and distribution, and pore wall thickness providing valuable knowledge to optimize scaffold design. These combined advantages over other morphological characterization techniques are well discussed in a review by Ho and Hutmacher [24] and, in our opinion, clearly justify why micro-CT has become a very popular technique for characterizing porous scaffolds [25,26,45] or bone ingrowth [21,22,46]. As a result, this methodology is very useful for quality control of scaffold fabrication processes and all data obtained for computational models will be helpful in further analyses, in order to improve our understanding of mechanical and biochemical stimuli on tissue formation.

In the present work, due to the above mentioned advantages, micro-CT was used to assess the morphometric relevant parameters and 3D reconstructions of porous structures allowing to visualize the internal cellular structure. Particle aggregation methodology allows for the production of suitable scaffolds for load-bearing bone applications. Trabecular bone typically consists of 30% bone tissue and 70% void volume [28,47]. Our effort was to fabricate scaffolds by the particle aggregation that should have a total pore volume similar to the percent bone, as previously reported [30,47]. It is expected that as an in vivo bone defect heals, bone tissue grows into the porous system of the scaffold, and the scaffold itself degrades completely (allowing for 30% ingrowth) to obtain healing of the bone defect. The chitosan scaffolds produced by this methodology have pores volume of approximate 30% as shown before in Figure 2. Furthermore, and using threshold inversion, micro-CT allows to visualize the pores network giving a clear image of scaffolds' porosity morphology which resemble the bone trabecular structure, as shown in Figure 13.

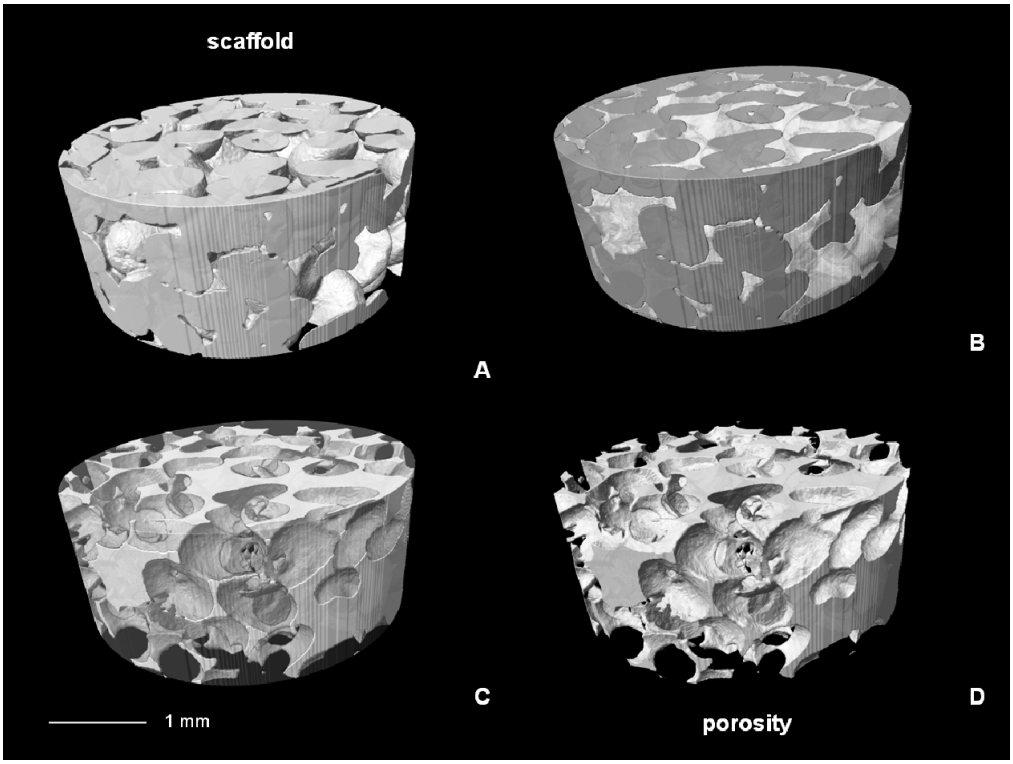

Figure 13. 3D virtual models of chitosan particle aggregated scaffolds (A) showing the gradual transition (B, C) till the inverse 3D model (D) evidencing the porosity morphology.

One can still consider that the porosity value is low for the typical reported requirements for tissue engineering scaffolding [1,3]. But we have to consider that there is also the compromise between porosity and mechanical behaviour. Since the scaffolds present a high interconnectivity degree, the mechanical performance appears as more critical when aiming at load bearing tissue engineering applications, such as bone and cartilage. Furthermore, pore size is another important factor for tissue ingrowth. Several researchers have studied bone ingrowth into porous material with different pore sizes [16,18,19] and the consensus seems to be that the optimal pore size for bone ingrowth is 100-400 μm [14-17,21-23]. The proposed scaffolds have shown to present a pore size distribution in the range of the optimal pore size (Figure 3). The 3D structures present pores with irregular shape and heterogeneous sizes (Figure 13) because pores are created by the interstices between the particles after aggregation. Again, the pore morphology resembles those in trabecular bone where pores are irregular in shape and size.

Another key issue on tissue engineering scaffolding is the interconnectivity which has direct implications for cell growth, cell migration, flow of nutrients and tissue growth into scaffolds. The proposed scaffolds are highly interconnected (Figure 2 and 13) to assure these biological requirements. For instances, Lu *et al* [17] reported the importance of interconnections for bone ingrowth and showed that interconnections larger than 50 μm were favourable for mineralized bone formation. This value was thought to be the minimum size of pore size for good tissue ingrowth as being also considered in the study by Otsuki *et al* [21,26] and, for that reason, was used to calculate the interconnectivity values in the present study, meaning that the interconnectivity only considers pore interconnections higher that 53 μm. If the pore interconnection is lower than 53 μm it is considered as a close pore. In general, this limit is not considered or at least is not reported in the majority of published morphometric studies and it is of major importance since it can change significantly the values of interconnectivity as shown in Table 2. If we used a lower value in the limit of pore size, the interconnectivity clearly increase as disclosed in Table 2. Nevertheless, the interconnectivity with low pore interconnection values will show no relevance when translated to *in vivo* situations, because the minimum pore size considered will not promote adequate tissue ingrowth. The results of the micro-CT analysis implied that the scaffolds have a suitable architecture for tissue engineering applications.

Table 2. Interconnectivity calculated with different voxels size.

LIMIT VOXELS	LIMIT VOXEL SIZE (μm) = PORE SIZE	INTERCONNECTIVITY (%)
2	17.58	99.27 ± 0.89
4	35.16	96.52 ± 1.55
6	52.74	94.99 ± 1.41

4.2. DYNAMIC MECHANICAL ANALYSIS (DMA)

The maintenance of sufficient structural integrity of scaffolds is critical in tissue engineering applications, more so since the cell and tissue remodelling is important for achieving stable biomechanical conditions at the host site. Additionally, in the case of load-bearing tissue such as articular cartilage and bone, the scaffold matrix must provide sufficient temporary mechanical support to withstand in vivo stresses and loading [3,48]. Previous work [30] has shown that chitosan scaffolds produced under the same conditions, with the same percentage porosity as the scaffolds used in this study had a compressive

modulus of 132 ± 7 MPa in dry state under static compression solicitation. The scaffolds showed a very good mechanical behaviour when compared to the typical mechanical properties obtained for chitosan based porous materials [5,6,49] normally presented as a combination of several polymers [5,6] or in a composite form [49] to improve their performance. The relatively high mechanical properties obtained by the particle aggregation methodology was further supported by other works, namely the work by Jiang *et al* [47] when using chitosan microspheres in this case with poly(lactic acid-glycolic acid) sintered together to obtain the final 3D structure.

Nevertheless, it is common to study the scaffolds mechanical performance in dry state and static conditions. In the present study, we have evaluated the mechanical performance of the chitosan particle aggregated scaffolds in hydrated state under dynamic solicitation, mimicking in this way the *in vivo* physiological condition in a post-implantation scenario. The dynamic mechanical behaviour of the scaffolds was characterized by DMA. Both storage and loss modulus (E' and E'') were measured in the frequency range 0.5-40 Hz, which are typical frequencies found in physiological situations in load bearing applications [42, 43]. The storage modulus (E') is about one order of magnitude higher than the loss modulus (E'') indicating an elastic nature of the chitosan scaffolds in the hydrated state.

The storage modulus increases with increasing frequency, E' while the loss modulus shows the inverse tendency except for high frequencies. This results in a decrease of the tan δ (loss factor) with increasing frequency with a small increase for high frequencies (inset graphic in Figure 5). This factor measures the proportion of the imposed mechanical stress that is dissipated in the form of heat. As tan δ is typically above 0.08 for f<1 Hz, one may conclude that the scaffolds possesses significant damping capability that may be useful to dissipate some cyclic mechanical energy that is imposed in an implantation scenario. Nevertheless, there is an increase in E'' for high frequencies, which suggests that the material exhibits some dissipation capability for high frequencies. The developed scaffolds present elastic and viscous modulus of 4.21±1.04 MPa and 0.36±0.07 MPa respectively at a frequency of 1Hz.

The obtained compression modulus in wet state of the scaffolds produced by the particle aggregation method presents considerable higher values when compared to other chitosan based scaffolds with fibre-based architectures produced by fibre bonding which present a higher porosity [50]. Furthermore, it is important to keep in mind that the mechanical properties may be further improved if desired with crosslinking or by incorporating a ceramic filler.

The relatively good mechanical performance of the chitosan particle aggregated scaffolds is attributed to the stable interface between the chitosan particles as shown in the 3D virtual model obtained by micro-CT (Figure 14). The 3D virtual model shows the bonding between the adjoining chitosan particles achieved by particle aggregation method process. This was achieved due to the bioadhesive character of the chitosan polymer that resulted in the merging of adjacent particles at their contact points to form the chitosan porous 3D matrices. The cross sections from the scaffolds' bulk stained with eosin (Figure 15) showed clearly the bonding areas on the particle surfaces. This chitosan-particles bonding leads to a very stable interface between the particles which assures the mechanical integrity and stability of the developed scaffolds.

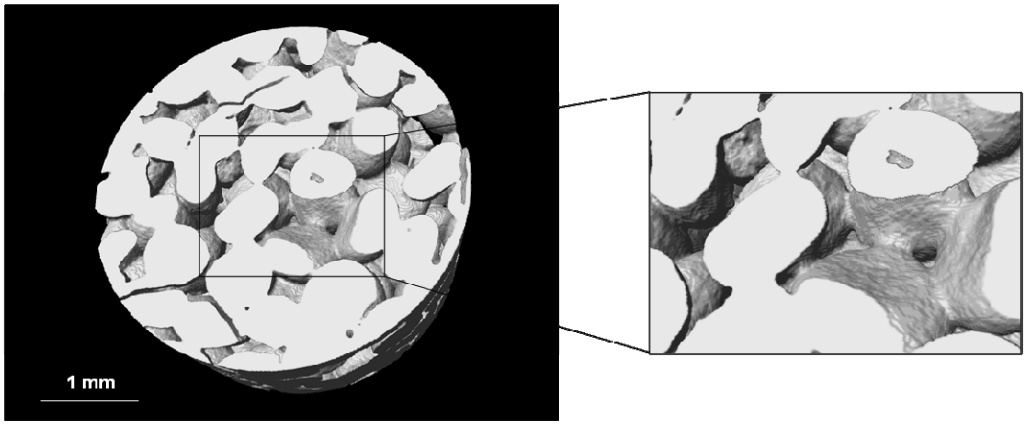

Figure 14. 3D virtual models of chitosan particle aggregated scaffolds evidencing the interface between the particles.

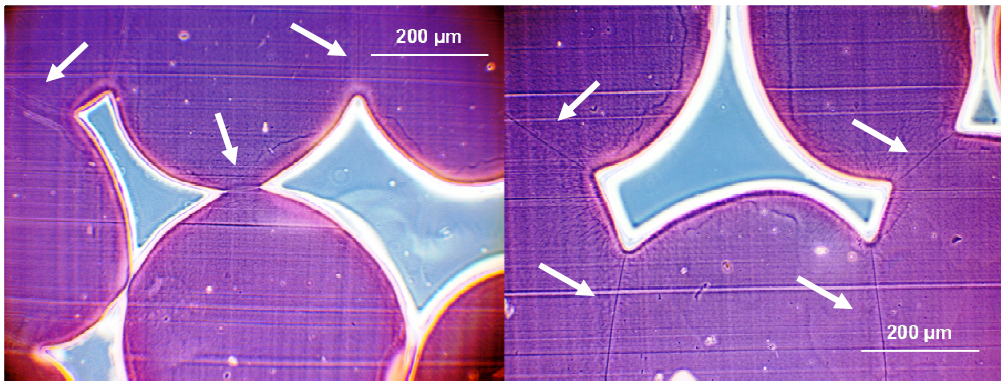

Figure 15. Cross-sections of chitosan particle aggregated scaffolds stained with eosin showing the particles' interface.

4.3. *IN VIVO* BIOCOMPATIBILITY

The non-cytotoxic behaviour of the chitosan particle aggregated scaffolds was evaluated in previous studies [30]. *In vitro* tests showed that the chitosan particle aggregated scaffolds were not cytotoxic to L929 fibroblast cell line and to human adipose stem cells [30]. However, it is critical to evaluate the scaffolds' performance in an *in vivo* environment when proposing scaffolds to be used in biomedical applications, namely tissue engineering. *In vivo* parameters such as inflammatory response, tissue ingrowth, vascularization potential and overall host response give the correct evidence to consider the biofunctionality of scaffolds. This is one of the obvious key requirements for tissue engineering applications.

After intramuscular implantation of the developed scaffolds, no systemic or regional surgical complications were seen in any of the rats. Under optical microscopy it is clear that the chitosan scaffolds architecture allowed for tissue ingrowth, being the feature more evident for longer periods of implantation (as shown previously in Figure 6). Micro-CT allowed also assessing the increase of spatial and temporal tissue ingrowth into the scaffolds, as shown in the 2D X-Ray cross-sections from the bulk of the implant (Figure 7). The increase in the connective tissue ingrowth provides a clear evidence that the interconnectivity of the developed scaffolds plays a key role in this process. The influence of interconnectivity on the tissue ingrowth was already demonstrated by Otsuki *et al* [21,26] by studying the effect of narrow pore throats on bone and tissue differentiation using bioactive porous titanium implants and micro-CT. The study revealed that narrow pore throats (e.g. low interconnectivity with low pore size limitation for its calculation) were inhibiting tissue differentiation in pores [21].

There is also a clear macroscopic indication of the presence of a vascularized tissue after 12 weeks of implantation that was further confirmed by the immunohistochemistry analyses. Again, scaffolds interconnectivity seems to be favourable for a good integration of the scaffolds in the host tissue, promoting the vascularization of the scaffolds which is critical in tissue engineering applications for cell growth, tissue ingrowth and nutrients flow. For tissue differentiation, vascularization is an important factor, and narrow pore interconnectivity may inhibit adequate vascularization [21,26].

After implantation of a medical device such as a biomaterial, the host tissue will inevitably be traumatized by the implantation procedure [51-54] triggering an inflammatory response. The recruitment

of cells after implantation of biomaterials mimics the one observed in a local inflammation [55] and this inflammatory response to biomaterials, together with the response to the trauma of implantation is, therefore, considered important in the overall biocompatibility [52]. Essentially, the purpose of inflammation is to destroy (or contain) the damaging agent, initiate the repair process and return the damaged tissue to useful function. It is subjectively divided into acute and chronic inflammation, but actually they form a continuum. Many causes of tissue damage provoke an acute inflammatory response but some types of injuries may elicit a typical chronic inflammatory reaction from the beginning, such as the viral infections, the foreign body reactions and the fungal infections [53].

An inflammatory response triggered by chitosan particle aggregated scaffolds was observed after 1, 2 and 12 weeks of intramuscular implantation in rats. One week after the implantation of the chitosan particle aggregated scaffolds, PMNs were the predominant inflammatory cell type (previous Figures 8.A, 8.B, 9.C and 9.D). These cells are normally recruited from blood circulation whenever there is tissue damage and the initiation of the process of wound healing [52-54]. In less extent, lymphocytes (Figures 10.C and 10.D) and macrophages (Figures 8.A and 8.B) were observed, following again the typical features of the implantation of foreign bodies [53,54,56]. The type of inflammatory infiltrate found in the surrounding tissue of the implanted chitosan particle aggregated scaffolds is the type of infiltrate expected when a foreign body is implanted in a host [52,54], showing a normal and mild inflammatory reaction towards the implants. Few new blood vessels can be found at this stage (Figures 11.C, 11.D, 12.C and 12.D). The neo-vascularization observed at this stage identified by the vWF expression (Figures 11.C and 11.D) is due to the initially formed clot in part to the inflammatory process that brings the leukocytes in circulation to the site of implantation after the surgical procedure. Even though, it is considered very important for the nutrition of the new tissue that is expected to grow in the spaces between the particles forming the scaffold.

In contrast with the 1 week of implantation, after 2 weeks, the principal cell type in the scaffold and surrounding tissue were without any doubt lymphocytes. These cells start to appear when the acute inflammation progresses to chronic inflammation, around the 2nd week after the tissue injury and if the damaging agent persists in the site [52-54,57]. When the implant has dimensions which the phagocytic cells are not able to phagocytose and the macrophages may fuse, forming foreign body giant cells [54,58]. Therefore, the observed reaction coincides with the patterns of a mild foreign body reaction [58].

The initially formed clot (resulting from the implantation procedure and consequent cascades of events for wound healing) is now less evident (Figure 11.E and 11.F).

After 12 weeks in the intramuscular environment, some foreign body giant cells were observed near the implanted particle aggregated chitosan scaffolds. Although some PMNs and lymphocytes were observed, the type of reaction showed to be non-granulomatous [53]. This type of inflammatory infiltrate, where mononuclear cells clearly predominate, is quite typical for foreign body reactions [56,58] and shows a normal response from the host to the chitosan particle aggregated scaffolds [58].

The neo-vascularization of the spaces between the particle forming the chitosan-based scaffolds was also achieved (Figure 12). One week after implantation, few new blood vessels were observed, responsible for the recruitment of leukocytes to the site of implantation. In early stages of inflammation and wound healing process, neo-vascularization is an important feature, since it allows the adequate nutrition of the new connective tissue that will grow around and between the scaffold structure [54,56,59]. With the increasing need of nutrition, justified by the increase of extracellular matrix formation, the density of vascularization increased as well after 2 and 12 weeks of implantation. After these periods of implantation, it was possible to observe that the scaffolds induced a marked angiogenic response promoted also by the high scaffolds interconnectivity (Figures 11.E-11.H, 12.E-12.H).

The neo-vascularization of the implants created by new blood vessels formation was clear even after only 2 weeks of implantation, becoming more significant as the implant remained for a longer period of time, showing that the scaffolds characteristics were favourable to the integration in the host tissue. These blood vessels established and developed as seen for 12 weeks after scaffolds implantation. In fact, the vascularization is another critical factor for a successful approach in tissue engineering. The chitosan scaffold architecture has shown its ability to allow for cells ingrowth, and subsequent migration into and through the matrix. This was accomplished given that the 3D materials enabled the mass transfer of nutrients and metabolites, and provided sufficient space for development and later remodelling of the organized tissue.

The formation of blood vessels developing inside the scaffold was a remarkable result since no angiogenic growth factor or previously seeded angiogenic cells were used in this study. This kind of evidence leads one to speculate that the good in vivo performance of the chitosan based scaffolds

produced by particle aggregation can be still further improved if using any angiogenic growth factor or cells important in vasculature. These results was also observed by Ehrenfreund-Kleinman *et al* [60] for chitosan/arabinogalactan-based sponges where the vascularization became clearer for 11 weeks of implantation period as detected by light microscopy and magnetic resonance imaging. The generation of extracellular matrix by the connective tissue cells between the spaces of the particle aggregated chitosan scaffolds was also identified (Figures 8.A and 8.B). Furthermore, the immunolabelling of smooth muscle actin (SMA) allowed, at the same time, for the observation of vessels' ingrowth, since it is one of the constituents of the vessel's walls.

At 1 week of implantation, it was possible to observe some extracellular matrix formed a still disorganized network between the particles of the scaffold (Figures 8.A, 8.B, 12.B and 12.C). This network increased in amount of extracellular matrix and organization along the time of implantation. These overall features show that the implanted particle aggregated chitosan scaffolds are well tolerated by the host. Furthermore, it was shown that the scaffolds architecture, namely pore interconnectivity, is favourable for cell ingrowth and subsequent production of extracellular matrix by the connective tissue cells.

The overall host response elicited by the intramuscular implantation of chitosan particle aggregated scaffolds was a mild and expected inflammatory response. It started with the normal acute inflammation initiated by the surgical procedure of implantation, noticed at the first week progressing to the normal chronic inflammation usually observed in the implantation of foreign bodies [57,58,61]. The increasing of neo-vascularization, as well as the presence of smooth muscle actin and the enhanced organization of the extracellular matrix with the time of implantation, demonstrates the good integration and scaffolds' biofunctionality. The high interconnectivity of the developed chitosan particle aggregated scaffolds might also play a key role in the scaffold integration with vascularization from the host tissue.

5. CONCLUSIONS

In this study, we manage to fabricate novel chitosan scaffolds based on a particle aggregation technique. These scaffolds have shown to fulfil three main key requirements for tissue engineering scaffolding: morphological adequacy, mechanical stability and in vivo functional biocompatibility. Micro-

CT allowed for an accurate morphometric characterization showing that the developed scaffolds had an adequate pore size range and an interconnected porous structure assuming a relevant interconnection limit. Furthermore, porosity morphology will allow for tissue ingrowth resembling those of trabecular bone, if this application is considered. In addition to all this, the mechanical properties demonstrated the scaffolds stability and suitability for load-bearing bone tissue engineering applications. From a biological point of view, it is possible to conclude that the chitosan particle aggregated scaffolds are suitable structures to allow tissue ingrowth with an induced minimal inflammatory response by the host in an intramuscular site. Furthermore, neo-vascularization as well as the enhanced organization of the extracellular matrix with the implantation time demonstrates scaffolds' biofunctionality. It is concluded that chitosan scaffolds produced by an innovative particle aggregation methodology are morphological and mechanically adequate for their aimed applications, presenting an *in vivo* biocompatible behaviour. Consequently they are without doubts potential candidates for being used in load-bearing tissue engineering applications.

REFERENCES

1. Hollister SJ. Porous scaffold design for tissue engineering. Nature Materials 2005;4(7):518-524.

2. Gomes ME, Reis RL. Tissue engineering: Key elements and some trends. Macromolecular Bioscience 2004;4(8):737-742.

3. Hutmacher DW, Schantz JT, Fu CX, Cheng LK, Lim TTC. State of the art and future directions of scaffold-based bone engineering from a biomaterials perspective. Journal of Tissue Engineering and Regenerative Medicine 2007;1(4):245-260.

4. Mano JF, Reis RL. Osteochondral defects: present situation and tissue engineering approaches. Journal of Tissue Engineering and Regenerative Medicine 2007;1(4):261-273.

5. Wan Y, Fang Y, Wu H, Cao X. Porous polylactide/chitosan scaffolds for tissue engineering. Journal of Biomedical Materials Research - Part A 2007;80A(4):776-789.

6. Huang Y, Onyeri S, Siewe M, Moshfeghian A, Madihally SV. In vitro characterization of chitosan-gelatin scaffolds for tissue engineering. Biomaterials 2005;26(36):7616-7627.

7. Cushnie EK, Khan YM, Laurencin CT. Amorphous hydroxyapatite-sintered polymeric scaffolds for bone tissue regeneration: Physical characterization studies. Journal of Biomedical Materials Research - Part A 2008;84(1):54-62.

8. Mano JF, Silva GA, Azevedo HS, Malafaya PB, Sousa RA, Silva SS, et al. Natural origin biodegradable systems in tissue engineering and regenerative medicine: Present status and some moving trends. Journal of the Royal Society Interface 2007;4(17):999-1030.

9. Gomes ME, Holtorf HL, Reis RL, Mikos AG. Influence of the porosity of starch-based fiber mesh scaffolds on the proliferation and osteogenic differentiation of bone marrow stromal cells cultured in a flow perfusion bioreactor. Tissue Engineering 2006;12(4):801-809.

10. Park H, Temenoff JS, Tabata Y, Caplan AI, Mikos AG. Injectable biodegradable hydrogel composites for rabbit marrow mesenchymal stem cell and growth factor delivery for cartilage tissue engineering. Biomaterials 2007;28(21):3217-3227.

11. Yamane S, Iwasaki N, Kasahara Y, Harada K, Majima T, Monde K, et al. Effect of pore size on in vitro cartilage formation using chitosan-based hyaluronic acid hybrid polymer fibers. Journal of Biomedical Materials Research - Part A 2007;81(3):586-593.

12. Noth U, Rackwitz L, Heymer A, Weber M, Baumann B, Steinert A, et al. Chondrogenic differentiation of human mesenchymal stem cells in collagen type I hydrogels. Journal of Biomedical Materials Research - Part A 2007;83(3):626-635.

13. Zhang Y, Ni M, Zhang M, Ratner B. Calcium Phosphate-Chitosan Composite Scaffolds for Bone Tissue Engineering. Tissue Engineering 2003;9(2):337-345.

14. Mastrogiacomo M, Scaglione S, Martinetti R, Dolcini L, Beltrame F, Cancedda R, et al. Role of scaffold internal structure on in vivo bone formation in macroporous calcium phosphate bioceramics. Biomaterials 2006;27(17):3230-3237.

15. Peyrin F, Mastrogiacomo M, Cancedda R, Martinetti R. SEM and 3D synchrotron radiation micro-tomography in the study of bioceramic scaffolds for tissue-engineering applications. Biotechnology and Bioengineering 2007;97(3):638-648.

16. Bobyn JD, Pilliar RM, Cameron HU, Weatherly GC. The optimum pore size for the fixation of porous surfaced metal implants by the ingrowth of bone. Clinical Orthopaedics and Related Research 1980;150:263-270.

17. Lu JX, Flautre B, Anselme K, Hardouin P, Gallur A, Descamps M, et al. Role of interconnections in porous bioceramics on bone recolonization in vitro and in vivo. Journal of Materials Science: Materials in Medicine 1999;10(2):111-120.

18. Whang K, Elenz DR, Nam EK, Tsai DC, Thomas CH, Nuber GW, et al. Engineering bone regeneration with bioabsorbable scaffolds with novel microarchitecture. Tissue Engineering 1999;5(1):35-51.

19. Holy CE, Fialkov JA, Davies JE, Shoichet MS. Use of a biomimetic strategy to engineer bone. Journal of Biomedical Materials Research - Part A 2003;65(4):447-453.

20. Komlev VS, Peyrin F, Mastrogiacomo M, Cedola A, Papadimitropoulos A, Rustichelli F, et al. Kinetics of In Vivo Bone Deposition by Bone Marrow Stromal Cells into Porous Calcium Phosphate Scaffolds: An X-Ray Computed Microtomography Study. Tissue Engineering 2006;12(12):3449-3458.

21. Otsuki B, Takemoto M, Fujibayashi S, Neo M, Kokubo T, Nakamura T. Pore throat size and connectivity determine bone and tissue ingrowth into porous implants: Three-dimensional micro-CT based structural analyses of porous bioactive titanium implants. Biomaterials 2006;27(35):5892-5900.

22. van Lenthe GH, Hagenmuller H, Bohner M, Hollister SJ, Meinel L, Muller R. Nondestructive micro-computed tomography for biological imaging and quantification of scaffold-bone interaction in vivo. Biomaterials 2007;28(15):2479-2490.

23. Liu C, Xia Z, Czernuszka JT. Design and development of three-dimensional scaffolds for tissue engineering. Chemical Engineering Research and Design 2007;85(7 A):1051-1064.

24. Ho ST, Hutmacher DW. A comparison of micro-CT with other techniques used in the characterization of scaffolds. Biomaterials 2006;27(8):1362-1376.

25. Jones JR, Poologasundarampillai G, Atwood RC, Bernard D, Lee PD. Non-destructive quantitative 3D analysis for the optimisation of tissue scaffolds. Biomaterials 2007;28(7):1404-1413.

26. Otsuki B, Takemoto M, Fujibayashi S, Neo M, Kokubo T, Nakamura T. Novel micro-CT based 3-dimentional structural analyses of porous biomaterials. Key Engineering Materials 2007;330-332 II:967-970.

27. Feldkamp LA, Goldstein SA, Parfitt AM, Jesion G, Kleerekoper M. The direct examination of three-dimensional bone architecture in vitro by computed tomography. Journal of Bone and Mineral Research 1989;4(1):3-11.

28. Hildebrand T, Laib A, Muller R, Dequeker J, Ruegsegger P. Direct three-dimensional morphometric analysis of human cancellous bone: Microstructural data from spine, femur, iliac crest, and calcaneus. Journal of Bone and Mineral Research 1999;14(7):1167-1174.

29. Mathieu LM, Mueller TL, Bourban P-E, Pioletti DP, Muller R, Manson J-AE. Architecture and properties of anisotropic polymer composite scaffolds for bone tissue engineering. Biomaterials 2006;27(6):905-916.

30. Malafaya PB, Pedro A, Peterbauer A, Gabriel C, Redl H, Reis RL. Chitosan particles agglomerated scaffolds for cartilage and osteochondral tissue engineering approaches with adipose tissue derived stem cells. Journal of Materials Science: Materials in Medicine 2005;16(12):1077.

31. Mastrogiacomo M, Komlev VS, Hausard M, Peyrin F, Turquier F, Casari S, et al. Synchrotron radiation microtomography of bone engineered from bone marrow stromal cells. Tissue Engineering 2004;10(11-12):1767-1774.

32. Ma PX. Biomimetic materials for tissue engineering. Advanced Drug Delivery Reviews 2008;60(2):184-198.

33. Malafaya PB, Silva GA, Reis RL. Natural-origin polymers as carriers and scaffolds for biomolecules and cell delivery in tissue engineering applications. Advanced Drug Delivery Reviews 2007;59(4-5):207-233.

34. Tan H, Gong Y, Lao L, Mao Z, Gao C. Gelatin/chitosan/hyaluronan ternary complex scaffold containing basic fibroblast growth factor for cartilage tissue engineering. Journal of Materials Science: Materials in Medicine 2007;18(10):1961-1968.

35. Nettles DL, Elder SH, Gilbert JA. Potential Use of Chitosan as a Cell Scaffold Material for Cartilage Tissue Engineering. Tissue Engineering 2002;8(6):1009-1016.

36. Kim I-Y, Seo S-J, Moon H-S, Yoo M-K, Park I-Y, Kim B-C, et al. Chitosan and its derivatives for tissue engineering applications. Biotechnology Advances 2008;26(1):1-21.

37. Tan W, Krishnaraj R, Desai TA. Evaluation of Nanostructured Composite Collagen-Chitosan Matrices for Tissue Engineering. Tissue Engineering 2001;7(2):203-210.

38. Wan Y, Wu H, Wen D. Porous-conductive chitosan scaffolds for tissue engineering, 1: Preparation and characterization. Macromolecular Bioscience 2004;4(9):882-890.

39. Mwale F, Iordanova M, Demers CN, Steffen T, Roughley P, Antoniou J. Biological Evaluation of Chitosan Salts Cross-Linked to Genipin as a Cell Scaffold for Disk Tissue Engineering. Tissue Engineering 2005;11(1-2):130-140.

40. Malafaya PB, Reis RL. Bilayered chitosan-based scaffolds for osteochondral tissue engineering: influence of hydroxylapatite on in-vitro cytotoxicity and dynamic bioactivity studies in a specific double chamber bioreactor. Acta Biomaterialia 2008:submitted.

41. Malafaya PB, Oliveira JT, Reis RL. The effect of insulin-loaded chitosan particle aggregated scaffolds in chondrogenic differentiation. Biomaterials 2008:submitted.

42. Garner E, Lakes R, Lee T, Swan C, Brand R. Viscoelastic dissipation in compact bone: Implications for stress- induced fluid flow in bone. Journal of Biomechanical Engineering 2000;122(2):166-172.

43. Barker MK, Seedhom BB. Articular cartilage deformation under physiological cyclic loading - Apparatus and measurement technique. Journal of Biomechanics 1997;30(4):377-381.

44. Hristov M, Weber C. Endothelial progenitor cells: Characterization, pathophysiology, and possible clinical relevance. Journal of Cellular and Molecular Medicine 2004;8(4):498-508.

45. Moore MJ, Jabbari E, Ritman EL, Lu L, Currier BL, Windebank AJ, et al. Quantitative analysis of interconnectivity of porous biodegradable scaffolds with micro-computed tomography. Journal of Biomedical Materials Research Part A 2004;71A(2):258-267.

46. Jones AC, Milthorpe B, Averdunk H, Limaye A, Senden TJ, Sakellariou A, et al. Analysis of 3D bone ingrowth into polymer scaffolds via micro-computed tomography imaging. Biomaterials 2004;25(20):4947-4954.

47. Jiang T, Abdel-Fattah WI, Laurencin CT. In vitro evaluation of chitosan/poly(lactic acid-glycolic acid) sintered microsphere scaffolds for bone tissue engineering. Biomaterials 2006;27(28):4894-4903.

48. Hutmacher DW. Scaffolds in tissue engineering bone and cartilage. Biomaterials 2000;21(24):2529-2543.

49. Yin Y, Ye F, Cui J, Zhang F, Li X, Yao K. Preparation and characterization of macroporous chitosan-gelatin/beta-tricalcium phosphate composite scaffolds for bone tissue engineering. Journal of Biomedical Materials Research - Part A 2003;67A(3):844-855.

50. Tuzlakoglu K, Alves CM, Mano JF, Reis RL. Production and characterization of chitosan fibers and 3-D fiber mesh scaffolds for tissue engineering applications. Macromolecular Bioscience 2004;4(8):811-819.

51. Babensee JE, Anderson JM, McIntire LV, Mikos AG. Host response to tissue engineered devices. Advanced Drug Delivery Reviews 1998;33(1-2):111-139.

52. Hunt JA. Inflammation. In: Buschow KHJ, Cahn RW, Flemings MC, (print) BI, Kramer EJ, Mahajan S, et al., editors. Encyclopedia of Materials: Science and Technology Amesterdam: Elsevier 2001. p. 4069-4075.

53. Stevens A, Lowe J, Young B. Wheater's Basic Histopathology: A Colour Atlas and Text. Edinburgh: Churchill Livingstone, 2002.

54. Williams DF. Biocompatibility Principles. In: Buschow KHJ, Cahn RW, Flemings MC, (print) BI, Kramer EJ, Mahajan S, et al., editors. Encyclopedia of Materials: Science and Technology Amesterdam: Elsevier 2001. p. 542-448.

55. Spargo BJ, Rudolph AS, Rollwagen FM. Recruitment of tissue resident cells to hydrogel composites: In vivo response to implant materials. Biomaterials 1994;15(10):853-858.

56. Marques AP, Reis RL, Hunt JA. An in vivo study of the host response to starch-based polymers and composites subcutaneously implanted in rats. Macromolecular Bioscience 2005;5(8):775-785.

57. Lickorish D, Chan J, Song J, Davies JE, Kirkpatrick J, Bongrand P. An in-vivo model to interrogate the transition from acute to chronic inflammation. European Cells and Materials 2004;8:12-20.

58. Luttikhuizen DT, Harmsen MC, Van Luyn MJA. Cellular and molecular dynamics in the foreign body reaction. Tissue Engineering 2006;12(7):1955-1970.

59. Junqueira LC, Carneiro J. Basic Histology: Text & Atlas. 11th edition ed. New York: McGraw-Hill. Medical Publishing Division, 2005.

60. Ehrenfreund-Kleinman T, Gazit Z, Gazit D, Azzam T, Golenser J, Domb AJ. Synthesis and biodegradation of arabinogalactan sponges prepared by reductive amination. Biomaterials 2002;23(23):4621-4631.

61. Hu WJ, Eaton JW, Tang L. Molecular basis of biomaterial-mediated foreign body reactions. Blood 2001;98(4):1231-1238.

SECTION 4.

CHAPTER VII.

General conclusions and final remarks

CHAPTER VII.

General conclusions and final remarks

1. GENERAL CONCLUSIONS AND FINAL REMARKS

The main goal of this thesis was to develop and assess the potential of several possible strategies for osteochondral tissue engineering. This includes: (1) the development of the cell culturing to be performed independently in the two components that are integrated before implantation; (2) the biphasic scaffold with adequate properties for both cartilage and bone parts to be used in a special bioreactor with two separate chambers where two different cell types can be seeded, and (3) the biphasic scaffold loaded with distinct differentiation agents able to provide the adequate biochemical cues to common progenitor cells. Furthermore, and as a key requisite for biomedical applications including tissue engineering, the presented work also tried to keep present the needs for (4) the *in vivo* biofunctionality of the new materials. The work described in this thesis intends mainly to be yet another positive contribute for the design of a successful approach for osteochondral tissue engineering.

Among the key requirements in tissue engineering scaffolding, in our opinion, three are a must for an ideal design: (i) a porous structure with adequate morphological characteristics, (ii) a suitable mechanical behaviour and (iii) a clear and undoubtable *in vivo* biocompatibility. Having this in mind, an innovative thodology for scaffolds production was herein proposed based in the agglomeration of pre-fabricated degradable particles. The main advantage of this methodology is that it allows to fabricate scaffolds with high interconnectivity and good mechanical performance. The particle aggregated polymeric scaffolds also demonstrated to be biocompatible not only *in vitro* but also *in vivo*. Specifically aiming at osteochondral applications, the particle aggregation methodology also enabled for the successful production of adequate bilayered structures.

The materials used for the scaffolds production were chitosan and hydroxylapatite. Chitosan was selected due to its interesting properties such as the structural similarity to glycosaminoglycans found in

extracellular matrices including native cartilage. On the other hand, hydroxylapatite was apply as bioactive ceramic filler, since it is the major mineral present in bone composition, approaching in this way the developed composite scaffolds to the bone composite structure.

The main relevant conclusions and final remarks for the experimental section, which includes Chapters III to VII, are summarized as following.

1.1. CELL CULTURING PERFORMED INDEPENDENTLY IN THE TWO COMPONENTS THAT ARE INTEGRATED BEFORE IMPLANTATION

In order to properly address this strategy, chitosan-based scaffolds were developed as described in Chapter III. SEM and micro-CT, showed that the developed scaffolds present an adequate morphology with pores ranging from 100 to 400 μm well distributed throughout the scaffolds and clearly interconnected. In addition, there was no compromise of the mechanical properties of the particle-based scaffolds. The developed polymeric scaffolds were non-cytotoxic *in vitro*, as evaluated by the MTS assay. To investigate the possibility of inducing osteogenic and chondrogenic differentiation using the developed polymeric scaffolds, preliminary cell seeding tests with mesenchymal stem cells isolated from human adipose tissue were carried out using osteogenic and chondrogenic inducing mediums. The results corroborated this hypothesis since the presence of cells with osteogenic and chondrogenic morphology in the 3D particle agglomerated scaffolds was observed. A simple strategy for the integration of the scaffolds to be applied prior to an *in vivo* implantation was developed, by means of using an adhesive material for obtaining the bilayered constructs.

1.2. BIPHASIC SCAFFOLD WITH ADEQUATE PROPERTIES FOR BOTH CARTILAGE AND BONE PARTS USED IN A SPECIAL BIOREACTOR WITH TWO SEPARATE CHAMBERS WHERE TWO DIFFERENT CELL TYPES CAN BE SEEDED

In tissue engineering, it has been better increasingly accepted that a bilayered structure would be more adequate to regenerate an osteochondral defect. Considering this, bilayered structures were successfully developed by means of assembling polymeric and composite particles, as reflected in

Chapter IV. A detailed morphometric analysis was carried out using micro-CT, from which the relevant parameters were retrieved, namely X-ray absorption histogram, scaffolds' porosity and interconnectivity, mean pore and particle size, pore size and ceramic phase distribution. This technique allowed also to confirm that the bilayered scaffolds presented a very good integration between both components avoiding any risk of possible delamination. The mechanical stability of the scaffolds was demonstrated by performing dynamic tests in wet state under compression dynamic solicitation, approaching the *in vivo* scenario. As proof of concept, dynamic bioactivity tests were also performed using a specific double-chamber bioreactor. This bioreactor was designed to allow, as an ultimate goal, for the simultaneous culturing of chondrocytes and osteoblasts or the same source of progenitor cells with distinct differentiation mediums.

1.3. BIPHASIC SCAFFOLD LOADED WITH DISTINCT DIFFERENTIATION AGENTS ABLE TO PROVIDE THE ADEQUATE BIOCHEMICAL CUES TO COMMON PROGENITOR CELLS

Another possible strategy for osteochondral tissue engineering would be to engineer *in vitro* a hybrid material able to provide the adequate biochemical cues to a single cell source, in order to promote the selective, but simultaneous, differentiation of both cartilage and bone tissues. This is the ideal and most challenging strategy for the regeneration of an osteochondral defect using tissue engineering principles. In this thesis, attention was paid primarily to the cartilage component by focusing on the development of insulin-loaded systems to induce chondrogenic differentiation. Insulin was selected as a bioactive substance, since its differentiating capacity in chondrocytes is well known. The novel systems could be successfully developed and characterized as demonstrated in Chapter V. The most promising results were obtained for pre-chondrogenic cells seeded in the higher insulin-loaded scaffolds that showed a round morphology typical of chondrocytes. The biological evaluation confirmed also that these cells were positively stained for toluidine blue, presented a high GAGs production, and expressed genes encoding cartilaginous markers, corroborating the chondro-inductive effect of the insulin-loaded scaffolds.

1.4. *IN VIVO* BIOFUNCTIONALITY

The scaffolds *in vivo* performance is an obvious requirement when designing a biomaterial for tissue engineering applications, since the implant materials must be non-toxic to the human body and should interact properly with the host tissue. Animal models are widely studied to preliminary assess this *in vivo* behaviour. In this thesis as described in Chapter VII, a well-established rat muscle pocket model was used to investigate the *in vivo* behaviour of polymeric chitosan scaffolds. The scaffolds properties shown to be favourable to the connective tissues ingrowth into the scaffolds, demonstrating a good integration with the host tissue. Furthermore, the scaffolds were able to promote an organization of the extracellular matrix and an increasing neo-vascularization with the time of implantation.

As a final remark, one can say that the work described in the present thesis intends to give yet another positive contribute for the development of a clinically needed successful approach for osteochondral tissue engineering, by means of addressing some of the possible strategies that are being currently applied in this research field. Each of the individual performed work opens the possibility to better accomplish an osteochondral hybrid strategy following the different discussed options. Chitosan-based scaffolds produced by particle aggregation were developed and optimized for a potential use in this field. The results obtained so far clearly indicate their suitability for pursuing osteochondral regeneration. The cumulative data generated from the work described in this thesis presents, and scientifically demonstrates, that chitosan-based particle aggregated scaffolds can be a valid alternative for the treatment of osteochondral defects and may have a distinct important role in the biomedical field. This is the main innovation coming from this thesis.

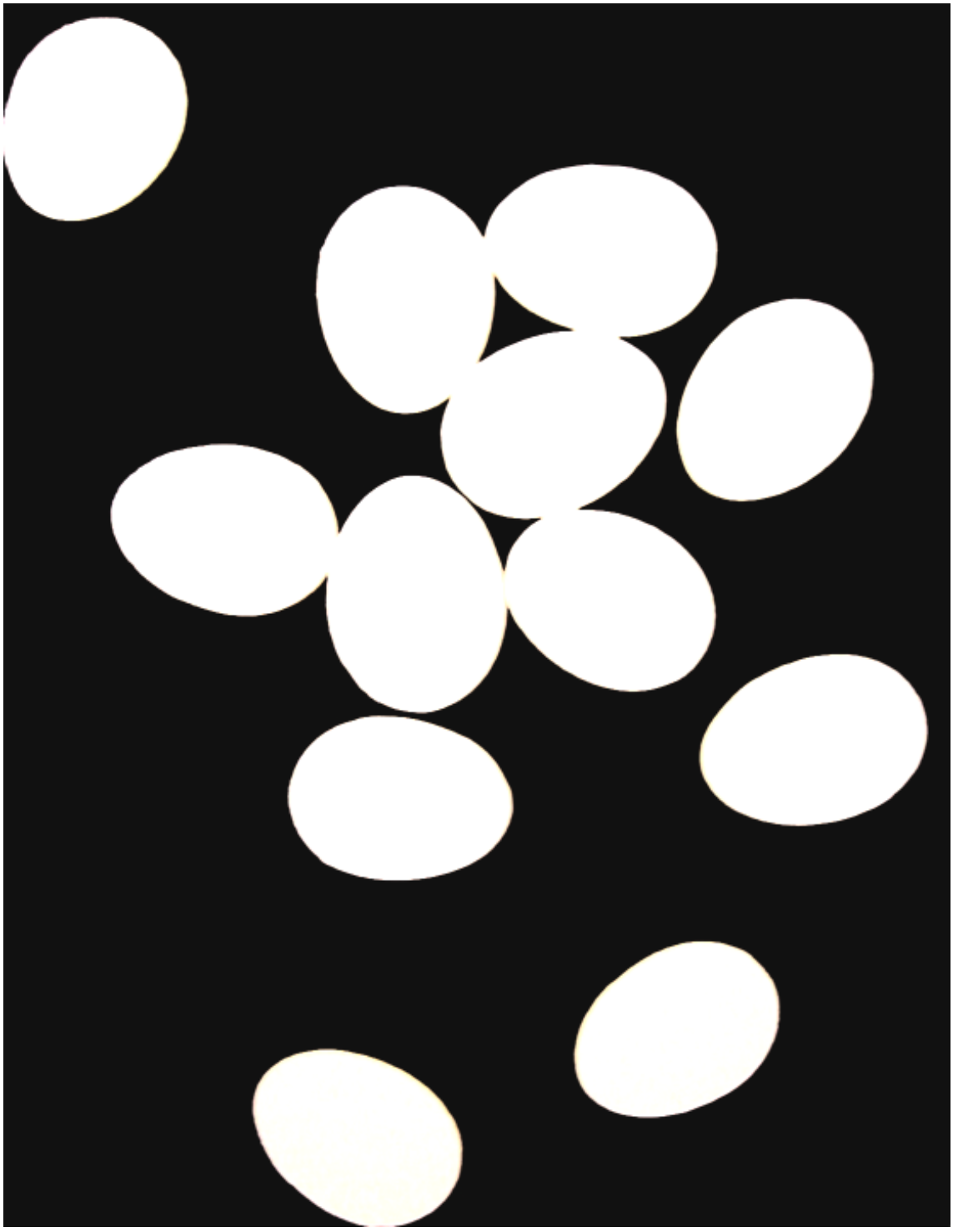

EGGS
Andy Warhol, 1982
Acrylic and silkscreen ink on canvas
Founding Collection, Contribution The Andy Warhol Foundation for the Visual Arts, Inc.
1998.1.259